

(NASA-CR-157182) OPTICAL AND INFRARED
TRANSFER FUNCTION OF THE LAGEOS
RETROREFLECTOR ARRAY (Smithsonian
Astrophysical Observatory) 193 P HC A09/ME
A01 CSCI 20F G3/74

N78-25892

Unclas
21380

OPTICAL AND INFRARED TRANSFER FUNCTION
OF THE LAGEOS RETROREFLECTOR ARRAY

Grant NGR 09-015-002

Author: David A. Arnold

May 1978

Prepared for
National Aeronautics and Space Administration
Washington, D. C. 20546

Smithsonian Institution
Astrophysical Observatory
Cambridge, Massachusetts 02138

The Smithsonian Astrophysical Observatory
and the Harvard College Observatory
are members of the
Center for Astrophysics



**OPTICAL AND INFRARED TRANSFER FUNCTION
OF THE LAGEOS RETROREFLECTOR ARRAY**

Grant NGR 09-015-002

Author: David A. Arnold

May 1978

**Prepared for
National Aeronautics and Space Administration
Washington, D. C. 20546**

**Smithsonian Institution
Astrophysical Observatory
Cambridge, Massachusetts 02138**

**The Smithsonian Astrophysical Observatory
and the Harvard College Observatory
are members of the
Center for Astrophysics**

TABLE OF CONTENTS

	<u>Page</u>
ABSTRACT	vi
1 INTRODUCTION	1
2 CUBE-CORNER SPECIFICATIONS	3
3 GEOMETRY OF THE ARRAY	5
4 METHOD OF COMPUTING THE TRANSFER FUNCTION	19
5 SIGNAL-STRENGTH COMPUTATION	21
6 OPTICAL CUBE-CORNER REFLECTIVITY	23
7 VARIATION OF TRANSFER FUNCTION WITH SATELLITE ORIENTA- TION	43
8 REFLECTIVITY HISTOGRAM	45
9 ARRAY REFLECTIVITY	53
10 RANGE CORRECTION	105
11 EFFECT OF OPTICAL COHERENCE	159
12 ACCURACY OF RESULTS	177
13 INFRARED TRANSFER FUNCTION	179
14 ACKNOWLEDGMENTS	189
15 REFERENCES	191

LIST OF FIGURES

<u>Figure</u>		<u>Page</u>
1	The Lageos satellite.	6
2	Cube-corner mount assembly.	7
3	Coordinate system for cube-corner orientation.	6
4	Coordinate system for incidence angles on cube-corner entrance face	23
5	Asymmetry of the input polarization vector with respect to $\theta = 30^\circ$. . .	26
6	Total reflectivity and average reflectivity in the 32- to 41- μ rad annulus for a Lageos optical cube corner	28
7	Reflectivity histogram of Lageos	47
8	Diffraction-pattern coordinate system	54
9	Contour plots of the gain-function matrices	87
10	Contour plots of the centroid range correction matrices.	142
11	Sample incoherent and coherent reflected pulse shapes.	162
12	Reflectivity of a Lageos infrared cube corner	182

LIST OF TABLES

<u>Table</u>	<u>Page</u>
1 Specifications for the rings of cube corners	5
2 Cube-corner positions and orientations	9
3 Cutoff angles for total internal reflection	25
4 Average reflectivity of a Lageos optical cube corner in the 32- to 41- μ rad annulus.	27
5 Apparent reflection points for various cube-corner incidence angles.	46
6 Percentage of total return in each 1-cm interval.	50
7 Gain function matrices	55
8 Gain function vs. velocity aberration.	71
9 Average gain in the 32-41 μ rad annulus	104
10 Variation of range correction with pulse length.	105
11 Codes for range contour plots in Figure 10.	106
12 Average range correction in the 32-41 μ rad annulus for various cases.	106
13 Range correction for four pulse detection techniques at selected points in the far field	108
14 Centroid range correction matrices	110
15 Centroid range correction vs. velocity aberration.	126
16 Difference between the average range correction for a set of coherent returns and the range correction for the incoherent return	160
17 Central angles between pairs of infrared cube corners.	179
18 Reflectivity of a Lageos infrared cube corner	181
19 Polarization of the reflection from a Lageos infrared cube corner	183
20 Absorptance/cm and transmission factor for the Lageos infrared reflectors.	183
21 Probability of getting reflections from more than one infrared reflector	184
22 Infrared range correction vs. incidence angle.	186

ABSTRACT

This report covers work done under NASA Grant NGR 09-015-002. The transfer function of the retroreflector array carried by the LAGEOS satellite (1976 39A) has been computed at three wavelengths: 5230, 6943, and 106000 Å. The range correction is given for extrapolating laser range measurements to the center of gravity of the satellite. The reflectivity of the array has been computed for estimating laser-echo signal strengths.

OPTICAL AND INFRARED TRANSFER FUNCTION OF THE LAGEOS RETROREFLECTOR ARRAY

David A. Arnold

1. INTRODUCTION

This is the fifth in a series of reports giving transfer functions for satellites with retroreflector arrays (Arnold, 1972, 1974, 1975a,b). A special analysis has been done for the infrared cube corners designed for use with lasers operating at $\lambda = 106000 \text{ \AA}$. The optical transfer function of the array was measured experimentally at Goddard Space Flight Center before the satellite was launched (Fitzmaurice, Minott, Abshire, and Rowe, 1977). Some preliminary transfer function analyses done on an earlier design of the satellite are given (Weiffenbach, 1973).

Data on the Lageos retroreflector array were obtained from Marshall Space Flight Center.

2. CUBE-CORNER SPECIFICATIONS

The cube corners on Lageos have a circular entrance face $1\frac{1}{5}$ (3.81 cm) in diameter, which gives an aperture of 11.4009 cm^2 . The length from vertex to face is 1.096 in. (2.78384 cm). The optical cube corners are made of fused silica and rely on total internal reflection rather than reflective coatings on the back faces. The dihedral angles between the back faces are $90^\circ + 1\frac{1}{2}25 \pm 0\frac{1}{2}5$ in order to compensate for velocity aberration. The infrared cube corners are made of single-crystal germanium and are also uncoated. The dihedral angles between the back faces are $90^\circ \pm 0\frac{1}{2}5$ with no offset.

The index of refraction of the fused silica is 1.455 at 6943 \AA and 1.461 at 5320 \AA . The refractive index of the germanium cube corners at 106000 \AA is 4.003. The surface flatness tolerance is $\sqrt{10}$ peak to peak for the optical cubes and $\lambda/4$ for the infrared cubes, where λ is the helium-neon wavelength used in measuring the flatness.

PRECEDING PAGE BLANK NOT FILMED

3. GEOMETRY OF THE ARRAY

The Lageos satellite is a sphere 60 cm in diameter with 426 retroreflectors distributed over the surface (Figure 1). Four of the cube corners are made of germanium for infrared wavelengths and the other 422 are made of fused silica for use at visible wavelengths. The sphere consists of two hemispheres bolted together. The cube corners are arranged in rings about the pole of each hemisphere. Table 1 lists for each ring, the number of cubes, the latitude, and the angle between the cubes as measured from the axis of the hemisphere.

Table 1. Specifications for the rings of cube corners on each hemisphere.

Ring number	Number of cubes	Latitude (deg.)	Angle between cubes (deg.)
1	32	4.865	11.250
2	32	13.252	11.250
3	31	22.982	11.613
4	31	31.231	11.613
5	27	40.961	13.333
6	23	50.691	15.652
7	18	60.421	20.000
8	12	70.151	30.000
9	6	79.881	60.000
10	1	90.000	360.000

Adjacent rings having the same number of cubes are meshed in order to get as many cubes on the sphere as possible. The cubes in ring two are positioned above the space between the cubes in row one. The cubes in rings three and four are meshed in a similar manner.

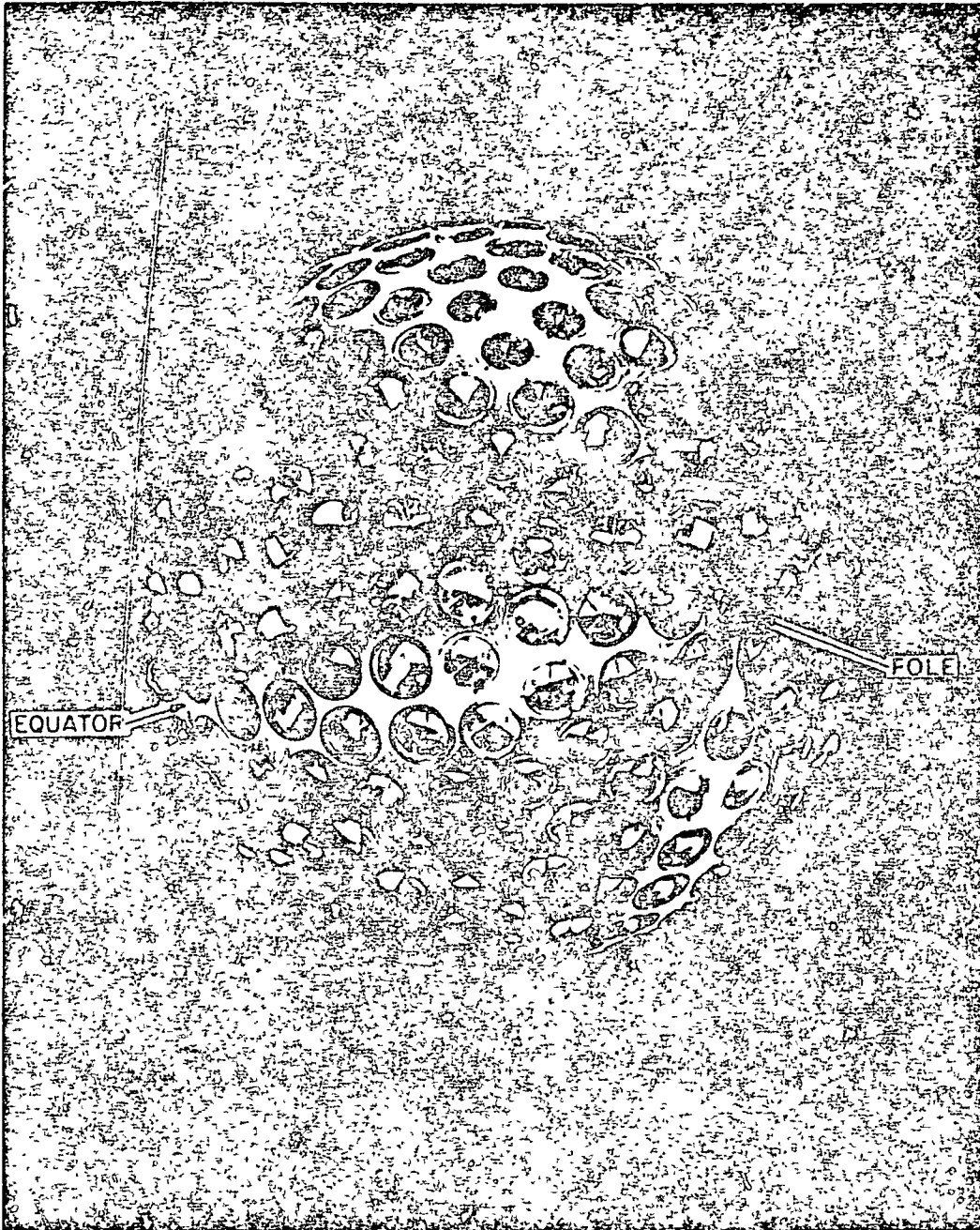


Figure 1. The Lageos satellite.

ORIGINAL PAGE IS
OF POOR QUALITY

The retroreflectors are recessed slightly below the surface of the sphere in order to prevent them from being damaged during handling. This recession, together with the fact that the front face of a cube corner is flat, places the center of the front face closer to the center of the satellite than the surface of the sphere. The cube corner is held in place by upper and lower mounting rings, which fit over tabs projecting from the cube corner. In order to minimize thermal conductance across the mounting tabs, there is a slight clearance between the tabs and the rings. The outermost hole into which the cube corner assembly is placed is 2.3813 cm in radius and 1.0236 cm deep (Figure 2). The bottom of the mounting rings are therefore

$$\sqrt{30^2 - 2.3813^2} - 1.0236 = 28.8818 \text{ cm}$$

from the center of the sphere. Adding to this the distance from the bottom of the rings to the center of the tab (0.5436 cm) and the distance from the center of the tab to the front face of the cube corner (0.3810 cm) places the front face at 29.807 cm from the center of the sphere.

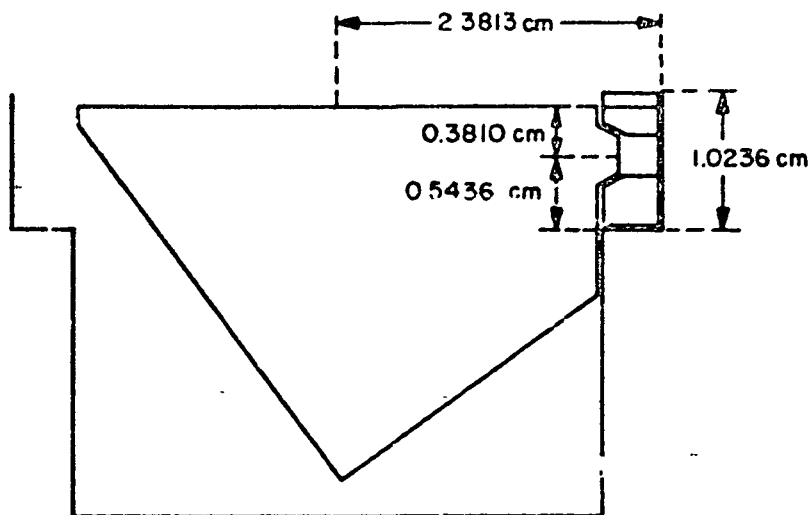


Figure 2. Cube-corner mount assembly.

Since the cube corners have no reflective coating on the back faces, retroreflection is by total internal reflection, which occurs only for certain directions of the incident beam. Any beam making an angle of less than about 17° with the normal to the front face will undergo total reflection. Beyond 17° , only certain azimuths give total reflection. In order to make the transfer function of the sphere more independent of satellite orientation, the cube corners have been installed so as to give a uniform distribution of orientations. In this way there is no satellite orientation where all the cube corners are either all totally reflecting or not totally reflecting, which would give an anomalous transfer function.

The coordinate system used to describe the geometry of the array is as follows. The position and orientation of each cube corner in the array are given by the six numbers, $x, y, z, \theta, \phi, \alpha$. The origin of the x - y - z coordinate system is the center of the satellite. The angles θ and ϕ are given in an x' - y' - z' coordinate, which is parallel to the x - y - z system (Figure 3a). The angle α is shown in Figure 3b. The β and γ axes point east and north, respectively; in other words, γ is in the direction of decreasing ϕ , and β is in the direction of increasing θ .

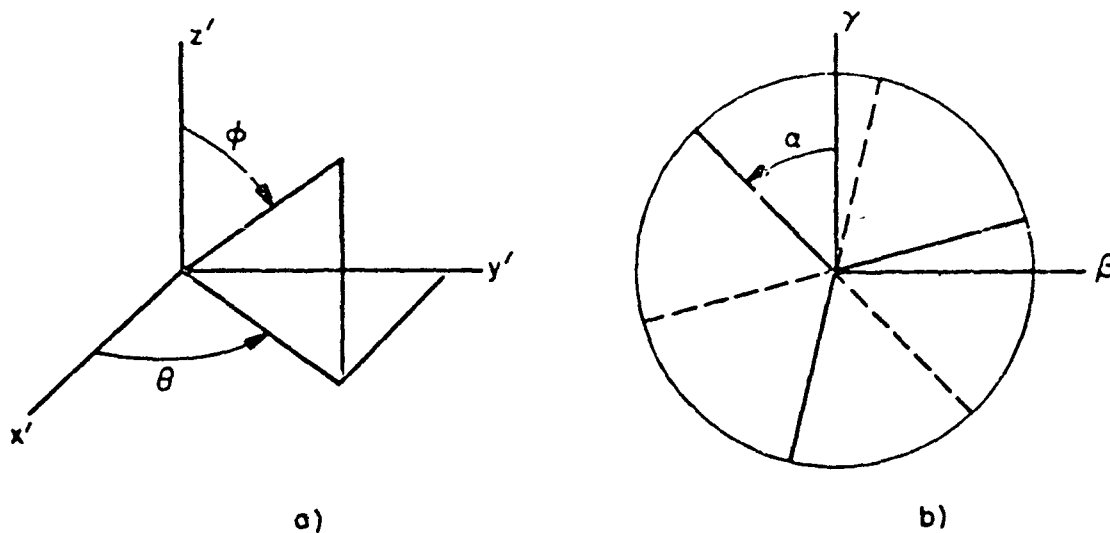


Figure 3. Coordinate system for cube-corner orientation.

Table 2 lists the position and orientation of the cube corners in the array.

Table 2. Cube corner positions (m) and orientations (degrees).

a) Infrared cube corners

HEMISPHERE	RING	RETRO	X	Y	Z	THETA	PHI	ALPHA
1	10	1	0.00000	0.00000	.29807	0.000	0.000	115.000
2	3	1	.27300	.02776	-.11638	5.806	112.982	170.000
2	3	11	-.14515	.23287	-.11638	121.936	112.982	150.000
2	3	21	-.14515	-.23287	-.11638	238.065	112.982	130.000

Table 2. (Cont.)

b) Optical cube corners.

HEMISPHERE	RING	RETRO	X	Y	Z	THETA	PHI	ALPHA
1	1	1	.29556	.02911	.02528	5.625	85.135	107.000
2	1	1	.29556	.02911	-.02528	5.625	94.865	154.000
1	1	2	.28421	.08621	.02528	16.875	85.135	81.000
2	1	2	.28421	.08621	-.02528	16.875	94.865	128.000
1	1	3	.26192	.14000	.02528	28.125	85.135	175.000
2	1	3	.26192	.14000	-.02528	28.125	94.865	102.000
1	1	4	.22958	.18841	.02528	39.375	85.135	149.000
2	1	4	.22958	.18841	-.02528	39.375	94.865	76.000
1	1	5	.18841	.22958	.02528	50.625	85.135	123.000
2	1	5	.18841	.22958	-.02528	50.625	94.865	170.000
1	1	6	.14000	.26192	.02528	61.875	85.135	97.000
2	1	6	.14000	.26192	-.02528	61.875	94.865	144.000
1	1	7	.08621	.28421	.02528	73.125	85.135	71.000
2	1	7	.08621	.28421	-.02528	73.125	94.865	118.000
1	1	8	.02911	.29556	.02528	84.375	85.135	165.000
2	1	8	.02911	.29556	-.02528	84.375	94.865	92.000
1	1	9	-.02911	.29556	.02528	95.625	85.135	139.000
2	1	9	-.02911	.29556	-.02528	95.625	94.865	66.000
1	1	10	-.08621	.28421	.02528	106.875	85.135	113.000
2	1	10	-.08621	.28421	-.02528	106.875	94.865	160.000
1	1	11	-.14000	.26192	.02528	118.125	85.135	87.000
2	1	11	-.14000	.26192	-.02528	118.125	94.865	134.000
1	1	12	-.18841	.22958	.02528	129.375	85.135	61.000
2	1	12	-.18841	.22958	-.02528	129.375	94.865	108.000
1	1	13	-.22958	.18841	.02528	140.625	85.135	155.000
2	1	13	-.22958	.18841	-.02528	140.625	94.865	82.000
1	1	14	-.26192	.14000	.02528	151.875	85.135	129.000
2	1	14	-.26192	.14000	-.02528	151.875	94.865	176.000
1	1	15	-.28421	.08621	.02528	163.125	85.135	103.000
2	1	15	-.28421	.08621	-.02528	163.125	94.865	150.000
1	1	16	-.29556	.02911	.02528	174.375	85.135	77.000
2	1	16	-.29556	.02911	-.02528	174.375	94.865	124.000
1	1	17	-.29556	-.02911	.02528	185.625	85.135	171.000
2	1	17	-.29556	-.02911	-.02528	185.625	94.865	98.000
1	1	18	-.28421	-.08621	.02528	196.875	85.135	145.000
2	1	18	-.28421	-.08621	-.02528	196.875	94.865	72.000
1	1	19	-.26192	-.14000	.02528	208.125	85.135	119.000
2	1	19	-.26192	-.14000	-.02528	208.125	94.865	166.000
1	1	20	-.22958	-.18841	.02528	219.375	85.135	93.000
2	1	20	-.22958	-.18841	-.02528	219.375	94.865	140.000
1	1	21	-.18841	-.22958	.02528	230.625	85.135	67.000
2	1	21	-.18841	-.22958	-.02528	230.625	94.865	114.000
1	1	22	-.14000	-.26192	.02528	241.875	85.135	161.000
2	1	22	-.14000	-.26192	-.02528	241.875	94.865	88.000
1	1	23	-.08621	-.28421	.02528	253.125	85.135	135.000
2	1	23	-.08621	-.28421	-.02528	253.125	94.865	62.000
1	1	24	-.02911	-.29556	.02528	264.375	85.135	109.000
2	1	24	-.02911	-.29556	-.02528	264.375	94.865	156.000
1	1	25	.02911	-.29556	.02528	275.625	85.135	83.000
2	1	25	.02911	-.29556	-.02528	275.625	94.865	130.000

Table 2. (Cont.)

HEMISPHERE	RING	RETRO	X	Y	Z	THETA	PHI	ALPHA
1	1	26	.08621	-.28421	.02528	286.875	85.135	177.000
2	1	26	.08621	-.28421	-.02528	286.875	94.865	104.000
1	1	27	.14000	-.26102	.02528	298.125	85.135	151.000
2	1	27	.14000	-.26102	-.02528	298.125	94.865	78.000
1	1	28	.18841	-.22958	.02528	309.375	85.135	125.000
2	1	28	.18841	-.22958	-.02528	309.375	94.865	172.000
1	1	29	.22958	-.18841	.02528	320.625	85.135	99.000
2	1	29	.22958	-.18841	-.02528	320.625	94.865	146.000
1	1	30	.26102	-.14000	.02528	331.875	85.135	73.000
2	1	30	.26102	-.14000	-.02528	331.875	94.865	120.000
1	1	31	.28421	-.08621	.02528	343.125	85.135	167.000
2	1	31	.28421	-.08621	-.02528	343.125	94.865	94.000
1	1	32	.29556	-.02911	.02528	354.375	85.135	141.000
2	1	32	.29556	-.02911	-.02528	354.375	94.865	68.000
1	2	1	.29013	0.00000	.06833	0.000	76.748	115.000
2	2	1	.29013	0.00000	-.06833	0.000	103.252	162.000
1	2	2	.28456	.05660	.06833	11.250	76.748	89.000
2	2	2	.28456	.05660	-.06833	11.250	103.252	136.000
1	2	3	.26804	.11103	.06833	22.500	76.748	63.000
2	2	3	.26804	.11103	-.06833	22.500	103.252	110.000
1	2	4	.24124	.16119	.06833	33.750	76.748	157.000
2	2	4	.24124	.16119	-.06833	33.750	103.252	84.000
1	2	5	.20515	.20515	.06833	45.000	76.748	131.000
2	2	5	.20515	.20515	-.06833	45.000	103.252	178.000
1	2	6	.16119	.24124	.06833	56.250	76.748	105.000
2	2	6	.16119	.24124	-.06833	56.250	103.252	152.000
1	2	7	.11103	.26804	.06833	67.500	76.748	74.000
2	2	7	.11103	.26804	-.06833	67.500	103.252	126.000
1	2	8	.05660	.28456	.06833	78.750	76.748	173.000
2	2	8	.05660	.28456	-.06833	78.750	103.252	100.000
1	2	9	0.00000	.29013	.06833	90.000	76.748	147.000
2	2	9	0.00000	.29013	-.06833	90.000	103.252	74.000
1	2	10	-.05660	.28456	.06833	101.250	76.748	121.000
2	2	10	-.05660	.28456	-.06833	101.250	103.252	168.000
1	2	11	-.11103	.26804	.06833	112.500	76.748	95.000
2	2	11	-.11103	.26804	-.06833	112.500	103.252	142.000
1	2	12	-.16119	.24124	.06833	123.750	76.748	69.000
2	2	12	-.16119	.24124	-.06833	123.750	103.252	116.000
1	2	13	-.20515	.20515	.06833	135.000	76.748	163.000
2	2	13	-.20515	.20515	-.06833	135.000	103.252	90.000
1	2	14	-.24124	.16119	.06833	146.250	76.748	137.000
2	2	14	-.24124	.16119	-.06833	146.250	103.252	64.000
1	2	15	-.26804	.11103	.06833	157.500	76.748	111.000
2	2	15	-.26804	.11103	-.06833	157.500	103.252	158.000
1	2	16	-.28456	.05660	.06833	168.750	76.748	85.000
2	2	16	-.28456	.05660	-.06833	168.750	103.252	132.000
1	2	17	-.29013	0.00000	.06833	180.000	76.748	179.000
2	2	17	-.29013	0.00000	-.06833	180.000	103.252	106.000
1	2	18	-.28456	-.05660	.06833	191.250	76.748	153.000
2	2	18	-.28456	-.05660	-.06833	191.250	103.252	80.000

Table 2. (Cont.)

HEMISPHERE	RING	RETRO	X	Y	Z	THETA	PHI	ALPHA
1	2	19	-.26804	-.11103	.06833	202.500	76.748	127.000
2	2	19	-.26804	-.11103	-.06833	202.500	103.252	174.000
1	2	20	-.24124	-.16119	.06833	213.750	76.748	101.000
2	2	20	-.24124	-.16119	-.06833	213.750	103.252	148.000
1	2	21	-.20515	-.20515	.06833	225.000	76.748	75.000
2	2	21	-.20515	-.20515	-.06833	225.000	103.252	122.000
1	2	22	-.16119	-.24124	.06833	236.250	76.748	169.000
2	2	22	-.16119	-.24124	-.06833	236.250	103.252	96.000
1	2	23	-.11103	-.26804	.06833	247.500	76.748	143.000
2	2	23	-.11103	-.26804	-.06833	247.500	103.252	70.000
1	2	24	-.05660	-.28456	.06833	258.750	76.748	117.000
2	2	24	-.05660	-.28456	-.06833	258.750	103.252	164.000
1	2	25	0.00000	-.29013	.06833	270.000	76.748	91.000
2	2	25	0.00000	-.29013	-.06833	270.000	103.252	138.000
1	2	26	.05660	-.28456	.06833	281.250	76.748	65.000
2	2	26	.05660	-.28456	-.06833	281.250	103.252	112.000
1	2	27	.11103	-.26804	.06833	292.500	76.748	159.000
2	2	27	.11103	-.26804	-.06833	292.500	103.252	86.000
1	2	28	.16119	-.24124	.06833	303.750	76.748	133.000
2	2	28	.16119	-.24124	-.06833	303.750	103.252	180.000
1	2	29	.20515	-.20515	.06833	315.000	76.748	107.000
2	2	29	.20515	-.20515	-.06833	315.000	103.252	154.000
1	2	30	.24124	-.16119	.06833	326.250	76.748	81.000
2	2	30	.24124	-.16119	-.06833	326.250	103.252	128.000
1	2	31	.26804	-.11103	.06833	337.500	76.748	175.000
2	2	31	.26804	-.11103	-.06833	337.500	103.252	102.000
1	2	32	.28456	-.05660	.06833	348.750	76.748	149.000
2	2	32	.28456	-.05660	-.06833	348.750	103.252	76.000
1	3	1	.27300	.02776	.11638	5.606	67.018	123.000
1	3	2	.26182	.08215	.11638	17.420	67.018	97.000
2	3	2	.26182	.08215	-.11638	17.420	112.982	144.000
1	3	3	.23992	.13317	.11638	29.032	67.018	71.000
2	3	3	.23992	.13317	-.11638	29.032	112.982	118.000
1	3	4	.20821	.17874	.11638	40.645	67.018	165.000
2	3	4	.20821	.17874	-.11638	40.645	112.982	92.000
1	3	5	.16797	.21699	.11638	52.258	67.018	139.000
2	3	5	.16797	.21699	-.11638	52.258	112.982	66.000
1	3	6	.12085	.24636	.11638	63.871	67.018	113.000
2	3	6	.12085	.24636	-.11638	63.871	112.982	160.000
1	3	7	.06878	.26565	.11638	75.484	67.018	87.000
2	3	7	.06878	.26565	-.11638	75.484	112.982	134.000
1	3	8	.01390	.27405	.11638	87.097	67.018	61.000
2	3	8	.01390	.27405	-.11638	87.097	112.982	108.000
1	3	9	-.04155	.27124	.11638	98.710	67.018	155.000
2	3	9	-.04155	.27124	-.11638	98.710	112.982	82.000
1	3	10	-.09530	.25732	.11638	110.322	67.018	129.000
2	3	10	-.09530	.25732	-.11638	110.322	112.982	176.000
1	3	11	-.14515	.23287	.11638	121.936	67.018	103.000
1	3	12	-.18905	.19889	.11638	133.548	67.018	77.000
2	3	12	-.18905	.19889	-.11638	133.548	112.982	124.000

Table 2. (Cont.)

HEMISPHERE	RING	RETRO	X	Y	Z	THETA	PHI	ALPHA
1	3	13	-.22522	.15676	-.11638	145.161	67.018	171.000
2	3	13	-.22522	.15676	-.11638	145.161	112.982	98.000
1	3	14	-.25217	.10822	-.11638	156.774	67.018	145.000
2	3	14	-.25217	.10822	-.11638	156.774	112.982	72.000
1	3	15	-.26879	.05524	-.11638	168.387	67.018	119.000
2	3	15	-.26879	.05524	-.11638	168.387	112.982	166.000
1	3	16	-.27441	0.00000	-.11638	180.000	67.018	93.000
2	3	16	-.27441	0.00000	-.11638	180.000	112.982	140.000
1	3	17	-.26879	-.05524	-.11638	191.613	67.018	67.000
2	3	17	-.26879	-.05524	-.11638	191.613	112.982	114.000
1	3	18	-.25217	-.10822	-.11638	203.226	67.018	161.000
2	3	18	-.25217	-.10822	-.11638	203.226	112.982	88.000
1	3	19	-.22522	-.15676	-.11638	214.839	67.018	135.000
2	3	19	-.22522	-.15676	-.11638	214.839	112.982	62.000
1	3	20	-.18905	-.19889	-.11638	226.452	67.018	109.000
2	3	20	-.18905	-.19889	-.11638	226.452	112.982	156.000
1	3	21	-.14515	-.23287	-.11638	238.065	67.018	83.000
1	3	22	-.09530	-.25732	-.11638	249.677	67.018	177.000
2	3	22	-.09530	-.25732	-.11638	249.677	112.982	10.000
1	3	23	-.04155	-.27124	-.11638	261.291	67.018	151.000
2	3	23	-.04155	-.27124	-.11638	261.291	112.982	78.000
1	3	24	.01390	-.27405	-.11638	272.903	67.018	125.000
2	3	24	.01390	-.27405	-.11638	272.903	112.982	172.000
1	3	25	.06878	-.26545	-.11638	284.516	67.018	99.000
2	3	25	.06878	-.26545	-.11638	284.516	112.982	1.6.000
1	3	26	.12085	-.24636	-.11638	296.129	67.018	73.000
2	3	26	.12085	-.24636	-.11638	296.129	112.982	170.000
1	3	27	.16797	-.21699	-.11638	307.742	67.018	167.000
2	3	27	.16797	-.21699	-.11638	307.742	112.982	9.000
1	3	28	.20821	-.17874	-.11638	319.355	67.018	141.000
2	3	28	.20821	-.17874	-.11638	319.355	112.982	68.000
1	3	29	.23992	-.13317	-.11638	330.968	67.018	115.000
2	3	29	.23992	-.13317	-.11638	330.968	112.982	162.000
1	3	30	.26182	-.08715	-.11638	342.581	67.018	89.000
2	3	30	.26182	-.08715	-.11638	342.581	112.982	136.000
1	3	31	.27300	-.02776	-.11638	354.193	67.018	63.000
2	3	31	.27300	-.02776	-.11638	354.193	112.982	110.000
1	4	1	.25487	0.00000	-.15455	0.000	58.769	157.000
2	4	1	.25487	0.00000	-.15455	0.000	121.231	84.000
1	4	2	.24965	.05131	-.15455	11.613	58.769	131.000
2	4	2	.24965	.05131	-.15455	11.613	121.231	178.000
1	4	3	.23422	.10051	-.15455	23.226	58.769	105.000
2	4	3	.23422	.10051	-.15455	23.226	121.231	152.000
1	4	4	.20919	.14560	-.15455	34.839	58.769	79.000
2	4	4	.20919	.14560	-.15455	34.839	121.231	176.000
1	4	5	.17560	.18473	-.15455	46.451	58.769	173.000
2	4	5	.17560	.18473	-.15455	46.451	121.231	100.000
1	4	6	.13482	.21630	-.15455	58.065	58.769	147.000
2	4	6	.13482	.21630	-.15455	58.065	121.231	74.000
1	4	7	.08852	.23901	-.15455	69.677	58.769	121.000

Table 2. (Cont.)

HEMISPHERE	RING	RETRO	X	Y	Z	THETA	PHI	ALPHA
2	4	7	.08852	.23901	-.15455	69.677	121.231	168.000
1	4	8	.03860	.25194	.15455	81.790	58.769	95.000
2	4	8	.03860	.25194	-.15455	81.790	121.231	142.000
1	4	9	-.01291	.25455	.15455	92.903	58.769	69.000
2	4	9	-.01291	.25455	-.15455	92.903	121.231	116.000
1	4	10	-.06389	.24674	.15455	104.516	58.769	163.000
2	4	10	-.06389	.24674	-.15455	104.516	121.231	90.000
1	4	11	-.11224	.22883	.15455	116.129	58.769	137.000
2	4	11	-.11224	.22883	-.15455	116.129	121.231	64.000
1	4	12	-.15601	.20154	.15455	127.742	58.769	111.000
2	4	12	-.15601	.20154	-.15455	127.742	121.231	158.000
1	4	13	-.19339	.16601	.15455	139.355	58.769	85.000
2	4	13	-.19339	.16601	-.15455	139.355	121.231	132.000
1	4	14	-.22285	.12369	.15455	150.968	58.769	179.000
2	4	14	-.22285	.12369	-.15455	150.968	121.231	106.000
1	4	15	-.24318	.07630	.15455	162.581	58.769	153.000
2	4	15	-.24318	.07630	-.15455	162.581	121.231	80.000
1	4	16	-.25357	.02578	.15455	174.193	58.769	127.000
2	4	16	-.25357	.02578	-.15455	174.193	121.231	174.000
1	4	17	-.25357	-.02578	.15455	185.806	58.769	101.000
2	4	17	-.25357	-.02578	-.15455	185.806	121.231	148.000
1	4	18	-.24318	-.07630	.15455	197.419	58.769	75.000
2	4	18	-.24318	-.07630	-.15455	197.419	121.231	122.000
1	4	19	-.22285	-.12369	.15455	209.032	58.769	169.000
2	4	19	-.22285	-.12369	-.15455	209.032	121.231	96.000
1	4	20	-.19339	-.16601	.15455	220.645	58.769	143.000
2	4	20	-.19339	-.16601	-.15455	220.645	121.231	70.000
1	4	21	-.15601	-.20154	.15455	232.258	58.769	117.000
2	4	21	-.15601	-.20154	-.15455	232.258	121.231	164.000
1	4	22	-.11224	-.22883	.15455	243.871	58.769	91.000
2	4	22	-.11224	-.22883	-.15455	243.871	121.231	138.000
1	4	23	-.06389	-.24674	.15455	255.484	58.769	65.000
2	4	23	-.06389	-.24674	-.15455	255.484	121.231	112.000
1	4	24	-.01291	-.25455	.15455	267.097	58.769	159.000
2	4	24	-.01291	-.25455	-.15455	267.097	121.231	86.000
1	4	25	.03859	-.25194	.15455	278.710	58.769	133.000
2	4	25	.03859	-.25194	-.15455	278.710	121.231	180.000
1	4	26	.08852	-.23901	.15455	290.322	58.769	107.000
2	4	26	.08852	-.23901	-.15455	290.322	121.231	154.000
1	4	27	.13482	-.21630	.15455	301.936	58.769	81.000
2	4	27	.13482	-.21630	-.15455	301.936	121.231	128.000
1	4	28	.17560	-.18473	.15455	313.548	58.769	175.000
2	4	28	.17560	-.18473	-.15455	313.548	121.231	102.000
1	4	29	.20919	-.14560	.15455	325.161	58.769	149.000
2	4	29	.20919	-.14560	-.15455	325.161	121.231	76.000
1	4	30	.23422	-.10051	.15455	336.774	58.769	123.000
2	4	30	.23422	-.10051	-.15455	336.774	121.231	170.000
1	4	31	.24965	-.05131	.15455	348.387	58.769	97.000
2	4	31	.24965	-.05131	-.15455	348.387	121.231	144.000
1	5	1	.22509	0.00000	.19539	0.000	49.039	71.000

Table 2. (Cont.)

HEMISPHERE	RING	RETRO	X	Y	Z	THETA	PHI	ALPHA
2	5	1	.22509	0.00000	-.19539	0.000	130.961	118.000
1	5	2	.21902	.05190	.19539	13.333	49.039	165.000
2	5	2	.21902	.05190	-.19539	13.333	130.961	92.000
1	5	3	.20115	.10102	.19539	26.667	49.039	139.000
2	5	3	.20115	.10102	-.19539	26.667	130.961	66.000
1	5	4	.17242	.14468	.19539	40.000	49.039	113.000
2	5	4	.17242	.14468	-.19539	40.000	130.961	160.000
1	5	5	.13441	.18055	.19539	53.333	49.039	87.000
2	5	5	.13441	.18055	-.19539	53.333	130.961	134.000
1	5	6	.08915	.20668	.19539	66.667	49.039	61.000
2	5	6	.08915	.20668	-.19539	66.667	130.961	108.000
1	5	7	.03909	.22166	.19539	80.000	49.039	155.000
2	5	7	.03909	.22166	-.19539	80.000	130.961	82.000
1	5	8	-.01309	.22470	.19539	93.333	49.039	129.000
2	5	8	-.01309	.22470	-.19539	93.333	130.961	176.000
1	5	9	-.06455	.21563	.19539	106.666	49.039	103.000
2	5	9	-.06455	.21563	-.19539	106.666	130.961	150.000
1	5	10	-.11254	.19493	.19539	120.000	49.039	77.000
2	5	10	-.11254	.19493	-.19539	120.000	130.961	124.000
1	5	11	-.15446	.16372	.19539	133.333	49.039	171.000
2	5	11	-.15446	.16372	-.19539	133.333	130.961	98.000
1	5	12	-.18805	.12369	.19539	146.666	49.039	145.000
2	5	12	-.18805	.12369	-.19539	146.666	130.961	72.000
1	5	13	-.21151	.07698	.19539	160.000	49.039	119.000
2	5	13	-.21151	.07698	-.19539	160.000	130.961	166.000
1	5	14	-.22356	.02613	.19539	173.333	49.039	93.000
2	5	14	-.22356	.02613	-.19539	173.333	130.961	140.000
1	5	15	-.22356	-.02613	.19539	186.666	49.039	67.000
2	5	15	-.22356	-.02613	-.19539	186.666	130.961	114.000
1	5	16	-.21151	-.07698	.19539	200.000	49.039	161.000
2	5	16	-.21151	-.07698	-.19539	200.000	130.961	88.000
1	5	17	-.18806	-.12369	.19539	213.333	49.039	135.000
2	5	17	-.18806	-.12369	-.19539	213.333	130.961	62.000
1	5	18	-.15447	-.16372	.19539	226.666	49.039	109.000
2	5	18	-.15447	-.16372	-.19539	226.666	130.961	156.000
1	5	19	-.11254	-.19493	.19539	239.999	49.039	83.000
2	5	19	-.11254	-.19493	-.19539	239.999	130.961	130.000
1	5	20	-.06456	-.21563	.19539	253.333	49.039	177.000
2	5	20	-.06456	-.21563	-.19539	253.333	130.961	104.000
1	5	21	-.01310	-.22470	.19539	266.666	49.039	151.000
2	5	21	-.01310	-.22470	-.19539	266.666	130.961	78.000
1	5	22	.03909	-.22166	.19539	279.999	49.039	125.000
2	5	22	.03909	-.22166	-.19539	279.999	130.961	172.000
1	5	23	.08915	-.20668	.19539	293.333	49.039	99.000
2	5	23	.08915	-.20668	-.19539	293.333	130.961	146.000
1	5	24	.13441	-.18055	.19539	306.666	49.039	73.000
2	5	24	.13441	-.18055	-.19539	306.666	130.961	120.000
1	5	25	.17242	-.14468	.19539	319.999	49.039	167.000
2	5	25	.17242	-.14468	-.19539	319.999	130.961	94.000
1	5	26	.20115	-.10103	.19539	333.333	49.039	141.000

Table 2. (Cont.)

HEMISPHERE	RING	RETRO	X	Y	Z	THETA	PHI	ALPHA
2	5	2A	.20115	-.10103	-.19539	333.333	130.961	68.000
1	5	27	.21902	-.05191	.19539	346.666	49.039	115.000
2	5	27	.21902	-.05191	-.19539	346.666	130.961	162.000
1	6	1	.18883	0.00000	.23063	0.000	39.309	89.000
2	6	1	.18883	0.00000	-.23063	0.000	140.691	136.000
1	6	2	.18182	.05095	.23063	15.652	39.309	63.000
2	6	2	.18182	.05095	-.23063	15.652	140.691	110.000
1	6	3	.16133	.09811	.23063	31.304	39.309	157.000
2	6	3	.16133	.09811	-.23063	31.304	140.691	84.000
1	6	4	.12888	.13801	.23063	46.957	39.309	131.000
2	6	4	.12888	.13801	-.23063	46.957	140.691	178.000
1	6	5	.08688	.16765	.23063	62.609	39.309	105.000
2	6	5	.08688	.16765	-.23063	62.609	140.691	152.000
1	6	6	.03842	.18488	.23063	78.261	39.309	77.000
2	6	6	.03842	.18488	-.23063	78.261	140.691	126.000
1	6	7	-.01289	.18839	.23063	93.913	39.309	173.000
2	6	7	-.01289	.18839	-.23063	93.913	140.691	100.000
1	6	8	-.06323	.17793	.23063	109.566	39.309	147.000
2	6	8	-.06323	.17793	-.23063	109.566	140.691	74.000
1	6	9	-.10889	.15427	.23063	125.218	39.309	121.000
2	6	9	-.10889	.15427	-.23063	125.218	140.691	168.000
1	6	10	-.14647	.11917	.23063	140.870	39.309	95.000
2	6	10	-.14647	.11917	-.23063	140.870	140.691	142.000
1	6	11	-.17320	.07523	.23063	156.522	39.309	69.000
2	6	11	-.17320	.07523	-.23063	156.522	140.691	116.000
1	6	12	-.18707	.02571	.23063	172.174	39.309	163.000
2	6	12	-.18707	.02571	-.23063	172.174	140.691	90.000
1	6	13	-.18707	-.02571	.23063	187.826	39.309	137.000
2	6	13	-.18707	-.02571	-.23063	187.826	140.691	64.000
1	6	14	-.17320	-.07523	.23063	203.479	39.309	111.000
2	6	14	-.17320	-.07523	-.23063	203.479	140.691	158.000
1	6	15	-.14647	-.11917	.23063	219.131	39.309	85.000
2	6	15	-.14647	-.11917	-.23063	219.131	140.691	132.000
1	6	16	-.10889	-.15427	.23063	234.783	39.309	179.000
2	6	16	-.10889	-.15427	-.23063	234.783	140.691	106.000
1	6	17	-.06323	-.17793	.23063	250.435	39.309	153.000
2	6	17	-.06323	-.17793	-.23063	250.435	140.691	80.000
1	6	18	-.01289	-.18839	.23063	266.087	39.309	127.000
2	6	18	-.01289	-.18839	-.23063	266.087	140.691	174.000
1	6	19	.03842	-.18488	.23063	281.739	39.309	101.000
2	6	19	.03842	-.18488	-.23063	281.739	140.691	148.000
1	6	20	.08688	-.16765	.23063	297.392	39.309	75.000
2	6	20	.08688	-.16765	-.23063	297.392	140.691	122.000
1	6	21	.12888	-.13800	.23063	313.044	39.309	169.000
2	6	21	.12888	-.13800	-.23063	313.044	140.691	96.000
1	6	22	.16133	-.09811	.23063	328.696	39.309	143.000
2	6	22	.16133	-.09811	-.23063	328.696	140.691	70.000
1	6	23	.18182	-.05095	.23063	344.348	39.309	117.000
2	6	23	.18182	-.05095	-.23063	344.348	140.691	164.000
1	7	1	.14713	0.00000	.25922	0.000	29.579	91.000

Table 2. (Cont.)

HEMISPHERE	RING	RETRO	X	Y	Z	THETA	PHI	ALPHA
2	7	1	.14713	0.00000	-.25922	0.000	150.421	138.000
1	7	2	.13825	.05032	.25922	20.000	29.579	65.000
2	7	2	.13825	.05032	-.25922	20.000	150.421	112.000
1	7	3	.11271	.09458	.25922	40.000	29.579	159.000
2	7	3	.11271	.09458	-.25922	40.000	150.421	86.000
1	7	4	.07356	.12741	.25922	60.000	29.579	133.000
2	7	4	.07356	.12741	-.25922	60.000	150.421	180.000
1	7	5	.02554	.14489	.25922	80.000	29.579	107.000
2	7	5	.02554	.14489	-.25922	80.000	150.421	154.000
1	7	6	-.02554	.14489	.25922	100.000	29.579	81.000
2	7	6	-.02554	.14489	-.25922	100.000	150.421	128.000
1	7	7	-.07356	.12741	.25922	120.000	29.579	175.000
2	7	7	-.07356	.12741	-.25922	120.000	150.421	102.000
1	7	8	-.11271	.09458	.25922	140.000	29.579	149.000
2	7	8	-.11271	.09458	-.25922	140.000	150.421	76.000
1	7	9	-.13825	.05032	.25922	160.000	29.579	123.000
2	7	9	-.13825	.05032	-.25922	160.000	150.421	170.000
1	7	10	-.14713	0.00000	.25922	180.000	29.579	97.000
2	7	10	-.14713	0.00000	-.25922	180.000	150.421	144.000
1	7	11	-.13825	-.05032	.25922	200.000	29.579	71.000
2	7	11	-.13825	-.05032	-.25922	200.000	150.421	118.000
1	7	12	-.11271	-.09458	.25922	220.000	29.579	165.000
2	7	12	-.11271	-.09458	-.25922	220.000	150.421	92.000
1	7	13	-.07356	-.12741	.25922	240.000	29.579	139.000
2	7	13	-.07356	-.12741	-.25922	240.000	150.421	86.000
1	7	14	-.02554	-.14489	.25922	260.000	29.579	113.000
2	7	14	-.02554	-.14489	-.25922	260.000	150.421	160.000
1	7	15	.02554	-.14489	.25922	280.000	29.579	87.000
2	7	15	.02554	-.14489	-.25922	280.000	150.421	134.000
1	7	16	.07356	-.12741	.25922	300.000	29.579	61.000
2	7	16	.07356	-.12741	-.25922	300.000	150.421	108.000
1	7	17	.11271	-.09458	.25922	320.000	29.579	155.000
2	7	17	.11271	-.09458	-.25922	320.000	150.421	82.000
1	7	18	.13825	-.05032	.25922	340.000	29.579	129.000
2	7	18	.13825	-.05032	-.25922	340.000	150.421	176.000
1	8	1	.10120	0.00000	.28036	0.000	19.848	103.000
2	8	1	.10120	0.00000	-.28036	0.000	160.151	150.000
1	8	2	.08764	.05060	.28036	30.000	19.848	77.000
2	8	2	.08764	.05060	-.28036	30.000	160.151	124.000
1	8	3	.05060	.08764	.28036	60.000	19.848	171.000
2	8	3	.05060	.08764	-.28036	60.000	160.151	98.000
1	8	4	0.00000	.10120	.28036	90.000	19.848	145.000
2	8	4	0.00000	.10120	-.28036	90.000	160.151	72.000
1	8	5	-.05060	.08764	.28036	120.000	19.848	119.000
2	8	5	-.05060	.08764	-.28036	120.000	160.151	166.000
1	8	6	-.08764	.05060	.28036	150.000	19.848	93.000
2	8	6	-.08764	.05060	-.28036	150.000	160.151	140.000
1	8	7	-.10120	0.00000	.28036	180.000	19.848	67.000
2	8	7	-.10120	0.00000	-.28036	180.000	160.151	114.000
1	8	8	-.08764	-.05060	.28036	210.000	19.848	101.000

Table 2. (Cont.)

HEMISPHERE	RING	RETRC	X	Y	Z	THETA	PHI	ALPHA
2	8	8	-.08764	-.05060	-.28036	210.000	160.151	88.000
1	8	9	-.05060	-.08764	.28036	240.000	19.848	125.000
2	8	9	-.05060	-.08764	-.28036	240.000	160.151	62.000
1	8	10	0.00000	-.10120	.28036	270.000	19.848	109.000
2	8	10	0.00000	-.10120	-.28036	270.000	160.151	156.000
1	8	11	.05060	-.08764	.28036	300.000	19.848	83.000
2	8	11	.05060	-.08764	-.28036	300.000	160.151	130.000
1	8	12	.08764	-.05060	.28036	330.000	19.848	177.000
2	8	12	.08764	-.05060	-.28036	330.000	160.151	104.000
1	9	1	.05236	0.00000	.29343	0.000	10.118	151.000
2	9	1	.05236	0.00000	-.29343	0.000	169.881	78.000
1	9	2	.02618	.04535	.29343	60.000	10.118	125.000
2	9	2	.02618	.04535	-.29343	60.000	169.881	172.000
1	9	3	-.02618	.04535	.29343	120.000	10.118	99.000
2	9	3	-.02618	.04535	-.29343	120.000	169.881	146.000
1	9	4	-.05236	0.00000	.29343	180.000	10.118	73.000
2	9	4	-.05236	0.00000	-.29343	180.000	169.881	120.000
1	9	5	-.02618	-.04535	.29343	240.000	10.118	167.000
2	9	5	-.02618	-.04535	-.29343	240.000	169.881	94.000
1	9	6	.02618	-.04535	.29343	300.000	10.118	141.000
2	9	6	.02618	-.04535	-.29343	300.000	169.881	68.000
2	10	1	0.00000	0.00000	-.29807	0.000	180.000	142.000

4. METHOD OF COMPUTING THE TRANSFER FUNCTION

In computing the reflectivity of the Lageos retroreflector array, the cube corners have been modeled as isothermal, geometrically perfect reflectors (except for the dihedral-angle offset) with no reflecting coatings on the back faces. The change in phase and amplitude on reflection from the back faces is computed for either ordinary reflection or total internal reflection, depending on the incidence angle at each face. The changes on transmission through the front face are also computed.

Computation of the range correction includes a correction for the optical path length of the ray within the cube corner. The range correction is the difference between the centroid of the actual return signal and the centroid of the return signal that would be received from a point reflector at the center of gravity of the satellite. The correction listed is the one-way correction.

The reflectivities and range corrections presented in all the tables are for the incoherent case; that is, the intensities of the reflections are added without taking into account coherent interference among the reflected signals from the individual cube corners.

The variation of the range correction due to optical coherence has been derived by statistical analysis of a set of coherent returns, which was constructed by assigning random phases to the reflection from each cube corner by means of a pseudo random-number generator. Since the computer time required to compute a coherent return increases as the square of the number of cube corners, the calculations were done with a reduced array obtained by omitting about a third of the cube corners. The total contribution of the omitted cubes is about 0.2% of the return energy because they reflect by ordinary reflection rather than total internal reflection and are at large incidence angles, and thus have small effective apertures. Reduced arrays have also been used in diffraction calculations. Except when the calculations have been performed for specific values of velocity aberration, the curves in Figure 6 (Section 6), giving the average reflectivity of the cube corners between velocity aberrations of 32 and 41 μ rad, have been used to compute the strength of the reflection from each cube corner. The curve for 5320 Å is used unless runs have been made for both wavelengths.

5. SIGNAL-STRENGTH COMPUTATION

The data contained in the tables presented later can be used to estimate signal strengths for laser ranging by use of the following equation:

$$N = \frac{E}{h\nu} G_T A_S G_S A_R \frac{T^2}{R^4} \eta ,$$

where

- N = number of photoelectrons,
- E = transmitted energy,
- h = Planck's constant,
- ν = frequency of laser light,
- G_T = "gain" of transmitter,
- A_S = active reflecting area of satellite,
- G_S = "gain" of satellite array,
- A_R = area of receiving telescope,
- T = atmospheric-transmission factor,
- R = range from station to satellite,
- η = constant, which includes the quantum efficiency of the photomultiplier and the optical transmission factors of the transmitter, the satellite, and the receiver.

If the transmitted beam is a uniform spot of solid angle Ω_T , the "gain" function of the transmitter is

$$G_T = \frac{1}{\Omega_T} .$$

The gain functions in this equation do not contain the factor of 4π used in the standard definition of gain. Those given in later sections can be converted to the standard definition by multiplying by 4π . The signal-strength equation above can be converted to the standard definition of gain by adding the factor $1/(4\pi)^2$.

6. OPTICAL CUBE-CORNER REFLECTIVITY

The reflectivity of the Lageos optical cube corners is given below as a function of incidence angle. The angle ϕ is measured from the normal to the front face, and the angle θ is the angle to the projection of the incident beam onto the front face; both these angles are shown in Figure 4. In each graph of Figure 6, the upper curve is the total reflectivity and the lower curve is the average reflectivity in the annulus between 32 and 41 μrad from the center of the reflected beam in the far field, which is approximately that region of the far field observed during laser ranging because of velocity aberration. All curves are normalized to unity at normal incidence. The total reflectivity at normal incidence is proportional to the area of the front face, which is 11.4009 cm^2 for a circular cube corner of radius 1.905 cm. For a perfect reflector of the same aperture, the gain at the center of the far-field pattern would be $G = A/\lambda^2$, where A is the area, λ the wavelength of the incident beam, and G the gain as defined in Section 5. (The standard expression for gain in this case is $4\pi A/\lambda^2$.) The program used to compute the reflectivity of the Lageos cube corners is normalized such that A/λ^2 is unity. The average intensity computed by this program between 32 and 41 μrad is 0.0262 at 5320 \AA and 0.0291 at 6943 \AA . To convert the reflectivities in the annulus to gain, values from Figure 6 are multiplied by G_{5320} or G_{6943} , where

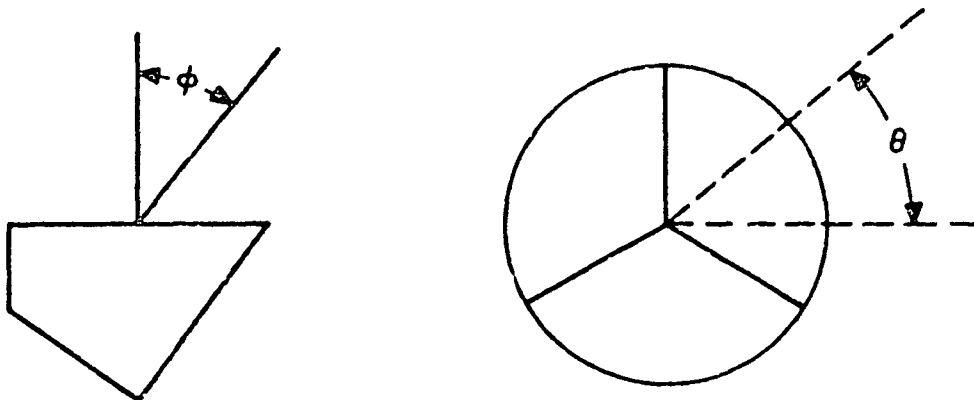


Figure 4. Direction of incident beam.

$$G_{5320} = 0.0262 (A/\lambda_{5320}^2) = 1.0554 \times 10^8$$

and

$$G_{6943} = 0.0291 (A/\lambda_{6943}^2) = 6.882 \times 10^7$$

The reflectivity of a cube corner depends on the polarization of the input beam. The reflection losses on entering and leaving the front face are different for the components of the radiation parallel and perpendicular to the plane of incidence. When the light is reflected from each of the back faces there is a change in phase for the parallel and perpendicular components of the radiation if the incidence angle is large enough to give total internal reflection, and a change in amplitude for each component if the incidence angle is less than the critical angle. It is possible for only one of the three back faces to lose total internal reflection at a time. The total reflectivity curve was generated by computing the active reflecting area and then correcting for all reflection losses assuming that the light is unpolarized at each encounter with a surface. The reflectivity in the annulus was computed for a circularly polarized input beam and all reflections and transmissions are treated rigorously. In general, the reflectivity in the annulus falls off more rapidly than the total reflectivity because diffraction spreads the beam more as the effective reflecting area decreases.

Since the front face of the cube corner is circular, the active reflecting area is independent of the azimuth angle θ . However, the reflectivity depends on θ primarily because of loss of total reflection, and to a lesser extent because of polarization effects. The reflectivity repeats exactly every 120° in θ starting at any of the three real back edges, which are at $\theta = -30^\circ$, 90° , and 210° . The cutoff angle for total internal reflection is symmetrical about the centers of each 120° interval, which are at $\theta = +30^\circ$, 120° , and 240° . The cutoff angle ϕ_c for total internal reflection is given from $\theta = -30^\circ$ to $+90^\circ$ in Table 3, for $n = 1.461$ and 1.455 , the refractive indices at 5320 and 6943 \AA , respectively. The cube corner never loses total internal reflection at $\theta = 30^\circ$. The cutoff angle listed for this azimuth is the angle where the active reflecting area goes to zero. This angle is computed from the formula

$$\phi_c(\theta = 30^\circ) = \sin^{-1} (n \sin \phi'_c) ,$$

where

$$\phi'_c = \tan^{-1} \frac{r}{l} ,$$

r = the radius of the front face (1.905 cm),

l = the length of the cube corner (2.7838 cm),

n = the index of refraction.

When the incidence angle is past the limit for total reflection, the cube corner reflects by ordinary reflection at one of the back faces. Figure 6-15 shows a detailed plot of the total reflectivity as a function of ϕ in the vicinity of the cutoff angle ϕ_c , which is $16^\circ 59.5$ for this case. The curve shows a discontinuity in slope at the cutoff angle, and the reflectivity decreases rapidly just past the cutoff. One degree past cutoff, the reflectivity is down to 42% of the value before cutoff, and two degrees past, it is down to 28%.

Table 3. Cutoff angle for total internal reflection.

θ	$\phi_c(5320 \text{ \AA})$	$\phi_c(6913 \text{ \AA})$
-30°	$16^\circ 9.98$	$16^\circ 59.5$
-20	17.315	16.903
-10	18.340	17.899
0	20.347	19.844
$+10$	24.079	23.416
$+20$	32.215	31.204
$+30$	55.597	55.255
$+40$	32.215	31.204
$+50$	24.079	23.416
$+60$	20.347	19.844
$+70$	18.340	17.899
$+80$	17.315	16.903
$+90$	16.998	16.595

The reflectivities listed in Table 4 are nearly symmetric about $\theta = 30^\circ$ because the total reflection cutoff is symmetric about this azimuth. The slight asymmetry is due to an asymmetry in the input polarization. The circular polarization vector used as input has components of equal magnitude perpendicular and parallel to the plane of incidence and a phase difference of 90° between the components. Figure 5 shows the input polarization vectors just before and just after $\theta = 30^\circ$. It is apparent that to obtain polarization symmetry about $\theta = 30^\circ$, the direction (or sign) of \vec{E}_\perp should be reversed when the symmetry angle is crossed. Some computer runs have been done reversing the sign, and exact symmetry is obtained. Since the polarization asymmetry is small, only the curves for $\theta = -30^\circ$ to $+30^\circ$ have been plotted in Figure 6.

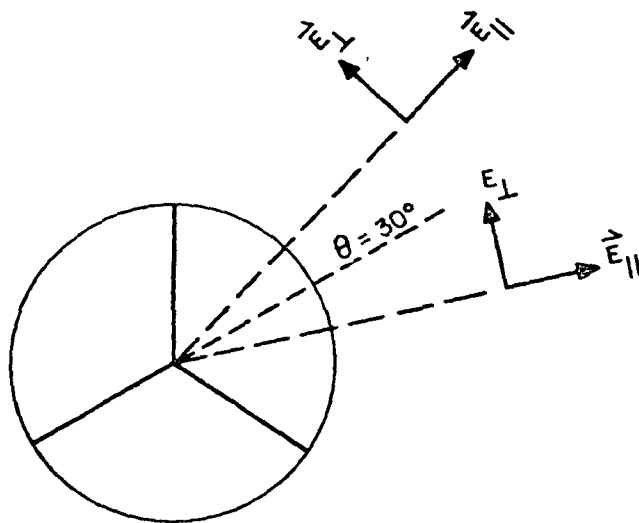


Figure 5. Asymmetry of the input polarization vector with respect to $\theta = 30^\circ$.

Table 4. Average reflectivity of a Lages optical cube corner in the 32- to 41- μ rad annulus of the far-field diffraction pattern. The angles θ and ϕ are defined in Figure 4.

		$\lambda = 5320 \text{ \AA}$															
		-30	-20	-10	0	10	20	30	40	50	60	70	80	90	θ		
0	1.00000	1.00000	1.00000	1.00000	1.00000	1.00000	1.00000	1.00000	1.00000	1.00000	1.00000	1.00000	1.00000	1.00000	1.00000	1.00000	
5	.84198	.83617	.84629	.84871	.85854	.86205	.85090	.86266	.87030	.85462	.84939	.85048	.84198				
10	.64899	.63828	.64889	.65020	.65551	.67307	.64814	.67917	.69342	.66777	.65883	.66000	.64899				
15	.49886	.47880	.47712	.46654	.46492	.48740	.46856	.50136	.52601	.51443	.50754	.51275	.49886				
20	.39065	.39184	.11770	.36279	.35001	.36816	.37029	.38399	.40637	.41819	.43598	.40329	.39065				
25	.33306	.33258	.03789	.32321	.32504	.32921	.29511	.29568	.30312	.24256	.26562	.26562	.33306				
30	.01451	.01383	.01524	.01977	.03582	.20427	.20948	.21923	.04711	.02765	.02011	.01663	.01451				
35	.00739	.00680	.00684	.00788	.01263	.04142	.05201	.05204	.02004	.01284	.00983	.00845	.00739				
40	.00411	.00382	.00380	.00415	.00601	.01564	.07214	.01929	.00898	.00617	.00506	.00453	.00411				
45	.00179	.00170	.00177	.00202	.00287	.00472	.03634	.00738	.00457	.00251	.00208	.00192	.00179				
50	.00038	.00038	.00038	.00050	.00072	.00165	.01047	.00163	.00077	.00053	.00045	.00042	.00038				
55	0.00000	0.00000	0.00000	0.00004	.00004	.00008	.00053	.00008	.00004	.00004	.00004	.00004	0.00000				
60	0.00000	0.00000	0.00000	0.00000	0.00000	0.00000	0.00000	0.00000	0.00000	0.00000	0.00000	0.00000	0.00000				

		$\lambda = 6943 \text{ \AA}$															
		-30	-20	-10	0	10	20	30	40	50	60	70	80	90	θ		
0	1.00000	1.00000	1.00000	1.00000	1.00000	1.00000	1.00000	1.00000	1.00000	1.00000	1.00000	1.00000	1.00000	1.00000	1.00000	1.00000	
5	.86265	.84987	.84522	.85373	.86285	.87386	.87436	.87022	.86810	.86660	.87019	.87151	.86265				
10	.77398	.75196	.73903	.75055	.76309	.78050	.78933	.78051	.78768	.78141	.79153	.79065	.77398				
15	.65893	.64083	.63247	.64606	.67000	.69407	.70599	.68484	.68950	.68783	.68602	.68021	.65893				
20	.5528	.54954	.54776	.56574	.59615	.62948	.63954	.62954	.62734	.62972	.62972	.62116	.5528				
25	.43626	.43537	.4076	.46025	.4821	.49284	.48295	.42854	.48711	.48302	.45436	.44187	.43626				
30	.31738	.31599	.31640	.32558	.37332	.22770	.25083	.27610	.23792	.23382	.22454	.21994	.31738				
35	.20967	.20895	.20882	.21001	.21533	.24696	.24816	.26053	.23260	.21586	.21451	.21076	.20967				
40	.05506	.05484	.05498	.05571	.06332	.02030	.09063	.02314	.01153	.00740	.00607	.00541	.05506				
45	.00196	.00196	.00206	.02248	.00364	.01838	.04604	.00859	.00394	.00275	.00230	.00206	.00196				
50	.00045	.00045	.00048	.00058	.00089	.00207	.01314	.00196	.00089	.00062	.00051	.00045	.00045				
55	0.00000	0.00000	0.00000	0.00003	.00003	.00007	.00052	.00007	.00003	.00003	.00003	.00003	0.00000				
60	0.00000	0.00000	0.00000	0.00000	0.00000	0.00000	0.00000	0.00000	0.00000	0.00000	0.00000	0.00000	0.00000				

This document is copyrighted by the American Institute of Physics (AIP) Publishing Company. This article is intended solely for the personal use of the individual user and is not to be disseminated broadly.

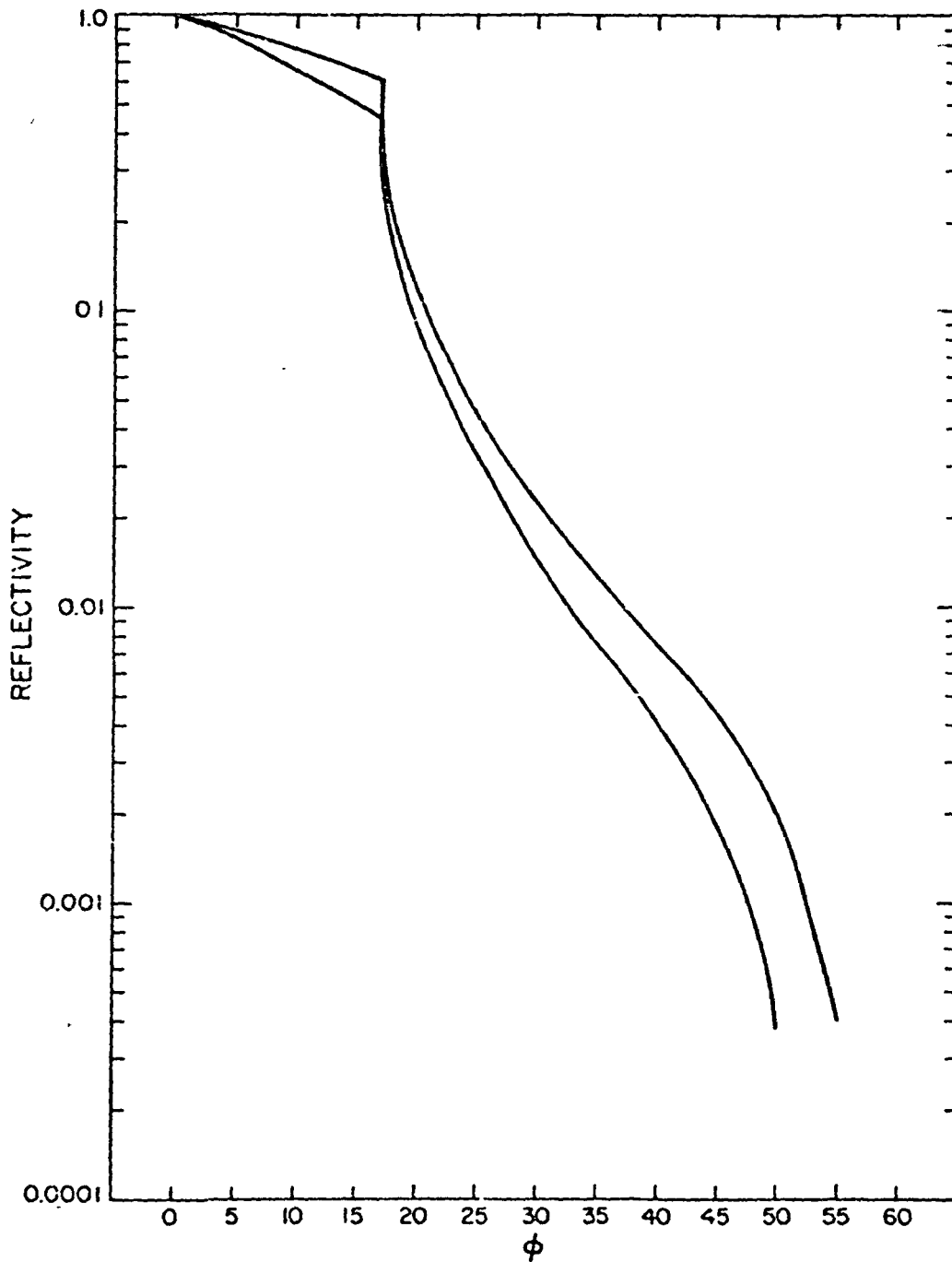


Figure 6(1-15). Total reflectivity (upper curve) and average reflectivity in the 32- to 41- μ rad annulus of the far-field pattern (lower curve) for a Lageos optical cube corner. The angles θ and ϕ are defined in Figure 4; the angle θ and the wavelength λ are listed for each set of curves. Figure 6-1. $\theta = -30^\circ$, $\lambda = 5320 \text{ \AA}$.

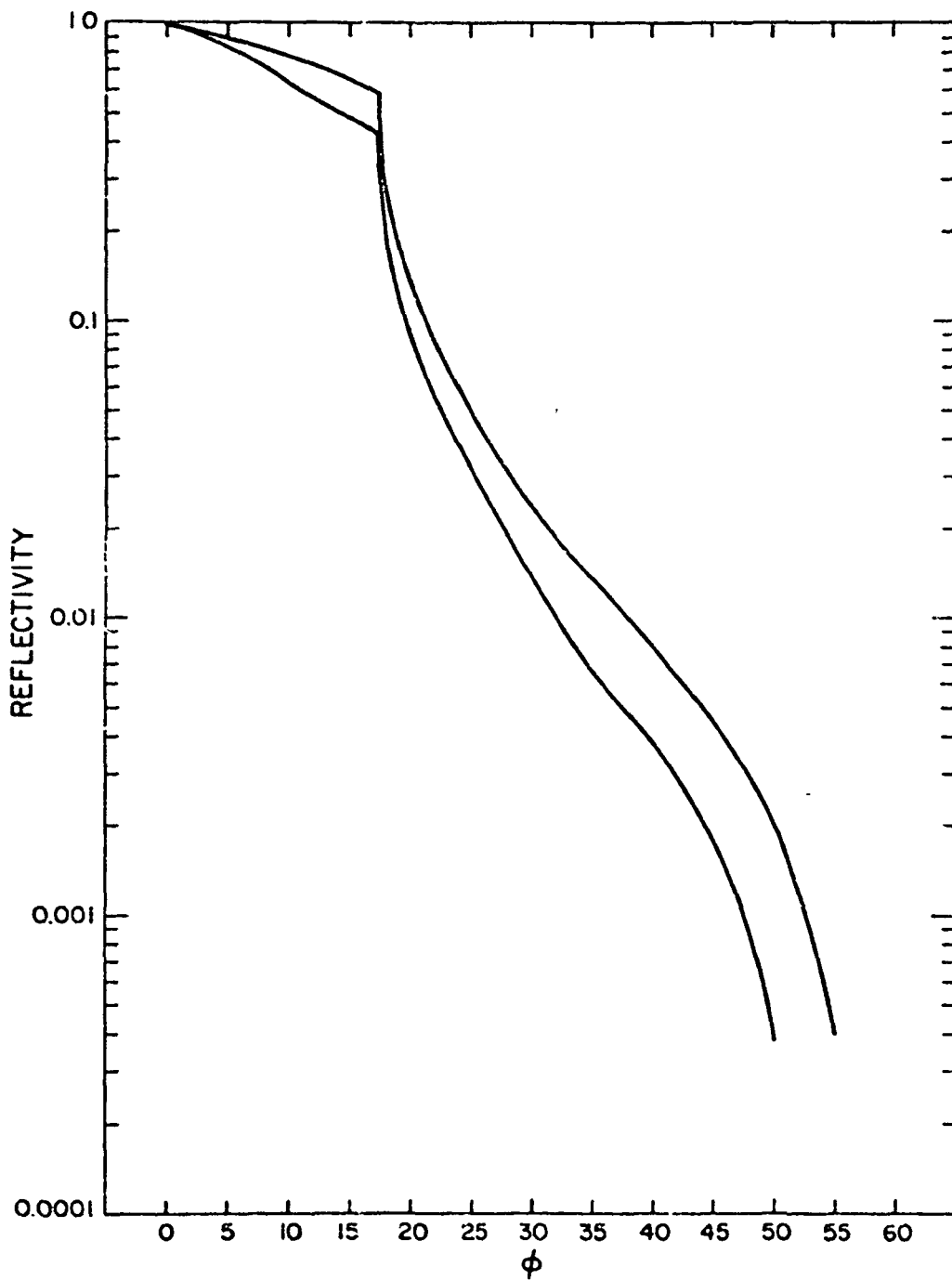


Figure 6-2. $\theta = -20^\circ$, $\lambda = 5320 \text{ \AA}$.

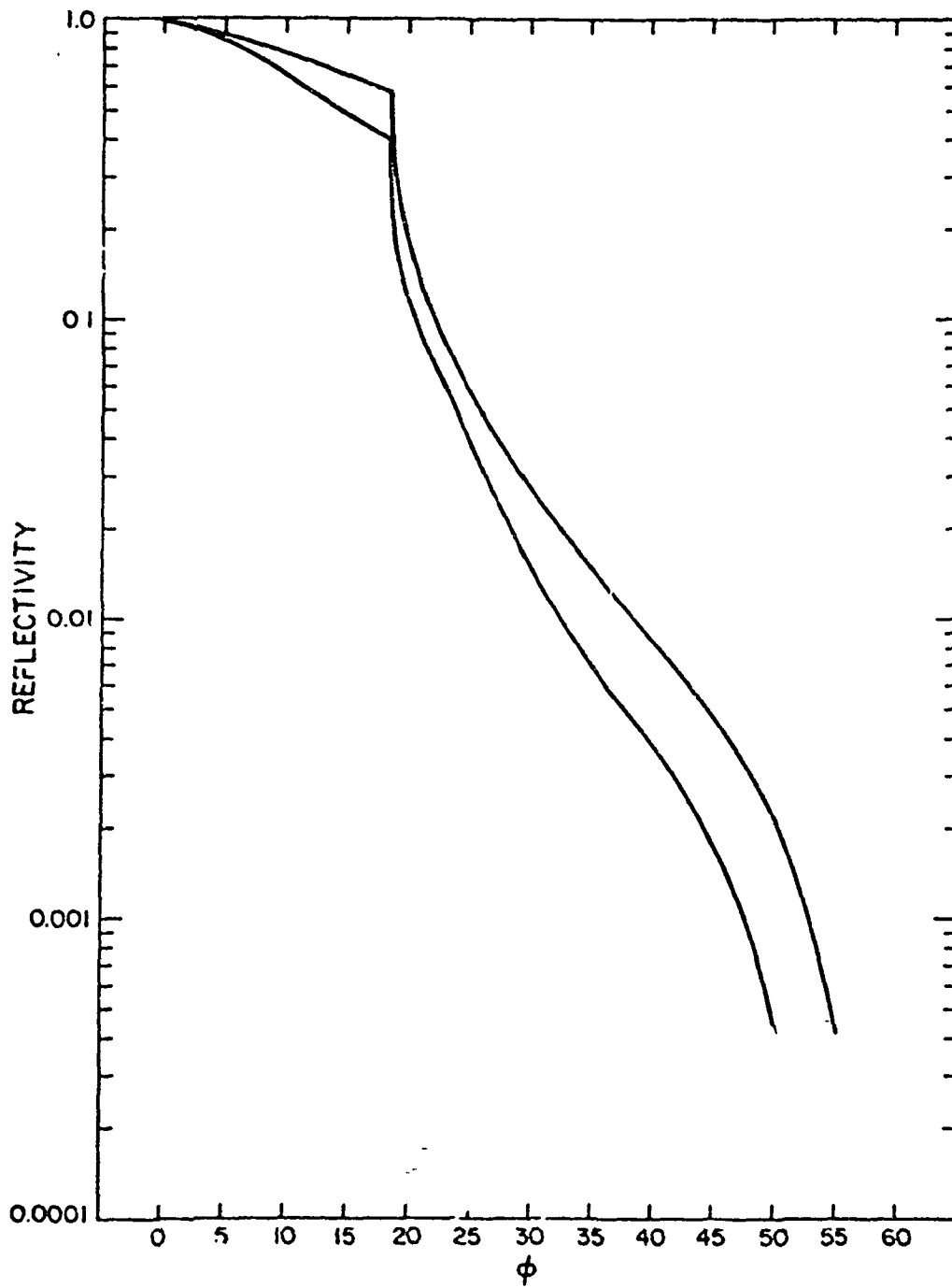


Figure 6-3. $\theta = -10^\circ$, $\lambda = 5320 \text{ \AA}$.

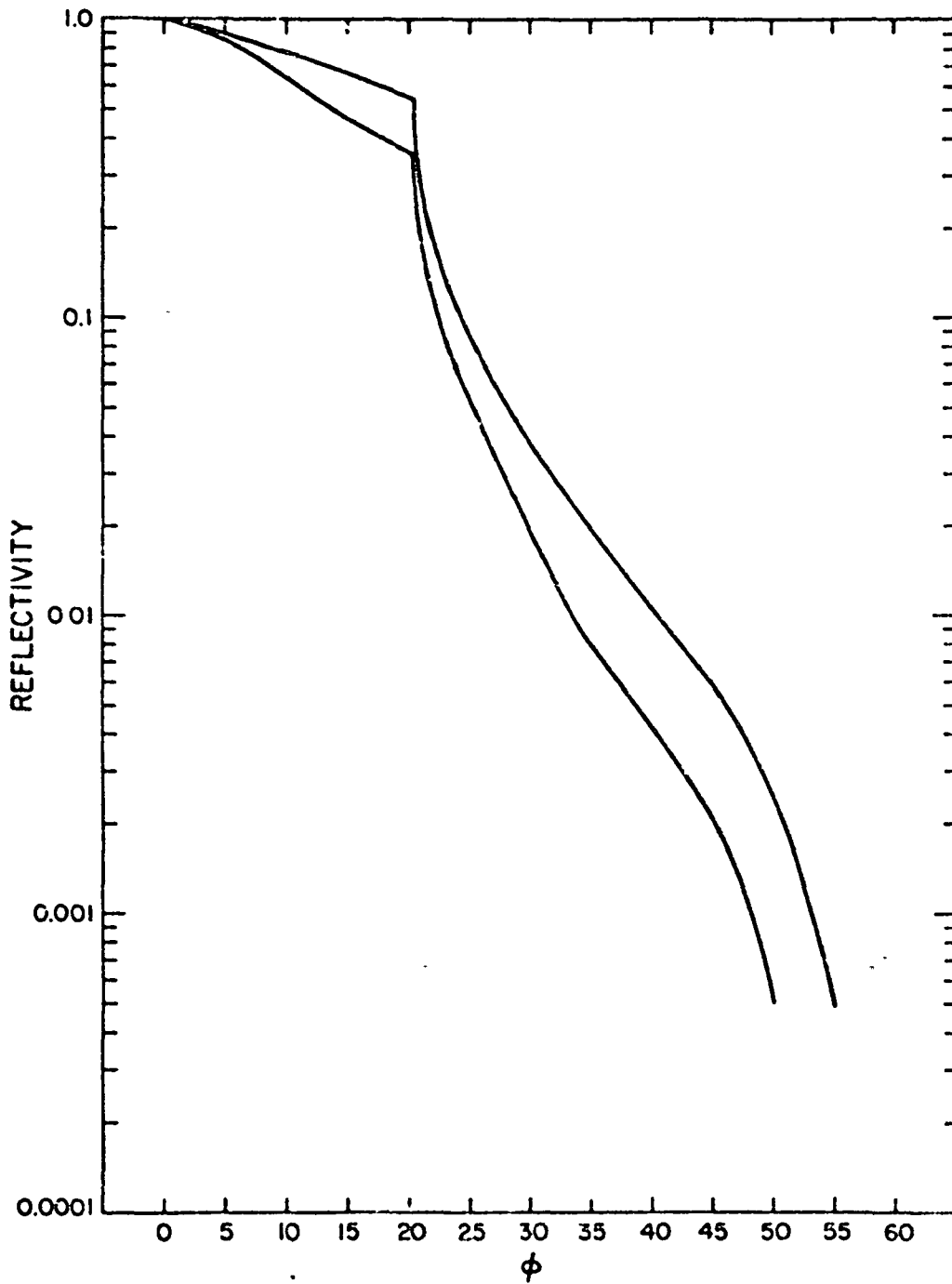


Figure 6-4. $\theta = 0^\circ$, $\lambda = 5320 \text{ \AA}$.

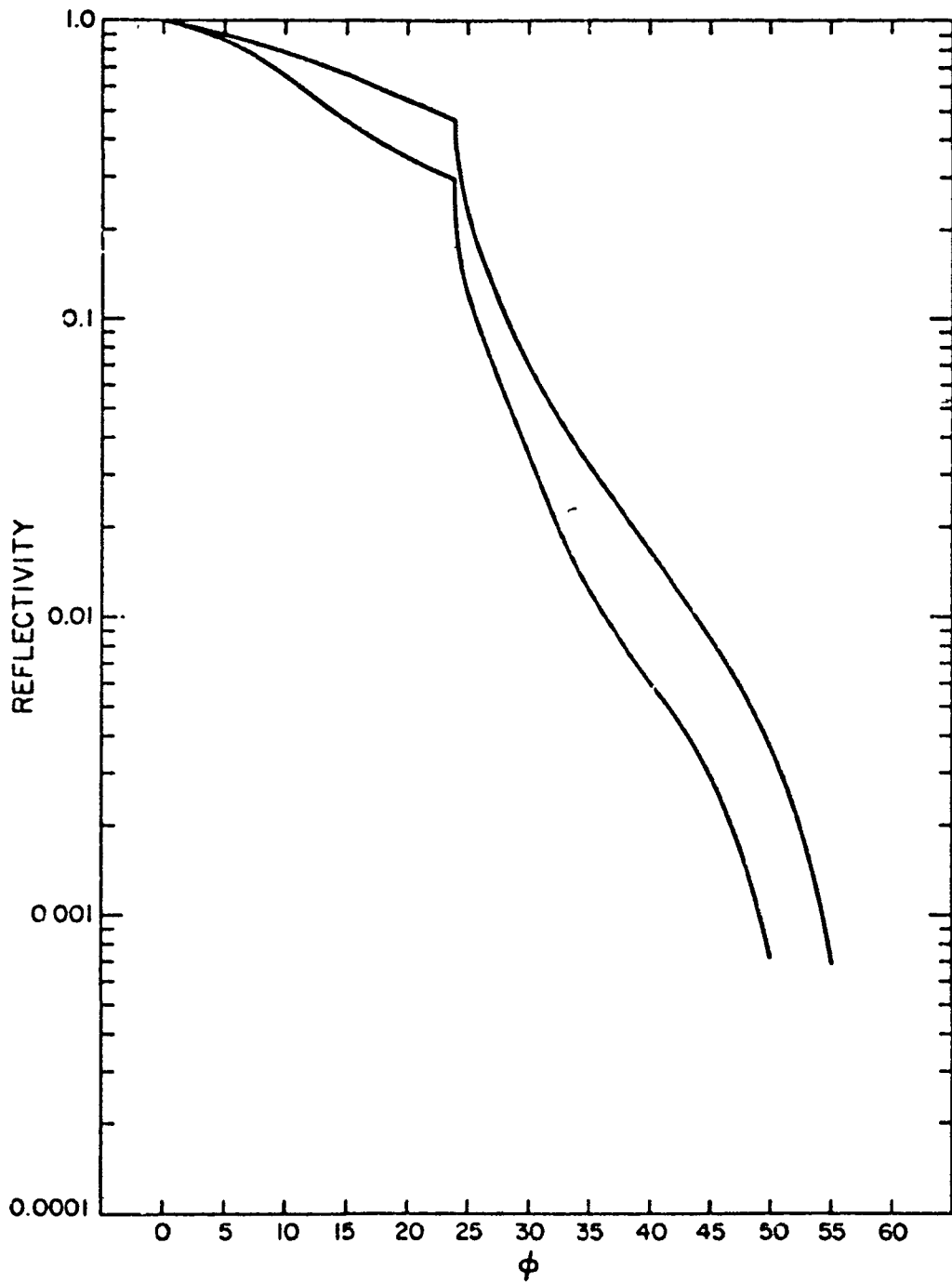


Figure 6-5. $\theta = 10^\circ$, $\lambda = 5320 \text{ \AA}$.

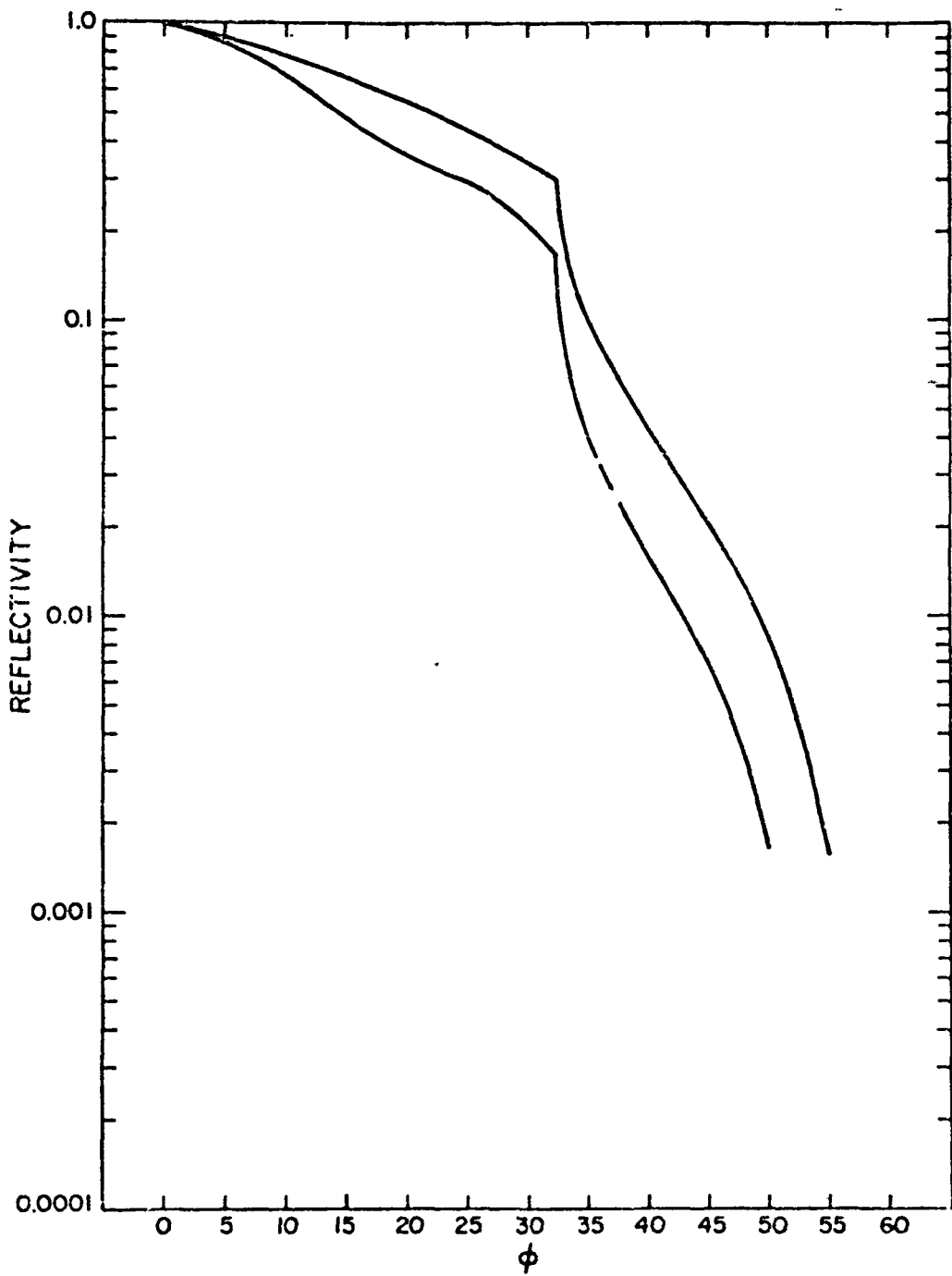


Figure 6-6. $\theta = 20^\circ$, $\lambda = 5320 \text{ \AA}$.

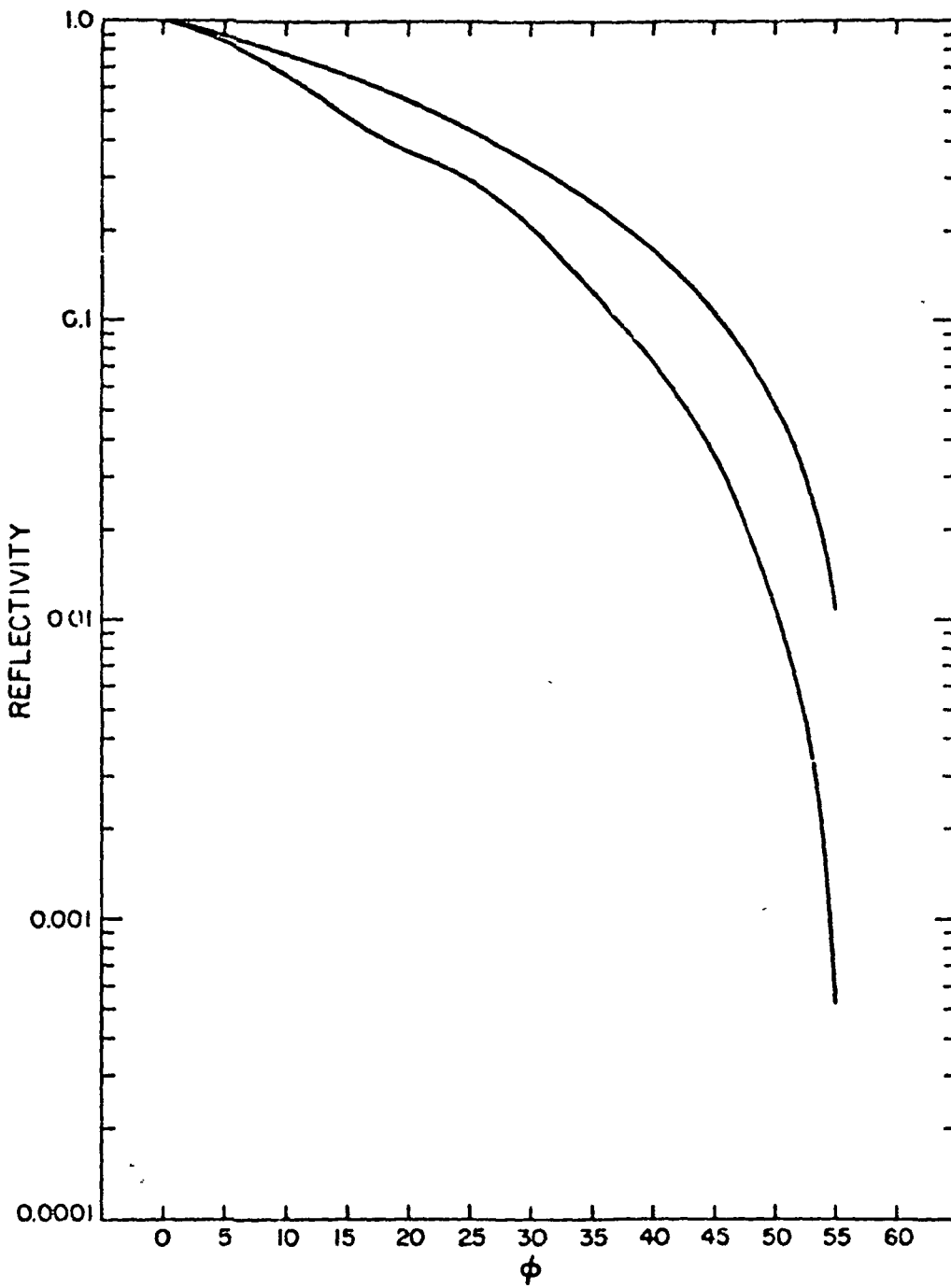


Figure 6-7. $\theta = 30^\circ$, $\lambda = 5320 \text{ \AA}$.

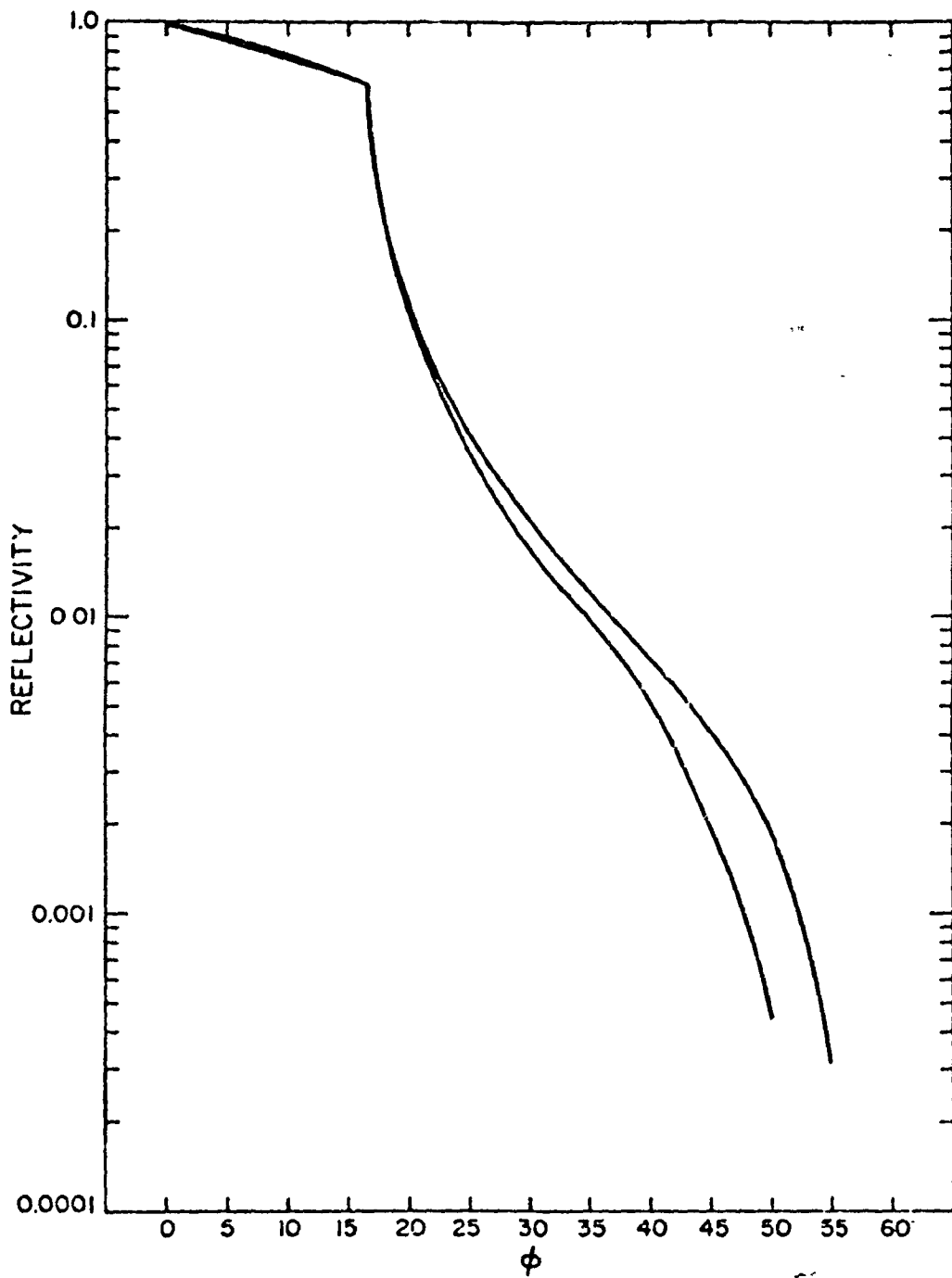


Figure G-8. $\theta = -30^\circ$, $\lambda = 6943 \text{ \AA}$.

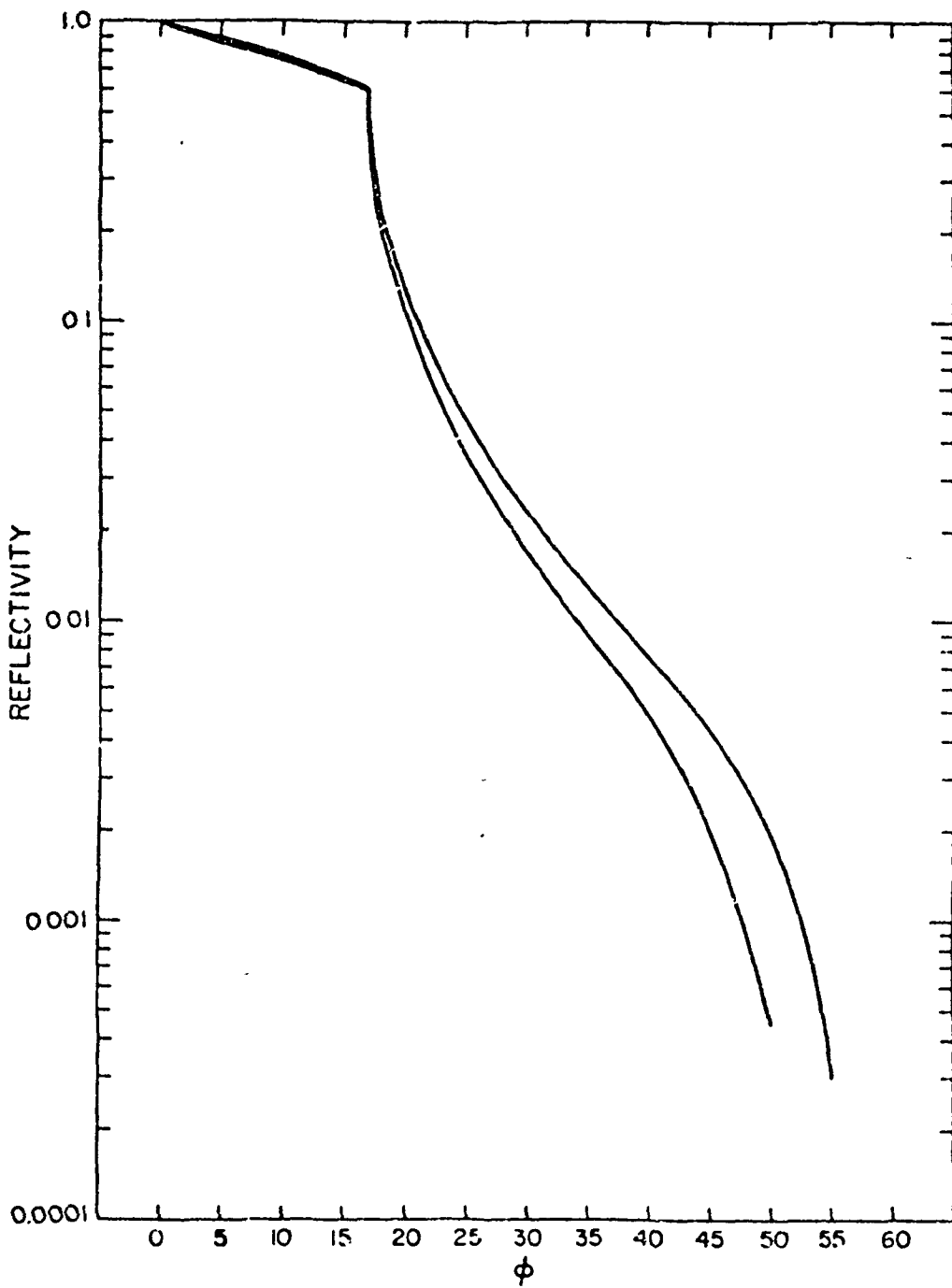


Figure G-9. $\theta = -20^\circ$, $\lambda = 6943 \text{ \AA}$.

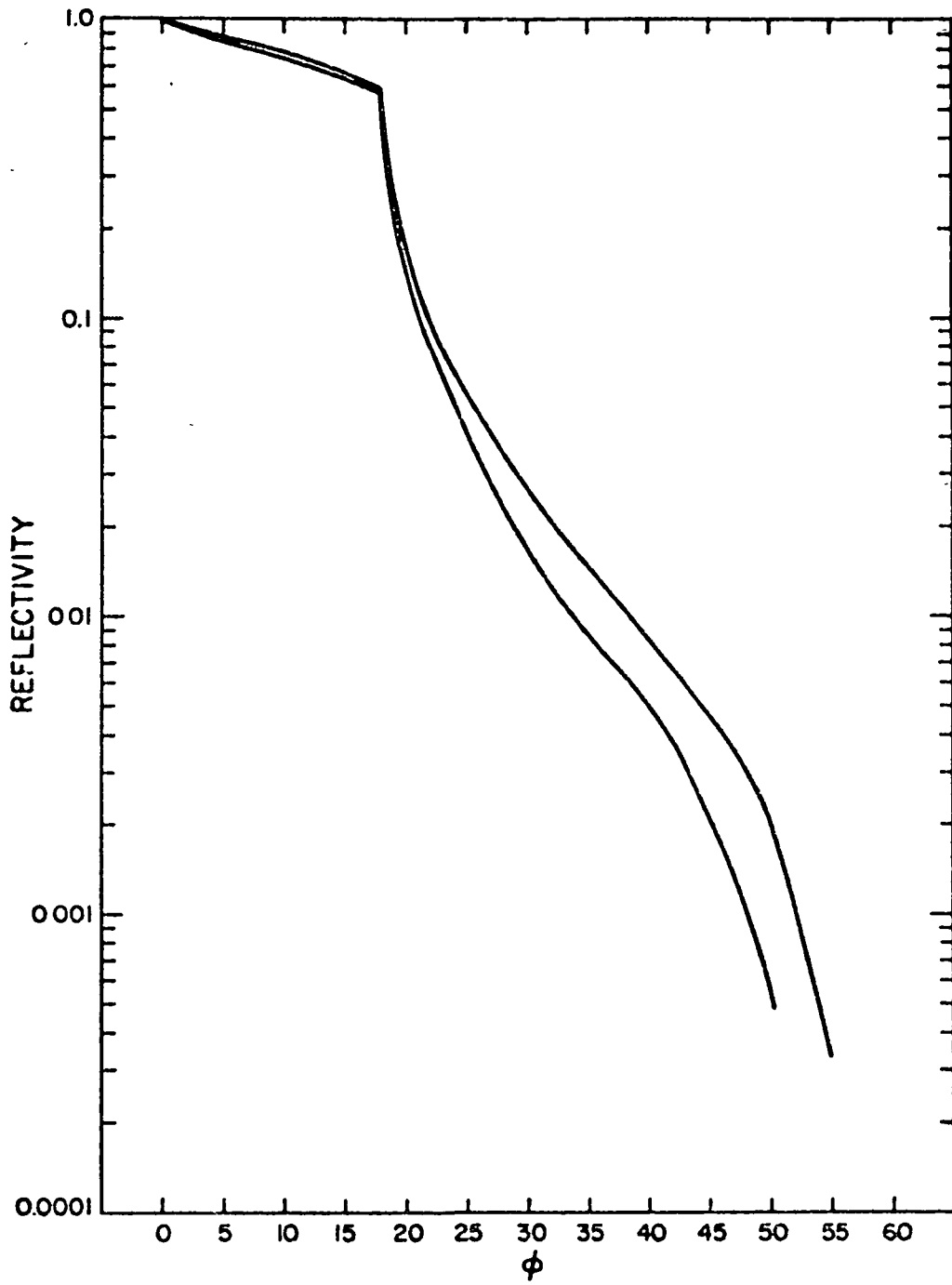


Figure G-10. $\theta = -10^\circ$, $\lambda = 6943 \text{ \AA}$.

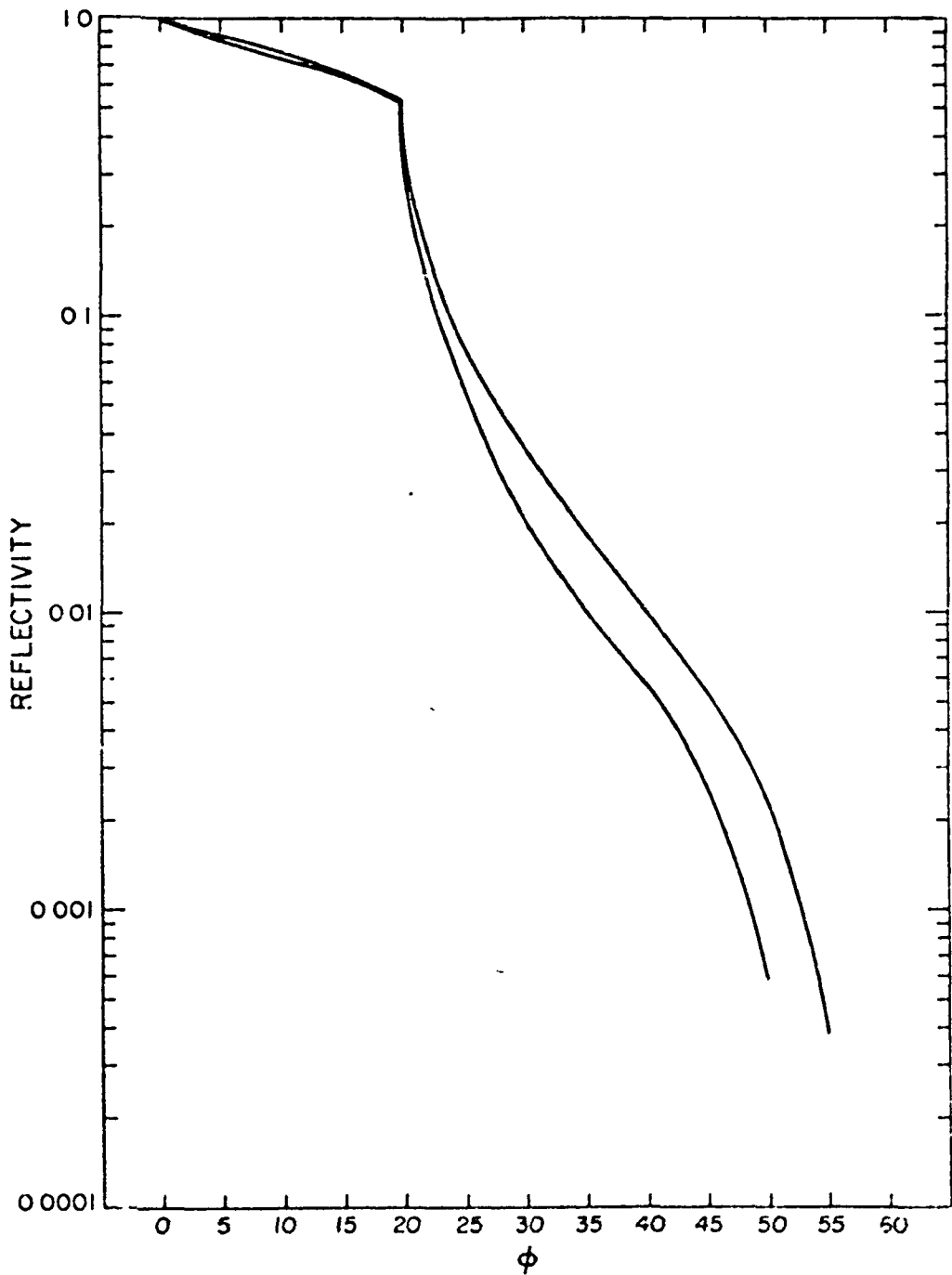


Figure 6-11. $\theta = 0^\circ$, $\lambda = 6943 \text{ \AA}$.

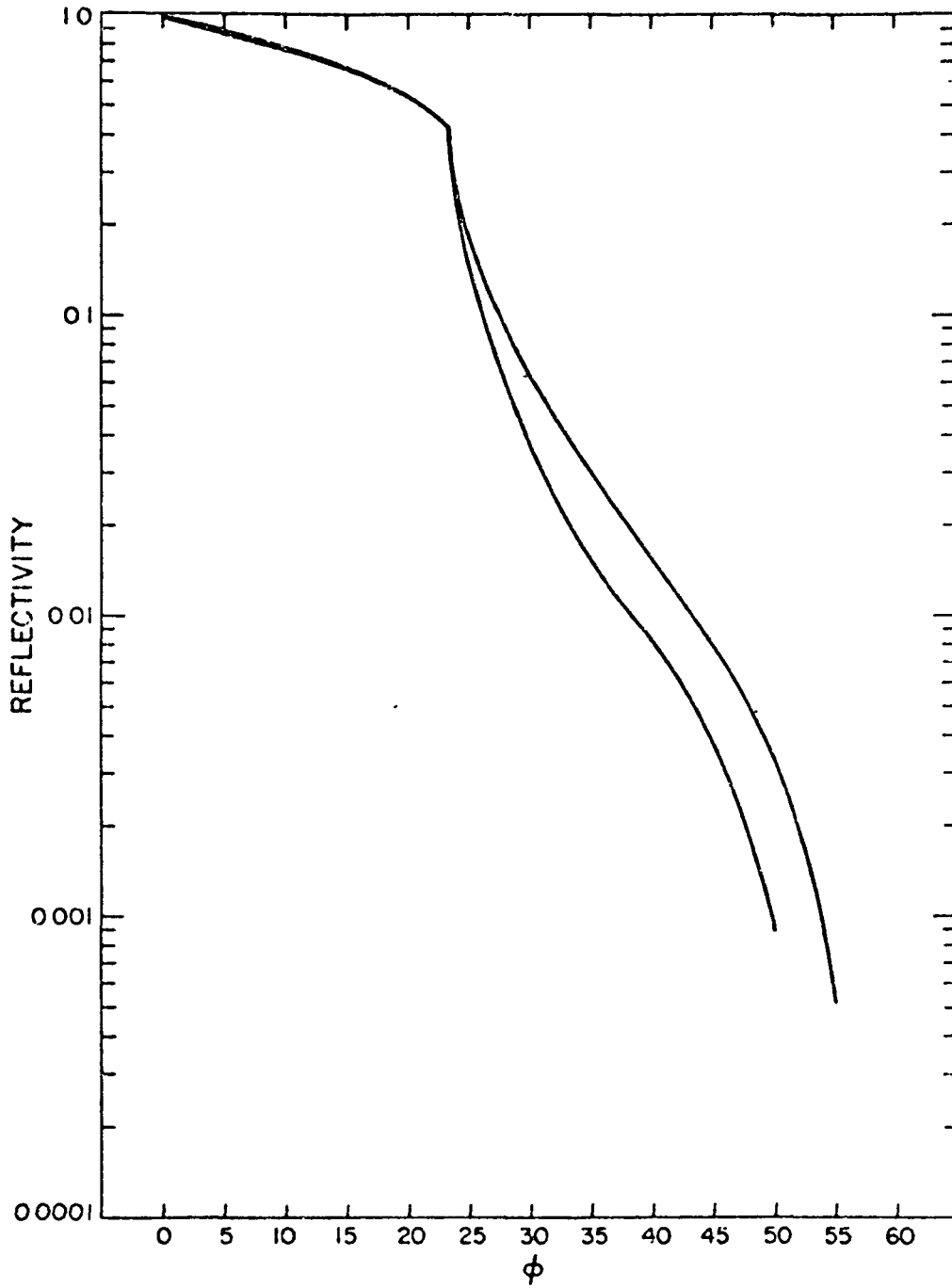


Figure 6-12. $\theta = 10^\circ$, $\lambda = 6943 \text{ \AA}$.

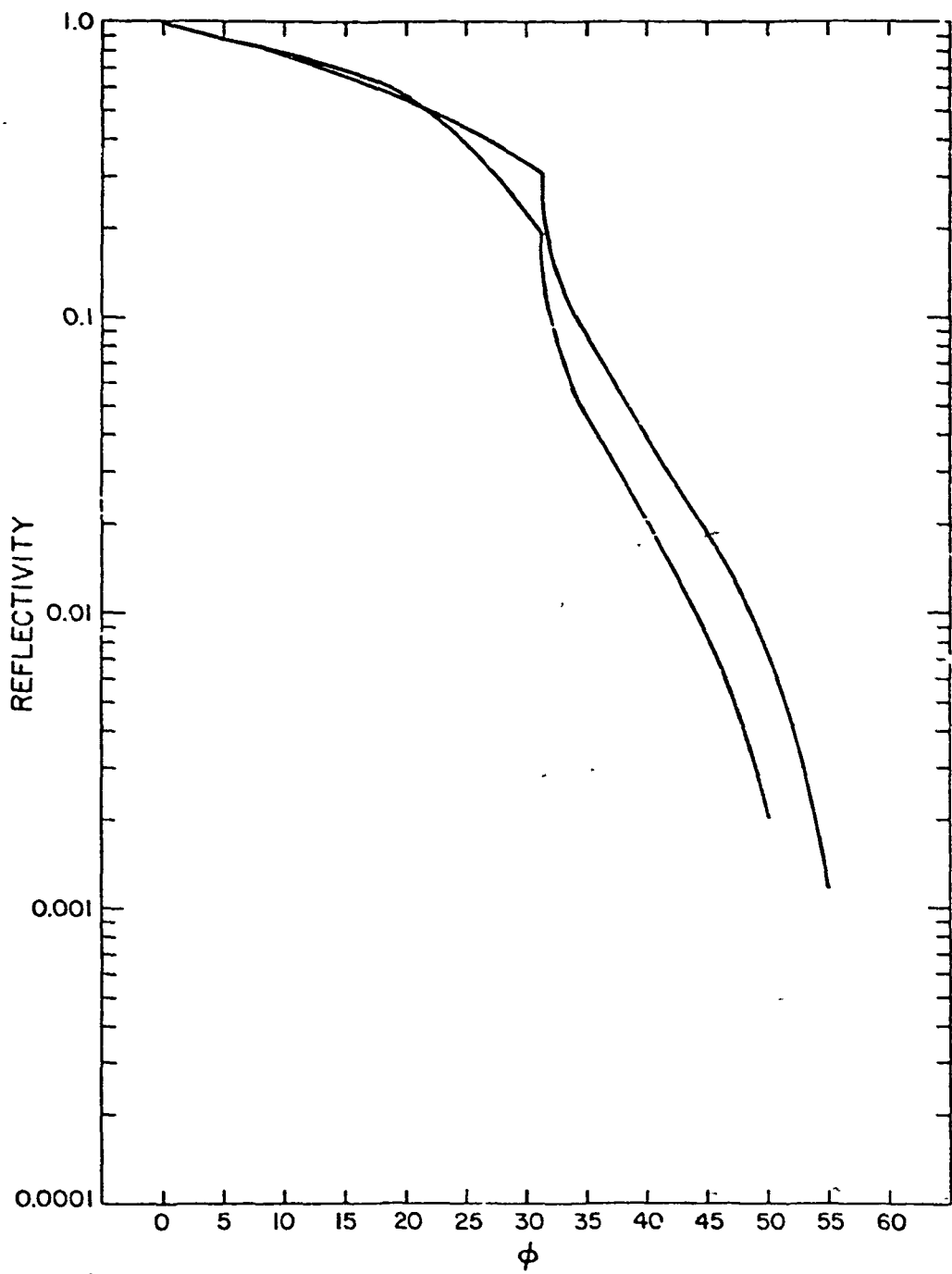


Figure 6-13. $\theta = 20^\circ$, $\lambda = 6943 \text{ \AA}$.

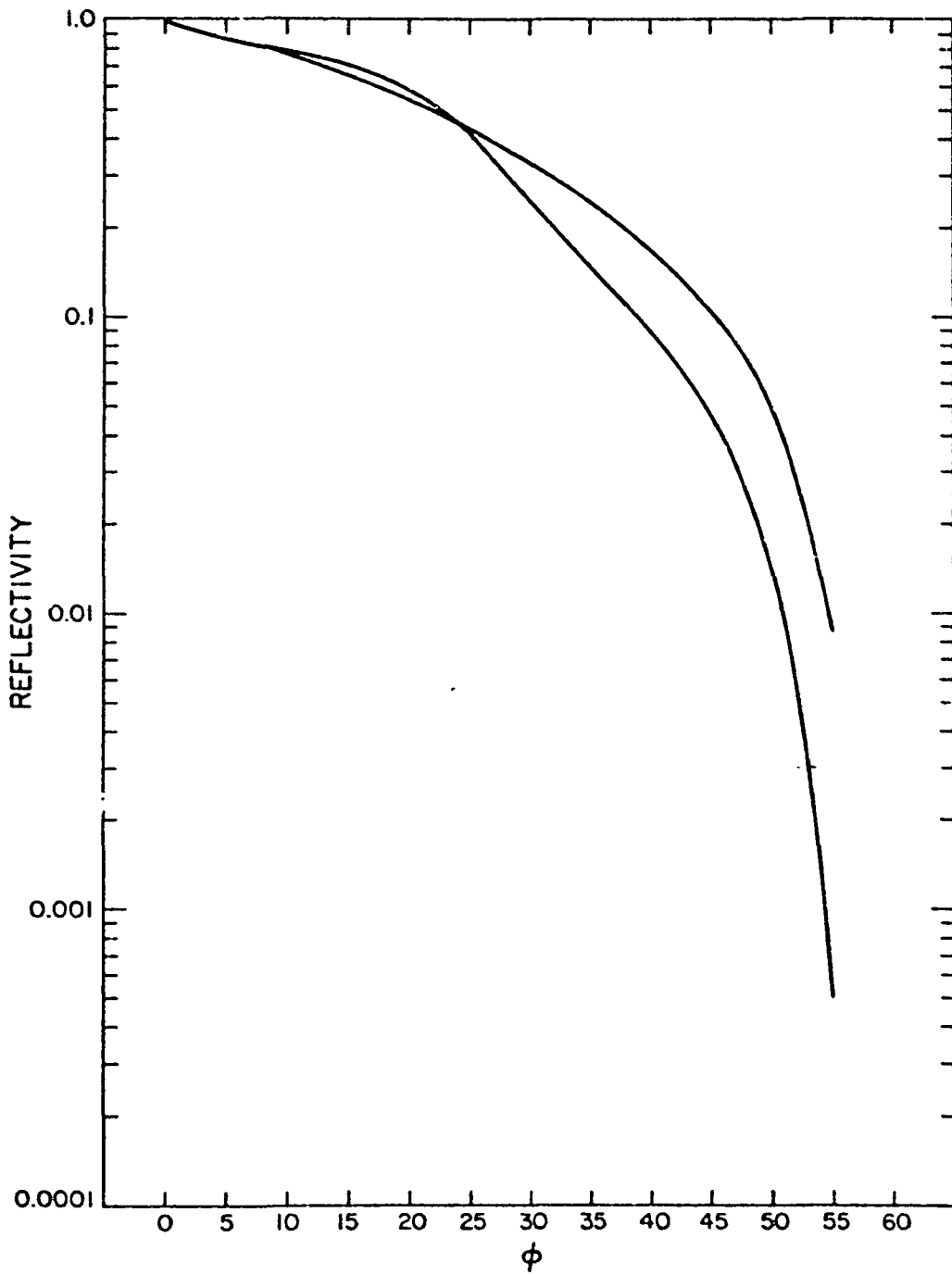


Figure 6-14. $\theta = 30^\circ$, $\lambda = 6943 \text{ \AA}$.

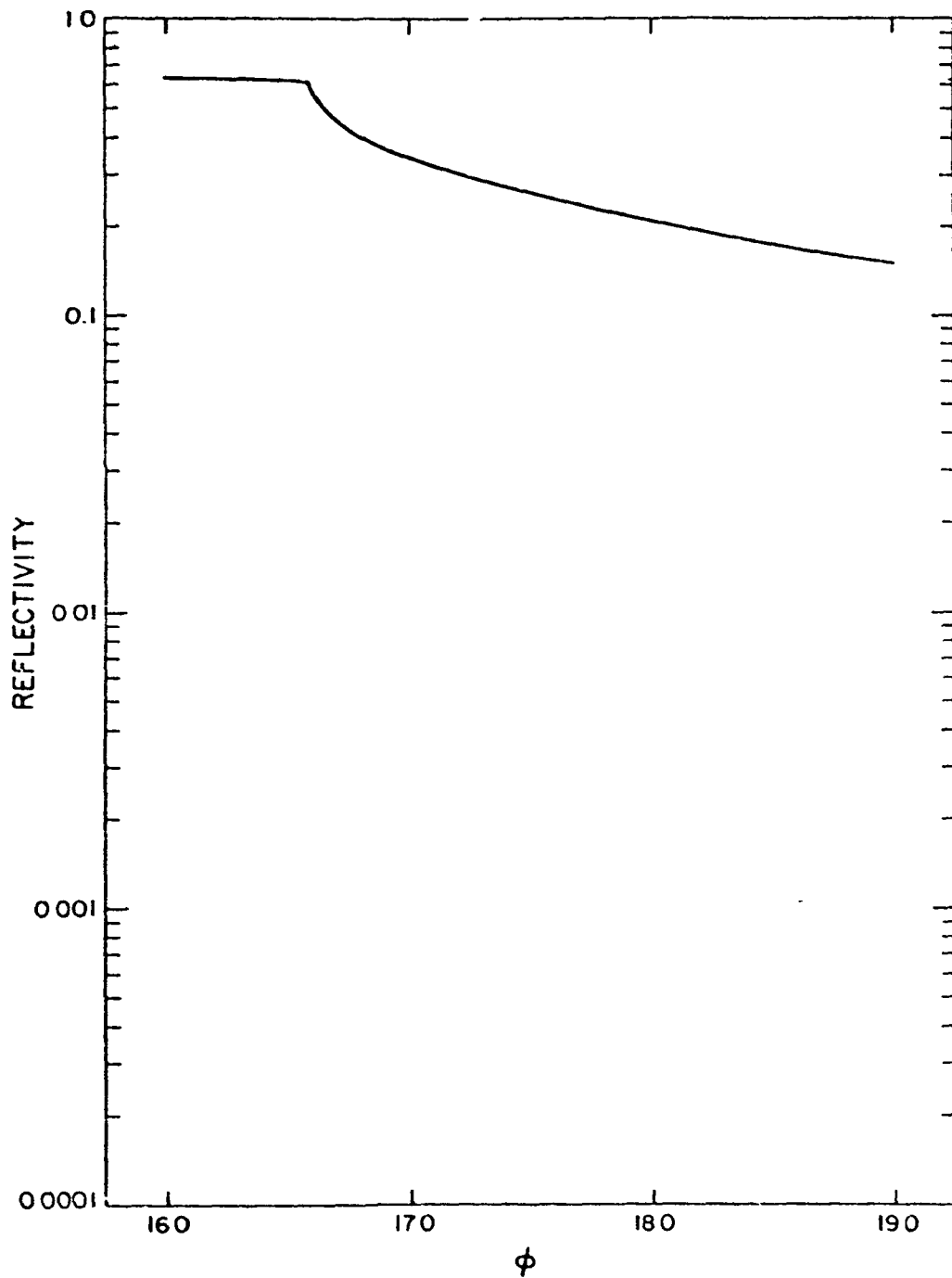


Figure 6-15. Total reflectivity for a Lageos optical cube corner in the vicinity of the cutoff for total internal reflection ($\theta = -30^\circ$, $\lambda = 6913 \text{ \AA}$).

7. VARIATION OF TRANSFER FUNCTION WITH SATELLITE ORIENTATION

The surface of the Lageos satellite is covered as uniformly as possible with cube corners to make the reflecting properties nearly independent of satellite orientation. Four of the cube corner locations have germanium reflectors for use by infrared lasers. Replacing an optical cube with a germanium cube, which is opaque to visible light, reduces the range correction by about 1.6 to 1.7 mm for a beam incident perpendicular to the face of the cube corner. The change in range was calculated by using the reflectivity curves for 5320 Å, with a 0.2-nsec incident pulse, and by computing the range correction for centroid, half-area, half-maximum, and peak detection methods.

A set of 138 sampling points was distributed over the surface of the sphere to study the variation of the transfer function with satellite orientation. The reflectivity curves for 5320 and 6943 Å were used to compute the reflectivity (in equivalent number of cube corners) and centroid range correction at each point. The rms variation of the centroid range correction is 0.85 mm and the variation of the reflected energy is about 6 or 7% over all satellite orientations. The difference between the maximum and minimum range corrections is 4.5 mm. The average range correction at each latitude has also been computed to look for systematic effects. Except at the north pole where there is an infrared cube corner, the average range corrections at all latitudes are contained within a 1-mm interval. The variation of the transfer function at points other than the location of germanium reflectors is due mainly to cube corners going in and out of total internal reflection, and, to a lesser extent, to differences in the configuration of the cube corners from different viewing angles. For the purpose of making more detailed studies of the transfer function, the sampling points have been looked at individually to find one whose properties are close to the average for all orientations. The point at $\theta = 20^\circ$, $\phi = 150^\circ$ has nearly the average reflectivity, range correction, and pulse spread, so it has been used for all the calculations in the following sections.

8. REFLECTIVITY HISTOGRAM

An important factor affecting the range accuracy obtainable from a retroreflector array is the spread in range along the line of sight of the cube corners contributing to the reflected signal. The return from Lageos comes from a spherical cap whose angular radius is the cutoff angle of the cube corners. In addition to the angle where the active reflecting area goes to zero, there is a sharp decrease in reflectivity when the incidence angle on a cube corner goes past the cutoff for total internal reflection. Table 5 below lists the apparent reflection points along the line of sight measured from the center of the satellite for three cases: the earliest possible reflection point (a cube corner whose face is normal to the incident beam); the earliest point where a cube corner can lose total internal reflection; and the last possible reflection point where the active reflecting area goes to zero. The apparent reflection point as a function of the angle ϕ between the incident beam and the normal to the front face of the cube corner is given by the expression

$$R \cos \phi - l \sqrt{n^2 - \sin^2 \phi} ,$$

where

R = the distance from the center of the satellite to the front face of the cube corner (29.807 cm),

ϕ = the incidence angle on the cube corner,

l = the length of the cube corner (2.7838 cm),

n = the index of refraction.

The cutoff angles (ϕ) for the cases listed are from Table 3 in Section 6.

The total range spread is a little over 12 cm. Total internal reflection is guaranteed for a little more than the first centimeter. Since the cube corners are spaced about 10° from each other on the surface, a beam incident in the center of a square of reflectors could be up to about 7° from the nearest cube corner. The apparent reflection point for $\phi = 7^\circ$ and $n = 1.461$ is 0.2553 m. Therefore, the maximum variation of the earliest reflection point is about 2 mm.

RESEARCH PHOTO BANK NOT FILMED

Table 5. Apparent reflection points for various incidence angles.

ϕ	λ	n	Apparent reflection point (m)	Description
0	6943	1.455	0.2576	Earliest reflection point
0	5320	1.461	0.2574	Earliest reflection point
16°595	6943	1.455	0.2459	Earliest T, I. R. cutoff
16°998	5320	1.461	0.2452	Earliest T. I. R. cutoff
55°255	6943	1.455	0.13645	Latest reflection point
55°597	5320	1.461	0.13485	Latest reflection point

Figures 7(a-c), are histograms of the contribution to the reflected signal from each 1-cm interval along the line of sight starting from the earliest reflection point. The origin of the distance scale is the center of the satellite. Table 6 lists the data used to plot the histograms. The calculations were done using the reflectivity curves of Figure 6. Over half the return energy comes from the first 1-cm interval, and over 90% comes from the first 4-cm interval. The centroid of the first two histograms is at 24.25 cm, which is 1.50 cm in back of the first reflection point. The effect of loss of total internal reflection in concentrating the energy toward the earliest reflection point can be seen by comparing the second histogram with the third, which is the energy distribution that would be obtained by coating the back reflecting faces of the cube corners. The centroid, if the cubes were coated, would be at 0.2314 m, which is a little over 2.50 cm from the earliest reflection point.

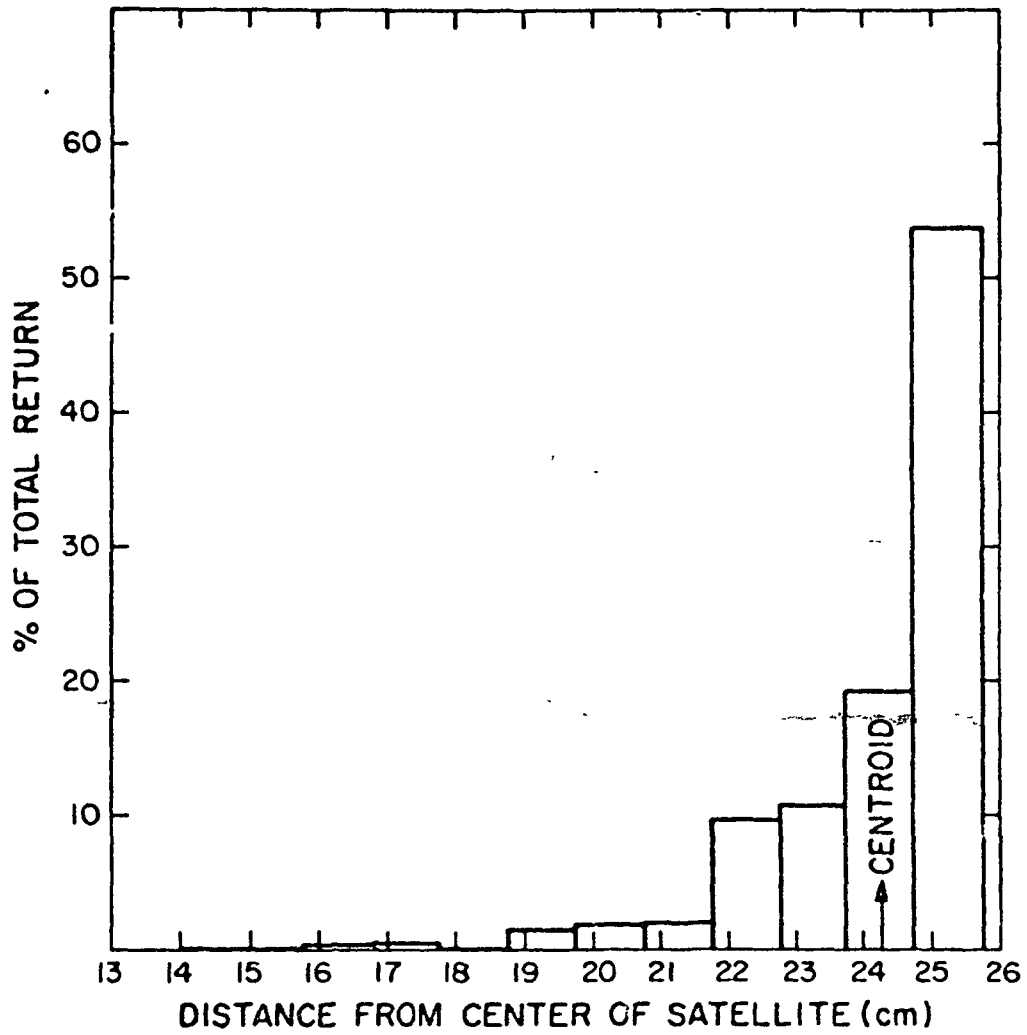


Figure 7a. Reflectivity histogram of Lageos using the reflectivity curve of Figure 6 for $\lambda = 5320 \text{ \AA}$ (uncoated cube corners).

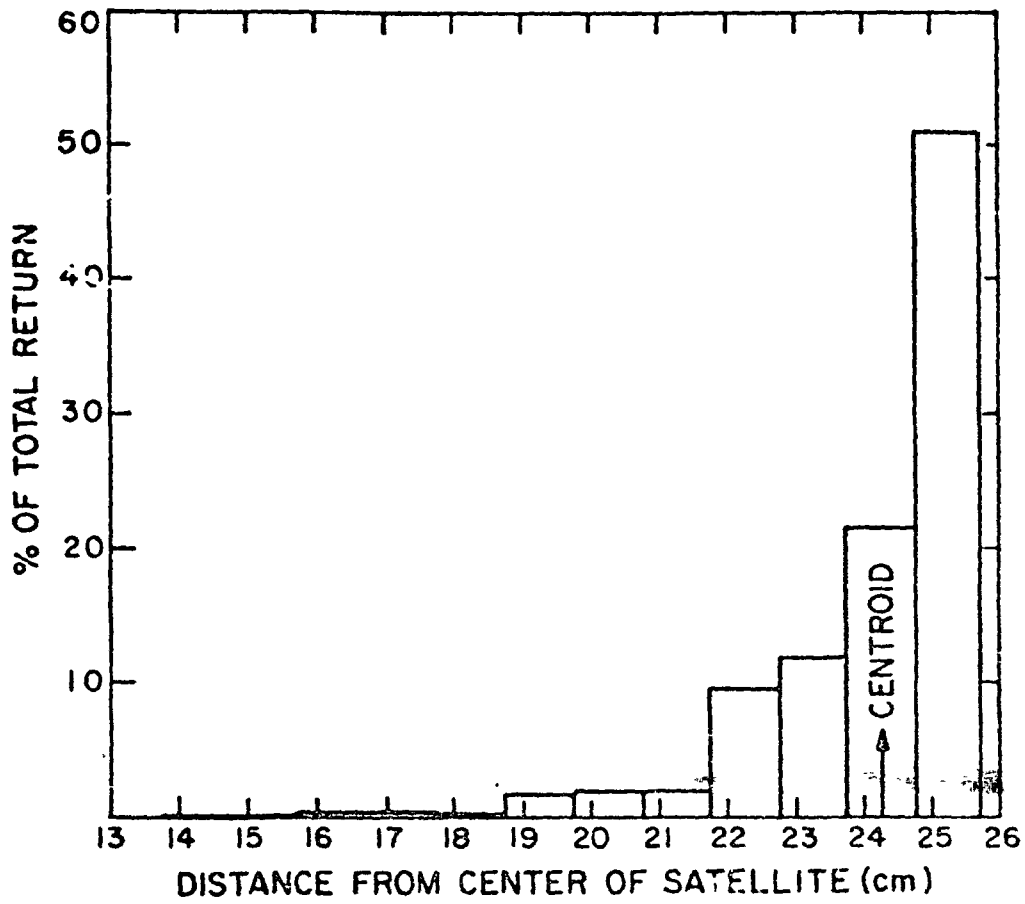


Figure 7b. Reflectivity histogram of LAGEOS using the reflectivity curve of Figure 6 for $\lambda = 6943 \text{ \AA}$ (uncoated cube corners).

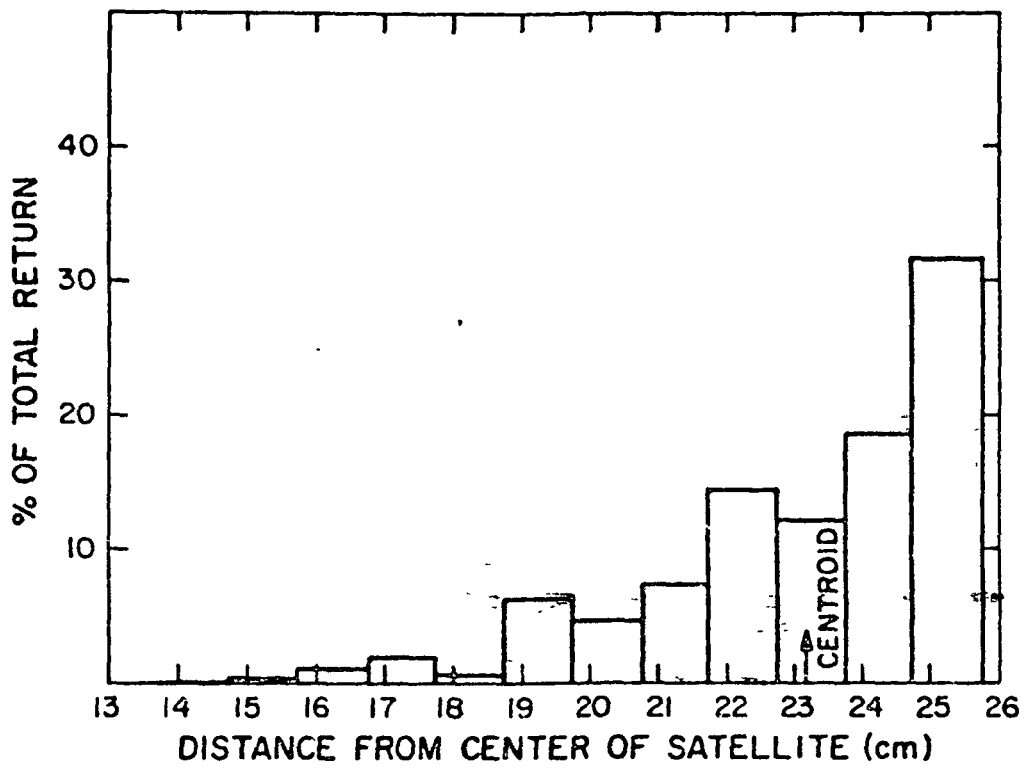


Figure 7c. Reflectivity histogram of Lageos using the reflectivity curve for cube corners with reflective coatings on the back faces ($\lambda = 6943 \text{ \AA}$).

Table 6a. Percentage of total return in each 1-cm interval starting from the earliest apparent reflection point ($\lambda = 5320$, uncoated cube corners).

Interval	% of total return	Cumulative %
1	53.89	53.89
2	19.35	73.24
3	10.76	84.00
4	9.72	93.72
5	2.01	95.73
6	1.88	97.60
7	1.57	99.17
8	0.07	99.24
9	0.35	99.59
10	0.31	99.90
11	0.09	99.99
12	0.01	100.00

Table 6b. Percentage of total return in each 1-cm interval starting from the earliest apparent reflection point ($\lambda = 6943$, uncoated cube corners).

Interval	% of total return	Cumulative %
1	51.10	51.10
2	21.57	72.67
3	11.70	84.37
4	9.45	93.82
5	1.95	95.77
6	1.85	97.62
7	1.57	99.19
8	0.06	99.26
9	0.34	99.60
10	0.30	99.90
11	0.09	99.99
12	0.01	100.00

Table 6c. Percentage of total return in each 1-cm interval starting from the earliest apparent reflection point ($\lambda = 6943$, coated cube corners).

Interval	% of total return	Cumulative %
1	31.86	31.86
2	18.77	50.63
3	12.29	62.91
4	14.62	77.54
5	7.32	84.86
6	4.73	89.59
7	6.39	95.97
8	0.69	96.66
9	1.93	98.59
10	1.02	99.61
11	0.30	99.91
12	0.08	100.00

9. ARRAY REFLECTIVITY

This section presents information on the reflectivity of the Lageos array that can be used to estimate signal strengths by use of the formula given in Section 5. The array reflectivity is given by the cross section, which is the product of the reflecting area and the gain. In computing the diffraction pattern of the array, it is essentially the cross section that is computed. The gain can be computed by dividing the cross section by the reflecting area, which must be determined separately. The reflecting area can be computed by multiplying the area of one cube corner (11.4009 cm^2) by the equivalent number of cube corners, which can be obtained using a reflectivity curve normalized to unity at normal incidence. The total reflected energy is equivalent to 12.60 cube corners at $\lambda = 5320 \text{ \AA}$ and 12.33 cube corners at $\lambda = 6943$. Multiplying these by the area of one cube gives 0.014361 and 0.014052 m^2 at 5320 and 6943 \AA , respectively. These are the areas to be used with the gain matrices of this section for computing signal strength. The effective number of cube corners can also be computed from the reflectivity curves in Section 6. The average effective number of cube corners over all orientations using these curves are 9.88 and 12.21 at 5320 and 6943 \AA , respectively. Multiplying these values by the area and gain of one cube corner at normal incidence gives cross sections of $1.198 \times 10^6 \text{ m}^2$ and $0.958 \times 10^6 \text{ m}^2$ at 5320 and 6943 \AA . (In standard units of gain and cross section, $15 \times 10^6 \text{ m}^2$ and $12 \times 10^6 \text{ m}^2$ are obtained, respectively, because of the factor of 4π in the standard definition.)

The gain matrix of the Lageos array has been computed for 5320 and 6943 \AA , with dihedral angle offsets of 0.75, 1.25, and 1.75 arcsec, and linear and circular polarization of the incident beam. In addition, an equal mixture of 0.75-, 1.25-, and 1.75-arcsec offsets has been used in an attempt to simulate the mixture of offsets present in the actual cube corners. The gain matrices are given in Table 7. The angles θ_1 and θ_2 , in microradians, are defined in Figure 8. The angle θ_2 is in the direction of decreasing ϕ in the plane containing the Z axis and the direction toward the illuminating laser (the vector \vec{V}). The angle θ_1 is normal to the plane in the direction of $\hat{Z} \times \vec{V}$.

PRECEDING PAGE LINK NOT FILMED

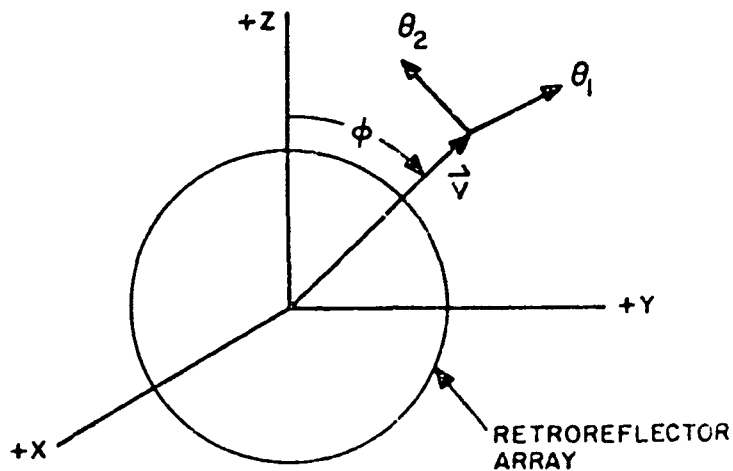


Figure 8. Diffraction-pattern coordinate system.

Table 8 shows how the array gain function varies with velocity aberration. The first column is the magnitude of the velocity aberration in microradians, and the second is the array gain function in units of 10^7 . In the computer-plotted graph, the gain function increases to the right and the velocity aberration, down the page. The gain function is the average value around a circle in the far field with radius equal to the velocity aberration. The second part of each table gives the root-mean-square (rms) variation of the gain around the circle.

Figure 9 consists of contour plots of the gain-function matrices given in Table 7. Circles have been drawn with radii of 32 and 11 μrad to mark the minimum and maximum values of velocity aberration. The contour levels plotted are 8, 1, 2, and 1×10^6 . The position of peaks in the pattern is indicated by asterisks. The contour plots for linearly polarized illumination show an asymmetry consisting of dumbbell-shaped contours aligned with the electric vector of the incident illumination. At 35 μrad from the center of the pattern, the intensity in the bright lobes is about a factor of 2^{1/2} higher than at points 90° away from the bright lobes. The asymmetry disappears if circularly polarized illumination is used. Test runs show that the asymmetry also disappears if there is no dihedral angle offset or if the back faces have metal coatings.

Table 7-2 Linear polarization

θ ₂	DIHEDRAL ANGLE 1.25		WAVELENGTH 5320		GAIN FUNCTION (1.E+7)																	
	1.08	1.51	2.04	3.02	4.06	4.34	3.98	3.44	3.01	2.75	2.51	1.92	1.43	1.07	0.80	0.69						
50	.83	1.03	1.45	2.07	2.85	3.74	4.78	5.87	6.68	6.98	6.70	6.16	5.27	4.56	4.22	3.86	3.17	2.33	1.63	1.07	.80	
45	.78	1.06	1.44	2.07	2.85	3.74	4.78	5.87	6.68	6.98	6.70	6.16	5.27	4.56	4.22	3.86	3.17	2.33	1.63	1.07	.77	
40	1.51	1.99	2.63	3.49	4.71	6.13	8.48	10.37	11.56	11.87	11.52	10.88	10.05	9.00	7.91	6.85	5.64	4.24	2.91	2.27	1.66	
35	1.90	2.58	3.42	4.53	5.89	7.57	9.52	11.43	12.80	13.23	12.77	11.67	10.35	9.02	7.95	6.89	5.64	4.24	2.91	2.27	1.66	
30	2.38	3.21	4.27	5.52	6.88	7.98	9.90	12.25	14.74	15.22	14.93	13.79	12.57	11.36	9.89	8.10	6.85	5.67	4.22	3.22	2.43	
25	2.81	3.74	4.89	5.98	6.61	7.12	9.70	12.01	12.94	13.85	14.59	13.76	12.16	11.02	9.70	8.41	7.09	6.01	4.68	3.83	2.92	
20	3.15	4.09	5.14	5.96	6.17	7.12	9.70	12.01	12.94	13.85	14.59	13.76	12.16	11.02	9.70	8.41	7.09	6.01	4.68	3.83	2.92	
15	3.30	4.19	5.14	5.76	5.80	6.78	8.31	9.37	8.88	10.27	11.96	10.68	8.54	8.42	8.60	7.49	6.92	6.31	5.43	4.58	3.51	
10	3.37	4.25	5.09	5.47	5.35	6.12	7.13	6.21	5.92	6.68	12.84	10.07	5.91	5.91	7.44	7.04	6.55	5.99	5.04	4.51	3.57	
5	3.45	4.30	5.15	5.28	5.02	5.64	6.07	4.64	5.06	10.48	14.34	10.59	5.44	4.84	6.70	6.55	5.99	5.36	5.23	4.51	3.66	
0	3.40	4.41	5.27	5.45	5.34	6.17	6.80	5.76	5.87	12.88	16.98	12.88	6.11	6.08	7.05	6.24	5.55	5.35	5.23	4.58	3.80	
-5	3.19	4.23	5.30	5.89	6.19	7.26	8.57	8.58	8.66	10.66	12.14	10.91	9.53	9.49	8.59	6.50	5.34	5.31	5.17	4.57	3.99	
-10	3.02	4.01	5.23	6.30	7.06	8.07	9.47	10.74	12.13	13.89	14.77	14.27	13.59	12.59	10.51	7.54	5.77	5.32	4.84	4.16	3.44	
-15	2.92	3.82	4.96	6.28	7.50	8.50	9.55	11.15	13.51	15.80	16.63	15.94	14.77	13.15	10.64	8.11	6.46	5.42	4.82	4.22	3.42	
-20	2.62	3.43	4.36	5.58	7.06	8.42	9.47	10.74	12.47	14.55	15.19	14.52	13.41	12.15	10.49	8.43	6.88	5.24	4.80	2.78	2.09	
-25	2.04	2.74	3.53	4.50	5.67	7.50	9.00	10.29	11.40	12.73	13.19	12.67	12.14	11.14	9.78	8.15	6.49	4.90	3.49	2.43	1.75	
-30	1.42	2.04	2.76	3.58	4.64	6.07	7.60	9.24	10.55	11.51	11.96	11.79	11.02	9.75	8.21	6.49	4.76	4.17	3.07	2.15	1.47	
-35	1.00	1.47	2.10	2.83	3.68	4.69	5.90	7.78	8.63	9.64	10.07	9.80	8.87	7.53	6.13	4.94	3.97	3.13	2.37	1.70	1.16	
-40	.77	1.09	1.49	2.02	2.70	3.43	4.20	5.13	6.16	6.96	7.24	6.91	6.11	5.12	4.19	3.38	2.67	2.06	1.60	1.22	.92	
-45	.61	.81	1.03	1.34	1.79	2.31	2.85	3.40	3.99	4.43	4.54	4.29	3.80	3.24	2.72	2.22	1.73	1.33	1.08	.90	.76	
-50																						
-55																						
-60																						
-65																						
-70																						
-75																						
-80																						
-85																						
-90																						

Table 7-3. Linear polarization.

θ ₂	DIPEDRAL ANGLE 1.75 WAVELENGTH 5320																					
	GAIN FUNCTION (1.E+7)																					
	-50	-45	-40	-35	-30	-25	-20	-15	-10	-5	0	5	10	15	20	25	30	35	40	45	50	
50	1.13	1.52	2.14	3.05	4.13	5.14	5.95	6.57	6.97	7.07	6.87	6.44	5.95	5.55	5.18	4.86	4.66	4.52	4.43	4.39	4.37	4.38
45	1.49	2.04	2.92	3.99	5.16	6.30	7.35	8.25	8.79	8.84	8.44	7.74	7.02	6.42	5.90	5.49	5.17	4.90	4.79	4.73	4.72	4.73
40	2.07	2.80	3.70	4.71	5.83	7.09	8.43	9.59	10.21	10.19	9.69	8.90	8.06	7.55	7.49	7.45	7.40	7.39	7.39	7.39	7.39	7.39
35	2.77	3.78	4.76	5.72	6.78	7.96	9.25	10.54	11.71	12.65	13.26	13.54	13.48	13.17	12.61	11.81	10.78	9.54	8.11	6.51	4.77	2.91
30	3.57	4.90	6.55	8.44	10.58	12.98	15.64	18.46	21.34	24.18	26.88	29.35	31.50	33.24	34.58	35.52	36.06	36.30	36.24	35.88	35.22	34.27
25	3.81	4.90	6.55	8.44	10.58	12.98	15.64	18.46	21.34	24.18	26.88	29.35	31.50	33.24	34.58	35.52	36.06	36.30	36.24	35.88	35.22	34.27
20	4.16	4.71	5.17	5.73	6.30	6.88	7.47	8.07	8.67	9.27	9.87	10.47	11.07	11.67	12.27	12.87	13.47	14.07	14.67	15.27	15.87	16.47
15	4.40	4.88	5.16	5.47	5.78	6.09	6.40	6.71	7.02	7.33	7.64	7.95	8.26	8.57	8.88	9.19	9.50	9.81	10.12	10.43	10.74	11.05
10	4.43	4.80	5.04	5.21	5.41	5.61	5.81	6.01	6.21	6.41	6.61	6.81	7.01	7.21	7.41	7.61	7.81	8.01	8.21	8.41	8.61	8.81
5	4.36	4.75	5.05	5.03	4.93	4.73	4.43	4.03	3.53	3.03	2.53	2.03	1.53	1.03	0.53	0.03	0.03	0.03	0.03	0.03	0.03	0.03
0	4.27	4.79	5.05	5.03	4.93	4.73	4.43	4.03	3.53	3.03	2.53	2.03	1.53	1.03	0.53	0.03	0.03	0.03	0.03	0.03	0.03	0.03
-5	4.21	4.77	5.17	5.02	4.51	4.08	3.65	3.21	2.76	2.31	1.86	1.41	0.96	0.51	0.06	0.06	0.06	0.06	0.06	0.06	0.06	0.06
-10	4.16	4.67	5.07	5.23	5.07	4.96	4.85	4.75	4.65	4.55	4.45	4.35	4.25	4.15	4.05	3.95	3.85	3.75	3.65	3.55	3.45	3.35
-15	4.10	4.54	5.11	5.54	5.52	5.50	5.50	5.52	5.51	5.49	5.47	5.45	5.43	5.41	5.39	5.37	5.35	5.33	5.31	5.29	5.27	5.25
-20	4.14	4.74	5.28	5.82	6.23	6.45	6.55	6.55	6.55	6.55	6.55	6.55	6.55	6.55	6.55	6.55	6.55	6.55	6.55	6.55	6.55	6.55
-25	3.93	4.75	5.38	5.81	6.51	6.92	7.05	7.05	7.05	7.05	7.05	7.05	7.05	7.05	7.05	7.05	7.05	7.05	7.05	7.05	7.05	7.05
-30	3.83	4.75	5.25	5.85	6.50	7.18	7.62	7.76	7.84	7.87	7.84	7.76	7.62	7.48	7.33	7.18	7.03	6.88	6.73	6.58	6.43	6.28
-35	3.69	4.72	5.25	5.88	6.50	7.18	7.76	8.11	8.27	8.33	8.33	8.27	8.11	7.96	7.81	7.66	7.51	7.36	7.21	7.06	6.91	6.76
-40	2.92	3.93	4.93	5.14	6.06	6.79	7.40	8.04	8.78	9.50	10.16	10.72	11.28	11.84	12.40	12.96	13.52	14.08	14.64	15.20	15.76	16.32
-45	1.92	2.93	3.15	4.13	5.12	5.97	6.62	7.20	7.82	8.40	8.76	8.79	8.45	7.81	6.96	5.96	4.90	3.89	2.87	1.82	0.77	0.78
-50	1.13	1.68	2.34	3.07	3.88	4.71	5.43	5.98	6.41	6.76	6.99	7.04	6.85	6.40	5.70	4.78	3.77	2.86	1.94	1.04	0.14	0.14

Figure 7-4 Linear polariz. horn, mixed dihedral angles

θ_2	DIPEDRAL ANGLE $\sqrt{33}$		WAVELENGTH 9320	
	0	180	0	180
50	1.03	1.31	3.02	3.43
45	1.01	1.37	4.38	5.23
40	1.43	2.97	5.98	7.31
35	2.01	3.69	7.49	9.04
30	2.46	3.73	8.77	10.49
25	2.72	4.33	9.57	11.99
20	2.94	4.75	9.85	12.72
15	3.10	5.52	8.65	11.37
10	3.13	5.89	7.39	8.36
5	3.14	5.80	6.32	5.74
0	3.23	5.54	5.95	4.84
-5	3.25	5.84	6.15	4.84
-10	3.14	5.80	6.49	5.80
-15	3.05	5.71	6.89	6.71
-20	2.96	5.59	7.19	7.05
-25	2.85	5.24	7.60	7.91
-30	2.66	4.31	7.01	7.28
-35	1.47	1.94	7.14	7.14
-40	1.08	1.49	5.97	5.97
-45	0.90	1.21	4.13	4.13
-50	0.78	1.00	3.16	3.16
50	1.83	1.71	2.52	3.02
45	1.75	2.29	3.59	4.38
40	2.39	3.68	4.67	5.98
35	3.08	4.52	5.80	7.49
30	3.73	5.50	6.82	8.77
25	4.33	6.12	7.39	9.57
20	4.75	6.90	8.65	11.37
15	5.52	5.35	6.01	8.65
10	5.89	5.13	5.62	7.39
5	5.80	5.16	5.64	6.32
0	5.54	5.03	5.24	5.95
-5	5.84	4.95	5.38	6.49
-10	5.80	5.02	5.61	6.89
-15	5.71	5.25	6.03	7.19
-20	5.59	5.38	6.49	7.60
-25	5.24	5.03	6.40	7.01
-30	4.31	4.31	4.92	4.92
-35	2.71	3.67	4.78	4.78
-40	2.18	3.11	4.13	4.13
-45	1.70	2.43	3.34	3.34
-50	1.30	1.79	2.48	2.48
50	1.03	1.36	7.51	8.84
45	1.32	1.87	9.60	11.26
40	1.54	2.33	11.84	14.13
35	1.80	2.68	14.13	17.01
30	2.23	3.03	16.42	19.88
25	2.81	3.49	18.71	22.75
20	3.07	4.06	21.00	25.62
15	3.07	4.60	23.29	28.50
10	3.21	4.90	25.58	31.37
5	3.25	4.92	27.87	34.25
0	3.30	4.82	30.16	37.12
-5	3.38	4.78	32.45	40.00
-10	3.37	4.68	34.74	42.87
-15	3.11	4.33	37.03	45.74
-20	2.68	3.77	39.32	48.61
-25	2.04	3.00	41.61	51.48
-30	1.63	2.43	43.90	54.35
-35	1.28	1.94	46.19	57.22
-40	1.00	1.51	48.48	60.09
-45	0.81	1.12	50.77	62.96
-50	0.69	0.86	53.06	65.83

Table 7-6 Linear Polarization.

θ_2	DIRECTIONAL ANGLE		WAVELENGTH		GAIN FUNCTION (1.E+7)		WAVELENGTH		DIRECTIONAL ANGLE												
	1.25	1.25	1.25	1.25	1.25	1.25	1.25	1.25	1.25	1.25											
50	1.92	1.17	1.52	2.03	2.70	3.46	4.17	4.69	4.94	4.95	4.83	4.62	4.34	3.95	3.32	3.11	2.74	2.36	1.92	1.46	1.06
45	1.59	1.54	2.00	2.64	3.65	4.34	5.18	5.81	6.15	6.19	6.01	5.74	5.44	5.07	4.60	4.04	3.46	2.89	2.33	1.78	1.30
40	1.59	2.05	2.60	3.31	4.18	5.17	6.17	7.03	7.61	7.79	7.58	7.14	6.57	6.19	5.84	4.85	4.20	3.65	3.11	2.51	1.92
35	2.04	2.59	3.15	3.83	4.75	5.93	7.25	8.52	9.52	10.03	9.92	9.30	8.46	7.53	6.80	5.89	4.93	4.02	3.21	2.51	1.92
30	2.64	3.39	4.27	5.13	6.63	8.33	9.97	11.36	12.28	12.43	11.75	10.55	9.24	8.00	6.80	5.57	4.50	3.63	2.92	2.31	1.78
25	2.73	3.21	3.56	4.15	5.19	7.18	9.00	10.56	11.94	13.13	13.62	13.05	11.68	10.11	8.68	7.28	5.93	4.77	3.91	3.27	2.70
20	2.93	3.31	3.49	4.22	5.60	7.36	8.77	9.71	10.75	12.06	12.88	12.44	11.00	9.45	8.26	7.16	5.94	4.80	4.01	3.51	3.03
15	2.96	3.33	3.59	4.25	5.57	6.92	7.54	7.77	8.72	10.51	11.72	11.13	9.24	7.82	6.91	6.50	5.72	4.73	4.01	3.62	3.23
10	2.65	3.26	3.44	4.06	5.10	5.81	5.71	5.77	6.74	10.39	12.14	10.94	7.89	5.74	5.20	5.41	5.01	4.64	3.97	3.61	3.28
5	2.91	3.10	3.22	3.68	4.38	4.55	4.08	4.51	4.42	11.73	13.94	12.10	7.78	4.90	4.60	4.82	5.06	4.51	3.87	3.50	3.19
0	2.91	3.01	3.07	3.68	4.00	3.92	3.35	4.11	7.71	12.65	15.06	12.76	7.83	4.71	3.24	4.37	4.74	4.27	3.67	3.32	3.03
-5	2.98	3.09	3.19	3.68	4.31	4.35	3.88	4.53	7.68	11.98	14.01	11.93	7.67	4.62	4.04	4.58	4.62	4.00	3.41	3.12	2.89
-10	3.08	3.30	3.55	4.20	5.08	5.51	5.38	5.62	7.94	10.86	12.71	10.81	8.57	6.13	5.08	5.16	4.87	3.88	3.23	2.97	2.79
-15	3.12	3.53	3.94	4.46	5.71	6.58	7.06	7.73	9.23	11.04	11.94	11.06	9.57	8.51	7.68	6.48	5.38	3.97	3.19	2.90	2.70
-20	3.07	3.64	4.18	4.90	5.86	6.95	6.05	6.98	11.01	12.46	12.99	12.44	11.44	10.51	9.52	7.78	5.80	4.19	3.49	2.87	2.55
-25	2.87	3.54	4.19	4.84	5.63	6.44	6.01	6.83	11.81	13.29	13.70	13.09	12.03	10.21	9.24	7.81	5.92	4.40	3.44	2.83	2.33
-30	2.49	3.16	3.88	4.57	5.22	6.04	7.27	8.01	10.81	12.57	12.58	11.92	10.84	9.22	8.23	7.16	5.72	4.48	3.52	2.75	2.10
-35	1.98	2.55	3.26	4.00	4.69	5.41	6.36	7.64	9.02	10.00	10.19	9.66	8.81	7.97	7.16	6.25	5.24	4.26	3.37	2.58	1.89
-40	1.48	1.90	2.49	3.22	3.98	4.73	5.51	6.58	7.77	7.80	7.92	7.51	7.08	6.52	5.93	5.25	4.40	3.69	2.96	2.28	1.69
-45	1.12	1.42	1.85	2.45	3.16	3.91	4.64	5.31	5.84	6.22	6.33	6.18	5.84	5.38	4.82	4.19	3.53	2.91	2.36	1.80	1.45
-50	0.91	1.13	1.44	1.86	2.40	3.02	3.65	4.23	4.69	4.99	5.10	5.00	4.71	4.25	3.69	3.12	2.58	2.13	1.76	1.44	1.16

Table 7-7 Linear polarization

θ ₂	DIMEDRAL ANGLE 1.75 WAVELENGTH 6943																				
	GAIN FUNCTION (1.E-7)																				
	-50	-45	-40	-35	-30	-25	-20	-15	-10	-5	0	5	10	15	20	25	30	35	40	45	50
50	1.59	1.99	2.50	3.16	3.96	4.83	5.87	6.19	6.47	6.69	6.37	6.01	5.58	5.09	4.62	4.26	3.96	3.60	3.10	2.49	1.89
45	1.91	2.31	2.93	3.66	4.54	5.45	6.26	6.83	7.10	7.09	6.89	6.61	6.28	5.88	5.43	4.97	4.53	4.06	3.50	2.86	2.21
40	2.29	2.81	3.42	4.14	4.94	5.78	6.55	7.15	7.42	7.40	7.14	6.83	6.54	6.26	5.89	5.42	4.89	4.34	3.75	3.11	2.49
35	2.70	3.24	3.82	4.41	5.08	5.80	6.50	7.00	7.23	7.09	6.81	6.50	6.20	5.89	5.57	5.24	4.89	4.50	4.03	3.51	2.99
30	3.03	3.58	4.14	4.74	5.39	6.07	6.76	7.23	7.46	7.31	7.01	6.69	6.37	6.04	5.70	5.35	4.99	4.60	4.16	3.74	3.31
25	3.22	3.82	4.38	4.92	5.52	6.14	6.76	7.23	7.46	7.31	7.01	6.69	6.37	6.04	5.70	5.35	4.99	4.60	4.16	3.74	3.31
20	3.28	3.95	4.51	5.02	5.58	6.14	6.70	7.17	7.46	7.31	7.01	6.69	6.37	6.04	5.70	5.35	4.99	4.60	4.16	3.74	3.31
15	3.25	3.93	4.48	5.00	5.52	6.04	6.56	7.03	7.31	7.16	6.86	6.54	6.22	5.89	5.57	5.24	4.91	4.58	4.20	3.81	3.42
10	3.18	3.79	4.31	4.80	5.28	5.76	6.22	6.67	7.03	6.88	6.58	6.26	5.94	5.61	5.28	4.95	4.62	4.30	3.98	3.66	3.34
5	3.14	3.71	4.21	4.68	5.14	5.59	6.03	6.45	6.83	6.68	6.38	6.06	5.74	5.41	5.08	4.75	4.42	4.10	3.78	3.46	3.14
0	3.14	3.69	4.18	4.64	5.09	5.53	5.96	6.37	6.74	6.60	6.30	5.98	5.66	5.34	5.01	4.68	4.35	4.03	3.71	3.39	3.07
-5	3.20	3.73	4.21	4.66	5.10	5.53	5.95	6.35	6.72	6.58	6.28	5.96	5.64	5.32	5.00	4.67	4.34	4.02	3.70	3.38	3.06
-10	3.27	3.78	4.25	4.69	5.12	5.54	5.95	6.34	6.71	6.57	6.27	5.95	5.63	5.31	4.99	4.66	4.33	4.01	3.69	3.37	3.05
-15	3.32	3.82	4.28	4.71	5.14	5.55	5.95	6.33	6.70	6.56	6.26	5.94	5.62	5.30	4.98	4.65	4.32	4.00	3.68	3.36	3.04
-20	3.35	3.84	4.29	4.72	5.14	5.54	5.94	6.32	6.69	6.55	6.25	5.93	5.61	5.29	4.97	4.64	4.31	3.99	3.67	3.35	3.03
-25	3.29	3.78	4.23	4.66	5.08	5.49	5.89	6.27	6.64	6.50	6.20	5.88	5.56	5.24	4.92	4.59	4.26	3.94	3.62	3.30	2.98
-30	3.09	3.58	4.02	4.45	4.87	5.28	5.68	6.07	6.44	6.30	6.00	5.68	5.36	5.04	4.72	4.39	4.07	3.75	3.43	3.11	2.79
-35	2.77	3.26	3.70	4.13	4.55	4.96	5.36	5.75	6.12	6.00	5.70	5.38	5.06	4.74	4.42	4.09	3.77	3.45	3.13	2.81	2.49
-40	2.50	2.99	3.43	3.86	4.28	4.69	5.09	5.48	5.85	5.75	5.45	5.13	4.81	4.49	4.17	3.85	3.53	3.21	2.89	2.57	2.25
-45	2.08	2.57	3.01	3.44	3.87	4.29	4.70	5.10	5.49	5.40	5.10	4.78	4.46	4.14	3.82	3.50	3.18	2.86	2.54	2.22	1.90
-50	1.73	2.11	2.53	3.01	3.56	4.17	4.82	5.45	6.09	6.09	5.78	5.46	5.14	4.82	4.50	4.18	3.86	3.54	3.22	2.90	2.58

Table 7-8 Linear polarization, mixed dihedral angles

θ ₂	DIPEDRAL ANGLE 1.25		WAVELENGTH 6943		GAIN FUNCTION (1.5σ ₁)																	
	0	180	0	180	0	15	20	25	30	35	40	45	50	θ ₁								
50	1.07	1.24	1.57	1.98	2.56	3.23	3.85	4.29	4.49	4.51	4.48	4.33	4.09	3.81	3.41	3.01	2.64	2.30	2.04	1.78	1.59	1.48
45	1.39	1.67	2.05	2.59	3.32	4.11	4.81	5.28	5.46	5.44	5.26	4.93	4.53	4.06	3.66	3.26	2.90	2.57	2.27	2.00	1.78	1.64
40	1.78	2.17	2.65	3.29	4.12	5.04	5.88	6.49	6.80	6.83	6.71	6.45	6.03	5.61	5.21	4.81	4.45	4.12	3.82	3.55	3.32	3.18
35	2.21	2.68	3.16	3.84	4.77	5.94	7.12	8.09	8.76	9.02	8.87	8.47	7.93	7.53	7.13	6.73	6.37	6.04	5.73	5.45	5.20	5.05
30	2.58	3.04	3.44	4.04	5.12	6.45	8.27	10.76	11.48	11.66	11.18	10.55	9.73	9.04	8.46	7.94	7.46	7.01	6.59	6.20	5.84	5.52
25	2.82	3.20	3.54	3.94	5.20	7.02	9.63	10.76	11.51	12.55	13.04	12.59	11.98	11.26	10.56	9.96	9.47	9.01	8.59	8.20	7.84	7.52
20	2.93	3.23	3.35	3.84	5.15	6.92	9.78	10.47	11.72	12.54	12.74	12.14	11.34	10.54	9.84	9.24	8.74	8.32	7.94	7.58	7.24	6.94
15	2.92	3.22	3.33	3.81	5.09	6.81	9.53	10.47	11.72	12.54	12.74	12.14	11.34	10.54	9.84	9.24	8.74	8.32	7.94	7.58	7.24	6.94
10	2.86	3.17	3.32	3.79	4.99	6.66	9.44	10.47	11.72	12.54	12.74	12.14	11.34	10.54	9.84	9.24	8.74	8.32	7.94	7.58	7.24	6.94
5	2.74	3.03	3.29	3.76	4.93	6.52	9.27	10.47	11.72	12.54	12.74	12.14	11.34	10.54	9.84	9.24	8.74	8.32	7.94	7.58	7.24	6.94
0	2.74	3.03	3.29	3.76	4.93	6.52	9.27	10.47	11.72	12.54	12.74	12.14	11.34	10.54	9.84	9.24	8.74	8.32	7.94	7.58	7.24	6.94
-5	2.74	3.04	3.38	4.01	5.65	7.39	9.96	10.47	11.72	12.54	12.74	12.14	11.34	10.54	9.84	9.24	8.74	8.32	7.94	7.58	7.24	6.94
-10	2.73	3.14	3.67	4.52	6.46	8.50	10.77	10.47	11.72	12.54	12.74	12.14	11.34	10.54	9.84	9.24	8.74	8.32	7.94	7.58	7.24	6.94
-15	2.67	3.17	3.71	4.65	6.84	9.31	12.09	10.47	11.72	12.54	12.74	12.14	11.34	10.54	9.84	9.24	8.74	8.32	7.94	7.58	7.24	6.94
-20	2.54	3.17	3.75	4.65	6.84	9.31	12.09	10.47	11.72	12.54	12.74	12.14	11.34	10.54	9.84	9.24	8.74	8.32	7.94	7.58	7.24	6.94
-25	2.28	2.89	3.60	4.33	5.12	6.11	7.49	9.70	10.47	11.72	12.54	12.74	12.14	11.34	10.54	9.84	9.24	8.74	8.32	7.94	7.58	7.24
-30	1.91	2.44	3.17	3.94	4.73	5.58	6.63	7.84	8.90	9.38	9.12	8.38	7.66	7.17	6.73	6.33	5.96	5.63	5.33	5.05	4.79	4.54
-35	1.54	1.98	2.59	3.3	4.09	4.84	5.66	6.40	6.96	7.15	6.93	6.47	6.03	5.72	5.42	5.14	4.89	4.64	4.41	4.19	3.98	3.78
-40	1.25	1.60	2.07	2.66	3.34	4.04	4.69	5.22	5.68	5.68	5.60	5.19	4.81	4.47	4.17	3.90	3.64	3.40	3.18	2.96	2.76	2.58
-45	1.06	1.35	1.71	2.15	2.65	3.19	3.73	4.18	4.51	4.69	4.52	4.23	3.91	3.61	3.34	3.09	2.84	2.60	2.36	2.14	1.94	1.76
-50																						

Table 7-9. Circular polarization

θ _z	DIRECTIONAL ANGLE		WAVELENGTH		GAIN FUNCTION (1 E-7)		ANGLE														
	θ _z	φ _z	λ	μ	θ _z	φ _z	0	5	10	15	20	25	30	35	40	45	50	0 _l			
50	1.52	.72	1.00	1.07	1.12	1.22	1.40	1.65	1.85	1.92	1.78	1.53	1.40	1.39	1.75	.97	.81	.84	.84	.84	.70
45	1.52	.70	1.04	1.27	1.42	1.56	2.48	3.00	3.31	3.33	3.08	2.72	2.45	2.24	1.89	1.41	1.08	.97	.90	.84	.76
40	1.52	.65	1.08	1.54	1.74	1.96	3.10	3.87	4.30	4.41	4.02	3.55	3.04	2.72	2.24	1.75	1.38	1.06	.84	.70	.65
35	1.52	.65	1.12	1.81	2.08	2.36	4.44	5.41	6.04	6.15	5.54	4.84	4.04	3.55	2.80	2.17	1.61	1.24	.90	.72	.65
30	1.52	.65	1.16	2.08	2.36	2.64	5.01	6.12	6.81	6.81	6.04	5.14	4.14	3.55	2.77	2.04	1.51	1.14	.84	.65	.65
25	1.52	.65	1.20	2.36	2.64	2.92	5.68	6.88	7.64	7.54	6.54	5.44	4.34	3.55	2.77	2.04	1.51	1.14	.84	.65	.65
20	1.52	.65	1.24	2.64	2.92	3.20	6.36	7.64	8.36	8.16	6.96	5.76	4.56	3.55	2.77	2.04	1.51	1.14	.84	.65	.65
15	1.52	.65	1.28	2.92	3.20	3.48	7.04	8.36	8.96	8.66	7.26	5.86	4.46	3.55	2.77	2.04	1.51	1.14	.84	.65	.65
10	1.52	.65	1.32	3.20	3.48	3.76	7.72	8.96	9.44	9.04	7.44	5.94	4.44	3.55	2.77	2.04	1.51	1.14	.84	.65	.65
5	1.52	.65	1.36	3.48	3.76	4.04	8.40	9.44	9.84	9.34	7.54	6.04	4.44	3.55	2.77	2.04	1.51	1.14	.84	.65	.65
0	1.52	.65	1.40	3.76	4.04	4.32	9.04	9.84	10.16	9.56	7.64	6.14	4.44	3.55	2.77	2.04	1.51	1.14	.84	.65	.65
-5	1.52	.65	1.44	4.04	4.32	4.60	9.64	10.16	10.48	9.76	7.72	6.24	4.44	3.55	2.77	2.04	1.51	1.14	.84	.65	.65
-10	1.52	.65	1.48	4.32	4.60	4.88	10.24	10.48	10.72	9.96	7.84	6.34	4.44	3.55	2.77	2.04	1.51	1.14	.84	.65	.65
-15	1.52	.65	1.52	4.60	4.88	5.16	10.84	10.72	10.88	10.04	7.92	6.44	4.44	3.55	2.77	2.04	1.51	1.14	.84	.65	.65
-20	1.52	.65	1.56	4.88	5.16	5.44	11.44	10.88	10.96	10.04	8.04	6.54	4.44	3.55	2.77	2.04	1.51	1.14	.84	.65	.65
-25	1.52	.65	1.60	5.16	5.44	5.72	12.04	11.04	11.04	10.04	8.14	6.64	4.44	3.55	2.77	2.04	1.51	1.14	.84	.65	.65
-30	1.52	.65	1.64	5.44	5.72	6.00	12.64	11.20	11.12	10.04	8.24	6.74	4.44	3.55	2.77	2.04	1.51	1.14	.84	.65	.65
-35	1.52	.65	1.68	5.72	6.00	6.28	13.24	11.36	11.16	10.04	8.34	6.84	4.44	3.55	2.77	2.04	1.51	1.14	.84	.65	.65
-40	1.52	.65	1.72	6.00	6.28	6.56	13.84	11.52	11.24	10.04	8.44	6.94	4.44	3.55	2.77	2.04	1.51	1.14	.84	.65	.65
-45	1.52	.65	1.76	6.28	6.56	6.84	14.44	11.68	11.36	10.04	8.54	7.04	4.44	3.55	2.77	2.04	1.51	1.14	.84	.65	.65
-50	1.52	.65	1.80	6.56	6.84	7.12	15.04	11.84	11.44	10.04	8.64	7.14	4.44	3.55	2.77	2.04	1.51	1.14	.84	.65	.65

Table 7-10 Circular polarization

θ ₂	DIPEDRAL ANGLE 1.25		WAVELENGTH 5320		GAIN FUNCTION (1.E+7)																						
	1.25	5320	1.25	5320	-50	-45	-40	-35	-30	-25	-20	-15	-10	-5	0	5	10	15	20	25	30	35	40	45	50		
50	1.05	1.42	1.70	1.94	2.22	2.57	2.98	3.42	3.78	3.90	3.67	3.26	2.69	2.09	1.48	1.00	0.60	0.33	0.18	0.10	0.06	0.04	0.03	0.02	0.01	0.01	0.01
45	1.21	1.64	2.03	2.47	2.96	3.51	4.10	4.62	5.07	5.36	5.37	5.07	4.39	3.50	2.50	1.50	0.90	0.50	0.28	0.16	0.09	0.05	0.03	0.02	0.01	0.01	0.01
40	1.37	1.84	2.33	2.87	3.46	4.10	4.68	5.19	5.64	5.85	5.67	5.17	4.20	3.10	2.00	1.30	0.80	0.45	0.25	0.14	0.08	0.05	0.03	0.02	0.01	0.01	0.01
35	1.54	2.04	2.61	3.24	3.93	4.67	5.44	6.14	6.75	7.00	6.75	6.14	5.00	3.80	2.60	1.70	1.10	0.65	0.38	0.22	0.13	0.08	0.05	0.03	0.02	0.01	0.01
30	1.71	2.24	2.91	3.67	4.46	5.31	6.14	6.94	7.61	7.85	7.46	6.50	5.20	3.90	2.70	1.80	1.15	0.70	0.42	0.26	0.16	0.10	0.06	0.04	0.03	0.02	0.01
25	1.88	2.44	3.18	4.07	5.00	5.97	6.94	7.89	8.75	9.00	8.50	7.20	5.80	4.50	3.30	2.30	1.50	0.95	0.55	0.32	0.19	0.12	0.08	0.05	0.03	0.02	0.01
20	2.05	2.64	3.45	4.46	5.50	6.57	7.64	8.69	9.64	9.90	9.20	7.70	6.20	4.90	3.70	2.60	1.70	1.05	0.60	0.36	0.22	0.14	0.09	0.06	0.04	0.03	0.02
15	2.22	2.84	3.75	4.87	6.00	7.24	8.48	9.71	10.94	11.20	10.30	8.60	6.90	5.50	4.30	3.20	2.20	1.40	0.85	0.48	0.28	0.17	0.11	0.07	0.05	0.03	0.02
10	2.39	3.04	4.05	5.27	6.50	7.84	9.27	10.69	12.10	12.40	11.40	9.50	7.60	6.00	4.70	3.50	2.50	1.60	0.95	0.52	0.30	0.19	0.13	0.08	0.05	0.03	0.02
5	2.56	3.19	4.30	5.61	6.94	8.37	9.89	11.50	13.10	13.50	12.40	10.30	8.30	6.50	5.10	3.90	2.90	1.90	1.10	0.58	0.32	0.20	0.14	0.09	0.06	0.04	0.03
0	2.73	3.36	4.57	5.98	7.50	9.01	10.61	12.29	14.06	14.50	13.40	11.20	9.00	7.00	5.50	4.30	3.30	2.30	1.50	0.85	0.45	0.26	0.16	0.10	0.07	0.05	0.03
-5	2.90	3.49	4.80	6.31	7.92	9.53	11.21	12.97	14.82	15.30	14.20	12.00	9.70	7.60	6.00	4.70	3.60	2.60	1.70	0.95	0.50	0.29	0.18	0.12	0.08	0.05	0.03
-10	3.07	3.66	5.01	6.52	8.13	9.84	11.60	13.45	15.39	15.90	14.80	12.60	10.30	8.20	6.50	5.10	4.00	3.00	2.10	1.30	0.75	0.40	0.24	0.15	0.10	0.07	0.05
-15	3.24	3.83	5.18	6.69	8.30	10.11	11.96	13.90	15.94	16.50	15.40	13.20	10.90	8.80	7.00	5.50	4.40	3.40	2.50	1.60	0.85	0.45	0.27	0.17	0.11	0.07	0.05
-20	3.41	4.00	5.35	6.86	8.47	10.28	12.21	14.24	16.37	17.00	15.90	13.70	11.40	9.30	7.40	5.80	4.60	3.60	2.70	1.80	0.95	0.50	0.30	0.19	0.13	0.08	0.05
-25	3.58	4.17	5.52	7.03	8.64	10.45	12.48	14.81	16.94	17.70	16.60	14.50	12.10	10.00	8.10	6.30	5.00	4.00	3.10	2.20	1.30	0.75	0.40	0.24	0.15	0.10	0.07
-30	3.75	4.34	5.69	7.20	8.81	10.62	12.75	15.28	17.77	18.60	17.50	15.30	12.90	10.80	8.90	6.90	5.50	4.50	3.60	2.70	1.80	0.85	0.45	0.27	0.17	0.11	0.07
-35	3.92	4.51	5.86	7.37	8.98	10.83	13.02	15.85	18.00	19.00	18.40	16.10	13.70	11.60	9.70	7.60	6.00	5.00	4.10	3.20	2.30	1.40	0.75	0.40	0.24	0.15	0.10
-40	4.09	4.68	6.03	7.54	9.15	11.04	13.27	16.52	18.50	19.50	19.30	17.00	14.50	12.40	10.50	8.40	6.70	5.50	4.60	3.70	2.80	1.90	1.00	0.75	0.40	0.24	0.15
-45	4.26	4.85	6.20	7.71	9.32	11.25	13.52	17.19	19.00	20.00	20.00	17.80	15.30	13.20	11.30	9.20	7.40	6.00	5.10	4.20	3.30	2.40	1.50	0.85	0.45	0.27	0.17
-50	4.43	5.02	6.37	7.88	9.49	11.46	13.77	17.88	19.50	20.50	20.50	18.60	16.10	14.00	12.10	10.00	7.90	6.50	5.60	4.70	3.80	2.90	2.00	1.10	0.85	0.45	0.27

Table 7-11. Circular polarization.

θ_2	DIMEAL ANGLE 1.75		WAVELENGTH 5320		GAIN FUNCTION (1.E+7)																							
	1.75	5.320	1.75	5.320	-50	-45	-40	-35	-30	-25	-20	-15	-10	-5	0	5	10	15	20	25	30	35	40	45	50			
50	1.16	1.73	2.41	3.09	3.76	4.40	4.93	5.26	5.48	5.58	5.56	5.35	5.10	4.96	4.79	4.36	3.75	3.14	2.53	1.85	1.23							
45	1.52	2.28	3.20	4.07	4.81	5.42	5.89	6.23	6.47	6.62	6.58	6.30	5.97	5.82	5.72	5.40	4.82	4.12	3.30	2.37	1.37							
40	2.22	3.10	4.05	4.88	5.57	6.22	6.83	7.27	7.50	7.57	7.37	7.08	6.82	6.69	6.56	6.25	5.75	5.09	4.16	3.02	2.04							
35	3.14	4.06	4.86	5.47	6.03	6.70	7.34	7.72	7.79	7.60	7.27	7.02	7.00	7.11	7.07	6.74	6.28	5.77	5.01	3.91	2.80							
30	4.47	5.57	6.40	6.94	7.06	6.83	6.58	6.48	6.48	6.34	6.00	5.74	5.68	6.06	6.36	7.04	6.70	6.28	5.75	4.06	3.70							
25	6.84	8.07	7.00	7.83	7.24	6.39	6.08	6.26	6.38	6.21	5.72	5.47	5.41	6.51	6.51	7.13	7.15	6.78	6.27	5.49	4.38							
20	9.13	10.37	7.84	7.80	7.05	6.00	5.95	6.16	6.31	6.31	6.07	5.72	5.41	6.20	6.00	6.82	7.26	7.01	6.43	5.62	4.60							
15	11.30	12.59	7.32	7.40	6.71	5.80	5.93	6.27	6.40	6.30	6.04	5.68	5.20	5.78	5.68	6.79	7.00	6.44	5.58	4.67	3.68							
10	13.43	14.77	7.03	7.19	6.41	5.81	5.72	6.26	6.36	6.20	5.92	5.56	5.07	5.50	5.40	6.42	6.23	6.44	6.83	6.55	5.85	4.98						
5	15.59	16.97	6.97	7.09	6.35	5.79	5.53	6.17	6.26	6.10	5.82	5.46	4.97	5.31	5.20	6.14	6.23	6.74	6.80	6.35	5.65	4.75						
0	17.74	19.16	7.08	7.28	6.54	5.97	5.58	6.34	6.42	6.26	5.98	5.62	5.13	5.46	5.35	6.18	6.26	6.78	7.01	6.72	5.75	4.85						
-5	19.86	21.31	7.03	7.41	6.78	6.03	5.74	6.44	6.50	6.34	6.06	5.70	5.21	5.54	5.43	6.10	6.18	6.70	7.17	6.82	5.74	4.85						
-10	21.94	23.40	7.28	7.48	6.93	6.28	5.92	6.20	6.37	6.20	5.92	5.56	5.07	5.40	5.29	6.05	6.15	6.67	7.20	7.23	6.59	5.53						
-15	23.98	25.48	7.00	7.00	6.97	6.63	6.21	5.59	6.02	6.10	5.82	5.46	5.00	5.33	5.22	6.11	6.15	6.68	6.98	6.99	6.48	5.41						
-20	25.98	27.54	6.62	6.62	6.87	6.91	6.60	6.03	5.92	6.18	5.90	5.54	5.07	5.40	5.29	6.17	6.26	6.48	6.98	6.96	6.48	5.41						
-25	27.94	29.58	6.13	6.25	6.73	7.03	7.06	6.47	6.18	6.18	5.97	5.60	5.13	5.46	5.35	6.11	6.21	6.07	6.77	7.06	6.97	6.52	5.94					
-30	29.88	31.58	5.56	6.25	6.73	7.03	7.06	6.47	6.18	6.18	5.97	5.60	5.13	5.46	5.35	6.11	6.21	6.07	6.77	7.06	6.97	6.52	5.94					
-35	31.81	33.55	4.91	5.85	6.56	6.98	7.06	6.90	6.60	6.95	7.25	7.42	7.59	7.25	7.04	6.68	6.08	6.17	5.60	4.92	4.06	3.09						
-40	33.74	35.48	4.22	5.21	6.04	6.56	6.61	6.43	6.51	6.97	7.39	7.39	7.05	6.66	6.38	6.08	6.06	6.53	4.09	3.12	2.22	1.23						
-45	35.67	37.36	3.46	4.25	5.01	5.62	5.79	5.64	5.73	6.19	6.25	6.25	5.91	5.45	5.21	5.45	5.11	4.57	3.89	3.08	2.24	1.22						
-50	37.59	39.20	2.68	3.27	3.85	4.53	4.73	4.74	4.83	5.20	5.49	5.47	5.23	4.93	4.55	4.03	3.42	2.82	2.23	1.63	1.11							

Table 7-12 Circular polarization, mixed dihedral angles

θ_z	Dihedral Angle 1.25		Wavelength 3320		Gain Function (1.E+7)																																																																																																																																																																																																																																																																																																																																																																																																																																																																																																																																																																																																																																																																																																																																																																																																																																																																																																																																																																																			
	1.25	3.25	1.25	3.25	0	5	10	15	20	25	30	35	40	45	50	55	60	65	70	75	80	85	90																																																																																																																																																																																																																																																																																																																																																																																																																																																																																																																																																																																																																																																																																																																																																																																																																																																																																																																																																																	
5C	1.02	1.25	1.71	2.12	2.48	2.76	2.94	3.04	3.11	3.29	3.36	3.41	3.57	3.60	3.71	3.81	3.78	3.90	3.97	3.97	3.90	3.78	3.61	3.42	3.20	2.97	2.74	2.51	2.28	2.05	1.82	1.59	1.36	1.14	.90																																																																																																																																																																																																																																																																																																																																																																																																																																																																																																																																																																																																																																																																																																																																																																																																																																																																																																																																																					
45	1.02	1.53	2.15	2.71	3.17	3.54	3.86	4.12	4.33	4.50	4.72	4.97	5.15	5.29	5.40	5.47	5.50	5.52	5.52	5.50	5.43	5.29	5.09	4.82	4.53	4.20	3.85	3.49	3.13	2.77	2.41	2.05	1.69	1.33	.97																																																																																																																																																																																																																																																																																																																																																																																																																																																																																																																																																																																																																																																																																																																																																																																																																																																																																																																																																					
40	1.44	2.04	2.75	3.34	3.83	4.34	4.93	5.56	6.15	6.77	7.40	8.03	8.64	9.21	9.73	10.20	10.61	10.96	11.25	11.48	11.65	11.74	11.76	11.71	11.59	11.40	11.13	10.80	10.40	9.94	9.43	8.87	8.26	7.60	6.89	6.14	5.36																																																																																																																																																																																																																																																																																																																																																																																																																																																																																																																																																																																																																																																																																																																																																																																																																																																																																																																																																			
35	2.01	2.76	3.52	4.25	4.97	5.25	5.97	6.73	7.54	8.40	9.30	10.23	11.18	12.14	13.11	14.08	15.04	16.00	16.95	17.89	18.81	19.71	20.58	21.42	22.22	22.97	23.67	24.31	24.89	25.41	25.88	26.30	26.67	27.00	27.29	27.54	27.75																																																																																																																																																																																																																																																																																																																																																																																																																																																																																																																																																																																																																																																																																																																																																																																																																																																																																																																																																			
30	2.47	3.40	4.41	5.25	6.05	6.95	8.02	9.26	10.64	12.14	13.74	15.42	17.17	18.98	20.84	22.74	24.67	26.62	28.58	30.54	32.50	34.45	36.38	38.29	40.18	42.04	43.86	45.64	47.37	49.04	50.65	52.20	53.69	55.12	56.49	57.81	59.00																																																																																																																																																																																																																																																																																																																																																																																																																																																																																																																																																																																																																																																																																																																																																																																																																																																																																																																																																			
25	2.71	3.73	4.90	6.09	7.56	8.92	10.59	12.54	14.74	17.17	19.81	22.64	25.64	28.79	32.07	35.47	38.97	42.56	46.23	49.97	53.77	57.61	61.48	65.38	69.29	73.20	77.11	81.01	84.89	88.74	92.55	96.31	100.03	103.71	107.34	110.91	114.42	117.88	121.29	124.64	127.93	131.16	134.33	137.45	140.51	143.51	146.45	149.33	152.15	154.91	157.61	160.25	162.83	165.35	167.81	170.21	172.55	174.83	177.05	179.21	181.32	183.37	185.36	187.29	189.15	190.94	192.66	194.31	195.89	197.41	198.87	200.27	201.61	202.89	204.11	205.27	206.38	207.44	208.45	209.41	210.32	211.18	212.00	212.77	213.49	214.16	214.78	215.35	215.87	216.34	216.76	217.13	217.45	217.72	217.94	218.11	218.23	218.30	218.33	218.32	218.27	218.18	218.05	217.88	217.66	217.40	217.09	216.74	216.35	215.92	215.45	214.94	214.39	213.80	213.17	212.50	211.79	211.04	210.25	209.42	208.55	207.64	206.69	205.70	204.67	203.60	202.49	201.34	200.15	198.92	197.65	196.34	194.99	193.60	192.17	190.70	189.19	187.64	186.05	184.42	182.75	181.04	179.29	177.50	175.67	173.80	171.89	170.94	169.95	168.92	167.85	166.74	165.58	164.38	163.13	161.84	160.50	159.12	157.70	156.24	154.74	153.20	151.62	150.00	148.34	146.63	144.87	143.06	141.20	139.29	137.33	135.32	133.26	131.15	129.00	126.80	124.55	122.25	119.91	117.52	115.09	112.61	110.09	107.53	104.93	102.29	99.61	96.89	94.13	91.33	88.49	85.61	82.69	79.73	76.73	73.69	70.61	67.49	64.33	61.13	57.89	54.61	51.29	47.93	44.53	41.09	37.61	34.09	30.53	26.93	23.29	19.61	15.89	12.13	8.33	4.49	0.61	-3.29	-7.13	-10.92	-14.66	-18.35	-22.00	-25.61	-29.18	-32.71	-36.20	-39.65	-43.06	-46.43	-49.75	-53.02	-56.25	-59.43	-62.56	-65.63	-68.65	-71.61	-74.51	-77.35	-80.13	-82.86	-85.53	-88.15	-90.71	-93.21	-95.66	-98.05	-100.39	-102.67	-104.90	-107.07	-109.18	-111.23	-113.22	-115.15	-117.02	-118.83	-120.58	-122.27	-123.90	-125.47	-126.98	-128.43	-129.82	-131.15	-132.42	-133.63	-134.78	-135.87	-136.90	-137.87	-138.79	-139.65	-140.46	-141.21	-141.90	-142.53	-143.10	-143.61	-144.06	-144.45	-144.78	-145.05	-145.27	-145.43	-145.54	-145.60	-145.61	-145.58	-145.50	-145.37	-145.19	-144.95	-144.65	-144.30	-143.89	-143.42	-142.89	-142.30	-141.65	-140.94	-140.17	-139.34	-138.45	-137.50	-136.49	-135.42	-134.29	-133.10	-131.85	-130.54	-129.17	-127.74	-126.25	-124.70	-123.09	-121.42	-119.69	-117.90	-116.05	-114.14	-112.17	-110.14	-108.05	-105.90	-103.69	-101.42	-99.09	-96.70	-94.25	-91.74	-89.17	-86.54	-83.85	-81.10	-78.29	-75.42	-72.49	-69.50	-66.45	-63.34	-60.17	-56.94	-53.65	-50.30	-46.89	-43.42	-39.89	-36.31	-32.67	-29.07	-25.41	-21.69	-17.91	-14.06	-10.15	-6.18	-2.15	1.94	6.06	10.19	14.33	18.47	22.61	26.75	30.88	35.00	39.11	43.21	47.30	51.38	55.45	59.50	63.53	67.54	71.53	75.50	79.45	83.38	87.29	91.18	95.05	98.89	102.70	106.48	110.23	113.94	117.61	121.24	124.83	128.38	131.89	135.36	138.79	142.18	145.53	148.84	152.11	155.34	158.53	161.68	164.79	167.86	170.89	173.87	176.81	179.71	182.57	185.39	188.17	190.91	193.61	196.27	198.89	201.47	204.01	206.51	208.97	211.39	213.77	216.11	218.41	220.67	222.89	225.07	227.21	229.31	231.37	233.39	235.37	237.31	239.21	241.07	242.89	244.66	246.39	248.07	249.70	251.28	252.81	254.29	255.72	257.10	258.43	259.71	260.94	262.12	263.25	264.33	265.36	266.33	267.25	268.11	268.92	269.68	270.39	271.05	271.66	272.22	272.73	273.19	273.60	273.96	274.27	274.53	274.75	274.92	275.05	275.13	275.17	275.17	275.13	275.05	274.92	274.75	274.53	274.27	273.96	273.60	273.19	272.73	272.22	271.66	271.05	270.39	269.68	268.92	268.11	267.25	266.33	265.36	264.33	263.25	262.12	260.94	259.71	258.43	257.10	255.72	254.29	252.81	251.28	249.70	248.07	246.39	244.66	242.89	241.07	239.21	237.31	235.37	233.39	231.37	229.31	227.21	225.07	222.89	220.67	218.41	216.11	213.77	211.39	208.97	206.51	204.01	201.47	198.89	196.27	193.61	190.91	188.17	185.39	182.57	179.71	176.81	173.87	170.89	167.86	164.79	161.68	158.53	155.34	152.11	148.84	145.53	142.18	138.79	135.36	131.89	128.38	124.83	121.24	117.61	113.94	110.23	106.48	102.70	98.89	95.05	91.18	87.29	83.38	79.45	75.50	71.53	67.49	63.34	59.17	54.94	50.65	46.30	41.89	37.42	32.89	28.31	23.67	19.07	14.41	9.69	4.93	0.13	-4.71	-9.48	-14.15	-18.72	-23.19	-27.56	-31.83	-36.00	-40.07	-44.04	-47.91	-51.68	-55.34	-58.90	-62.36	-65.72	-68.98	-72.14	-75.20	-78.17	-81.04	-83.81	-86.48	-89.05	-91.52	-93.89	-96.16	-98.33	-100.40	-102.37	-104.24	-106.01	-107.68	-109.25	-110.72	-112.09	-113.36	-114.53	-115.60	-116.57	-117.44	-118.21	-118.88	-119.45	-119.92	-120.29	-120.56	-120.73	-120.80	-120.77	-120.64	-120.41	-120.08	-119.65	-119.12	-118.49	-117.76	-116.93	-116.00	-114.97	-113.84	-112.61	-111.28	-109.85	-108.32	-106.69	-105.06	-103.33	-101.50	-99.57	-97.54	-95.41	-93.18	-90.85	-88.42	-85.89	-83.26	-80.53	-77.70	-74.77	-71.74	-68.61	-65.38	-62.05	-58.62	-55.09	-51.46	-47.73	-43.90	-39.97	-35.94	-31.81	-27.58	-23.25	-18.82	-14.29	-9.66	-4.93	0.00	4.97	9.94	14.91	19.88	24.85	29.82	34.79	39.76	44.73	49.69	54.66	59.63	64.59	69.56	74.53	79.49	84.46	89.43	94.39	99.36	104.33	109.29	114.26	119.23	124.19	129.16	134.13	139.09	144.06	149.03	154.00	158.97	163.94	168.91	173.88	178.85	183.82	188.79	193.76	198.73	203.69	208.66	213.63	218.60	223.57	228.54	233.51	238.48	243.45	248.42	253.39	258.36	263.33	268.30	273.27	278.24	283.21	288.18	293.15	298.12	303.09	308.06	313.03	318.00	323.00	328.00	333.00	338.00	343.00	348.00	353.00	358.00	363.00	368.00	373.00	378.00	383.00	388.00	393.00	398.00	403.00	408.00	413.00	418.00	423.00	428.00	433.00	438.00	443.00	448.00	453.00	458.00	463.00	468.00	473.00	478.00	483.00	488.00	493.00	498.00	503.00	508.00	513.00	518.00	523.00	528.00	533.00	538.00	543.00	548.00	553.00	558.00	563.00	568.00	573.00	578.00	583.00	588.00	593.00	598.00	603.00	608.00	613.00	618.00	623.00	628.00	633.00	638.00	643.00	648.00	653.00	658.00	663.00	668.00	673.00	678.00	683.00	688.00	693.00	698.00	703.00	708.00	713.00	718.00	723.00	728.00	733.00	738.00	743.00	748.00	753.00	758.00	763.00	768.00	773.00	778.00	783.00	788.00	793.00	798.00	803.00	808.00	813.00	818.00	823.00	828.00	833.00	838.00	843.00	848.00	853.00	858.00	863.00	868.00	873.00	878.00	883.00	888.00	893.00	898.00	903.00	908.00	913.00	918.00	923.00	928.00	933.00	938.00	943.00	948.00	953.00	958.00	963.00	968.00	973.00	978.00	983.00	988.00	993.00	998.00	1003.00	1008.00	1013.00	1018.00	1023.00	1028.00	1033.00	1038.00	1043.00	1048.00	1053.00	1058.00	1063.00	1068.00	1073.00	1078.00	1083.00	1088.00	1093.00	1098.00	1103.00	1108.00	1113.00	1118.00	1123.00	1128.00	1133.00	1138.00	1143.00	1148.00	1153.00	1158.00	1163.00	1168.00	1173.00	1178.00	1183.00	1188.00	1193.00	1198.00	1203.00	1208.00	1213.00	1218.00	1223.00	1228.00	1233.00	1238.00	1243.00	1248.00	1253.00	1258.00	1263.00	1268.00	1273.00	1278.00	1283.00	1288.00	1293.00	1298.00	1303.00	1308.00	1313.00	1318.00	1323.00	1328.00	1333.00	1338.00	1343.00	1348.00	1

Table 7-13 Circular Polarization

DIME- DRA- L AN- GLE	GAIN FUNCTION (1.E+7)																			
	-50	-45	-40	-35	-30	-25	-20	-15	-10	0	5	10	15	20	25	30	35	40	45	50
0	1.00	1.00	1.00	1.00	1.00	1.00	1.00	1.00	1.00	1.00	1.00	1.00	1.00	1.00	1.00	1.00	1.00	1.00	1.00	1.00
5	1.00	1.00	1.00	1.00	1.00	1.00	1.00	1.00	1.00	1.00	1.00	1.00	1.00	1.00	1.00	1.00	1.00	1.00	1.00	1.00
10	1.00	1.00	1.00	1.00	1.00	1.00	1.00	1.00	1.00	1.00	1.00	1.00	1.00	1.00	1.00	1.00	1.00	1.00	1.00	1.00
15	1.00	1.00	1.00	1.00	1.00	1.00	1.00	1.00	1.00	1.00	1.00	1.00	1.00	1.00	1.00	1.00	1.00	1.00	1.00	1.00
20	1.00	1.00	1.00	1.00	1.00	1.00	1.00	1.00	1.00	1.00	1.00	1.00	1.00	1.00	1.00	1.00	1.00	1.00	1.00	1.00
25	1.00	1.00	1.00	1.00	1.00	1.00	1.00	1.00	1.00	1.00	1.00	1.00	1.00	1.00	1.00	1.00	1.00	1.00	1.00	1.00
30	1.00	1.00	1.00	1.00	1.00	1.00	1.00	1.00	1.00	1.00	1.00	1.00	1.00	1.00	1.00	1.00	1.00	1.00	1.00	1.00
35	1.00	1.00	1.00	1.00	1.00	1.00	1.00	1.00	1.00	1.00	1.00	1.00	1.00	1.00	1.00	1.00	1.00	1.00	1.00	1.00
40	1.00	1.00	1.00	1.00	1.00	1.00	1.00	1.00	1.00	1.00	1.00	1.00	1.00	1.00	1.00	1.00	1.00	1.00	1.00	1.00
45	1.00	1.00	1.00	1.00	1.00	1.00	1.00	1.00	1.00	1.00	1.00	1.00	1.00	1.00	1.00	1.00	1.00	1.00	1.00	1.00
50	1.00	1.00	1.00	1.00	1.00	1.00	1.00	1.00	1.00	1.00	1.00	1.00	1.00	1.00	1.00	1.00	1.00	1.00	1.00	1.00

Table 7-14 Circular polarization

θ_2	DIMERAL ANGLE 1.25 WAVELENGTH 6943																			
	GAIN FUNCTION (1.E+7)																			
50	1.45	1.61	1.90	2.30	2.79	3.32	3.80	4.13	4.25	4.15	3.92	3.68	3.47	3.27	3.00	2.61	2.11	1.62	1.23	.94
45	1.52	1.81	2.11	2.47	2.92	3.45	4.02	4.55	4.94	5.07	4.97	4.73	4.42	4.05	3.70	3.30	2.71	2.08	1.56	1.18
40	1.96	2.39	2.77	3.15	3.59	4.10	4.67	5.28	5.81	6.05	5.87	5.55	5.14	4.65	4.30	4.04	3.48	2.76	2.09	1.57
35	2.49	3.07	3.50	3.87	4.30	4.88	5.57	6.33	7.04	7.45	7.31	6.95	6.50	6.04	5.86	5.59	4.81	3.96	2.80	2.13
30	3.03	3.72	4.17	4.57	5.15	5.97	6.85	7.86	8.78	9.31	9.05	8.58	8.07	7.52	7.34	7.04	6.04	4.84	3.52	2.71
25	3.46	4.27	4.72	5.27	6.19	7.32	8.21	9.65	10.88	11.41	10.95	10.35	9.72	9.07	8.85	8.54	7.34	6.04	4.51	3.43
20	3.70	4.52	5.14	5.98	7.29	8.57	9.08	10.78	12.25	12.55	12.05	11.35	10.62	9.87	9.64	9.24	7.94	6.54	4.91	3.60
15	3.72	4.60	5.41	6.57	8.15	9.30	9.19	10.22	11.78	12.01	11.45	10.72	9.98	9.23	8.99	8.59	7.29	5.89	4.32	3.56
10	3.63	4.51	5.49	6.90	8.56	9.41	8.98	9.48	10.53	11.01	10.45	9.72	8.98	8.23	8.00	7.60	6.30	4.90	3.33	3.58
5	3.58	4.43	5.44	6.94	8.57	9.21	8.55	8.32	9.67	10.25	10.01	9.45	8.72	7.97	7.74	7.34	6.04	4.64	3.07	3.53
0	3.62	4.40	5.36	6.84	8.43	8.90	8.34	8.08	9.66	10.21	10.01	9.45	8.72	7.97	7.74	7.34	6.04	4.64	3.07	3.53
-5	3.75	4.44	5.32	6.71	8.26	8.90	8.25	7.51	7.87	9.10	9.59	8.93	8.20	7.45	7.22	6.82	5.52	4.12	2.55	3.55
-10	3.82	4.51	5.28	6.54	8.04	8.77	8.14	7.28	7.27	7.27	7.23	6.55	5.82	5.07	4.84	4.44	3.14	1.74	1.13	3.55
-15	3.74	4.44	5.20	6.33	7.69	8.48	7.84	7.17	7.22	7.25	7.20	6.52	5.79	5.04	4.81	4.41	3.11	1.71	1.10	3.45
-20	3.52	4.24	5.04	6.04	7.18	7.91	7.84	7.16	7.13	7.20	7.24	6.56	5.82	5.07	4.84	4.44	3.14	1.74	1.13	3.20
-25	3.16	3.93	4.73	5.64	6.53	7.04	7.16	6.48	6.44	6.54	6.58	5.90	5.16	4.41	4.18	3.78	2.48	1.08	0.47	3.00
-30	2.70	3.43	4.23	5.07	5.78	6.14	6.18	5.50	5.23	5.20	5.24	4.56	3.82	3.07	2.84	2.44	1.14	0.54	0.00	2.81
-35	2.17	2.81	3.56	4.35	4.98	5.26	5.17	4.47	4.50	4.46	4.51	3.82	3.07	2.32	2.09	1.69	0.39	0.00	0.00	2.55
-40	1.68	2.21	2.86	3.57	4.16	4.47	4.50	3.82	3.82	3.82	3.82	3.13	2.38	1.63	1.40	1.00	0.00	0.00	0.00	2.38
-45	1.29	1.73	2.26	2.85	3.37	3.70	3.64	3.00	3.00	3.00	3.00	2.31	1.56	0.81	0.58	0.18	0.00	0.00	0.00	1.92
-50	1.01	1.35	1.78	2.24	2.64	2.91	3.08	3.24	3.40	3.82	4.12	4.21	3.40	2.65	2.59	2.19	1.50	1.00	0.63	1.20

Table 7-15 Circular polarization

DIPEDRAL ANGLE	WAVELENGTH		GA[M FUNCTION (1.F-7)		WAVELENGTH		DIPEDRAL ANGLE	
	1.75	6943	1.75	6943	1.75	6943	1.75	6943
0	1.86	2.17	2.49	2.57	3.14	3.89	4.32	4.69
5	1.86	2.17	2.49	2.57	3.14	3.89	4.32	4.69
10	1.86	2.17	2.49	2.57	3.14	3.89	4.32	4.69
15	1.86	2.17	2.49	2.57	3.14	3.89	4.32	4.69
20	1.86	2.17	2.49	2.57	3.14	3.89	4.32	4.69
25	1.86	2.17	2.49	2.57	3.14	3.89	4.32	4.69
30	1.86	2.17	2.49	2.57	3.14	3.89	4.32	4.69
35	1.86	2.17	2.49	2.57	3.14	3.89	4.32	4.69
40	1.86	2.17	2.49	2.57	3.14	3.89	4.32	4.69
45	1.86	2.17	2.49	2.57	3.14	3.89	4.32	4.69
50	1.86	2.17	2.49	2.57	3.14	3.89	4.32	4.69
55	1.86	2.17	2.49	2.57	3.14	3.89	4.32	4.69
60	1.86	2.17	2.49	2.57	3.14	3.89	4.32	4.69
65	1.86	2.17	2.49	2.57	3.14	3.89	4.32	4.69
70	1.86	2.17	2.49	2.57	3.14	3.89	4.32	4.69
75	1.86	2.17	2.49	2.57	3.14	3.89	4.32	4.69
80	1.86	2.17	2.49	2.57	3.14	3.89	4.32	4.69
85	1.86	2.17	2.49	2.57	3.14	3.89	4.32	4.69
90	1.86	2.17	2.49	2.57	3.14	3.89	4.32	4.69

Table 7-16 Circular polarization, mixed dihedral angles.

θ	DIPEDRAL ANGLE 1.25		WAVELENGTH 6943		GAIN FUNCTION (1.E+7)																							
	1.25	1.25	1.25	1.25	0	5	10	15	20	25	30	35	40	45	50	0	5	10	15	20	25	30	35	40	45	50		
50	1.32	1.56	1.78	2.06	2.42	2.83	3.21	3.52	3.71	3.76	3.70	3.59	3.46	3.33	3.17	2.94	2.61	2.21	1.79	1.42	1.11							
45	1.67	1.96	2.25	2.59	3.00	3.44	3.86	4.20	4.43	4.50	4.43	4.26	4.10	3.96	3.82	3.58	3.20	2.70	2.17	1.69	1.30							
40	2.08	2.49	2.85	3.22	3.63	4.08	4.52	4.93	5.27	5.46	5.41	5.15	4.82	4.55	4.31	4.19	3.87	3.35	2.72	2.10	1.60							
35	2.56	3.10	3.51	3.88	4.32	4.87	5.45	6.02	6.53	6.89	6.97	6.56	5.98	5.46	5.12	4.89	4.59	4.10	3.41	2.67	2.03							
30	3.05	3.70	4.12	4.50	5.10	5.92	6.73	7.38	7.92	8.31	8.39	8.01	7.34	6.67	6.17	5.78	5.34	4.76	4.04	3.24	2.50							
25	3.59	4.20	4.63	5.11	5.99	7.13	8.02	8.42	8.59	8.76	8.78	8.50	8.04	7.64	7.30	6.80	6.08	5.25	4.42	3.62	2.86							
20	3.77	4.23	5.02	5.69	6.87	8.15	8.76	8.60	8.28	8.24	8.26	8.05	7.85	7.95	8.11	7.77	6.82	5.63	4.61	3.79	3.06							
15	3.84	4.34	5.28	6.17	7.54	8.98	8.80	8.02	7.94	8.36	8.67	8.29	7.77	7.90	8.46	8.46	7.47	6.01	4.75	3.86	3.16							
10	3.73	4.27	5.33	6.46	7.90	9.76	8.76	8.29	10.37	13.64	15.25	13.62	10.40	8.33	8.14	8.42	7.85	6.32	4.91	3.94	3.24							
5	3.57	4.21	5.30	6.61	8.06	9.86	8.26	8.29	10.37	13.64	15.25	13.62	10.40	8.33	8.14	8.42	7.85	6.32	4.91	3.94	3.24							
0	3.48	4.24	5.25	6.67	8.16	9.88	8.18	8.42	11.02	14.83	16.58	14.58	10.70	8.06	7.62	7.94	7.55	6.41	5.18	4.20	3.42							
-5	3.44	4.21	5.18	6.64	8.17	9.75	8.08	7.91	9.75	12.71	14.01	12.27	9.16	7.30	7.27	7.67	7.31	6.30	5.24	4.33	3.52							
-10	3.36	4.10	5.03	6.44	7.95	8.57	7.92	7.19	7.75	9.25	9.93	8.91	7.41	6.97	7.52	7.82	7.22	6.17	5.22	4.41	3.59							
-15	2.94	3.67	4.52	5.63	6.83	7.58	7.55	7.21	7.26	7.76	7.68	7.48	7.25	7.67	8.24	8.07	7.06	5.91	5.06	4.35	3.55							
-20	2.63	3.39	4.19	5.17	6.13	6.77	6.98	7.12	7.62	8.41	9.00	8.18	6.96	6.60	8.11	7.09	5.89	4.99	4.32	3.73	2.99							
-25	2.27	2.95	3.76	4.63	5.40	5.87	6.07	6.33	6.93	7.75	8.33	8.38	8.00	7.64	8.75	5.91	5.07	4.39	3.83	3.27	2.59							
-30	1.89	2.49	3.23	4.00	4.65	5.03	5.16	5.28	5.64	6.17	6.57	6.60	6.30	5.84	6.82	4.28	3.78	3.30	2.78	2.21	1.66							
-35	1.56	2.08	2.70	3.36	3.94	4.31	4.46	4.52	4.65	4.91	5.15	5.21	5.05	4.74	4.38	3.97	3.54	3.12	2.70	2.29	1.84							
-40	1.31	1.77	2.28	2.82	3.29	3.65	3.87	4.00	4.14	4.33	4.51	4.58	4.45	4.14	3.73	3.29	2.86	2.48	2.15	1.85	1.54							
-45	1.17	1.53	1.93	2.37	2.72	2.98	3.18	3.38	3.62	3.88	4.07	4.10	3.92	3.55	3.09	2.64	2.26	1.96	1.71	1.48	1.24							
-50																												

Table 9(1-16). Gain function vs. velocity aberration. The average and rms fluctuations are computed around a circle in the far field whose radius is the velocity aberration listed in the first column in microradians. Table 8-J Linear polarization

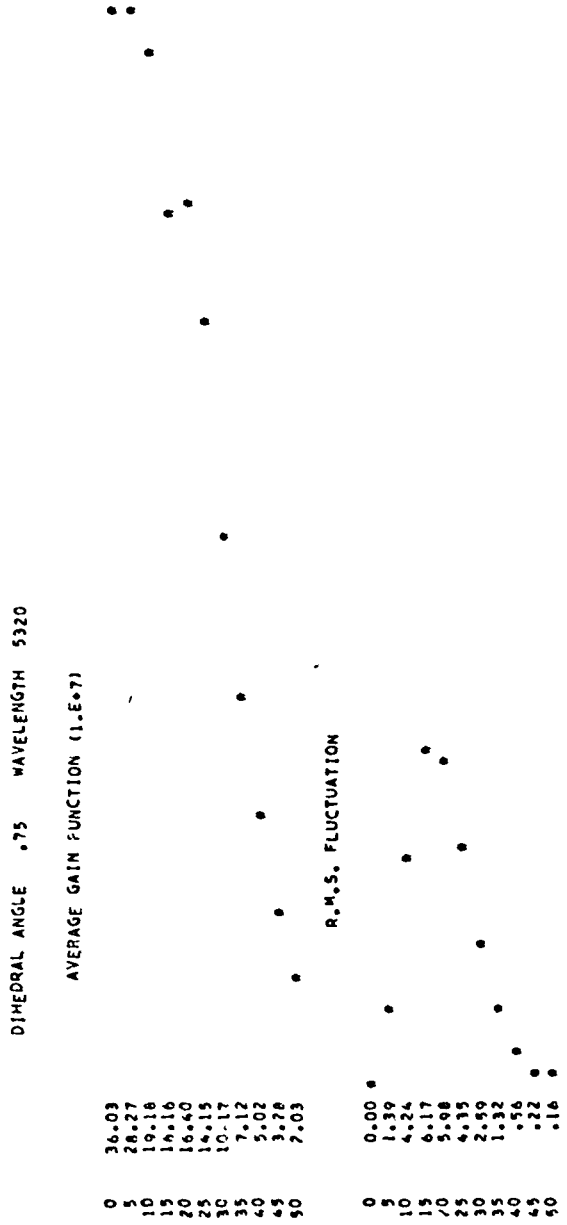


Table 8-2 Linear polarization.

DIHEDRAL ANGLE 1.25 WAVELENGTH 5320

AVERAGE GAIN FUNCTION (1.E+7)

0	14.34
5	11.25
10	8.70
15	9.66
20	11.26
25	10.70
30	9.36
35	8.43
40	7.19
45	5.47
50	3.84

R.M.S. FLUCTUATION

0	0.00
5	.74
10	2.33
15	3.36
20	3.49
25	3.17
30	2.78
35	2.28
40	1.82
45	.92
50	.89

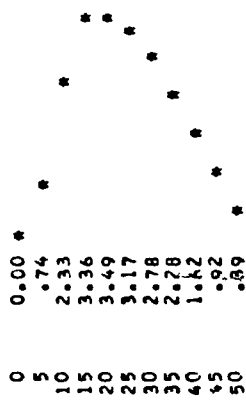
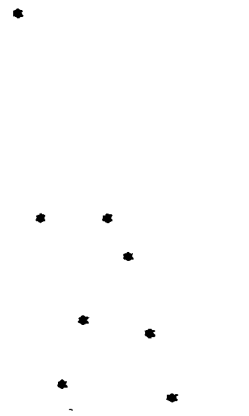


Table 8-3. Linear polarization.

DIHEDRAL ANGLE 1.75 WAVELENGTH 5320

AVERAGE GAIN FUNCTION (I.E.*7)



R.M.S. FLUCTUATION

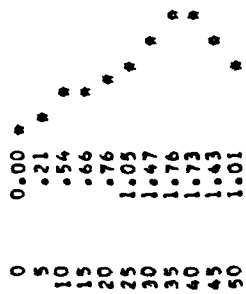


Table 8-4 Linear polarization, mixed dihedral angles.

DIHEDRAL ANGLE 1.23 WAVELENGTH 5320

AVERAGE GAIN FUNCTION (i.e. σ)

0	18.12
5	14.22
10	10.35
15	10.22
20	11.27
25	10.38
30	8.70
35	7.54
40	6.40
45	5.02
50	3.77

R.M.S. FLUCTUATION

0	0.00
5	.82
10	2.51
15	3.58
20	3.54
25	2.96
30	2.37
35	1.85
40	1.36
45	.84
50	.46

Table 8-5. Linear polarization.

DIMEDRAL ANGLE .75 WAVELENGTH 6943

AVERAGE GAIN FUNCTION (1.0E+7)

0	26.45
5	22.78
10	16.81
15	12.08
20	10.47
25	10.42
30	9.67
35	7.73
40	5.54
45	3.90
50	2.81

R.M.S. FLUCTUATION

0	0.00
5	.55
10	1.69
15	2.95
20	3.65
25	3.57
30	2.86
35	1.92
40	1.13
45	.59
50	.27

Table 8-6. Linear polarization.

DIHEDRAL ANGLE 1.25 WAVELENGTH 6943

AVERAGE GAIN FUNCTION (1.E+7)

0	15.06
5	12.98
10	9.87
15	7.94
20	8.01
25	8.63
30	8.33
35	7.08
40	5.74
45	4.76
50	3.94

R.M.S. FLUCTUATION

0	0.00
5	.43
10	1.51
15	2.62
20	3.25
25	3.24
30	2.80
35	2.19
40	1.62
45	1.13
50	.74

Table 8-7. Linear polarization.

DIHEDRAL ANGLE 1.75 WAVELENGTH 6943

AVERAGE GAIN FUNCTION (1.E+7)

0	6.93
5	5.72
10	4.62
15	4.29
20	5.09
25	5.95
30	6.04
35	5.60
40	5.22
45	4.99
50	4.62

R.M.S. FLUCTUATION

0	0.00
5	.23
10	.79
15	1.34
20	1.65
25	1.72
30	1.68
35	1.62
40	1.54
45	1.40
50	1.16

Table 8-8. Linear polarization, mixed dihedral angles.

DIHEDRAL ANGLE 1.25 WAVELENGTH 6943

AVERAGE GAIN FUNCTION (1.E+7)

0 16.07
 5 13.83
 10 10.41
 15 8.14
 20 7.95
 25 8.46
 30 8.12
 35 6.86
 40 5.51
 45 4.52
 50 3.75

R.M.S. FLUCTUATION

0 0.00
 5 .43
 10 1.43
 15 2.48
 20 3.05
 25 3.01
 30 2.54
 35 1.96
 40 1.44
 45 1.03
 50 .71

Table 8-9. Circular polarization.

DIHEDRAL ANGLE .75 WAVELENGTH 5320

AVERAGE GAIN FUNCTION (I.E.+7)

0	36.86
5	28.80
10	19.76
15	15.96
20	16.16
25	13.97
30	10.08
35	7.13
40	5.07
45	3.32
50	2.03

R.M.S. FLUCTUATION

0	0.00
5	.92
10	.91
15	.64
20	.80
25	.78
30	.68
35	.52
40	.37
45	.25
50	.18

Table 8-10. Circular polarization.

DIHEDRAL ANGLE 1.25 WAVELENGTH 5320

AVERAGE GAIN FUNCTION (1.E+7)

0	14.97
5	11.66
10	8.79
15	9.58
20	11.15
25	10.57
30	9.25
35	8.38
40	7.19
45	5.46
50	1.83

R.M.S. FLUCTUATION

0	0.00
5	.29
10	.25
15	.39
20	.67
25	.59
30	.45
35	.37
40	.35
45	.29
50	.22

Table 8-11. Circular polarization.

DIHEDRAL ANGLE 1.75 WAVELENGTH 9320

AVERAGE GAIN FUNCTION (1.E+7)

0	5.57	*
5	4.05	*
10	3.15	*
15	4.20	*
20	5.45	*
25	5.82	*
30	6.32	*
35	7.02	*
40	7.06	*
45	6.44	*
50	5.55	*

R.M.S. FLUCTUATION

0	0.00	*
5	0.10	*
10	0.10	*
15	0.27	*
20	0.39	*
25	0.33	*
30	0.23	*
35	0.22	*
40	0.24	*
45	0.22	*
50	0.19	*

This document contains information which is classified "Secret" under Executive Order 12958, Section 1.4, and is intended for the use of the personnel of the Department of Defense only. It is to be controlled, stored, transmitted, and disposed of in accordance with the provisions of Executive Order 12958, Section 1.4.

Table 8-12 Circular polarization, mixed dihedral angles.

DIHEDRAL ANGLE $\overline{1.25}$ WAVELENGTH 5320

AVERAGE GAIN FUNCTION (1.E+7)

0	19.26
5	15.02
10	10.62
15	10.08
20	11.00
25	10.1A
30	8.65
35	7.56
40	6.40
45	4.94
50	3.72

R.M.S. FLUCTUATION

0	0.00
5	.61
10	.53
15	.47
20	.58
25	.50
30	.37
35	.35
40	.41
45	.30
50	.27

Table 8-13 Circular Polarization

DIMEDRAL ANGLE .75 WAVELENGTH 6963

AVERAGE GAIN FUNCTION (1.5E+7)

0	26.93
5	23.14
10	16.98
15	12.06
20	10.33
25	10.25
30	9.53
35	7.64
40	5.50
45	3.91
50	2.84

R.M.S. FLUCTUATION

0	0.10
5	.57
10	.73
15	.67
20	.50
25	.50
30	.54
35	.49
40	.43
45	.34
50	.24

Table 8-14. Circular polarization.

DIHEDRAL ANGLE 1.25 WAVELENGTH 6943

AVERAGE GAIN FUNCTION (1.E+7)

0	15.59
5	13.39
10	10.07
15	7.95
20	7.91
25	8.51
30	8.21
35	6.98
40	5.68
45	4.74
50	3.95

R.M.S. FLUCTUATION

0	0.00
5	.30
10	.36
15	.31
20	.32
25	.47
30	.50
35	.43
40	.36
45	.29
50	.25

*

*

*

*

*

*

*

*

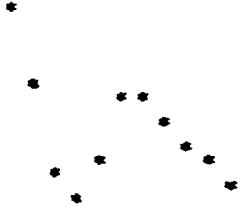
*

Table 8-16. Circular polarization.

DIMEDRAL ANGLE 1.75 WAVELENGTH 6943

AVERAGE GAIN FUNCTION (1.E+7)

0	7.31
5	6.22
10	4.77
15	4.31
20	5.06
25	5.90
30	5.98
35	5.53
40	5.16
45	4.95
50	4.60



R.M.S. FLUCTUATION

0	0.00
5	.12
10	.12
15	.11
20	.26
25	.39
30	.39
35	.31
40	.24
45	.20
50	.21

[Faint, illegible handwritten notes and markings along the right edge of the page.]

Table 8-16. Circular polarization, mixed dihedral angles.

DIHEDRAL ANGLE $\overline{1.25}$ WAVELENGTH 6943

AVERAGE GAIN FUNCTION (1.E+7)

0	16.58
5	14.24
10	10.44
15	8.19
20	7.87
25	8.32
30	7.97
35	6.75
40	5.46
45	4.53
50	3.77

R.M.S. FLUCTUATION

0	0.00 *
5	.48 *
10	.60 *
15	.46 *
20	.40 *
25	.45 *
30	.41 *
35	.31 *
40	.25 *
45	.21 *
50	.22 *

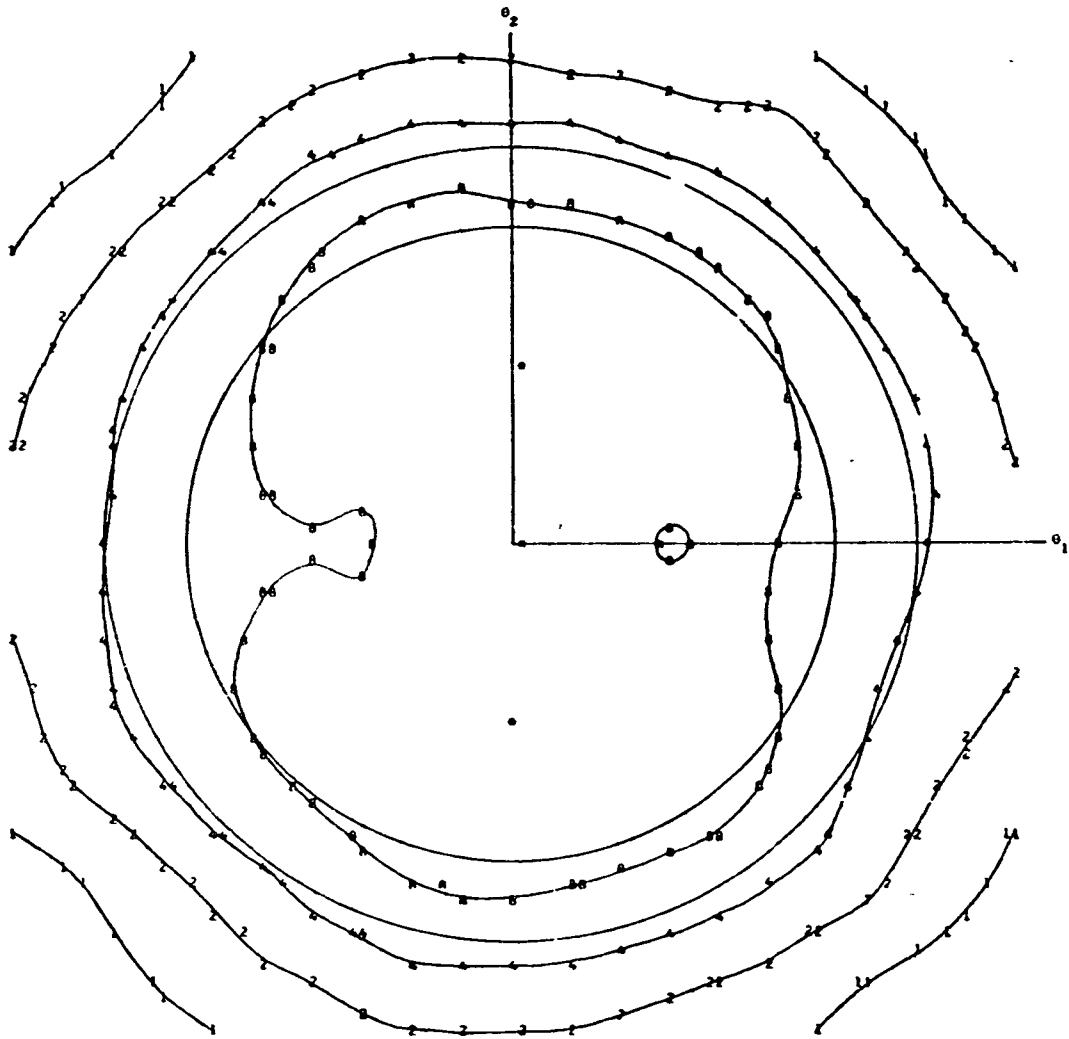


Figure 9(1-16) Contour plots of the gain-function matrices given in Table 7. Circles 32 and 41 μrad in radius are shown to mark the minimum and maximum values of velocity aberration. The numbers are the gain in units of 10^7 . The dihedral-angle offset δ and the wavelength λ are given for each figure. Figure 9-1: Linear polarization, $\delta = 0^\circ 75$, $\lambda = 53.0 \text{ \AA}$.

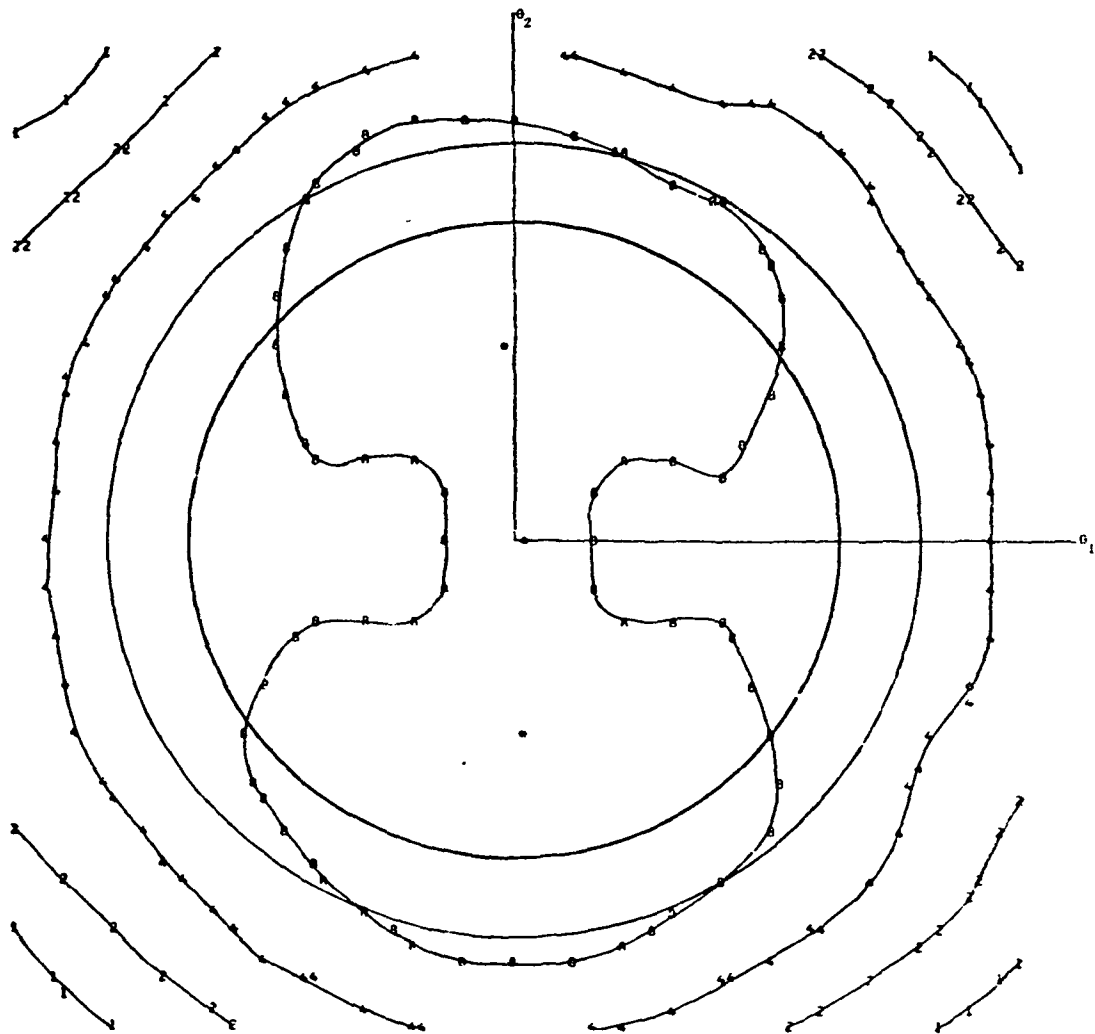


Figure 9-2 Linear polarization, $\delta = 1''25$, $\lambda = 5320 \text{ \AA}$

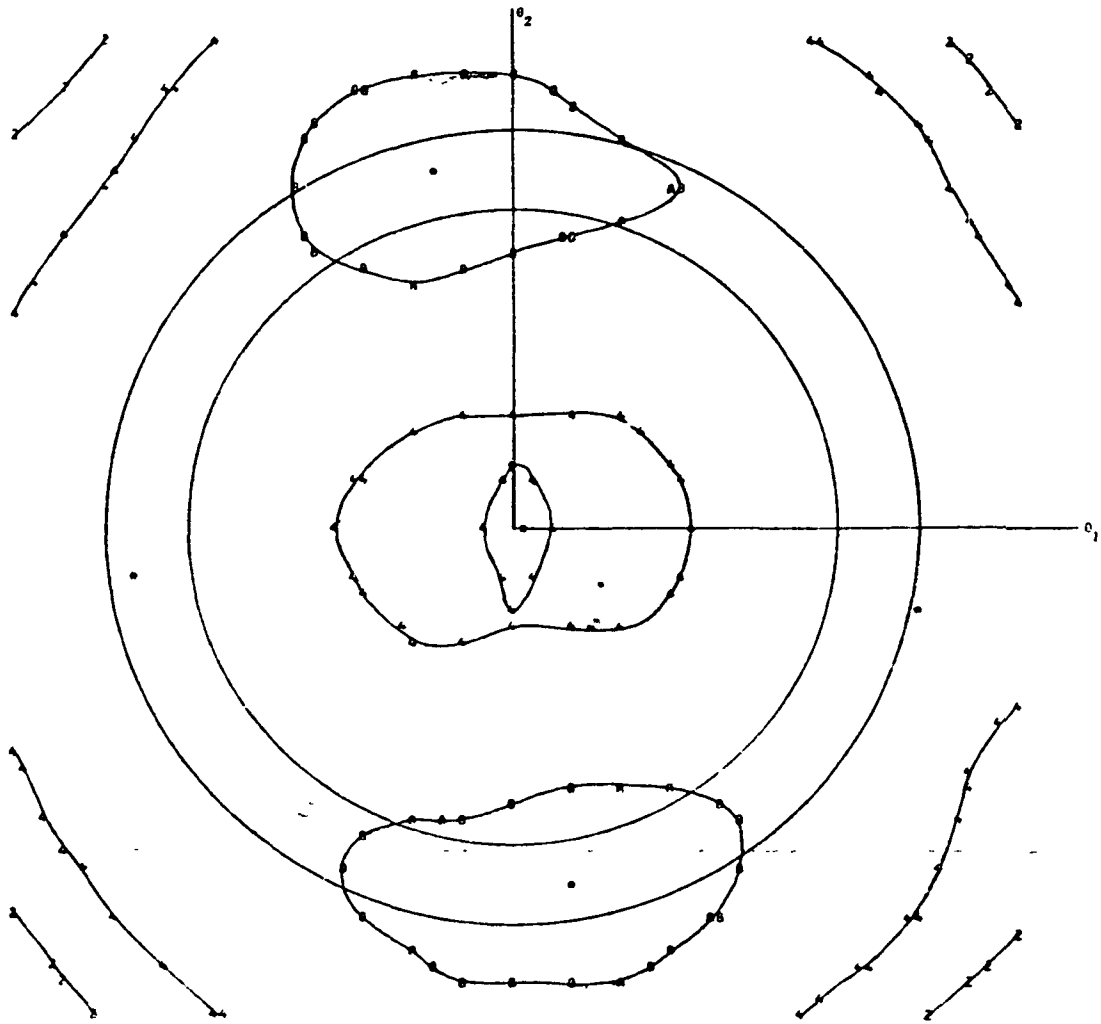


Figure 9-3 Linear polarization $\delta = 1^{\circ}75$, $\lambda = 5320 \text{ \AA}$

This document is the property of the U.S. Government and is loaned to your organization; it and its contents are not to be distributed outside your organization.

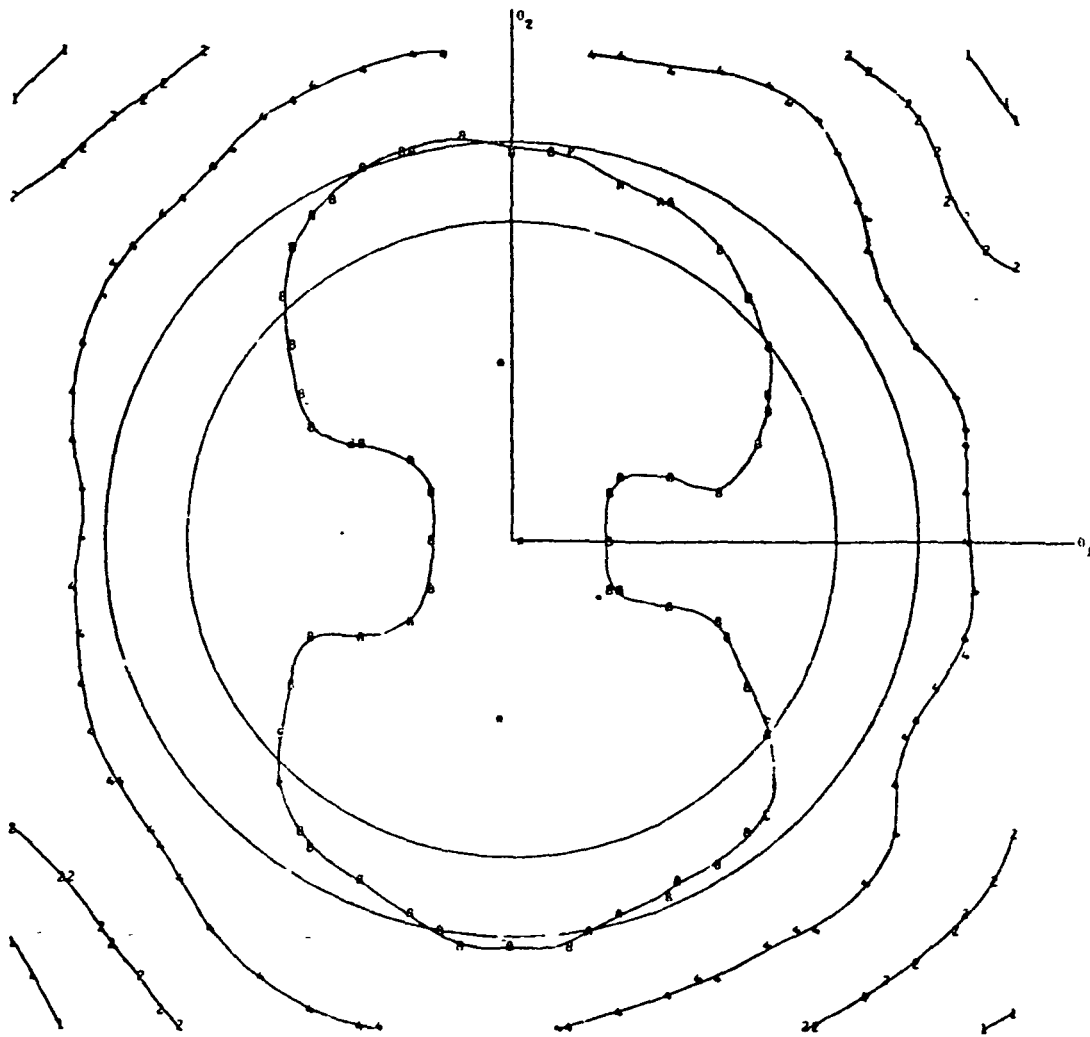


Figure 9-4. Linear polarization, $\delta = 1^{\circ}25'$ (mixed dihedral angles), $\lambda = 5320 \text{ \AA}$.

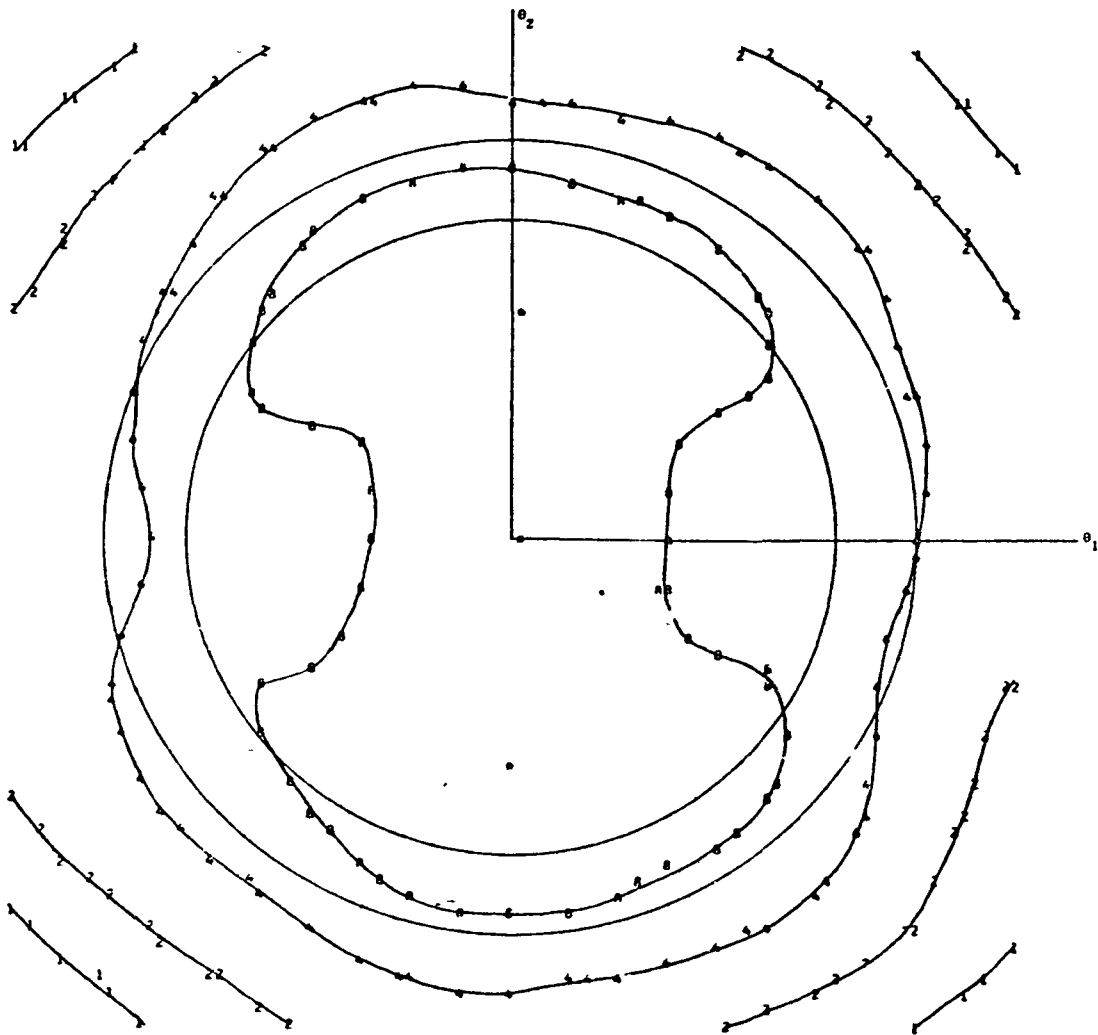


Figure 9-5 Linear polarization, $\delta = 0.75$, $\lambda = 6943 \text{ \AA}$.

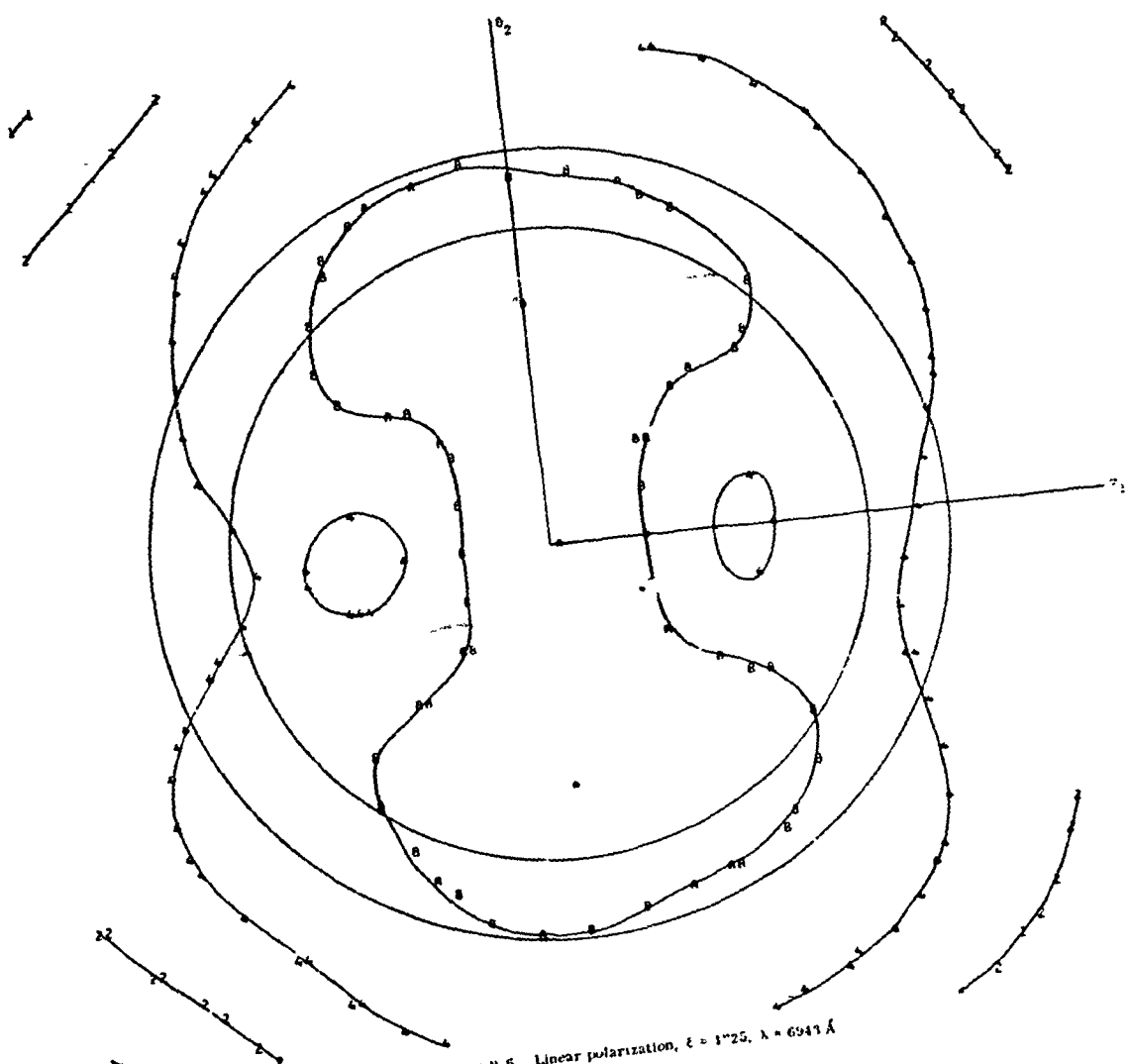


Figure 9-6 Linear polarization, $\xi = 1.25$, $\lambda = 6941 \text{ \AA}$

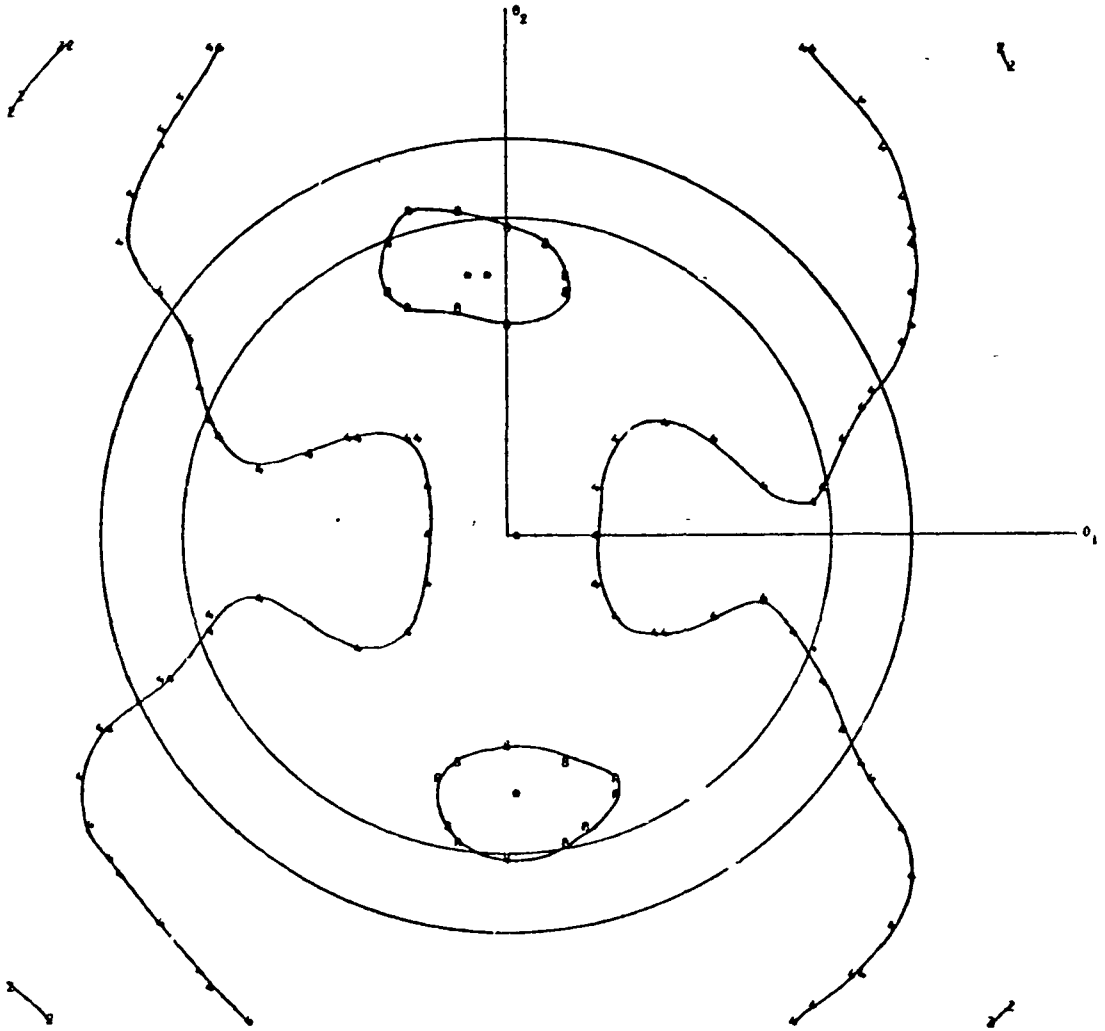


Figure 9-7 Linear polarization, $\delta = 1''75$, $\lambda = 6943 \text{ \AA}$

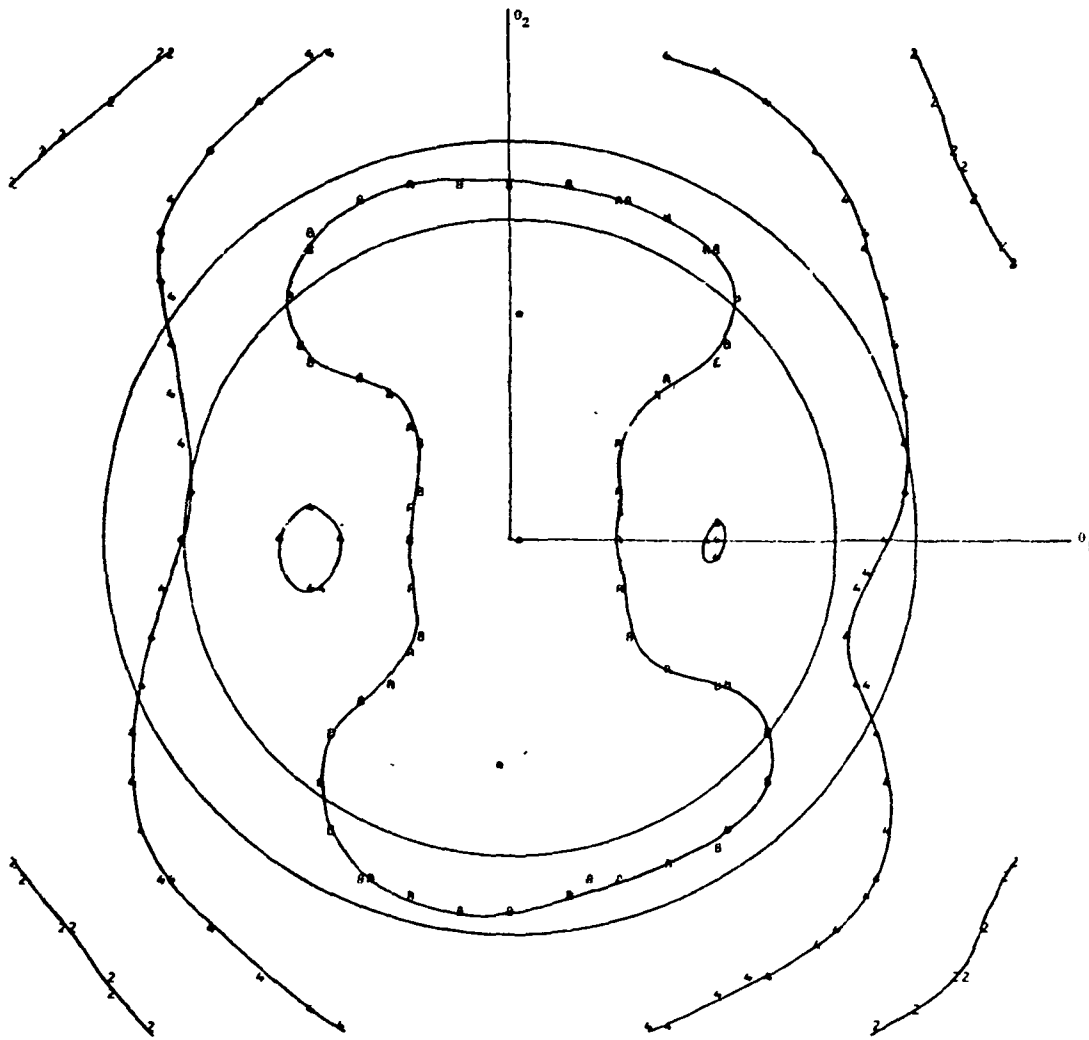


Figure 9-b Linear polarization $Z = 1.25$ (mixed dihedral angles) $\lambda = 6.947 \text{ \AA}$

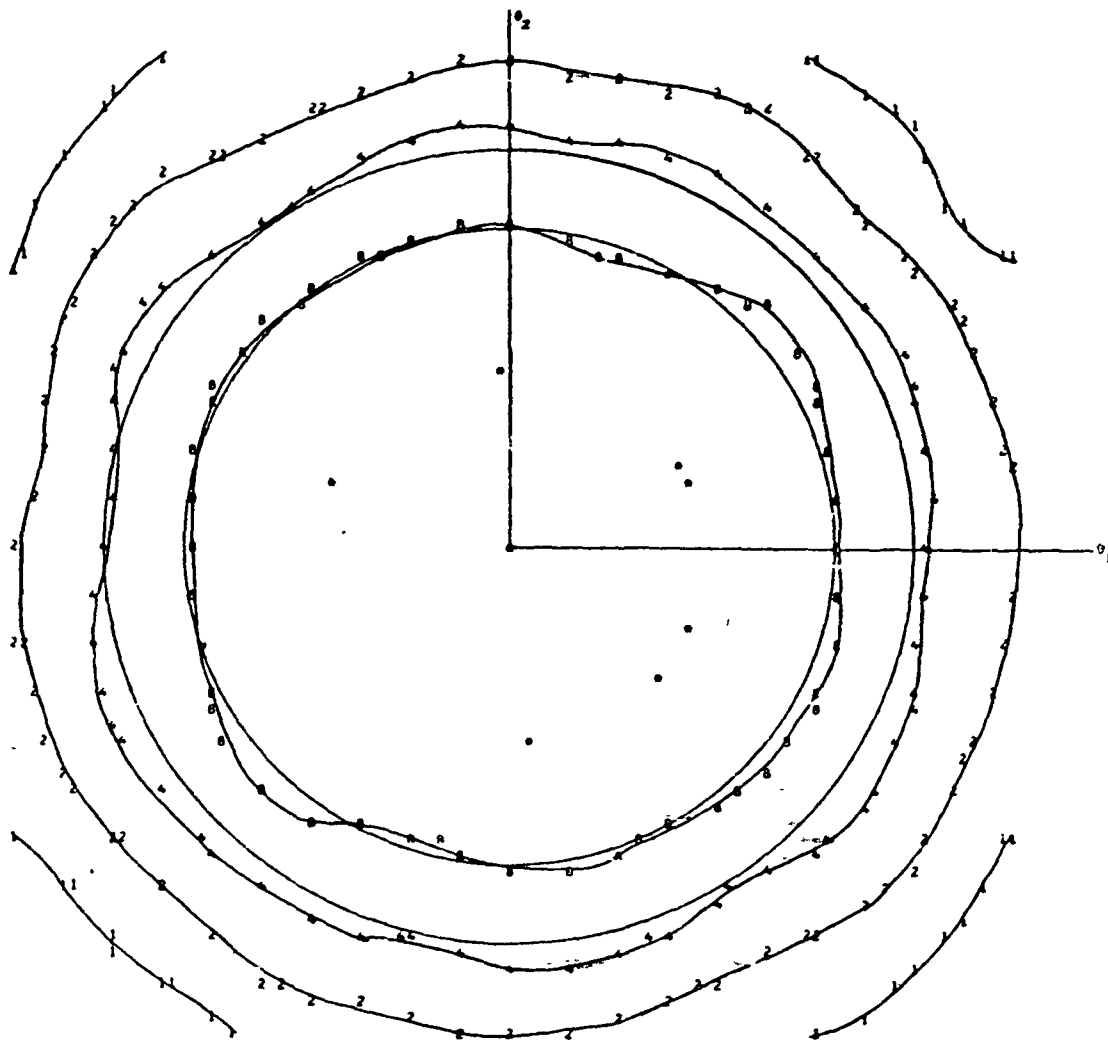
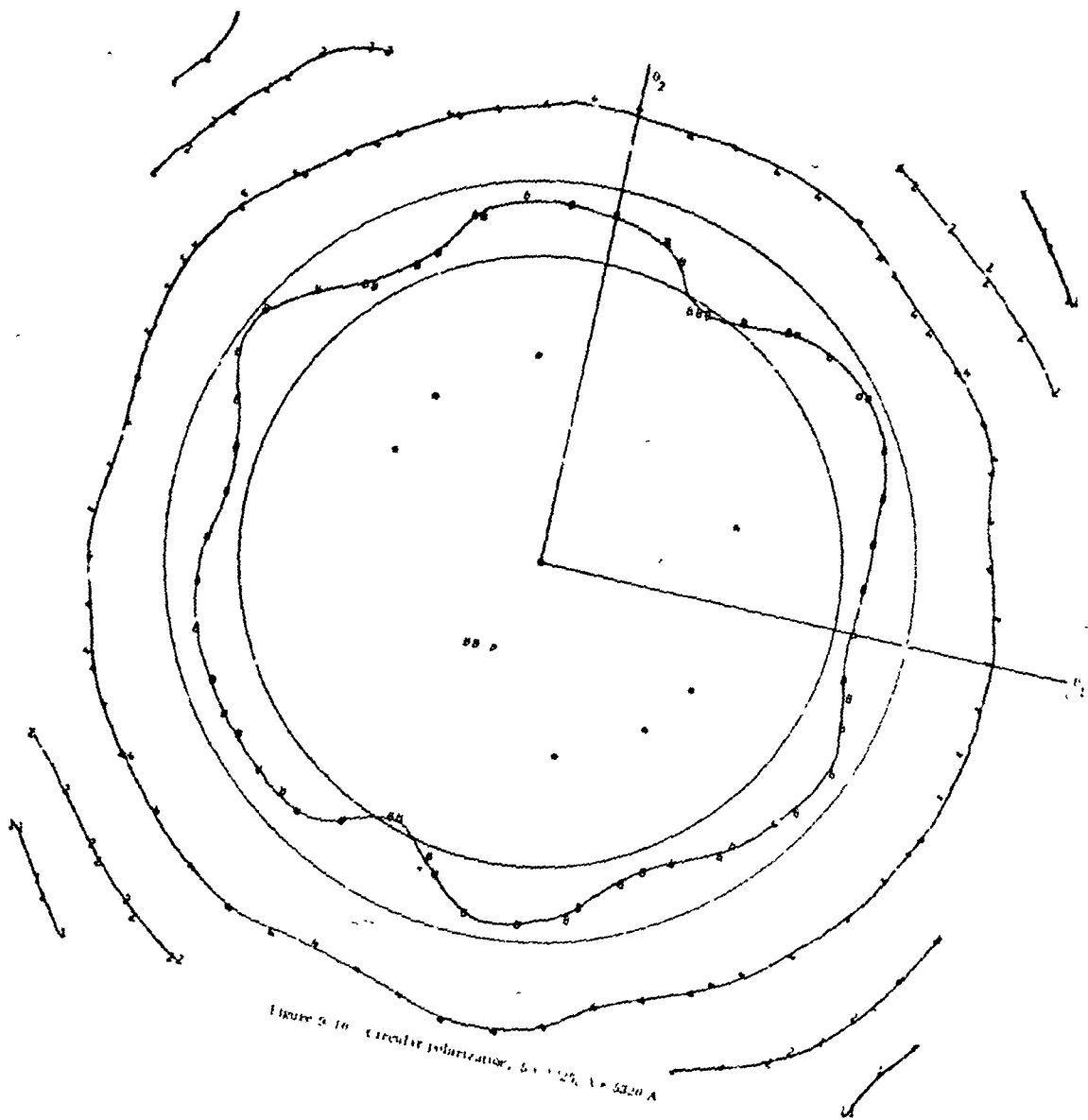


Figure 9-9. Circular polarization, $\epsilon = 0.75$, $\lambda = 5320 \text{ \AA}$

This document is the property of the U.S. Government and is loaned to your organization; it and its contents are not to be distributed outside your organization.



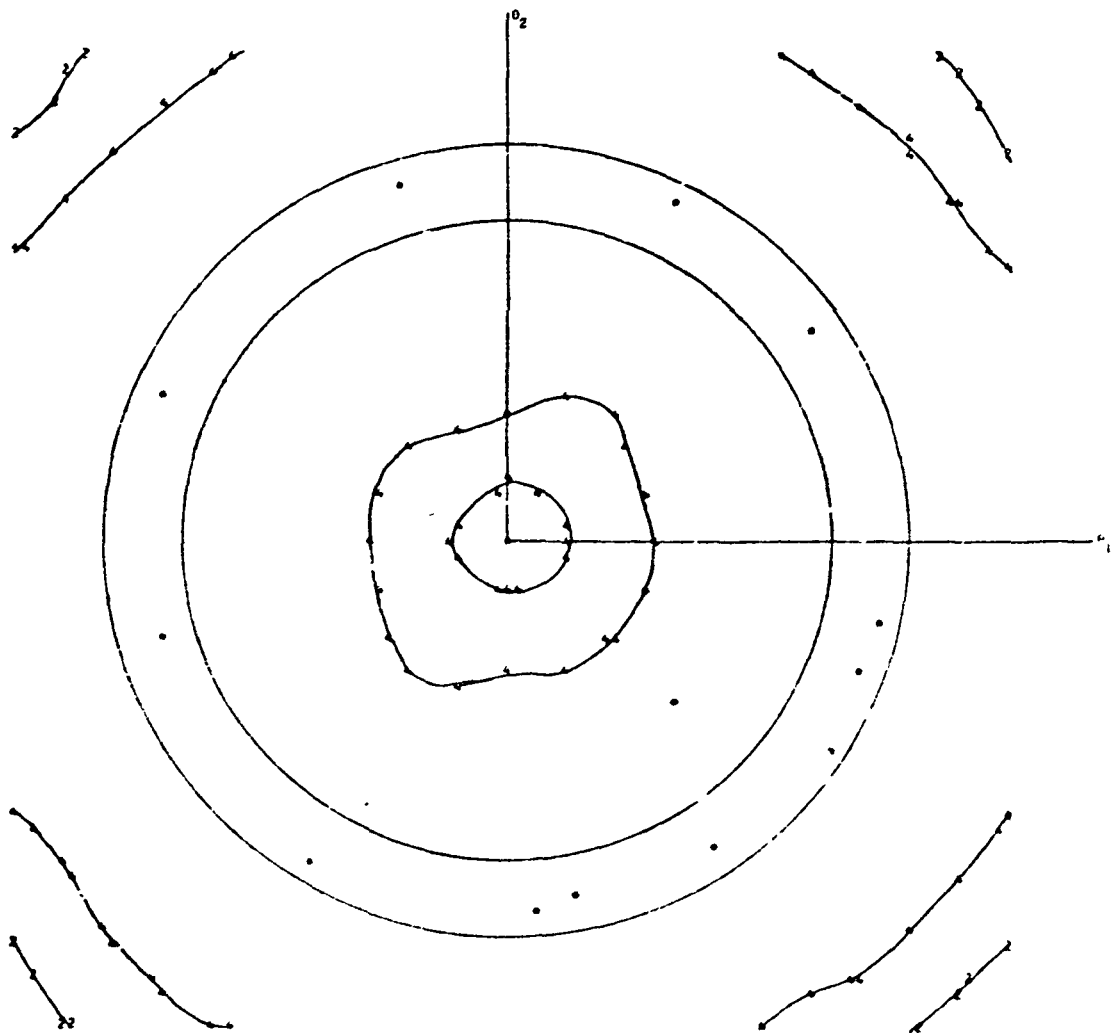
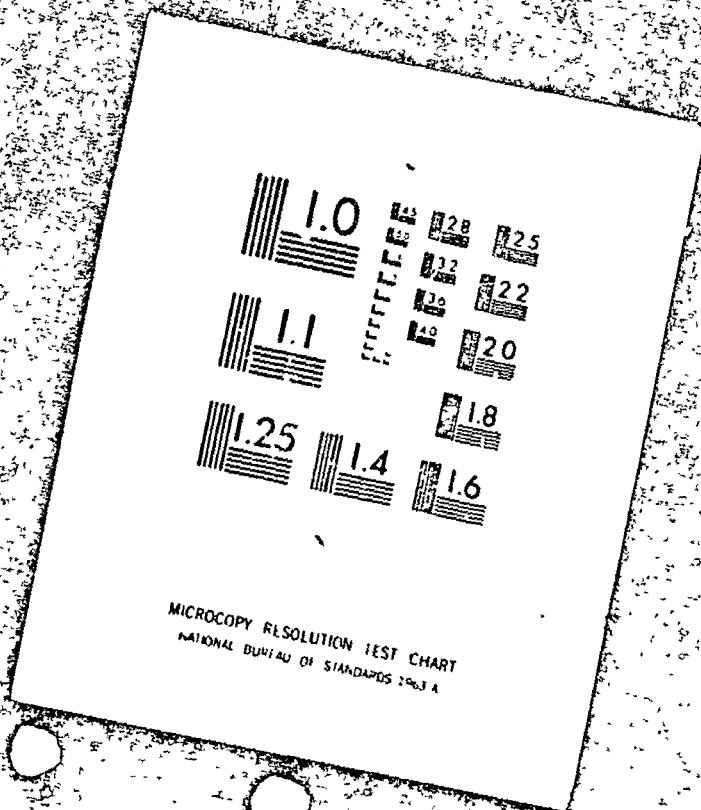


FIGURE 9-11 Circular polarization, $f = 1775 \text{ \AA}$, 5320 \AA

2 OF 2

78 25892 UNCLAS



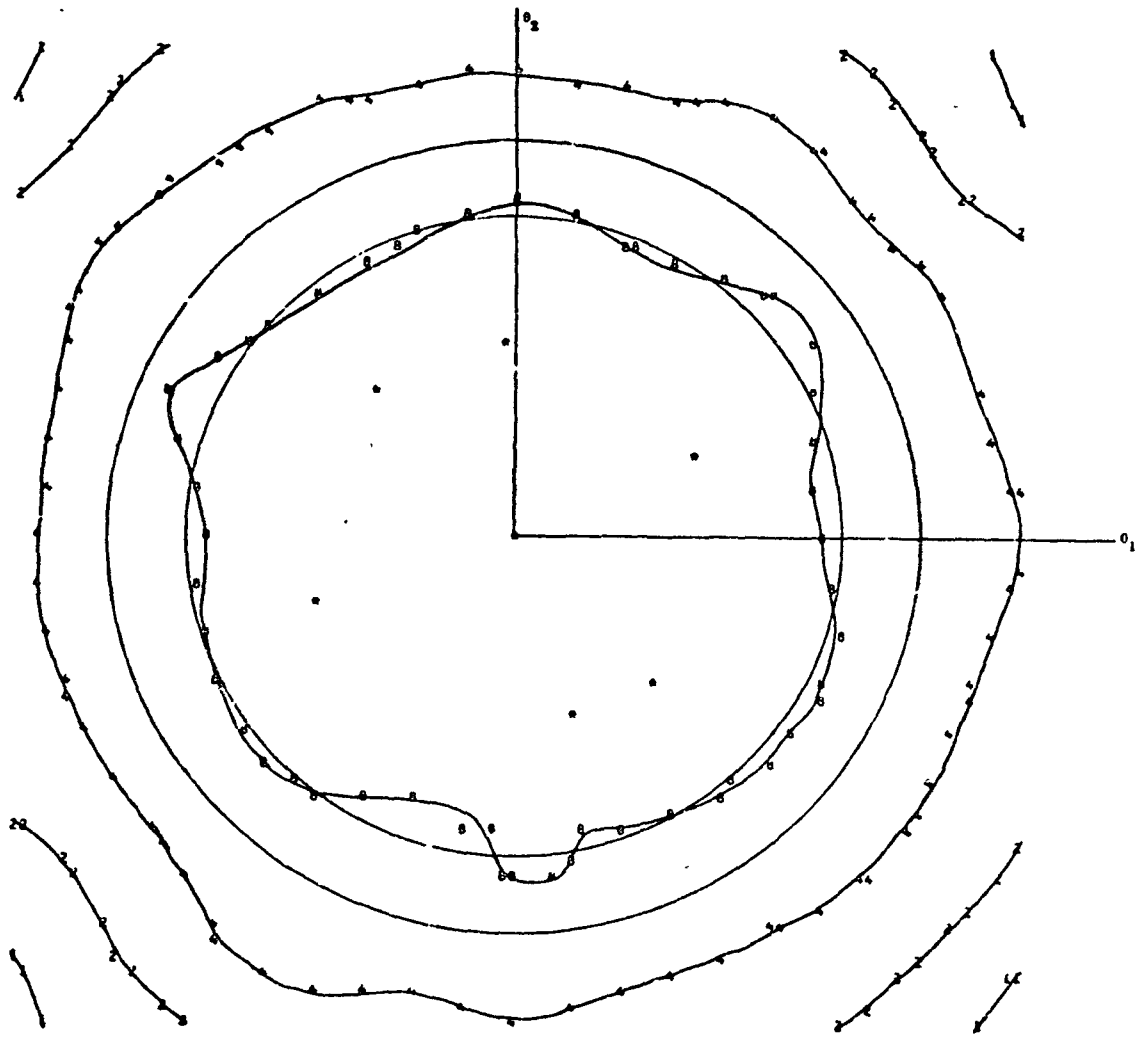


Figure 9-12 Circular polarization, $\delta = 1''25$ (mixed dihedral angles), $\lambda = 5320 \text{ \AA}$

C-2

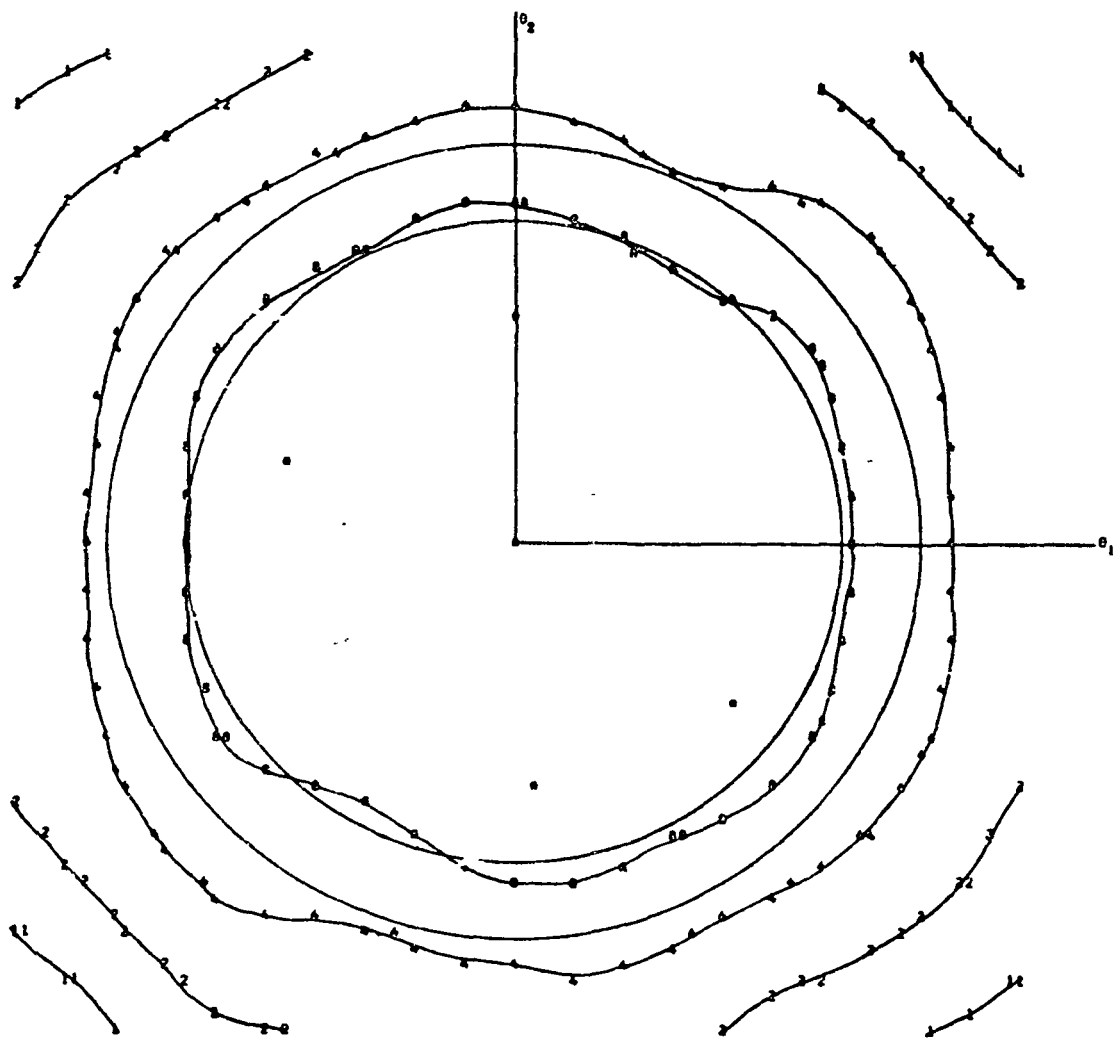


Figure 9-13 Circular polarization, $\delta = 0.75$, $\lambda = 6943 \text{ \AA}$.

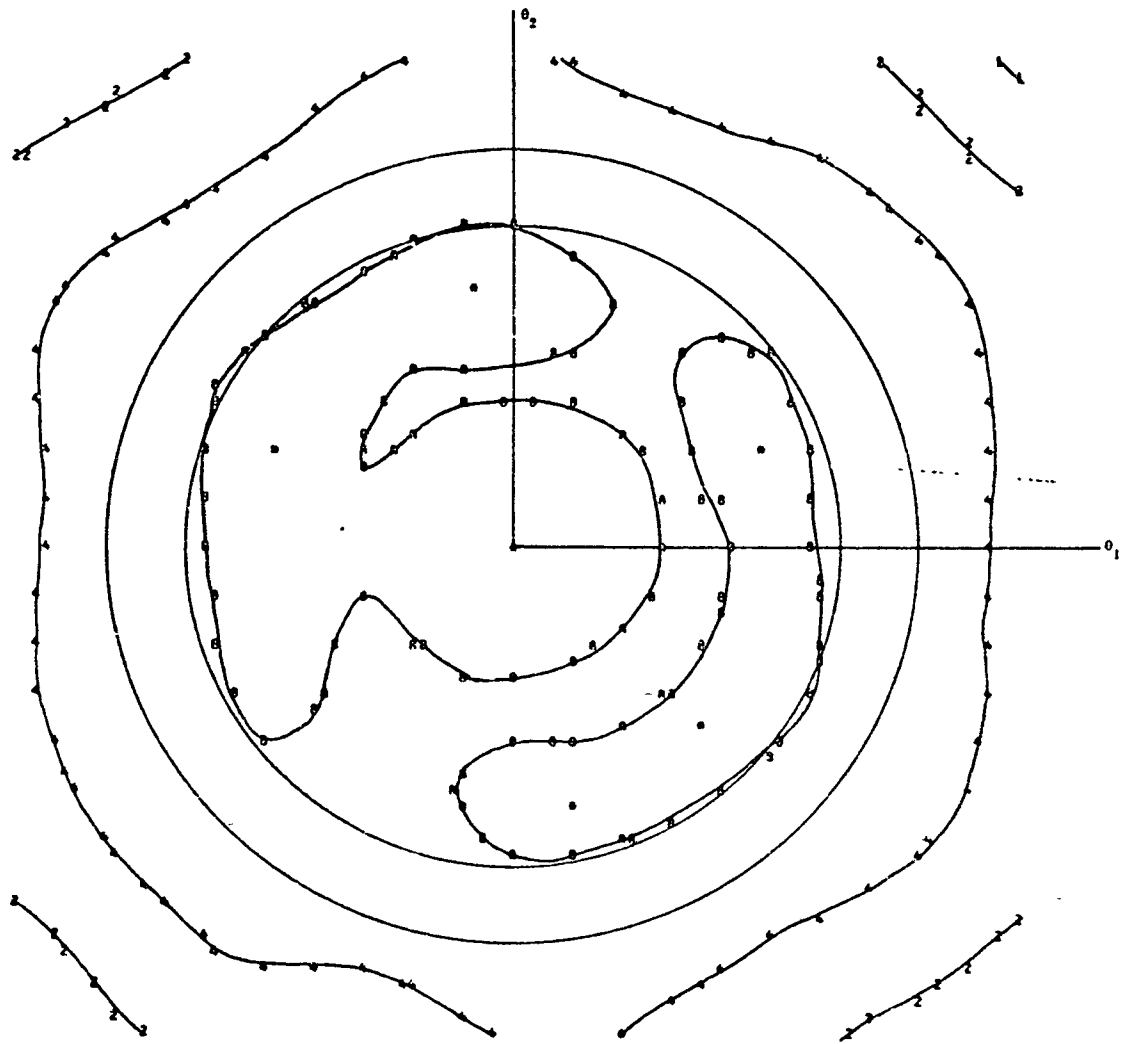


Figure 9-14 Circular polarization, $\delta = 1''25$, $\lambda = 6943 \text{ \AA}$.

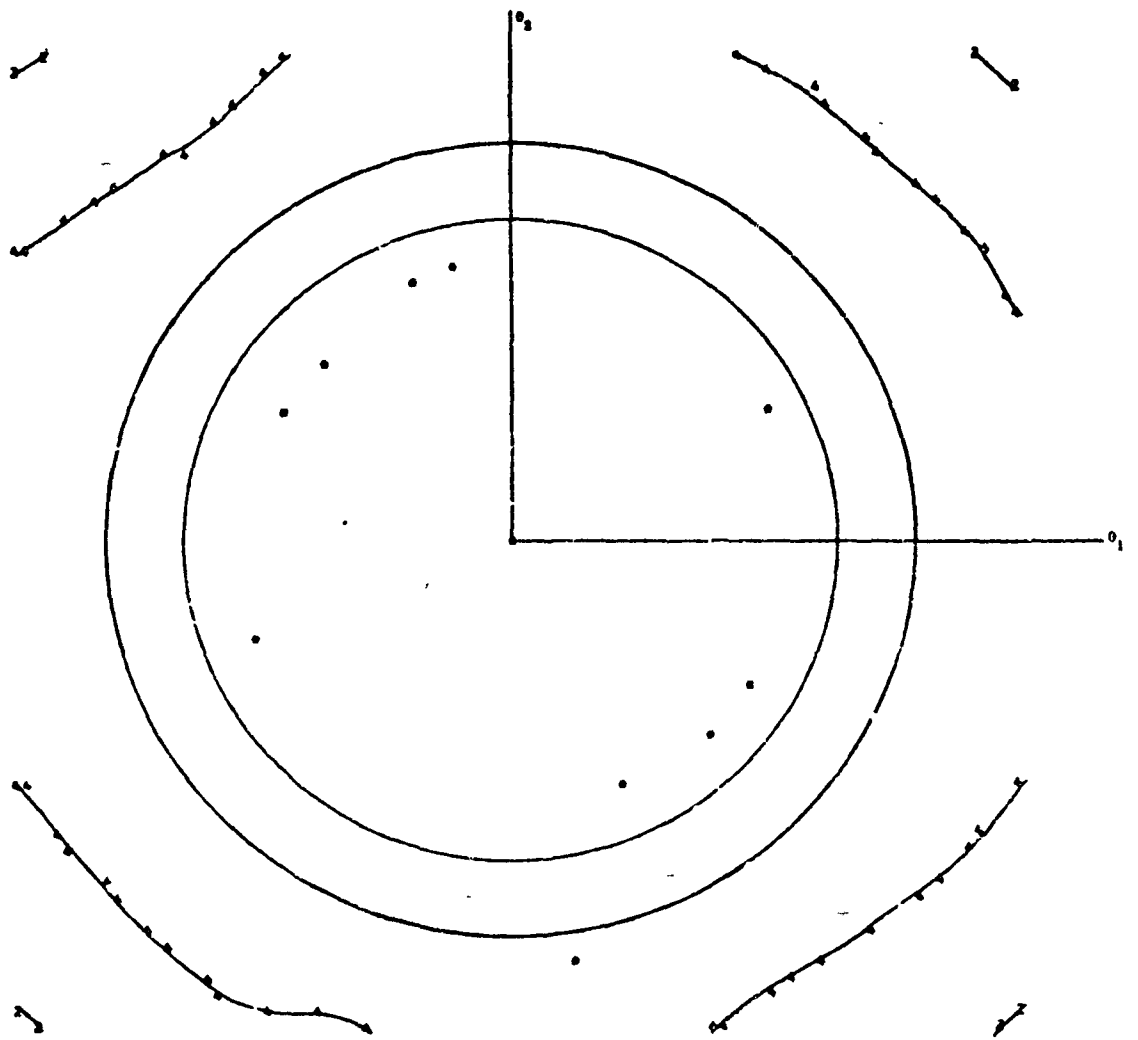


Fig. 9-10. Circular polarization, $\delta = 1.71$, $\lambda = 6943 \text{ \AA}$

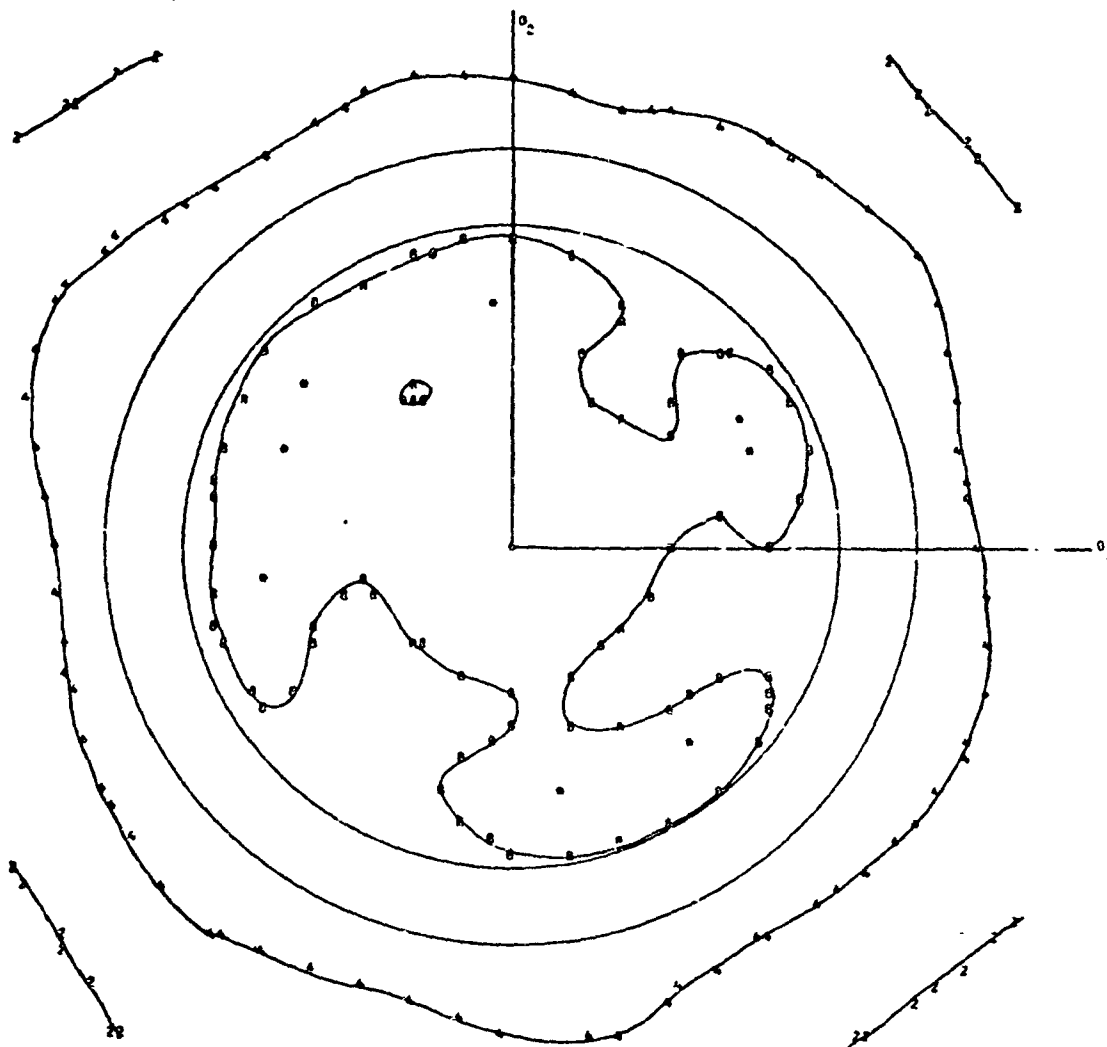


Figure 9-16 Circular polarisation, $\delta = 1^{\circ}25'$ (mixed dihedral angles), $\lambda = 6943 \text{ \AA}$.

Table 9 gives the average gain in the 32- to 41- μ rad annulus for each of the array diffraction patterns computed. At 5320 Å the strongest signal is obtained with the 1.25-arcsec dihedral angle offset. At 6943 Å the intensity is slightly higher at the 0.75-arcsec offset. As can be seen from Table 8, the energy is concentrated in the center of the pattern for small dihedral angle offsets and shifts outward as the offset is increased. At 6943 Å the pattern is wider than at 5320 Å due to diffraction effects, and, in fact, the dihedral angle offset is not really essential at 6943 Å. The phase changes due to total internal reflection at the back faces also help to widen the pattern at both wavelengths. At 5320 Å, the diffraction pattern is sharper than at 6943 Å, and it is possible to obtain a better concentration of energy in the desired range of velocity aberration. Using a mixture of dihedral angle offsets with an average of 1.25 arcsec reduces the gain in the annulus compared to having all the offsets 1.25 arcsec. The effect is greater at 5320 Å because the pattern is sharper at this wavelength. The results for a mixture of offsets are probably more representative of the behavior of the actual array. Multiplication of the gains for linear polarization and mixed offsets by the area for each wavelength gives cross sections of $1.03 \times 10^6 \text{ m}^2$ and $0.90 \times 10^6 \text{ m}^2$ at 5320 Å and 6943 Å, respectively ($13.0 \times 10^6 \text{ m}^2$ and $11.3 \times 10^6 \text{ m}^2$ in standard cross section units).

Table 9. Average gain in the 32-41 μ rad annulus for the gain matrices in Table 7.

Polarization	λ	δ	$G(10^7)$
Linear	5320	0.75	6.4086
		1.25	8.0338
		1.75	7.079134
		<u>1.25</u>	7.191611
	6943	0.75	6.95308
		1.25	6.6090
		1.75	5.47506
		<u>1.25</u>	6.3981
Circular	5320	0.75	6.4418
		1.25	8.01035
		1.75	7.06848
		<u>1.25</u>	7.1942
	6943	0.75	6.8869
		1.25	6.522986
		1.75	5.39929
		<u>1.25</u>	6.295369

10. RANGE CORRECTION

The range corrections presented in this section give the difference between the range that would be measured to a point reflector at the center of the satellite and the range measured to the retroreflector array. All values are for the incoherent case. The effect of coherent interference is discussed in Section 11. The centroid of the total reflected energy (which can be measured only in the laboratory) is 0.2394 m from the center of the satellite. When diffraction is taken into account, the centroid moves to about 0.2425 m. For long incident pulses, the range correction is the same for all pulse detection methods because there is negligible pulse distortion. For short pulses, the range correction is a function of pulse length for methods other than centroid detection. The table below gives range corrections (m) computed for three pulse lengths using the reflectivity curve for 5320 Å in Figure 6 (Section 6).

Table 10. Variation of range correction with pulse length.

Pulse length (nanosecs)	Centroid	Half area	Peak	Half maximum
20.0	0.2427	0.2427	0.2427	0.2428
5.0	0.2427	0.2427	0.2428	0.2431
0.2	0.2427	0.2451	0.2483	0.2506

Tables 14 and 15, and Figure 10 give the centroid range correction matrices, the range correction vs velocity aberration, and contour plots of the range correction matrices. The information is for the same conditions and in the same formats as the gain information in Section 9. The range correction vs velocity aberration in Table 15 is plotted at a scale of one millimeter per horizontal print position. The contour plots of Figure 10 are plotted using the codes in Table 11 below.

Circles of radius 32 and 41 μ rad are drawn to mark the minimum and maximum velocity aberration. The average value of the range correction in the 32- to 41- μ rad annulus is listed for each case in Table 12.

Table 11. Codes for range contour plots in Figure 10.

Range correction (m)	Plot code
0.2380	8
0.2400	0
0.2410	1
0.2420	2
0.2430	3
0.2440	4
0.2450	5

Table 12. Average range correction in the 32-41 μ rad annulus for various cases.

Polarization	Wavelength (\AA)	Dihedral angle offset (arcsecs)	Range correction (m)
Linear	5320	0.75	0.2411
		1.25	0.2426
		1.75	0.2421
		1.25	0.2424
	6943	0.75	0.2425
		1.25	0.2421
		1.75	0.2412
		1.25	0.2424
Circular	5320	0.75	0.2412
		1.25	0.2428
		1.75	0.2424
		1.25	0.2426
	6943	0.75	0.2427
		1.25	0.2426
		1.75	0.2418
		1.25	0.2427

The range corrections for pulse detection methods other than centroid have been computed at selected points in the far field to see how much these corrections vary with velocity aberration. The results are given in Table 13. The standard deviation of the corrections computed (excluding the point at the center of the diffraction pattern) was 1.2 mm for centroid detection, 1.0 mm for half area, 0.9 mm for peak, and 0.7 mm for half maximum detection, and the average values were 0.2429, 0.2456, 0.2490, and 0.2509 m, respectively. A single dihedral angle of 1.25 arcsecs was used.

In summary, the range correction for Lageos for centroid detection is about 0.2425 m for all pulse lengths and wavelengths. For other pulse detection methods, the range correction varies with pulse length and is different for each method.

Table 13. Range correction for four pulse detection techniques at selected points in the far field.

Polarization	Wavelength (Å)	θ_1	θ_2	Centroid	Half area	Peak	Half maximum
Linear	5320	0	0	0.2353	0.2388	0.2458	0.2497
		0	30	0.2428	0.2455	0.2489	0.2508
		0	35	0.2437	0.2464	0.2496	0.2513
		0	40	0.2441	0.2467	0.2497	0.2513
		30	0	0.2391	0.2425	0.2475	0.2502
		35	0	0.2410	0.2444	0.2490	0.2512
		40	0	0.2425	0.2457	0.2496	0.2512
		21.2	21.2	0.2424	0.2446	0.2475	0.2501
		24.7	24.7	0.2431	0.2454	0.2483	0.2506
		28.3	28.3	0.2431	0.2454	0.2482	0.2504
Linear	9643	0	0	0.2389	0.2423	0.2477	0.2503
		0	30	0.2449	0.2472	0.2499	0.2515
		0	35	0.2440	0.2464	0.2494	0.2512
		0	40	0.2432	0.2459	0.2493	0.2511
		30	0	0.2420	0.2457	0.2496	0.2512
		35	0	0.2414	0.2449	0.2489	0.2507
		40	0	0.2410	0.2444	0.2488	0.2510
		21.2	21.2	0.2425	0.2447	0.2473	0.2496
		24.7	24.7	0.2425	0.2446	0.2470	0.2493
		28.3	28.3	0.2427	0.2447	0.2472	0.2497
Circular	5320	0	0	0.2357	0.2391	0.2463	0.2495
		0	0	0.2429	0.2457	0.2490	0.2509
		0	5	0.2442	0.2469	0.2498	0.2514
		0	40	0.2449	0.2474	0.2500	0.2513
		30	0	0.2410	0.2441	0.2482	0.2504
		35	0	0.2417	0.2448	0.2489	0.2508
		40	0	0.2426	0.2456	0.2493	0.2508
		21.2	21.2	0.2428	0.2456	0.2495	0.2517
		24.7	24.7	0.2436	0.2465	0.2502	0.2522
		28.3	28.3	0.2434	0.2461	0.2497	0.2517

Table 13. (Cont.)

Polarization	Wavelength (Å)	θ_1	θ_2	Centroid	Half area	Peak	Half maximum
Circular	6943	0	0	0.2392	0.2426	0.2481	0.2505
		0	30	0.2440	0.2465	0.2495	0.2512
		0	35	0.2438	0.2463	0.2493	0.2510
		0	40	0.2438	0.2465	0.2496	0.2513
		30	0	0.2433	0.2462	0.2492	0.2507
		35	0	0.2424	0.2453	0.2485	0.2502
		40	0	0.2416	0.2446	0.2482	0.2502
		21.2	21.2	0.2438	0.2466	0.2501	0.2519
		24.7	24.7	0.2435	0.2461	0.2496	0.2516
28.3	28.3	0.2434	0.2460	0.2497	0.2518		

Table 14. Centroid range correction matrices. The angles θ_1 and θ_2 in micro-radians, are defined in Figure 8. Table 14-1. Linear polarization.

θ_2	DICHROIC ANGLE .75		WAVELENGTH 5-20		RANGE CORRECTION (METERS)										
	θ_1	0	10	20	25	30	35	40	45	50	60	70	80	90	
50	2368	2370	2346	2330	2319	2310	2308	2305	2304	2303	2302	2301	2300	2299	
45	2366	2353	2341	2338	2348	2347	2347	2347	2347	2347	2347	2347	2347	2347	
40	2356	2351	2344	2337	2335	2332	2330	2328	2326	2324	2322	2320	2318	2316	
35	2348	2354	2367	2378	2392	2405	2416	2426	2434	2441	2447	2451	2454	2456	
30	2337	2362	2395	2439	2480	2511	2533	2548	2558	2564	2568	2571	2573	2574	
25	2326	2386	2451	2517	2584	2641	2688	2726	2755	2775	2788	2795	2799	2801	
20	2314	2401	2478	2547	2603	2645	2678	2703	2720	2729	2735	2739	2741	2742	
15	2309	2406	2479	2532	2572	2600	2618	2628	2633	2636	2638	2639	2640	2640	
10	2306	2399	2472	2522	2557	2582	2598	2606	2610	2612	2613	2614	2614	2614	
5	2303	2390	2467	2513	2545	2568	2582	2589	2593	2595	2596	2597	2597	2597	
0	2300	2387	2464	2509	2539	2561	2574	2580	2583	2584	2585	2585	2585	2585	
-5	2300	2397	2474	2519	2549	2571	2584	2590	2593	2595	2596	2597	2597	2597	
-10	2306	2394	2471	2516	2546	2568	2581	2587	2590	2592	2593	2594	2594	2594	
-15	2319	2394	2471	2516	2546	2568	2581	2587	2590	2592	2593	2594	2594	2594	
-20	2338	2391	2468	2513	2543	2565	2578	2584	2587	2589	2590	2591	2591	2591	
-25	2364	2374	2451	2496	2526	2548	2561	2567	2570	2572	2573	2574	2574	2574	
-30	2351	2350	2427	2472	2502	2524	2537	2543	2546	2548	2549	2550	2550	2550	
-35	2348	2338	2414	2459	2489	2511	2524	2530	2533	2535	2536	2537	2537	2537	
-40	2379	2365	2441	2486	2516	2538	2551	2557	2560	2562	2563	2564	2564	2564	
-45	2407	2394	2464	2509	2539	2561	2574	2580	2583	2585	2586	2587	2587	2587	
-50	2405	2399	2464	2509	2539	2561	2574	2580	2583	2585	2586	2587	2587	2587	

Table 14-2. Linear polarization.

θ_2	DIPEDRAL ANGLE 1.25 WAVELENGTH 5320																				
	RANGE CORRECTIO (METERS)																				
	50	45	40	35	30	25	20	15	10	5	0	-5	-10	-15	-20	-25	-30	-35	-40	-45	-50
50	2350	2339	2331	2327	2326	2325	2325	2325	2325	2325	2325	2325	2325	2325	2325	2325	2325	2325	2325	2325	2325
45	2352	2340	2334	2330	2329	2328	2328	2328	2328	2328	2328	2328	2328	2328	2328	2328	2328	2328	2328	2328	2328
40	2364	2367	2374	2381	2385	2388	2390	2391	2392	2393	2394	2395	2396	2397	2398	2399	2400	2401	2402	2403	2404
35	2378	2383	2391	2399	2407	2416	2423	2429	2434	2437	2441	2443	2445	2447	2448	2449	2450	2451	2452	2453	2454
30	2386	2397	2409	2418	2427	2436	2443	2449	2454	2457	2460	2462	2464	2466	2467	2468	2469	2470	2471	2472	2473
25	2397	2411	2425	2433	2438	2441	2445	2448	2450	2452	2454	2456	2457	2458	2459	2460	2461	2462	2463	2464	2465
20	2411	2420	2433	2437	2442	2447	2450	2453	2455	2457	2459	2460	2461	2462	2463	2464	2465	2466	2467	2468	2469
15	2420	2423	2432	2434	2438	2442	2445	2448	2450	2452	2454	2456	2457	2458	2459	2460	2461	2462	2463	2464	2465
10	2420	2419	2425	2425	2425	2425	2425	2425	2425	2425	2425	2425	2425	2425	2425	2425	2425	2425	2425	2425	2425
5	2419	2414	2415	2409	2387	2388	2404	2347	2288	2321	2349	2326	2285	2363	2412	2400	2390	2391	2391	2391	2391
0	2418	2412	2406	2391	2364	2373	2368	2316	2233	2319	2357	2321	2237	2327	2404	2399	2391	2391	2391	2391	2391
-5	2412	2409	2403	2384	2360	2375	2366	2354	2282	2323	2348	2324	2286	2352	2395	2388	2389	2389	2389	2389	2389
-10	2399	2404	2405	2396	2381	2391	2410	2401	2370	2363	2369	2366	2377	2400	2400	2384	2390	2414	2414	2414	2414
-15	2395	2403	2413	2416	2410	2408	2414	2416	2414	2412	2412	2413	2419	2420	2408	2382	2400	2415	2415	2415	2415
-20	2395	2405	2417	2428	2432	2427	2420	2426	2426	2430	2427	2424	2424	2421	2413	2409	2415	2418	2418	2418	2418
-25	2398	2405	2413	2426	2438	2440	2434	2429	2429	2430	2432	2431	2426	2422	2421	2422	2425	2428	2428	2428	2428
-30	2391	2398	2405	2416	2430	2440	2443	2441	2439	2437	2435	2431	2429	2428	2428	2427	2427	2427	2427	2427	2427
-35	2372	2386	2398	2409	2421	2431	2439	2443	2445	2445	2443	2440	2435	2429	2425	2425	2425	2425	2425	2425	2425
-40	2352	2370	2388	2404	2416	2423	2428	2435	2442	2446	2445	2441	2432	2420	2411	2409	2413	2414	2414	2414	2414
-45	2346	2357	2368	2387	2405	2413	2416	2423	2430	2439	2440	2433	2421	2404	2391	2386	2384	2381	2380	2380	2380
-50	2343	2344	2345	2355	2377	2393	2400	2408	2419	2427	2427	2420	2404	2383	2366	2356	2351	2351	2351	2351	2351

Table 14-3 Linear polarization.

θ ₂	DIMEDRAL ANGLE 1.75 WAVELENGTH 5320																					
	RANGE CORRECTION (METERS)																					
	-50	-45	-40	-35	-30	-25	-20	-15	-10	-5	0	5	10	15	20	25	30	35	40	45	50 θ ₁	
0																						
5	2348	2355	2372	2395	2414	2425	2430	2430	2432	2435	2438	2440	2439	2439	2441	2445	2442	2433	2423	2415	2402	2373
10	2369	2380	2396	2411	2423	2430	2433	2433	2435	2439	2441	2447	2440	2437	2439	2446	2440	2441	2430	2420	2408	2384
15	2390	2398	2408	2418	2425	2430	2432	2432	2435	2437	2440	2441	2439	2435	2435	2442	2440	2432	2420	2408	2391	
20	2404	2407	2412	2419	2424	2427	2428	2428	2429	2430	2432	2433	2433	2432	2431	2436	2440	2429	2417	2406	2396	
25	2412	2411	2415	2421	2425	2425	2421	2417	2415	2413	2411	2411	2413	2420	2427	2431	2432	2422	2412	2406	2403	
30	2418	2418	2419	2426	2427	2418	2407	2400	2398	2394	2387	2387	2400	2414	2421	2423	2423	2416	2409	2408	2409	
35	2427	2422	2422	2427	2421	2399	2385	2377	2379	2379	2381	2378	2386	2397	2403	2409	2415	2414	2410	2411	2413	
40	2434	2424	2420	2422	2406	2375	2374	2368	2368	2365	2359	2359	2370	2385	2396	2397	2401	2412	2415	2415	2416	
45	2432	2419	2409	2402	2378	2361	2382	2389	2382	2382	2374	2369	2378	2378	2378	2385	2370	2402	2418	2420	2420	
50	2427	2416	2405	2391	2361	2352	2376	2367	2367	2366	2356	2347	2358	2351	2369	2392	2370	2402	2418	2424	2426	
-5	2418	2411	2407	2396	2356	2352	2379	2361	2361	2352	2342	2354	2346	2351	2368	2391	2374	2407	2419	2428	2436	
-10	2405	2402	2400	2392	2373	2366	2383	2380	2380	2372	2362	2374	2364	2370	2373	2382	2386	2410	2419	2429	2438	
-15	2399	2399	2402	2405	2399	2389	2385	2382	2370	2358	2354	2363	2381	2387	2377	2376	2396	2410	2415	2424	2434	
-20	2403	2405	2408	2414	2420	2415	2401	2388	2382	2381	2378	2378	2383	2387	2390	2400	2411	2411	2408	2413	2421	
-25	2408	2413	2415	2420	2429	2432	2425	2412	2400	2394	2390	2380	2391	2399	2409	2420	2424	2418	2408	2403	2406	
-30	2408	2417	2422	2426	2432	2437	2438	2432	2425	2419	2416	2415	2415	2419	2427	2432	2432	2428	2417	2405	2398	
-35	2399	2414	2426	2435	2440	2442	2441	2439	2438	2437	2436	2434	2430	2427	2427	2431	2435	2438	2424	2410	2398	
-40	2385	2406	2417	2427	2434	2440	2443	2442	2442	2444	2444	2444	2439	2431	2429	2431	2433	2430	2422	2411	2398	
-45	2374	2399	2411	2422	2432	2445	2450	2448	2445	2447	2447	2444	2439	2434	2430	2437	2433	2415	2407	2402	2396	
-50	2364	2392	2408	2421	2435	2444	2446	2445	2445	2446	2445	2443	2438	2432	2425	2417	2405	2390	2379	2378	2383	

Table 14-4 Linear polarization, mixed dihedral angles.

DIPEDRAL ANGLE	WAVELENGTH (MICRONS)		WAVELENGTH (MICRONS)		WAVELENGTH (MICRONS)		WAVELENGTH (MICRONS)		WAVELENGTH (MICRONS)		WAVELENGTH (MICRONS)		WAVELENGTH (MICRONS)		WAVELENGTH (MICRONS)		WAVELENGTH (MICRONS)		WAVELENGTH (MICRONS)		
	1.25	1.35	1.25	1.35	1.25	1.35	1.25	1.35	1.25	1.35	1.25	1.35	1.25	1.35	1.25	1.35	1.25	1.35	1.25	1.35	
0	2391	2347	2347	2319	2319	2300	2300	2287	2287	2287	2287	2287	2287	2287	2287	2287	2287	2287	2287	2287	2287
5	2388	2347	2347	2319	2319	2300	2300	2287	2287	2287	2287	2287	2287	2287	2287	2287	2287	2287	2287	2287	2287
10	2385	2347	2347	2319	2319	2300	2300	2287	2287	2287	2287	2287	2287	2287	2287	2287	2287	2287	2287	2287	2287
15	2382	2347	2347	2319	2319	2300	2300	2287	2287	2287	2287	2287	2287	2287	2287	2287	2287	2287	2287	2287	2287
20	2379	2347	2347	2319	2319	2300	2300	2287	2287	2287	2287	2287	2287	2287	2287	2287	2287	2287	2287	2287	2287
25	2376	2347	2347	2319	2319	2300	2300	2287	2287	2287	2287	2287	2287	2287	2287	2287	2287	2287	2287	2287	2287
30	2373	2347	2347	2319	2319	2300	2300	2287	2287	2287	2287	2287	2287	2287	2287	2287	2287	2287	2287	2287	2287
35	2370	2347	2347	2319	2319	2300	2300	2287	2287	2287	2287	2287	2287	2287	2287	2287	2287	2287	2287	2287	2287
40	2367	2347	2347	2319	2319	2300	2300	2287	2287	2287	2287	2287	2287	2287	2287	2287	2287	2287	2287	2287	2287
45	2364	2347	2347	2319	2319	2300	2300	2287	2287	2287	2287	2287	2287	2287	2287	2287	2287	2287	2287	2287	2287
50	2361	2347	2347	2319	2319	2300	2300	2287	2287	2287	2287	2287	2287	2287	2287	2287	2287	2287	2287	2287	2287
55	2358	2347	2347	2319	2319	2300	2300	2287	2287	2287	2287	2287	2287	2287	2287	2287	2287	2287	2287	2287	2287
60	2355	2347	2347	2319	2319	2300	2300	2287	2287	2287	2287	2287	2287	2287	2287	2287	2287	2287	2287	2287	2287
65	2352	2347	2347	2319	2319	2300	2300	2287	2287	2287	2287	2287	2287	2287	2287	2287	2287	2287	2287	2287	2287
70	2349	2347	2347	2319	2319	2300	2300	2287	2287	2287	2287	2287	2287	2287	2287	2287	2287	2287	2287	2287	2287
75	2346	2347	2347	2319	2319	2300	2300	2287	2287	2287	2287	2287	2287	2287	2287	2287	2287	2287	2287	2287	2287
80	2343	2347	2347	2319	2319	2300	2300	2287	2287	2287	2287	2287	2287	2287	2287	2287	2287	2287	2287	2287	2287
85	2340	2347	2347	2319	2319	2300	2300	2287	2287	2287	2287	2287	2287	2287	2287	2287	2287	2287	2287	2287	2287
90	2337	2347	2347	2319	2319	2300	2300	2287	2287	2287	2287	2287	2287	2287	2287	2287	2287	2287	2287	2287	2287
95	2334	2347	2347	2319	2319	2300	2300	2287	2287	2287	2287	2287	2287	2287	2287	2287	2287	2287	2287	2287	2287
100	2331	2347	2347	2319	2319	2300	2300	2287	2287	2287	2287	2287	2287	2287	2287	2287	2287	2287	2287	2287	2287

Table 14-5 Linear polarization

DIMEDRAL ANGLE .75 WAVELENGTH .943

RANGE CORRECTION (METERS)

θ_2	-30	-25	-20	-15	-10	-5	0	5	10	15	20	25	30	35	40	45	50	θ_1		
0	2354	2345	2339	2341	2352	2367	2381	2391	2394	2390	2382	2376	2379	2381	2382	2383	2382	2377	2360	2363
5	2359	2355	2350	2352	2367	2382	2394	2404	2407	2407	2393	2393	2396	2403	2403	2398	2391	2384	2375	2364
10	2367	2367	2367	2382	2397	2412	2423	2424	2423	2417	2413	2414	2417	2423	2423	2419	2413	2405	2396	2371
15	2378	2379	2381	2396	2411	2426	2439	2446	2446	2440	2433	2428	2433	2439	2439	2433	2427	2420	2409	2383
20	2415	2412	2398	2390	2396	2405	2421	2433	2444	2452	2455	2456	2459	2462	2462	2459	2454	2447	2437	2407
25	2426	2422	2406	2400	2410	2422	2429	2435	2442	2450	2455	2456	2459	2462	2462	2459	2454	2447	2437	2407
30	2431	2429	2418	2417	2427	2435	2443	2452	2459	2466	2472	2477	2482	2487	2487	2484	2480	2475	2465	2435
35	2448	2441	2426	2420	2430	2440	2447	2455	2463	2470	2477	2483	2489	2494	2494	2491	2487	2482	2472	2442
40	2418	2424	2424	2432	2441	2450	2459	2468	2476	2484	2492	2500	2508	2515	2522	2529	2536	2543	2550	2514
45	2402	2406	2409	2412	2421	2430	2439	2448	2457	2466	2475	2484	2493	2502	2511	2520	2529	2538	2547	2511
50	2389	2388	2392	2409	2420	2430	2436	2443	2450	2457	2464	2471	2478	2485	2492	2500	2507	2514	2521	2485
55	2385	2381	2388	2409	2424	2434	2441	2448	2455	2462	2469	2476	2483	2490	2497	2504	2511	2518	2525	2489
60	2391	2387	2395	2417	2433	2443	2450	2457	2464	2471	2478	2485	2492	2499	2506	2513	2520	2527	2534	2498
65	2401	2400	2406	2421	2436	2446	2453	2460	2467	2474	2481	2488	2495	2502	2509	2516	2523	2530	2537	2501
70	2411	2414	2415	2422	2430	2439	2448	2457	2466	2475	2484	2493	2502	2511	2520	2529	2538	2547	2556	2520
75	2416	2422	2423	2421	2420	2423	2430	2438	2446	2454	2462	2470	2478	2486	2494	2502	2510	2518	2526	2490
80	2410	2421	2424	2419	2412	2411	2421	2430	2438	2446	2454	2462	2470	2478	2486	2494	2502	2510	2518	2482
85	2398	2406	2415	2414	2408	2401	2412	2421	2429	2437	2445	2453	2461	2469	2477	2485	2493	2501	2509	2473
90	2398	2395	2391	2399	2401	2401	2407	2418	2428	2437	2446	2455	2464	2473	2482	2491	2500	2509	2518	2482
95	2342	2349	2361	2374	2386	2396	2401	2407	2415	2423	2431	2439	2447	2455	2463	2471	2479	2487	2495	2459
100	2355	2352	2353	2358	2367	2377	2386	2392	2398	2399	2399	2399	2399	2399	2399	2399	2399	2399	2399	2371

Table 14-7. Linear polarization.

θ_2	DIPEDRAL ANGLE 1.75		WAVELENGTH 6943		RANGE CORRECTION (METERS)																		
	-50	-45	-40	-35	-30	-25	-20	-15	-10	-5	0	5	10	15	20	25	30	35	40	45	50		
50	2393	2400	2408	2414	2422	2428	2434	2439	2443	2446	2447	2447	2445	2440	2436	2435	2435	2435	2435	2435	2435	2435	2410
45	2404	2410	2416	2421	2425	2428	2430	2430	2430	2430	2430	2430	2430	2430	2430	2430	2430	2430	2430	2430	2430	2430	2411
40	2417	2423	2429	2433	2436	2438	2439	2439	2439	2439	2439	2439	2439	2439	2439	2439	2439	2439	2439	2439	2439	2439	2411
35	2428	2433	2438	2442	2445	2447	2448	2448	2448	2448	2448	2448	2448	2448	2448	2448	2448	2448	2448	2448	2448	2448	2413
30	2438	2443	2448	2452	2455	2457	2458	2458	2458	2458	2458	2458	2458	2458	2458	2458	2458	2458	2458	2458	2458	2458	2413
25	2449	2454	2459	2463	2466	2468	2469	2469	2469	2469	2469	2469	2469	2469	2469	2469	2469	2469	2469	2469	2469	2469	2413
20	2459	2464	2469	2473	2476	2478	2479	2479	2479	2479	2479	2479	2479	2479	2479	2479	2479	2479	2479	2479	2479	2479	2413
15	2469	2474	2479	2483	2486	2488	2489	2489	2489	2489	2489	2489	2489	2489	2489	2489	2489	2489	2489	2489	2489	2489	2413
10	2479	2484	2489	2493	2496	2498	2499	2499	2499	2499	2499	2499	2499	2499	2499	2499	2499	2499	2499	2499	2499	2499	2413
5	2489	2494	2499	2503	2506	2508	2509	2509	2509	2509	2509	2509	2509	2509	2509	2509	2509	2509	2509	2509	2509	2509	2413
0	2499	2504	2509	2513	2516	2518	2519	2519	2519	2519	2519	2519	2519	2519	2519	2519	2519	2519	2519	2519	2519	2519	2413
-5	2509	2514	2519	2523	2526	2528	2529	2529	2529	2529	2529	2529	2529	2529	2529	2529	2529	2529	2529	2529	2529	2529	2413
-10	2519	2524	2529	2533	2536	2538	2539	2539	2539	2539	2539	2539	2539	2539	2539	2539	2539	2539	2539	2539	2539	2539	2413
-15	2529	2534	2539	2543	2546	2548	2549	2549	2549	2549	2549	2549	2549	2549	2549	2549	2549	2549	2549	2549	2549	2549	2413
-20	2539	2544	2549	2553	2556	2558	2559	2559	2559	2559	2559	2559	2559	2559	2559	2559	2559	2559	2559	2559	2559	2559	2413
-25	2549	2554	2559	2563	2566	2568	2569	2569	2569	2569	2569	2569	2569	2569	2569	2569	2569	2569	2569	2569	2569	2569	2413
-30	2559	2564	2569	2573	2576	2578	2579	2579	2579	2579	2579	2579	2579	2579	2579	2579	2579	2579	2579	2579	2579	2579	2413
-35	2569	2574	2579	2583	2586	2588	2589	2589	2589	2589	2589	2589	2589	2589	2589	2589	2589	2589	2589	2589	2589	2589	2413
-40	2579	2584	2589	2593	2596	2598	2599	2599	2599	2599	2599	2599	2599	2599	2599	2599	2599	2599	2599	2599	2599	2599	2413
-45	2589	2594	2599	2603	2606	2608	2609	2609	2609	2609	2609	2609	2609	2609	2609	2609	2609	2609	2609	2609	2609	2609	2413
-50	2599	2604	2609	2613	2616	2618	2619	2619	2619	2619	2619	2619	2619	2619	2619	2619	2619	2619	2619	2619	2619	2619	2413

Table 14-8. Linear polarization, mixed dihedral angles

θ_2	DIPEDRAL ANGLE 1.25		WAVELENGTH 6943		RANGE CORRECTION (METERS)																								
	0	180	0	180	-5	0	5	10	15	20	25	30	35	40	45	50	55	60	65	70	75	80	85	90					
50	2381	2380	2378	2381	2388	2398	2408	2416	2420	2422	2422	2421	2419	2416	2415	2416	2418	2418	2417	2408	2393								
45	2366	2366	2366	2368	2403	2410	2417	2422	2422	2422	2420	2420	2423	2427	2428	2428	2428	2428	2427	2414	2403	2384							
40	2412	2415	2414	2412	2416	2418	2423	2426	2427	2428	2428	2428	2428	2428	2428	2428	2428	2428	2427	2414	2401	2376							
35	2428	2431	2426	2417	2421	2422	2423	2426	2427	2428	2428	2428	2428	2428	2428	2428	2428	2428	2427	2414	2401	2376							
30	2430	2440	2430	2417	2415	2422	2430	2435	2440	2442	2443	2441	2437	2435	2433	2433	2433	2433	2432	2419	2406	2381							
25	2445	2444	2444	2413	2414	2425	2433	2437	2440	2442	2444	2442	2437	2435	2433	2433	2433	2433	2432	2419	2406	2381							
20	2445	2443	2426	2417	2419	2431	2435	2431	2428	2429	2431	2430	2425	2422	2422	2422	2422	2422	2416	2403	2378								
15	2440	2440	2425	2416	2426	2435	2429	2410	2399	2402	2407	2404	2397	2397	2412	2424	2424	2416	2403	2378									
10	2430	2431	2421	2418	2429	2432	2408	2369	2364	2382	2391	2384	2385	2380	2396	2408	2413	2404	2391	2366	2341								
5	2408	2406	2400	2407	2424	2418	2370	2323	2349	2382	2394	2383	2350	2322	2371	2426	2430	2427	2421	2408	2383								
0	2403	2399	2395	2405	2418	2409	2354	2309	2346	2385	2397	2385	2359	2320	2360	2407	2416	2432	2427	2421	2408								
-5	2404	2400	2397	2407	2420	2418	2387	2352	2359	2361	2397	2388	2378	2381	2403	2418	2419	2415	2415	2415	2415								
-10	2410	2409	2405	2409	2419	2421	2411	2396	2394	2401	2406	2409	2414	2425	2434	2432	2418	2404	2405	2407	2419								
-15	2416	2421	2415	2419	2425	2420	2422	2423	2425	2428	2430	2432	2437	2444	2444	2437	2422	2408	2405	2407	2419								
-20	2410	2428	2429	2424	2419	2420	2425	2433	2440	2442	2442	2444	2446	2444	2444	2437	2426	2415	2414	2417	2419								
-25	2413	2427	2433	2432	2427	2424	2428	2436	2442	2444	2444	2444	2446	2444	2444	2437	2426	2415	2414	2417	2419								
-30	2369	2416	2428	2433	2433	2432	2433	2436	2440	2442	2444	2444	2446	2444	2444	2437	2426	2415	2414	2417	2419								
-35	2364	2400	2416	2417	2433	2436	2437	2437	2440	2442	2444	2444	2446	2444	2444	2437	2426	2415	2414	2417	2419								
-40	2378	2391	2404	2417	2426	2432	2436	2435	2435	2435	2435	2435	2435	2435	2435	2435	2435	2435	2435	2435	2435								
-45	2379	2391	2402	2410	2417	2423	2431	2433	2433	2433	2433	2433	2433	2433	2433	2433	2433	2433	2433	2433	2433								
-50																													

Table 14-9. Circular polarization.

θ	DIMEAL ANGLE .75 WAVELENGTH 5320		RANGE CORRECTION (METERS)																							
	0	90	-50	-45	-40	-35	-30	-25	-20	-15	-10	-5	0	5	10	15	20	25	30	35	40	45	50	θ		
50	2373	2382	2370	2379	2389	2395	2399	2399	2399	2399	2399	2399	2399	2399	2399	2399	2399	2399	2399	2399	2399	2399	2399	2399	2399	2399
45	2362	2374	2367	2375	2382	2389	2395	2399	2399	2399	2399	2399	2399	2399	2399	2399	2399	2399	2399	2399	2399	2399	2399	2399	2399	2399
40	2353	2365	2360	2367	2373	2379	2384	2389	2393	2396	2399	2399	2399	2399	2399	2399	2399	2399	2399	2399	2399	2399	2399	2399	2399	2399
35	2348	2361	2355	2362	2368	2373	2378	2382	2386	2389	2392	2395	2397	2399	2399	2399	2399	2399	2399	2399	2399	2399	2399	2399	2399	2399
30	2331	2362	2356	2362	2368	2373	2378	2382	2386	2389	2392	2395	2397	2399	2399	2399	2399	2399	2399	2399	2399	2399	2399	2399	2399	2399
25	2326	2375	2369	2375	2380	2384	2388	2391	2394	2396	2398	2399	2399	2399	2399	2399	2399	2399	2399	2399	2399	2399	2399	2399	2399	2399
20	2315	2392	2386	2392	2397	2401	2404	2406	2408	2409	2410	2411	2411	2411	2411	2411	2411	2411	2411	2411	2411	2411	2411	2411	2411	2411
15	2302	2398	2393	2398	2402	2405	2408	2410	2412	2413	2414	2414	2414	2414	2414	2414	2414	2414	2414	2414	2414	2414	2414	2414	2414	2414
10	2308	2393	2426	2418	2422	2425	2427	2428	2429	2429	2429	2429	2429	2429	2429	2429	2429	2429	2429	2429	2429	2429	2429	2429	2429	2429
5	2386	2369	2410	2422	2431	2435	2438	2440	2441	2441	2441	2441	2441	2441	2441	2441	2441	2441	2441	2441	2441	2441	2441	2441	2441	2441
0	2400	2396	2399	2392	2405	2410	2413	2415	2416	2416	2416	2416	2416	2416	2416	2416	2416	2416	2416	2416	2416	2416	2416	2416	2416	2416
-5	2397	2396	2396	2392	2405	2410	2413	2415	2416	2416	2416	2416	2416	2416	2416	2416	2416	2416	2416	2416	2416	2416	2416	2416	2416	2416
-10	2376	2380	2398	2395	2403	2420	2425	2428	2430	2431	2431	2431	2431	2431	2431	2431	2431	2431	2431	2431	2431	2431	2431	2431	2431	2431
-15	2350	2380	2401	2405	2409	2423	2428	2430	2432	2432	2432	2432	2432	2432	2432	2432	2432	2432	2432	2432	2432	2432	2432	2432	2432	2432
-20	2342	2370	2398	2411	2418	2428	2432	2434	2435	2435	2435	2435	2435	2435	2435	2435	2435	2435	2435	2435	2435	2435	2435	2435	2435	2435
-25	2330	2359	2382	2404	2418	2423	2425	2426	2426	2426	2426	2426	2426	2426	2426	2426	2426	2426	2426	2426	2426	2426	2426	2426	2426	2426
-30	2320	2332	2356	2383	2405	2412	2414	2415	2415	2415	2415	2415	2415	2415	2415	2415	2415	2415	2415	2415	2415	2415	2415	2415	2415	2415
-35	2310	2321	2338	2364	2388	2401	2402	2402	2402	2402	2402	2402	2402	2402	2402	2402	2402	2402	2402	2402	2402	2402	2402	2402	2402	2402
-40	2300	2310	2324	2344	2369	2385	2391	2391	2391	2391	2391	2391	2391	2391	2391	2391	2391	2391	2391	2391	2391	2391	2391	2391	2391	2391
-45	2285	2285	2291	2311	2331	2352	2362	2362	2362	2362	2362	2362	2362	2362	2362	2362	2362	2362	2362	2362	2362	2362	2362	2362	2362	2362
-50	2297	2292	2284	2282	2276	2266	2258	2250	2243	2238	2233	2228	2226	2226	2226	2226	2226	2226	2226	2226	2226	2226	2226	2226	2226	2226

Table 14-10. Circular polarization.

θ_2	DIELECTRIC ANGLE 1.25		WAVELENGTH 5320		RANGE CORRECTION (METERS)																							
	0	10	0	10	-50	-45	-40	-35	-30	-25	-20	-15	-10	-5	0	5	10	15	20	25	30	35	40	45	50	θ_1		
50	2355	2367	2364	2353	2369	2356	2371	2393	2416	2435	2444	2439	2423	2412	2411	2405	2379	2367	2339	2342	2333							
45	2351	2368	2377	2389	2370	2378	2392	2410	2429	2443	2449	2443	2429	2419	2418	2416	2401	2376	2356	2338	2311							
40	2346	2374	2374	2374	2378	2390	2406	2422	2437	2447	2449	2443	2433	2426	2423	2420	2409	2382	2362	2343	2309							
35	2342	2374	2387	2384	2386	2396	2410	2424	2436	2443	2447	2443	2436	2429	2428	2424	2414	2400	2385	2368	2345							
30	2332	2403	2407	2406	2403	2401	2404	2413	2424	2430	2432	2429	2421	2418	2423	2420	2413	2400	2385	2368	2347							
25	2400	2418	2428	2430	2419	2403	2395	2402	2413	2420	2422	2417	2416	2416	2425	2438	2438	2439	2414	2400	2389							
20	2412	2430	2443	2446	2431	2409	2401	2406	2413	2420	2422	2417	2414	2418	2425	2433	2438	2435	2422	2404	2386							
15	2423	2437	2451	2453	2435	2421	2419	2418	2406	2392	2386	2389	2400	2424	2426	2421	2424	2421	2421	2404	2383							
10	2430	2438	2449	2451	2430	2432	2433	2419	2373	2332	2327	2332	2419	2427	2423	2411	2407	2413	2417	2411	2398							
5	2434	2436	2441	2440	2431	2432	2435	2407	2336	2325	2340	2359	2432	2402	2423	2411	2402	2419	2423	2421	2423							
0	2432	2437	2433	2427	2417	2424	2432	2399	2333	2340	2356	2359	2331	2389	2418	2416	2410	2417	2426	2434	2436							
-5	2420	2475	2477	2420	2458	2414	2428	2405	2341	2328	2337	2336	2336	2399	2421	2420	2423	2431	2435	2439	2439							
-10	2403	2415	2425	2421	2408	2412	2424	2412	2363	2327	2335	2338	2338	2378	2410	2414	2416	2422	2442	2439	2434							
-15	2390	2407	2423	2418	2418	2415	2418	2411	2391	2383	2391	2403	2415	2421	2416	2417	2434	2445	2443	2434	2424							
-20	2389	2403	2419	2427	2423	2423	2418	2407	2401	2411	2425	2428	2422	2413	2406	2414	2431	2441	2436	2425	2410							
-25	2388	2397	2410	2421	2428	2423	2423	2418	2402	2411	2424	2428	2417	2408	2406	2415	2426	2430	2426	2413	2397							
-30	2375	2384	2398	2411	2422	2426	2418	2412	2417	2427	2431	2425	2417	2413	2414	2405	2400	2394	2397	2392	2381							
-35	2350	2386	2387	2405	2419	2423	2422	2420	2424	2435	2445	2446	2439	2426	2414	2406	2396	2391	2389	2386	2381							
-40	2322	2351	2377	2400	2417	2423	2421	2420	2424	2442	2454	2453	2441	2422	2406	2396	2391	2389	2386	2381	2377							
-45	2312	2343	2360	2381	2408	2420	2413	2404	2417	2441	2454	2450	2432	2409	2391	2383	2378	2378	2376	2372	2367							
-50	2322	2336	2335	2347	2384	2409	2408	2401	2413	2437	2448	2441	2420	2394	2372	2356	2348	2348	2346	2342	2339							

Table 14-11. Circular polarization.

θ ₂	DIPHERAL ANGLE 1.75		WAVELENGTH 5320		RANGE CORRECTION (METERS)																					
	0	180	0	180	-50	-45	-40	-35	-30	-25	-20	-15	-10	-5	0	5	10	15	20	25	30	35	40	45	50	
50	2348	2166	2378	2386	2395	2406	2418	2427	2436	2443	2456	2465	2473	2480	2487	2494	2501	2508	2515	2522	2529	2536	2543	2550	2557	2564
45	2365	2397	2400	2400	2406	2412	2418	2424	2432	2440	2455	2465	2473	2480	2487	2494	2501	2508	2515	2522	2529	2536	2543	2550	2557	2564
40	2390	2395	2400	2403	2408	2413	2419	2424	2430	2436	2450	2460	2468	2476	2483	2490	2497	2504	2511	2518	2525	2532	2539	2546	2553	2560
35	2409	2409	2407	2405	2404	2411	2417	2422	2428	2435	2450	2460	2468	2476	2483	2490	2497	2504	2511	2518	2525	2532	2539	2546	2553	2560
30	2422	2421	2417	2413	2411	2418	2424	2429	2435	2442	2457	2467	2475	2483	2490	2497	2504	2511	2518	2525	2532	2539	2546	2553	2560	2567
25	2432	2437	2430	2427	2420	2408	2396	2390	2391	2393	2399	2409	2420	2430	2438	2445	2452	2459	2466	2473	2480	2487	2494	2501	2508	2515
20	2441	2441	2430	2427	2420	2401	2381	2372	2372	2372	2377	2387	2398	2408	2416	2423	2430	2437	2444	2451	2458	2465	2472	2479	2486	2493
15	2451	2448	2448	2446	2428	2395	2363	2368	2383	2360	2354	2369	2367	2365	2362	2359	2356	2353	2350	2347	2344	2341	2338	2335	2332	2329
10	2457	2451	2444	2443	2423	2393	2363	2369	2383	2361	2292	2264	2264	2262	2260	2257	2254	2251	2248	2245	2242	2239	2236	2233	2230	2227
5	2457	2451	2443	2434	2411	2381	2353	2373	2378	2358	2288	2263	2263	2260	2257	2254	2251	2248	2245	2242	2239	2236	2233	2230	2227	2224
0	2452	2445	2437	2425	2399	2383	2390	2361	2262	2207	2137	2082	2082	2080	2077	2074	2071	2068	2065	2062	2059	2056	2053	2050	2047	2044
5	2440	2434	2432	2421	2395	2377	2385	2367	2277	2221	2151	2096	2096	2094	2091	2088	2085	2082	2079	2076	2073	2070	2067	2064	2061	2058
10	2426	2426	2427	2422	2401	2379	2382	2375	2316	2259	2189	2134	2134	2132	2129	2126	2123	2120	2117	2114	2111	2108	2105	2102	2099	2096
15	2417	2419	2424	2424	2411	2392	2384	2376	2353	2333	2303	2273	2273	2270	2267	2264	2261	2258	2255	2252	2249	2246	2243	2240	2237	2234
20	2415	2418	2421	2423	2419	2408	2394	2381	2357	2337	2308	2278	2278	2275	2272	2269	2266	2263	2260	2257	2254	2251	2248	2245	2242	2239
25	2416	2417	2418	2420	2420	2418	2411	2397	2381	2378	2353	2323	2323	2320	2317	2314	2311	2308	2305	2302	2299	2296	2293	2290	2287	2284
30	2408	2412	2415	2419	2422	2423	2421	2413	2402	2402	2404	2407	2409	2413	2418	2420	2420	2419	2418	2417	2416	2415	2414	2413	2412	2411
35	2396	2406	2414	2422	2428	2430	2425	2420	2420	2426	2432	2432	2432	2432	2432	2432	2432	2432	2432	2432	2432	2432	2432	2432	2432	2432
40	2382	2400	2412	2423	2433	2438	2438	2438	2438	2438	2438	2438	2438	2438	2438	2438	2438	2438	2438	2438	2438	2438	2438	2438	2438	2438
45	2371	2397	2409	2418	2431	2440	2437	2429	2429	2429	2429	2429	2429	2429	2429	2429	2429	2429	2429	2429	2429	2429	2429	2429	2429	2429
50	2363	2391	2402	2409	2423	2435	2437	2433	2433	2433	2433	2433	2433	2433	2433	2433	2433	2433	2433	2433	2433	2433	2433	2433	2433	2433

Table 14-12. Circular polarization, mixed dihedral angles

θ	DIPEDRAL ANGLE 1.25		WAVELENGTH 5320																					
	RANGE CORRECTION (METERS)																							
	-50	-45	-40	-35	-30	-25	-20	-15	-10	-5	0	5	10	15	20	25	30	35	40	45	50	θ		
50	2367	2358	2350	2342	2334	2326	2318	2310	2302	2294	2286	2278	2270	2262	2254	2246	2238	2230	2222	2214	2206	2198	2190	
45	2375	2366	2358	2350	2342	2334	2326	2318	2310	2302	2294	2286	2278	2270	2262	2254	2246	2238	2230	2222	2214	2206	2198	2190
40	2381	2372	2364	2356	2348	2340	2332	2324	2316	2308	2300	2292	2284	2276	2268	2260	2252	2244	2236	2228	2220	2212	2204	2196
35	2390	2381	2373	2365	2357	2349	2341	2333	2325	2317	2309	2301	2293	2285	2277	2269	2261	2253	2245	2237	2229	2221	2213	2205
30	2397	2388	2380	2372	2364	2356	2348	2340	2332	2324	2316	2308	2300	2292	2284	2276	2268	2260	2252	2244	2236	2228	2220	2212
25	2403	2394	2386	2378	2370	2362	2354	2346	2338	2330	2322	2314	2306	2298	2290	2282	2274	2266	2258	2250	2242	2234	2226	2218
20	2415	2406	2398	2390	2382	2374	2366	2358	2350	2342	2334	2326	2318	2310	2302	2294	2286	2278	2270	2262	2254	2246	2238	2230
15	2429	2420	2412	2404	2396	2388	2380	2372	2364	2356	2348	2340	2332	2324	2316	2308	2300	2292	2284	2276	2268	2260	2252	2244
10	2444	2435	2427	2419	2411	2403	2395	2387	2379	2371	2363	2355	2347	2339	2331	2323	2315	2307	2299	2291	2283	2275	2267	2259
5	2459	2450	2442	2434	2426	2418	2410	2402	2394	2386	2378	2370	2362	2354	2346	2338	2330	2322	2314	2306	2298	2290	2282	2274
0	2473	2464	2456	2448	2440	2432	2424	2416	2408	2400	2392	2384	2376	2368	2360	2352	2344	2336	2328	2320	2312	2304	2296	2288
-5	2482	2473	2465	2457	2449	2441	2433	2425	2417	2409	2401	2393	2385	2377	2369	2361	2353	2345	2337	2329	2321	2313	2305	2297
-10	2499	2490	2482	2474	2466	2458	2450	2442	2434	2426	2418	2410	2402	2394	2386	2378	2370	2362	2354	2346	2338	2330	2322	2314
-15	2513	2504	2496	2488	2480	2472	2464	2456	2448	2440	2432	2424	2416	2408	2400	2392	2384	2376	2368	2360	2352	2344	2336	2328
-20	2528	2519	2511	2503	2495	2487	2479	2471	2463	2455	2447	2439	2431	2423	2415	2407	2399	2391	2383	2375	2367	2359	2351	2343
-25	2537	2528	2520	2512	2504	2496	2488	2480	2472	2464	2456	2448	2440	2432	2424	2416	2408	2400	2392	2384	2376	2368	2360	2352
-30	2562	2553	2545	2537	2529	2521	2513	2505	2497	2489	2481	2473	2465	2457	2449	2441	2433	2425	2417	2409	2401	2393	2385	2377
-35	2586	2577	2569	2561	2553	2545	2537	2529	2521	2513	2505	2497	2489	2481	2473	2465	2457	2449	2441	2433	2425	2417	2409	2401
-40	2612	2603	2595	2587	2579	2571	2563	2555	2547	2539	2531	2523	2515	2507	2499	2491	2483	2475	2467	2459	2451	2443	2435	2427
-45	2638	2629	2621	2613	2605	2597	2589	2581	2573	2565	2557	2549	2541	2533	2525	2517	2509	2501	2493	2485	2477	2469	2461	2453
-50	2665	2656	2648	2640	2632	2624	2616	2608	2600	2592	2584	2576	2568	2560	2552	2544	2536	2528	2520	2512	2504	2496	2488	2480

Table 14-13. Circular polarization.

θ	DIRECTIONAL ANGLE .75 WAVELENGTH 6943																				
	RANGE CORRECTION (METERS)																				
50	2364	2357	2358	2332	2342	2364	2361	2414	2420	2434	2427	2414	2399	2389	2385	2384	2379	2369	2355	2343	2347
45	2365	2357	2347	2343	2351	2369	2372	2410	2427	2434	2429	2416	2401	2391	2390	2384	2379	2368	2354	2344	2349
40	2375	2373	2365	2358	2361	2372	2374	2410	2427	2436	2435	2425	2409	2396	2394	2388	2380	2368	2354	2344	2349
35	2393	2394	2383	2374	2374	2383	2383	2414	2430	2441	2444	2438	2425	2410	2406	2402	2392	2378	2364	2354	2359
30	2412	2400	2391	2383	2383	2392	2392	2422	2434	2445	2448	2445	2436	2425	2420	2420	2412	2400	2386	2376	2380
25	2426	2427	2417	2411	2414	2424	2424	2428	2429	2432	2437	2440	2438	2434	2432	2433	2431	2425	2421	2411	2399
20	2432	2435	2430	2430	2437	2440	2437	2428	2429	2432	2437	2440	2438	2434	2432	2433	2431	2425	2421	2411	2399
15	2437	2435	2437	2440	2437	2440	2437	2428	2429	2432	2437	2440	2438	2434	2432	2433	2431	2425	2421	2411	2399
10	2443	2435	2444	2444	2449	2448	2448	2436	2437	2438	2439	2439	2438	2435	2434	2434	2433	2427	2423	2413	2394
5	2396	2410	2426	2444	2453	2448	2426	2397	2387	2397	2402	2397	2390	2380	2401	2400	2400	2400	2400	2400	2383
0	2394	2394	2419	2430	2451	2445	2428	2391	2395	2409	2415	2409	2396	2395	2420	2443	2444	2430	2407	2387	2377
-5	2380	2384	2406	2434	2451	2448	2433	2397	2397	2409	2413	2405	2389	2387	2413	2436	2441	2435	2424	2413	2394
-10	2382	2383	2401	2428	2448	2450	2430	2401	2399	2409	2413	2405	2389	2387	2413	2436	2441	2435	2424	2413	2394
-15	2382	2383	2401	2428	2448	2450	2430	2401	2399	2409	2413	2405	2389	2387	2413	2436	2441	2435	2424	2413	2394
-20	2393	2397	2407	2423	2435	2438	2428	2417	2411	2413	2415	2415	2403	2398	2412	2434	2444	2430	2407	2387	2377
-25	2398	2405	2416	2423	2428	2427	2421	2419	2426	2431	2436	2433	2420	2420	2436	2438	2430	2418	2405	2385	2375
-30	2397	2404	2416	2423	2428	2427	2421	2419	2426	2431	2436	2433	2420	2420	2436	2438	2430	2418	2405	2385	2375
-35	2397	2404	2416	2423	2428	2427	2421	2419	2426	2431	2436	2433	2420	2420	2436	2438	2430	2418	2405	2385	2375
-40	2397	2404	2416	2423	2428	2427	2421	2419	2426	2431	2436	2433	2420	2420	2436	2438	2430	2418	2405	2385	2375
-45	2397	2404	2416	2423	2428	2427	2421	2419	2426	2431	2436	2433	2420	2420	2436	2438	2430	2418	2405	2385	2375
-50	2397	2404	2416	2423	2428	2427	2421	2419	2426	2431	2436	2433	2420	2420	2436	2438	2430	2418	2405	2385	2375

Table 14-14. Circular polarization.

θ ₂	DIMEGRAL ANGLE 1.25		WAVELENGTH 6943		RANGE CORRECTION (METERS)	
	ANGLE	WAVELENGTH	ANGLE	WAVELENGTH	ANGLE	WAVELENGTH
50	2367	2361	2360	2367	2362	2400
45	2378	2375	2377	2388	2402	2419
40	2397	2396	2391	2388	2398	2410
35	2418	2417	2408	2397	2391	2408
30	2435	2434	2422	2407	2398	2400
25	2447	2446	2434	2419	2410	2420
20	2453	2453	2443	2432	2431	2430
15	2451	2451	2447	2442	2444	2444
10	2444	2444	2443	2445	2450	2447
5	2432	2433	2434	2441	2449	2443
0	2422	2420	2422	2436	2446	2443
-5	2417	2417	2412	2426	2442	2443
-10	2416	2410	2408	2421	2438	2443
-15	2418	2414	2412	2420	2434	2439
-20	2420	2421	2420	2423	2433	2433
-25	2420	2426	2428	2429	2427	2419
-30	2414	2426	2430	2431	2424	2414
-35	2401	2415	2426	2431	2424	2414
-40	2395	2403	2416	2425	2429	2423
-45	2373	2397	2407	2416	2419	2418
-50	2364	2384	2402	2411	2411	2409
-55						
-60						
-65						
-70						
-75						
-80						
-85						
-90						
-95						
-100						
-105						
-110						
-115						
-120						
-125						
-130						
-135						
-140						
-145						
-150						
-155						
-160						
-165						
-170						
-175						
-180						
-185						
-190						
-195						
-200						
-205						
-210						
-215						
-220						
-225						
-230						
-235						
-240						
-245						
-250						
-255						
-260						
-265						
-270						
-275						
-280						
-285						
-290						
-295						
-300						
-305						
-310						
-315						
-320						
-325						
-330						
-335						
-340						
-345						
-350						
-355						
-360						
-365						
-370						
-375						
-380						
-385						
-390						
-395						
-400						
-405						
-410						
-415						
-420						
-425						
-430						
-435						
-440						
-445						
-450						
-455						
-460						
-465						
-470						
-475						
-480						
-485						
-490						
-495						
-500						

Table 14-15 Circular polarization.

θ_2	DIPEDRAL ANGLE 1.75		WAVELENGTH 6943		RANGE CORRECTION (METERS)																			
	-10	-5	0	5	10	15	20	25	30	35	40	45	50	55	60	65	70	75	80	85	90			
50	2366	2384	2388	2395	2406	2418	2429	2439	2447	2451	2452	2448	2442	2437	2432	2430	2428	2419	2409	2397				
45	2395	2393	2396	2400	2408	2418	2428	2436	2442	2445	2444	2440	2436	2434	2436	2434	2428	2421	2409	2395				
40	2411	2408	2406	2406	2406	2413	2419	2427	2432	2434	2432	2427	2423	2425	2430	2433	2435	2429	2421	2413				
35	2428	2426	2420	2412	2405	2404	2408	2415	2422	2426	2428	2426	2419	2413	2414	2422	2422	2419	2411	2403				
30	2442	2441	2432	2416	2403	2399	2403	2410	2418	2424	2426	2424	2416	2413	2411	2417	2417	2413	2404	2399				
25	2452	2451	2440	2421	2407	2404	2408	2412	2419	2425	2426	2424	2416	2413	2411	2419	2419	2415	2406	2399				
20	2457	2456	2445	2427	2418	2416	2418	2421	2428	2433	2434	2432	2424	2421	2419	2428	2428	2424	2415	2408				
15	2458	2456	2446	2433	2429	2430	2422	2399	2365	2341	2334	2338	2361	2399	2423	2427	2423	2416	2409	2403				
10	2453	2451	2442	2434	2435	2435	2418	2373	2322	2310	2315	2315	2326	2374	2415	2423	2417	2413	2406	2401				
5	2446	2441	2432	2429	2434	2434	2409	2351	2312	2326	2338	2379	2318	2352	2401	2420	2415	2406	2401	2406				
0	2439	2437	2422	2421	2429	2430	2404	2345	2318	2338	2369	2338	2317	2341	2393	2418	2417	2414	2414	2422				
-5	2434	2424	2414	2413	2424	2424	2407	2353	2317	2328	2336	2326	2312	2347	2398	2419	2420	2419	2424	2432				
-10	2432	2424	2413	2413	2429	2428	2412	2368	2317	2320	2317	2309	2326	2375	2411	2423	2423	2425	2434	2442				
-15	2431	2427	2417	2418	2416	2422	2414	2386	2350	2334	2337	2349	2375	2404	2420	2423	2421	2426	2439	2448				
-20	2431	2431	2425	2418	2418	2418	2412	2397	2385	2387	2395	2404	2412	2419	2420	2416	2415	2425	2440	2449				
-25	2429	2433	2431	2427	2423	2418	2409	2401	2402	2412	2422	2426	2424	2420	2414	2409	2412	2424	2438	2446				
-30	2424	2431	2433	2433	2430	2422	2411	2402	2406	2415	2425	2428	2423	2415	2409	2407	2414	2425	2435	2439				
-35	2417	2424	2431	2434	2433	2428	2418	2409	2408	2415	2423	2426	2423	2417	2413	2413	2418	2426	2429	2429				
-40	2409	2419	2427	2431	2432	2430	2425	2420	2420	2425	2432	2433	2428	2423	2420	2420	2419	2419	2418	2417				
-45	2404	2416	2425	2430	2430	2428	2426	2427	2432	2440	2447	2449	2445	2438	2429	2422	2416	2412	2409	2407				
-50	2399	2414	2425	2431	2429	2424	2422	2427	2438	2449	2456	2457	2451	2441	2429	2419	2411	2406	2403	2400				

Table 14-16. Circular polarization, mixed dihedral angles.

θ_2	DIHEDRAL ANGLE 1.25		WAVELENGTH 6943		RANGE CORRECTION (METERS)																				
	-50	-45	-40	-35	-30	-25	-20	-15	-10	-5	0	5	10	15	20	25	30	35	40	45	50				
50	2370	2367	2365	2369	2376	2392	2409	2424	2435	2439	2436	2428	2419	2413	2410	2410	2409	2409	2398	2388	2376				
45	2380	2378	2375	2376	2386	2396	2410	2424	2433	2435	2431	2423	2417	2414	2415	2416	2415	2415	2402	2389	2373				
40	2396	2395	2390	2386	2387	2396	2405	2417	2426	2430	2427	2421	2414	2412	2416	2416	2424	2423	2416	2402	2383				
35	2414	2415	2407	2396	2391	2394	2403	2413	2423	2430	2430	2426	2419	2415	2417	2424	2431	2435	2432	2422	2403				
30	2433	2433	2422	2407	2399	2402	2409	2417	2425	2431	2434	2431	2426	2422	2423	2428	2435	2442	2432	2422	2403				
25	2447	2448	2436	2420	2415	2418	2422	2424	2425	2426	2427	2426	2425	2427	2431	2434	2436	2441	2438	2427					
20	2456	2457	2446	2434	2432	2435	2433	2434	2435	2436	2437	2436	2435	2437	2441	2443	2443	2443	2438	2427					
15	2457	2459	2451	2445	2446	2446	2446	2445	2445	2445	2445	2445	2445	2445	2445	2445	2445	2445	2445	2445					
10	2451	2453	2449	2449	2453	2450	2452	2450	2450	2450	2450	2450	2450	2450	2450	2450	2450	2450	2450	2450					
5	2440	2442	2442	2448	2454	2450	2454	2451	2451	2451	2451	2451	2451	2451	2451	2451	2451	2451	2451	2451					
0	2428	2430	2433	2443	2453	2449	2421	2393	2378	2393	2399	2391	2376	2379	2411	2435	2439	2432	2425	2423					
-5	2420	2421	2425	2438	2451	2445	2423	2382	2369	2381	2386	2378	2364	2373	2409	2434	2438	2435	2435	2436					
-10	2417	2418	2421	2433	2446	2447	2426	2384	2357	2360	2364	2358	2344	2355	2420	2437	2439	2439	2439	2439					
-15	2417	2420	2421	2430	2440	2441	2425	2383	2347	2362	2365	2358	2343	2353	2433	2439	2443	2443	2443	2443					
-20	2418	2424	2425	2428	2433	2431	2421	2404	2395	2398	2405	2412	2422	2432	2437	2434	2429	2431	2441	2449					
-25	2415	2424	2429	2430	2429	2424	2415	2408	2412	2423	2432	2437	2437	2435	2431	2423	2417	2421	2432	2440					
-30	2406	2421	2429	2431	2420	2420	2410	2404	2413	2427	2437	2440	2436	2429	2420	2411	2407	2412	2422	2428					
-35	2393	2411	2422	2427	2426	2419	2409	2403	2408	2420	2431	2434	2430	2421	2411	2403	2401	2404	2410	2412					
-40	2381	2400	2413	2420	2422	2418	2411	2406	2408	2418	2428	2433	2430	2422	2411	2402	2396	2395	2396	2396					
-45	2379	2398	2410	2415	2416	2414	2411	2406	2406	2416	2426	2431	2429	2421	2414	2400	2389	2383	2382	2382					
-50	2365	2401	2412	2416	2413	2407	2405	2410	2421	2435	2445	2446	2443	2430	2411	2393	2380	2374	2372	2372					

Table 15. Centroid range correction vs. velocity aberration. The average and rms deviation are computed around a circle in the far field whose radius is the velocity aberration listed, in microradians, in the first column. Table 15-1. Linear polarization.

DIMEDRAL ANGLE .75 WAVELENGTH 5320

AVERAGE RANGE CORRECTION (METERS)

0	.2403
5	.2390
10	.2370
15	.2389
20	.2424
25	.2427
30	.2416
35	.2412
40	.2409
45	.2393
50	.2370



R.M.S. FLUCTUATION

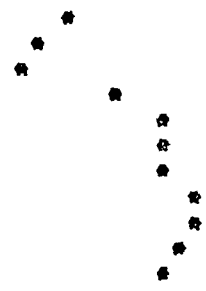
0	0.0020	*
5	.0004	*
10	.0028	*
15	.0036	*
20	.0016	*
25	.0011	*
30	.0012	*
35	.0009	*
40	.0010	*
45	.0015	*
50	.0020	*

Table 15-2. Linear polarization.

DIHEDRAL ANGLE 1.25 WAVELENGTH 5320

AVERAGE RANGE CORRECTION (METERS)

0	.2352
5	.2332
10	.2319
15	.2376
20	.2412
25	.2412
30	.2412
35	.2423
40	.2428
45	.2422
50	.2411



R.M.S. FLUCTUATION

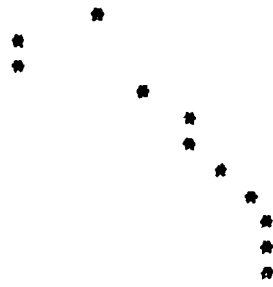
0	0.0000	*
5	.0009	*
10	.0044	*
15	.0028	*
20	.0013	*
25	.0016	*
30	.0020	*
35	.0015	*
40	.0010	*
45	.0008	*
50	.0010	*

Table 15-3. Linear polarization.

DIMEDRAL ANGLE 1.75 WAVELENGTH 5320

AVERAGE RANGE CORRECTION (METERS)

0	.2314
5	.2273
10	.2266
15	.2348
20	.2380
25	.2381
30	.2306
35	.2417
40	.2425
45	.2428
50	.2429



R.M.S. FLUCTUATION

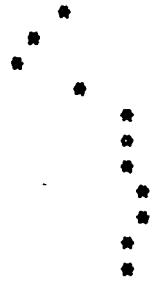
0	0.0000	*
5	.0008	*
10	.0027	*
15	.0007	*
20	.0004	*
25	.0012	*
30	.0017	*
35	.0014	*
40	.0012	*
45	.0012	*
50	.0013	*

Table 15-4. Linear polarization, mixed dihedral angles.

DIHEDRAL ANGLE $\overline{1.25}$ WAVELENGTH 5320

AVERAGE RANGE CORRECTION (METERS)

0	.2372
5	.2355
10	.2341
15	.2323
20	.2412
25	.2412
30	.2416
35	.2422
40	.2424
45	.2417
50	.2409



R.M.S. FLUCTUATION

0	0.0090	*
5	.0006	*
10	.0031	*
15	.0024	*
20	.0010	*
25	.0009	*
30	.0011	*
35	.0008	*
40	.0008	*
45	.0010	*
50	.0015	*

Table 15-5. Linear polarization.

DIHEDRAL ANGLE .75 WAVELENGTH 6943

AVERAGE RANGE CORRECTION (METERS)

0	.2417
5	.2410
10	.2394
15	.2383
20	.2401
25	.2478
30	.2437
35	.2430
40	.2417
45	.2408
50	.2402



R.M.S. FLUCTUATION

0	0.0000	*
5	.0002	*
10	.0011	*
15	.0027	**
20	.0029	**
25	.0016	**
30	.0010	*
35	.0009	*
40	.0009	*
45	.0009	*
50	.0013	*

Table 18-6. Linear polarization.

DIMEDRAL ANGLE 1.25 WAVELENGTH 6943

AVERAGE RANGE CORRECTION (METERS)

0	.2389
5	.2380
10	.2362
15	.2357
20	.2390
25	.2422
30	.2429
35	.2423
40	.2419
45	.2422
50	.2426



R.M.S. FLUCTUATION

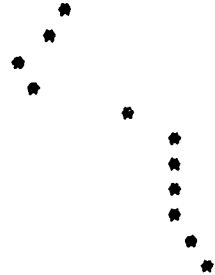
0	0.0000 *
5	.0004 *
10	.0020 *
15	.0045 *
20	.0037 *
25	.0019 *
30	.0014 *
35	.0015 *
40	.0016 *
45	.0013 *
50	.0009 *

Table 15-7. Linear polarization.

DIHEDRAL ANGLE 1.75 WAVELENGTH 6943

AVERAGE RANGE CORRECTION (METERS)

0	.2345
5	.2331
10	.2309
15	.2326
20	.2382
25	.2411
30	.2414
35	.2411
40	.2415
45	.2426
50	.2433



R.M.S. FLUCTUATION

0	0.0000	*
5	.0005	*
10	.0029	*
15	.0045	*
20	.0023	*
25	.0011	*
30	.0012	*
35	.0019	*
40	.0021	*
45	.0016	*
50	.0012	*

Table 15-8. Linear polarization, mixed dihedral angles.

DIHEDRAL ANGLE 1.23 WAVELENGTH 6943

AVERAGE RANGE CORRECTION (METERS)

0	.2397
5	.2388
10	.2370
15	.2365
20	.2395
25	.2425
30	.2432
35	.2426
40	.2421
45	.2422
50	.2423



R.M.S. FLUCTUATION

0	0.0000	*
5	.0003	*
10	.0016	*
15	.0035	*
20	.0029	*
25	.0013	*
30	.0009	*
35	.0009	*
40	.0010	*
45	.0008	*
50	.0008	*

Table 15-9. Circular polarization.

DIHEDRAL ANGLE .75 WAVELENGTH 5320

AVERAGE RANGE CORRECTION (METERS)

0	.2406
5	.2392
10	.2378
15	.2403
20	.2431
25	.2431
30	.2418
35	.2413
40	.2409
45	.2394
50	.2372



R.M.S. FLUCTUATION

0	0.0000	*
5	.0002	*
10	.0003	*
15	.0005	*
20	.0008	*
25	.0008	*
30	.0011	*
35	.0015	*
40	.0017	*
45	.0018	*
50	.0020	*

Table 15-10. Circular polarization.

DIHEDRAL ANGLE 1.25 WAVELENGTH 5320

AVERAGE RANGE CORRECTION (METERS)

0	.2356
5	.2336
10	.2333
15	.2387
20	.2418
25	.2418
30	.2418
35	.2427
40	.2430
45	.2473
50	.2412



R.M.S. FLUCTUATION

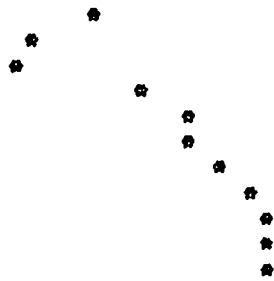
0	0.0000	*
5	.0002	*
10	.0004	*
15	.0007	*
20	.0008	*
25	.0007	*
30	.0009	*
35	.0011	*
40	.0012	*
45	.0014	*
50	.0017	*

Table 15-11. Circular polarization.

DIHEDRAL ANGLE 1.75 WAVELENGTH 5320

AVERAGE RANGE CORRECTION (METERS)

0	.2321
5	.2279
10	.2271
15	.2349
20	.2382
25	.2385
30	.2401
35	.2421
40	.2429
45	.2431
50	.2431



R.M.S. FLUCTUATION

0	0.0000 *
5	.0004 *
10	.0007 *
15	.0011 *
20	.0008 *
25	.0005 *
30	.0006 *
35	.0007 *
40	.0009 *
45	.0011 *
50	.0013 *

Table 15-12. Circular polarization, mixed dihedral angles.

DIHEDRAL ANGLE $\overline{1.25}$ WAVELENGTH 5320

AVERAGE RANGE CORRECTION (METERS)

0	.2378
5	.2381
10	.2351
15	.2360
20	.2420
25	.2421
30	.2420
35	.2426
40	.2426
45	.2418
50	.2410



R.M.S. FLUCTUATION

0	0.0000	*
5	.0006	*
10	.0009	*
15	.0011	*
20	.0012	*
25	.0011	*
30	.0011	*
35	.0013	*
40	.0014	*
45	.0015	*
50	.0018	*

Table 15-13. Circular polarization.

DIHEDRAL ANGLE .75 WAVELENGTH 6943

AVERAGE RANGE CORRECTION (METERS)

0	.2419
5	.2412
10	.2398
15	.2391
20	.2411
25	.2434
30	.2440
35	.2432
40	.2418
45	.2408
50	.2402



R.M.S. FLUCTUATION

0	0.0000 *
5	.0001 *
10	.0003 *
15	.0004 *
20	.0005 *
25	.0007 *
30	.0009 *
35	.0009 *
40	.0012 *
45	.0016 *
50	.0019 *

Table 15-14. Circular polarization.

DIMEDRAL ANGLE 1.25 WAVELENGTH 6943

AVERAGE RANGE CORRECTION (METERS)

0	.2392
5	.2383
10	.2368
15	.2372
20	.2405
25	.2430
30	.2434
35	.2428
40	.2423
45	.2425
50	.2427



R.M.S. FLUCTUATION

0	0.0000	*
5	.0001	*
10	.0003	*
15	.0004	*
20	.0006	*
25	.0008	*
30	.0008	*
35	.0009	*
40	.0011	*
45	.0014	*
50	.0016	*

Table 15-15. Circular polarization.

DIHEDRAL ANGLE 1.75 WAVELENGTH 6943

AVERAGE RANGE CORRECTION (METERS)

0	.2349
5	.2335
10	.2316
15	.2340
20	.2390
25	.2416
30	.2420
35	.2417
40	.2421
45	.2431
50	.2436



R.M.S. FLUCTUATION

0	0.0000	*
5	.0002	*
10	.0003	*
15	.0005	*
20	.0008	*
25	.0008	*
30	.0007	*
35	.0007	*
40	.0009	*
45	.0011	*
50	.0011	*

Table 15-16. Circular polarization, mixed dihedral angles.

DIHEDRAL ANGLE $\overline{1.25}$ WAVELENGTH 6943

AVERAGE RANGE CORRECTION (METERS)

0	.2399
5	.2390
10	.2374
15	.2376
20	.2405
25	.2430
30	.2435
35	.2429
40	.2424
45	.2424
50	.2425



R.M.S. FLUCTUATION

0	0.0000	*
5	.0004	*
10	.0007	*
15	.0008	*
20	.0010	*
25	.0011	*
30	.0011	*
35	.0010	*
40	.0011	*
45	.0014	*
50	.0016	*

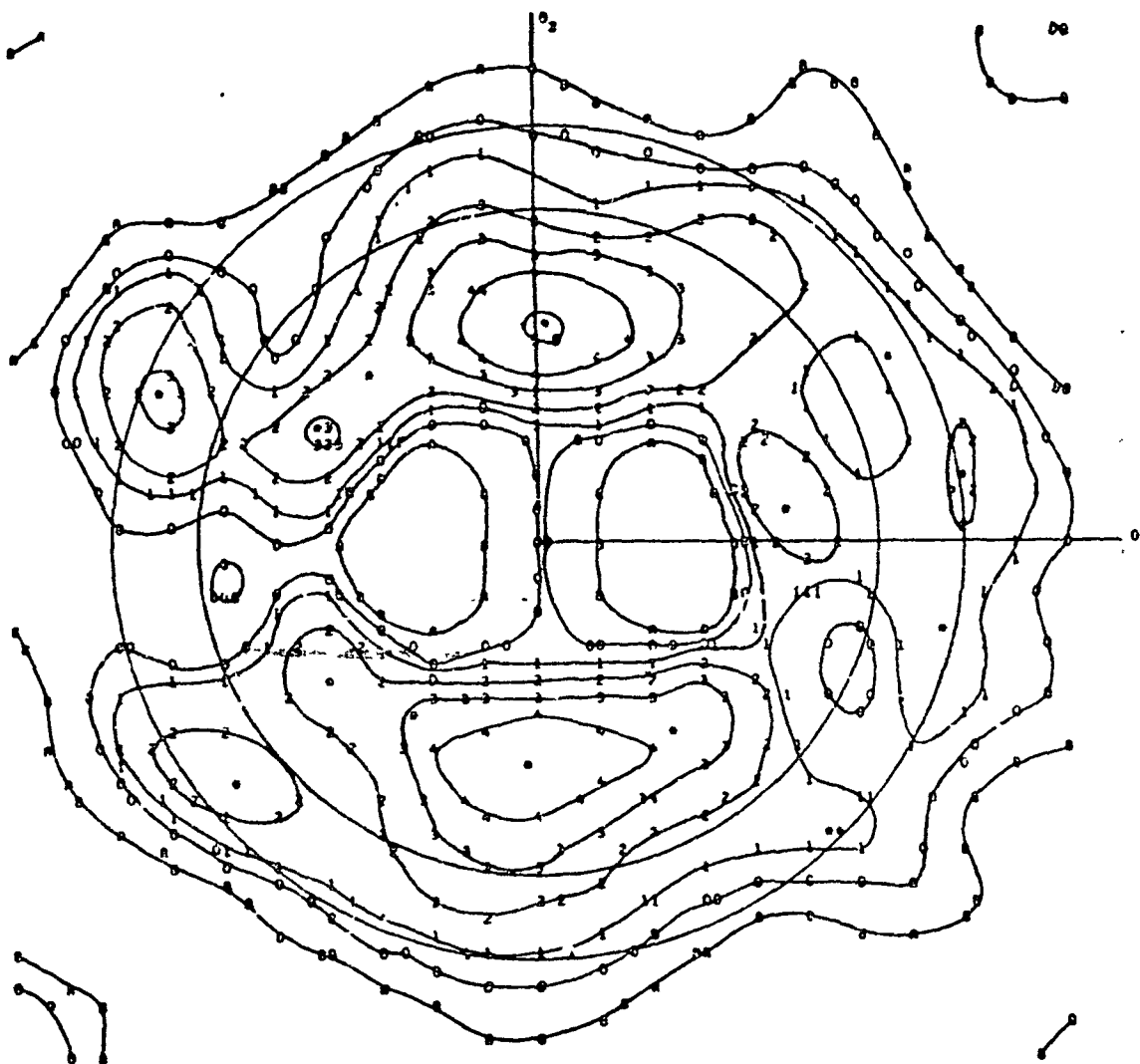


Figure 10. Contour plots of the centroid range correction matrices given in Table 14. Circles of radius 22 and 41 μ rad are shown to mark the minimum and maximum values of the velocity aberration. Table 11 lists the range correction corresponding to the numbers used to mark each contour. The polarization, dihedral angle offset δ , and wavelength λ are given for each figure. Figure 10-1. Linear polarization, $\delta = 0^\circ 75'$, $\lambda = 6320 \text{ \AA}$.

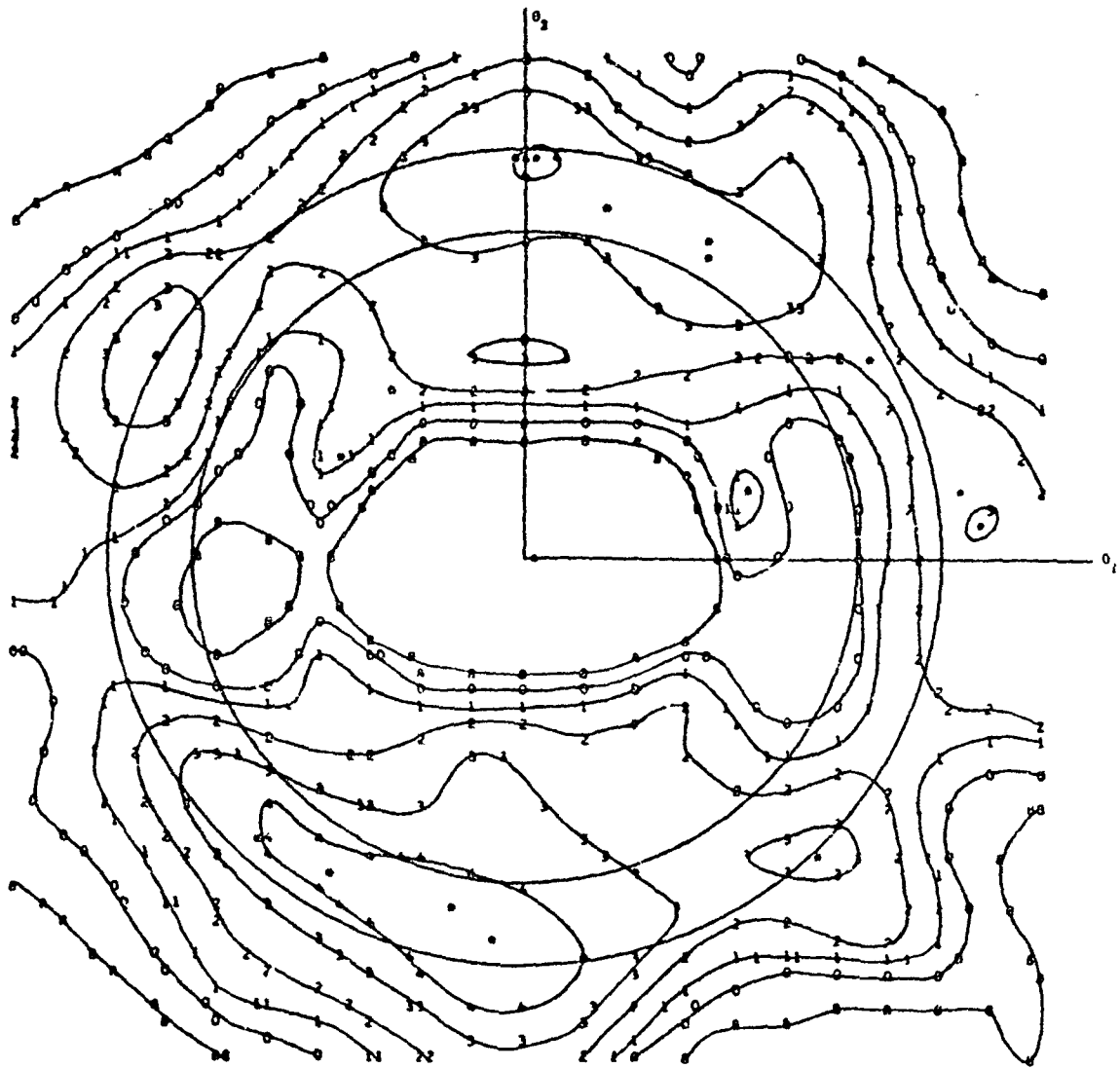


Figure 10-2 Linear polarization, $\delta = 1.725$, $\lambda = 5320 \text{ \AA}$

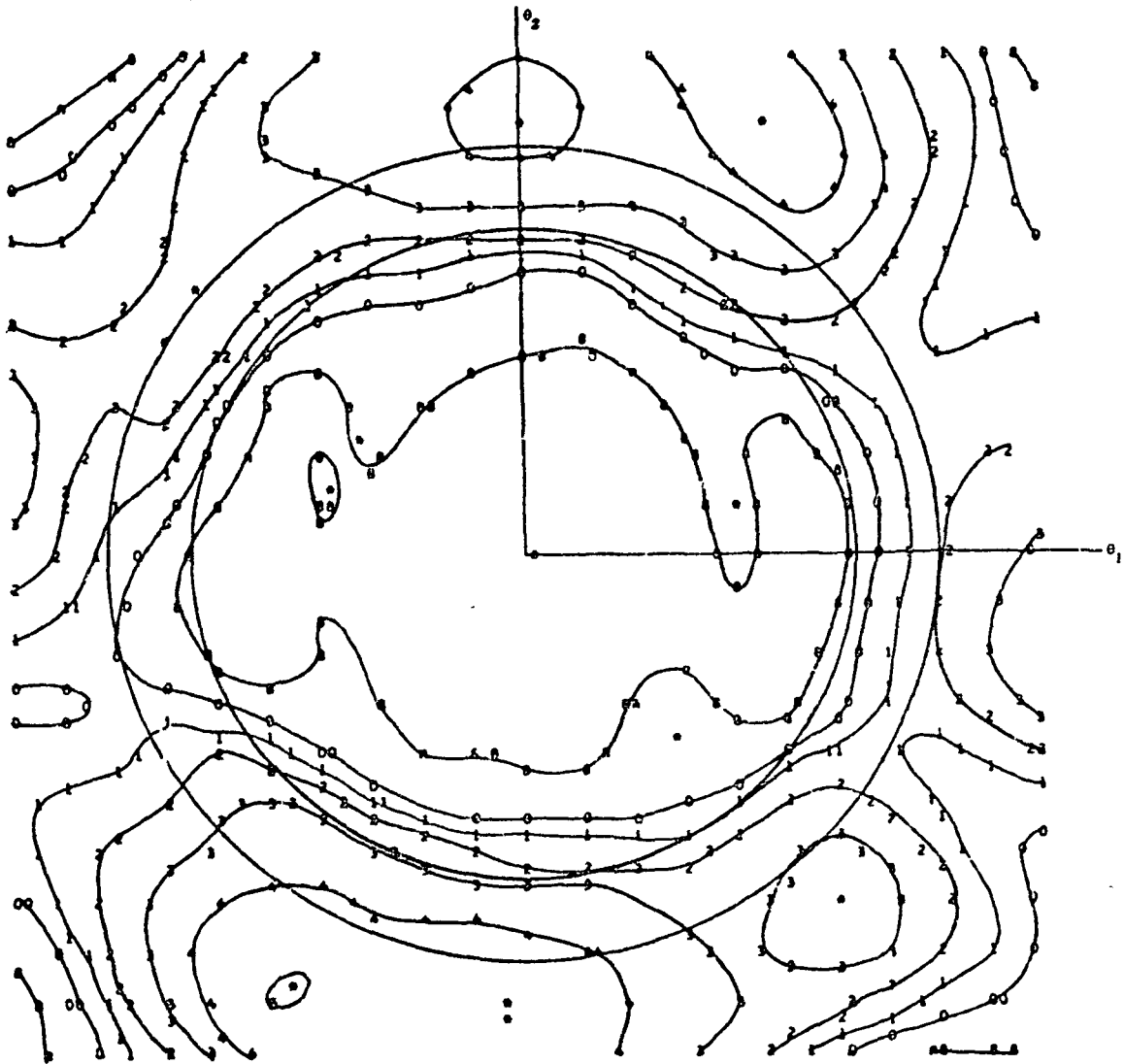


Figure 10-3. Linear polarization, $\delta = 1^{\circ}75$, $\lambda = 6320 \text{ \AA}$.

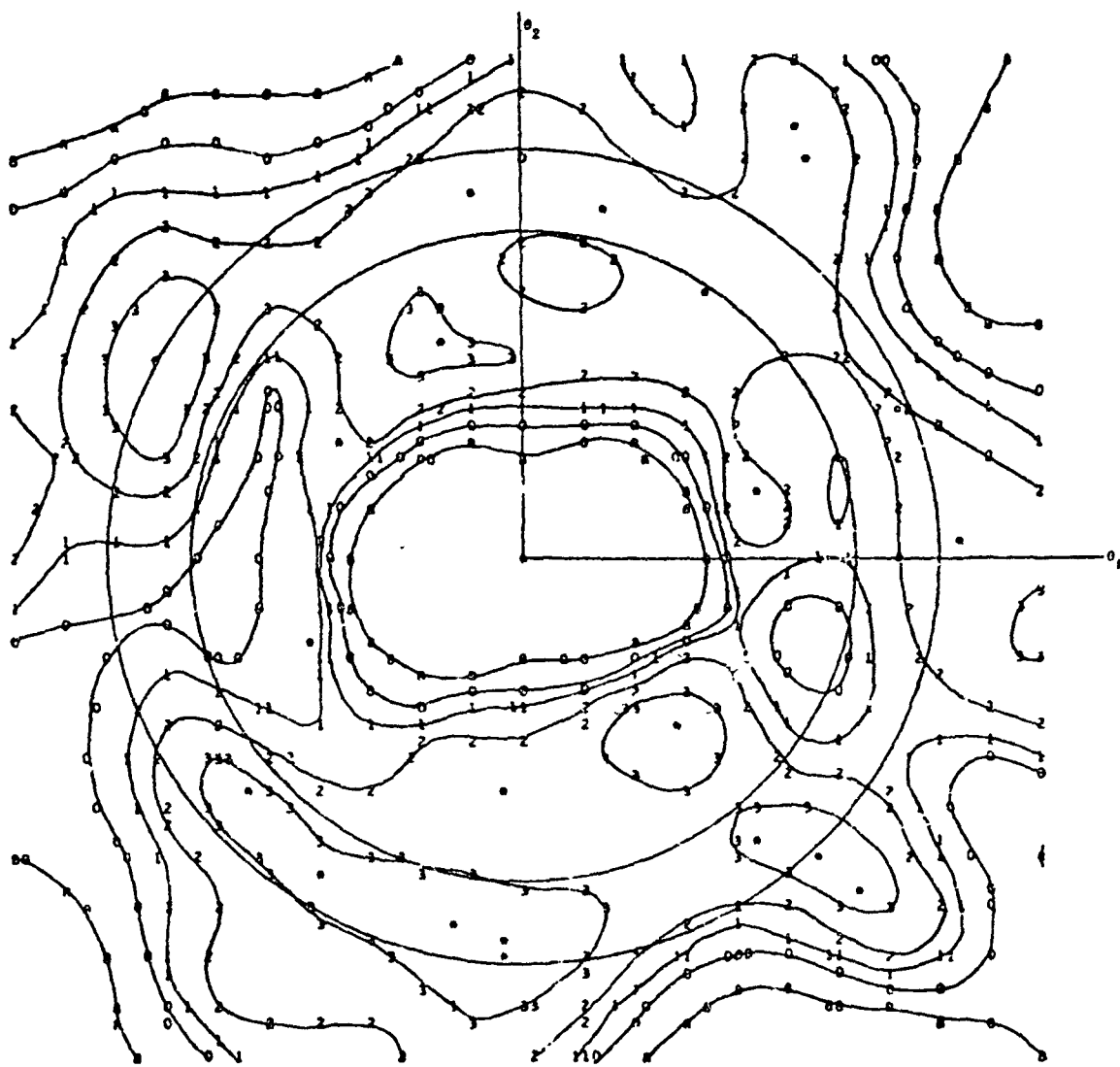


Figure 10-4. Linear polarization, $\delta = 1^{\circ}25'$ (mixed dihedral angles), $\lambda = 5320 \text{ \AA}$

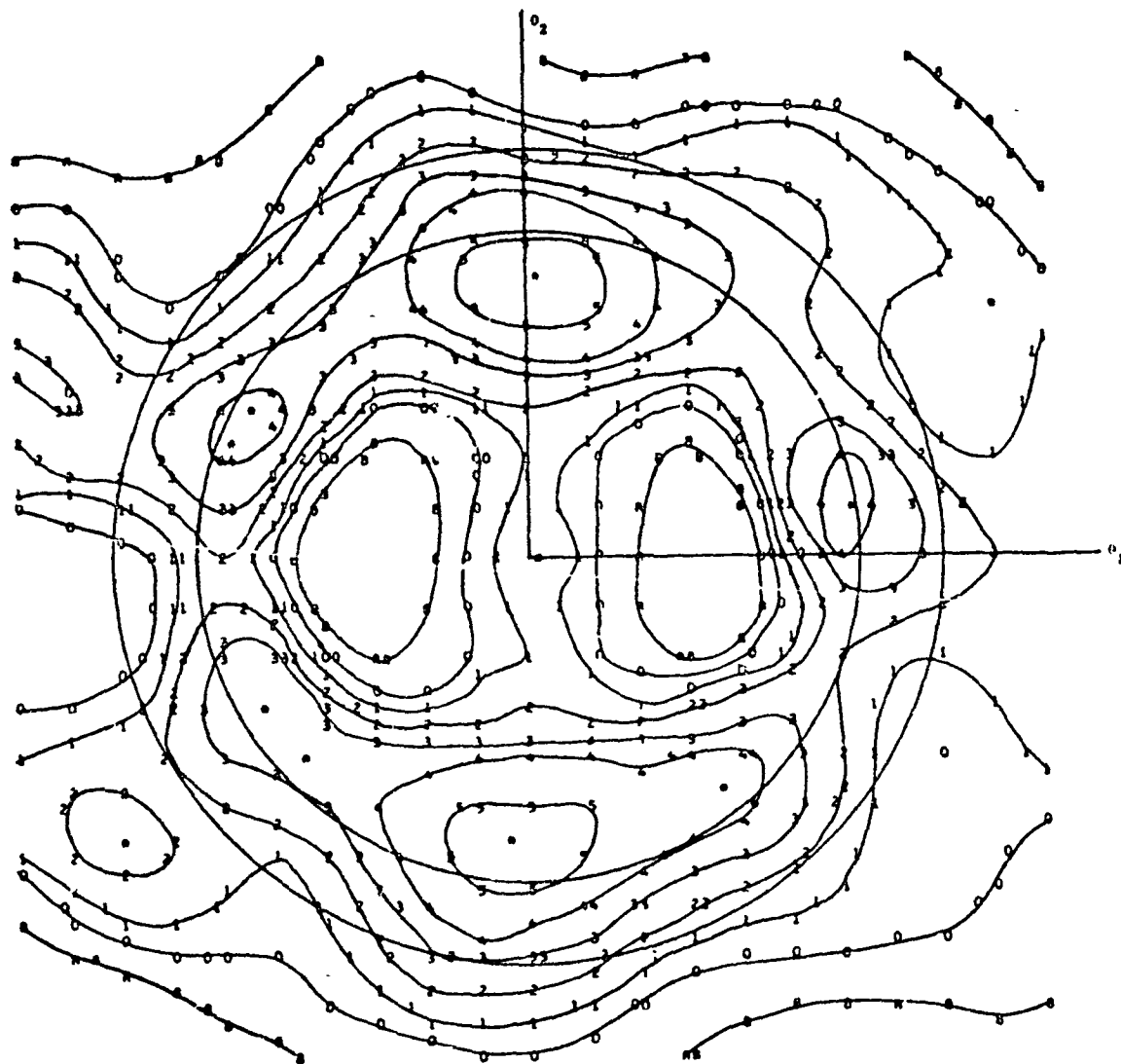


Figure 10 G. Linear polarization, $\delta = 0''75$, $\lambda = 6943 \text{ \AA}$.

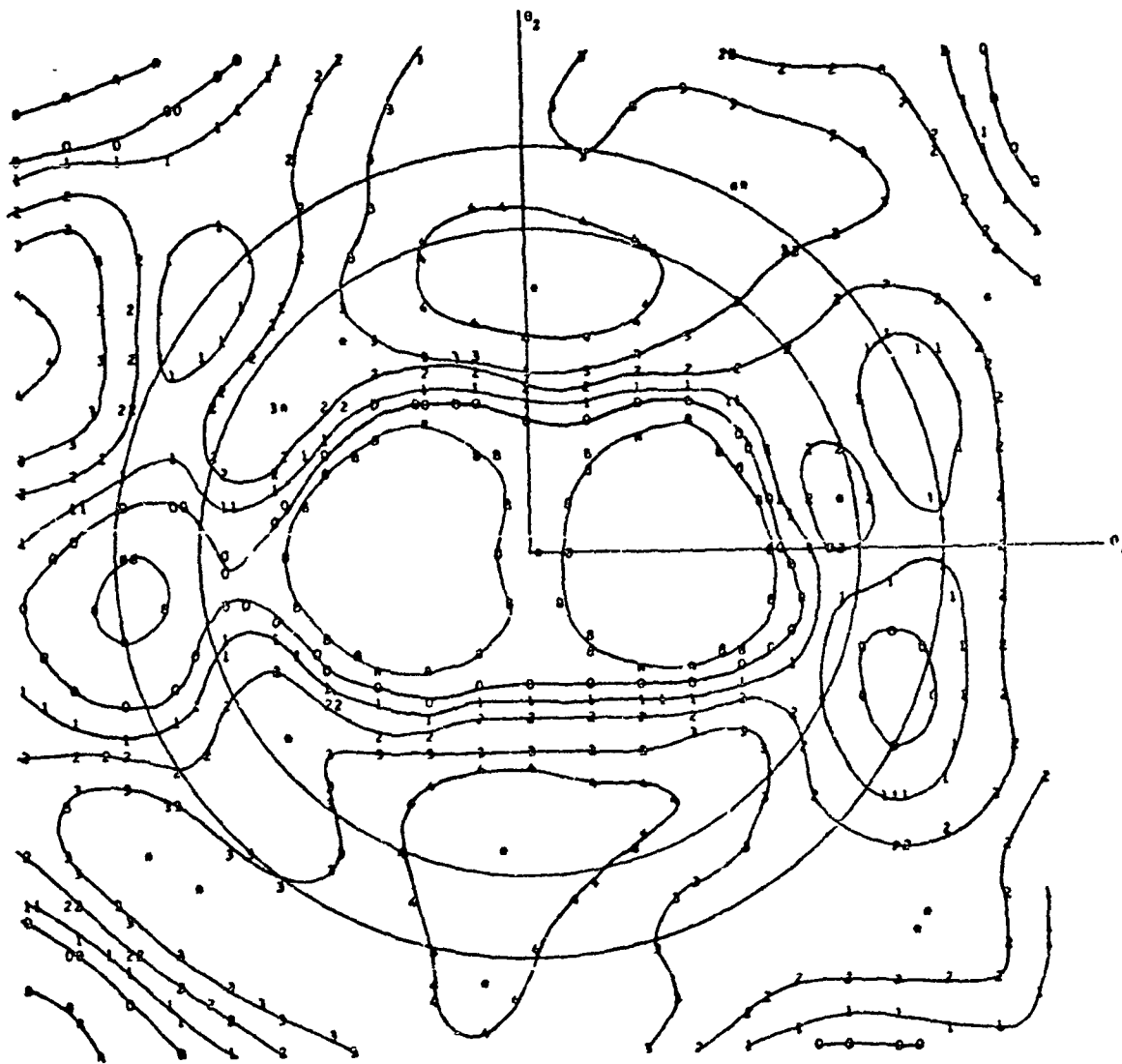


Figure 10-6. Linear polarization, $\delta = 1.25$, $\lambda = 6943 \text{ \AA}$

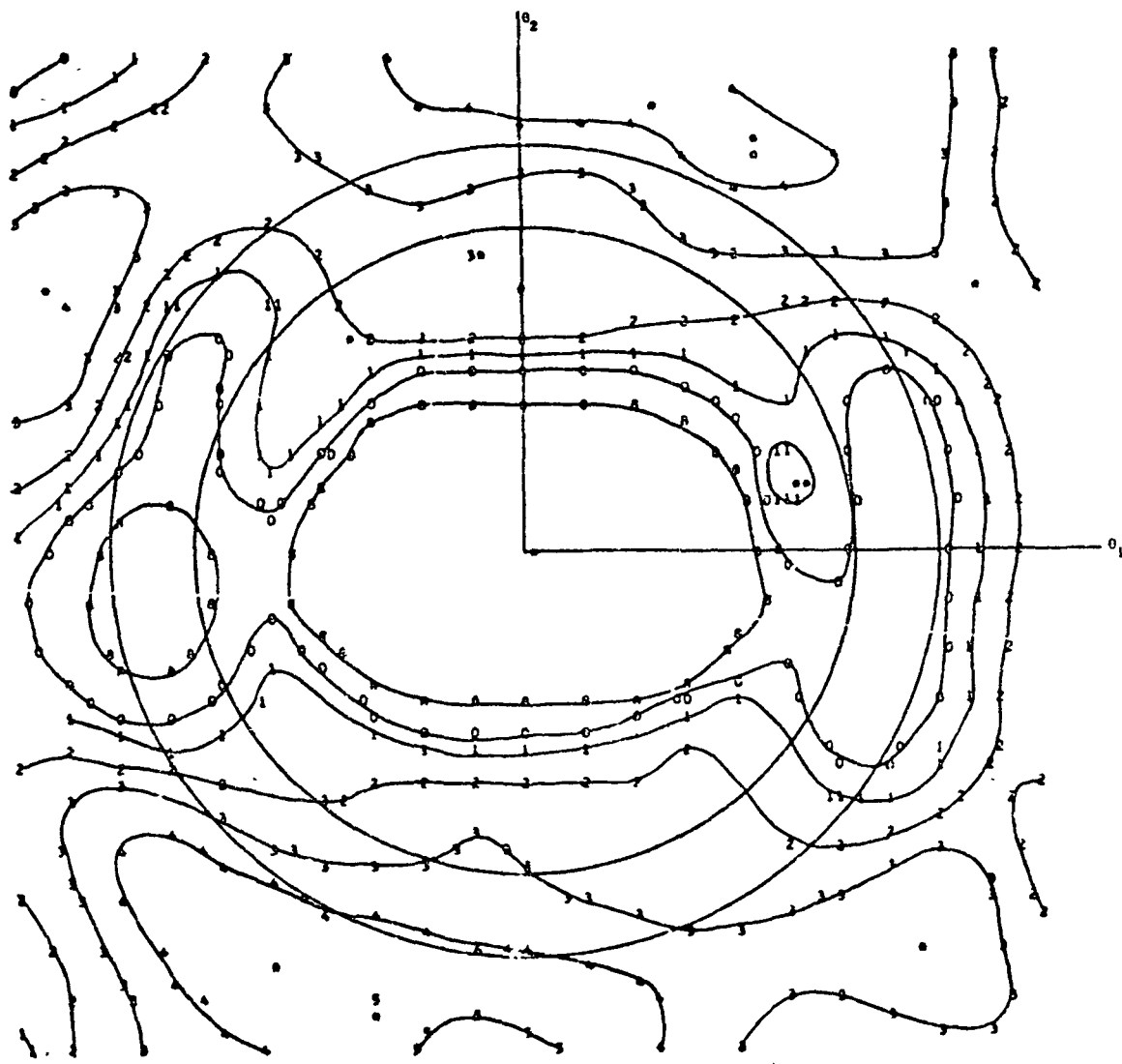


Figure 10-7. Linear polarization, $L = 1775$, $\lambda = 6943 \text{ \AA}$.

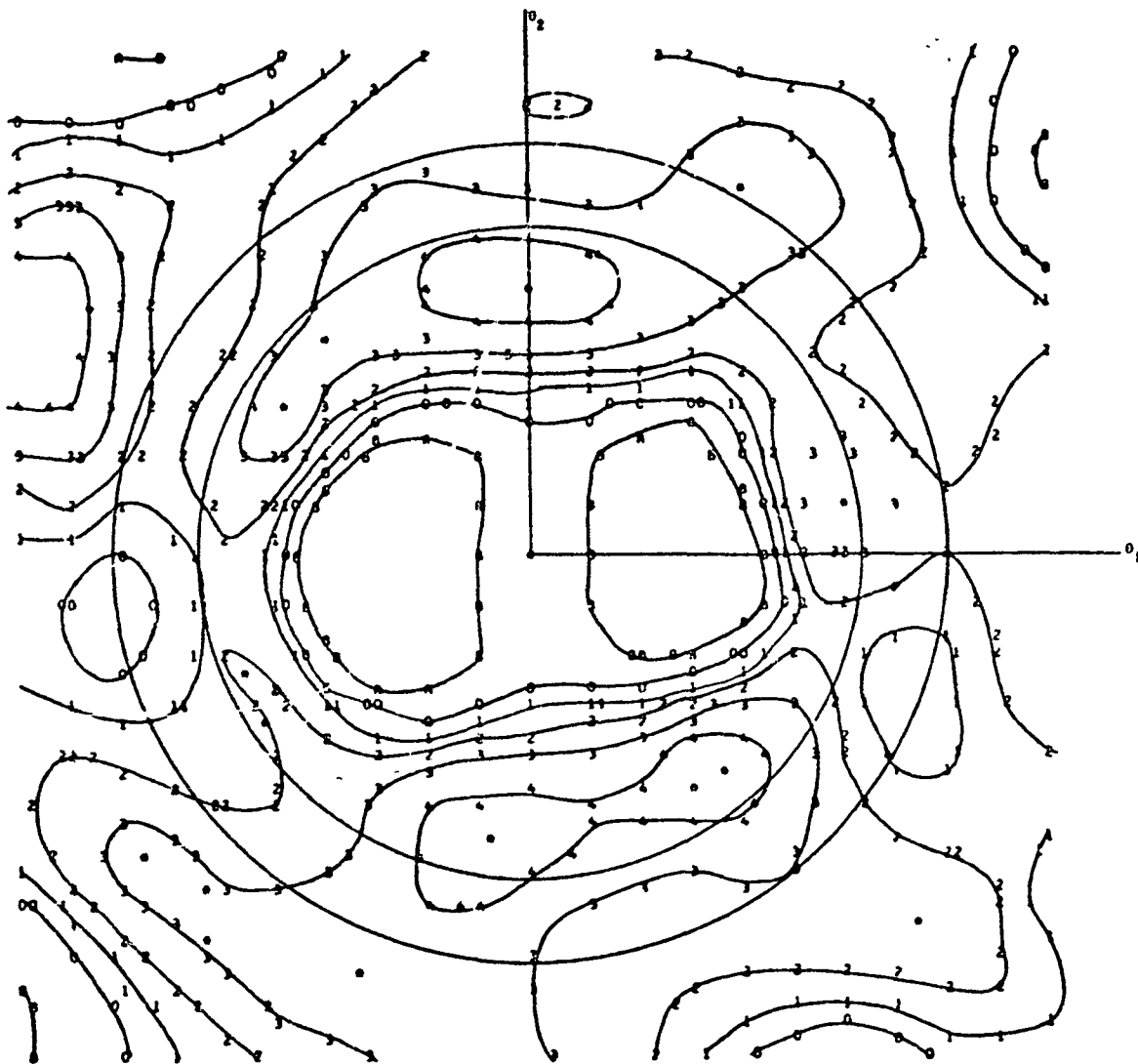


Figure 10-8 Linear polarization, $\delta = 725$ (mixed dihedral angles), $\lambda = 6943 \text{ \AA}$

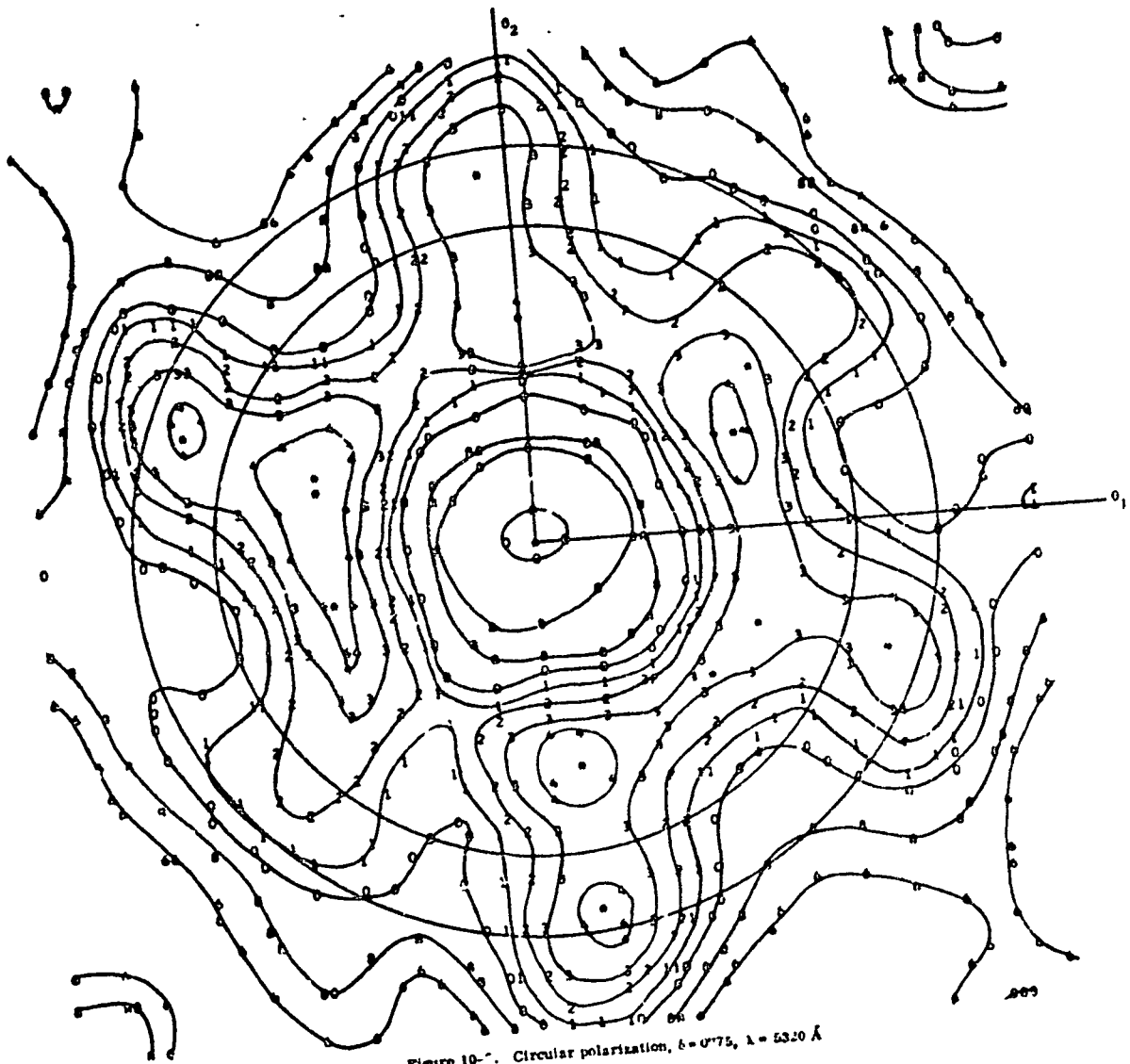


Figure 10-7. Circular polarization, $\delta = 0.75$, $\lambda = 5320 \text{ \AA}$

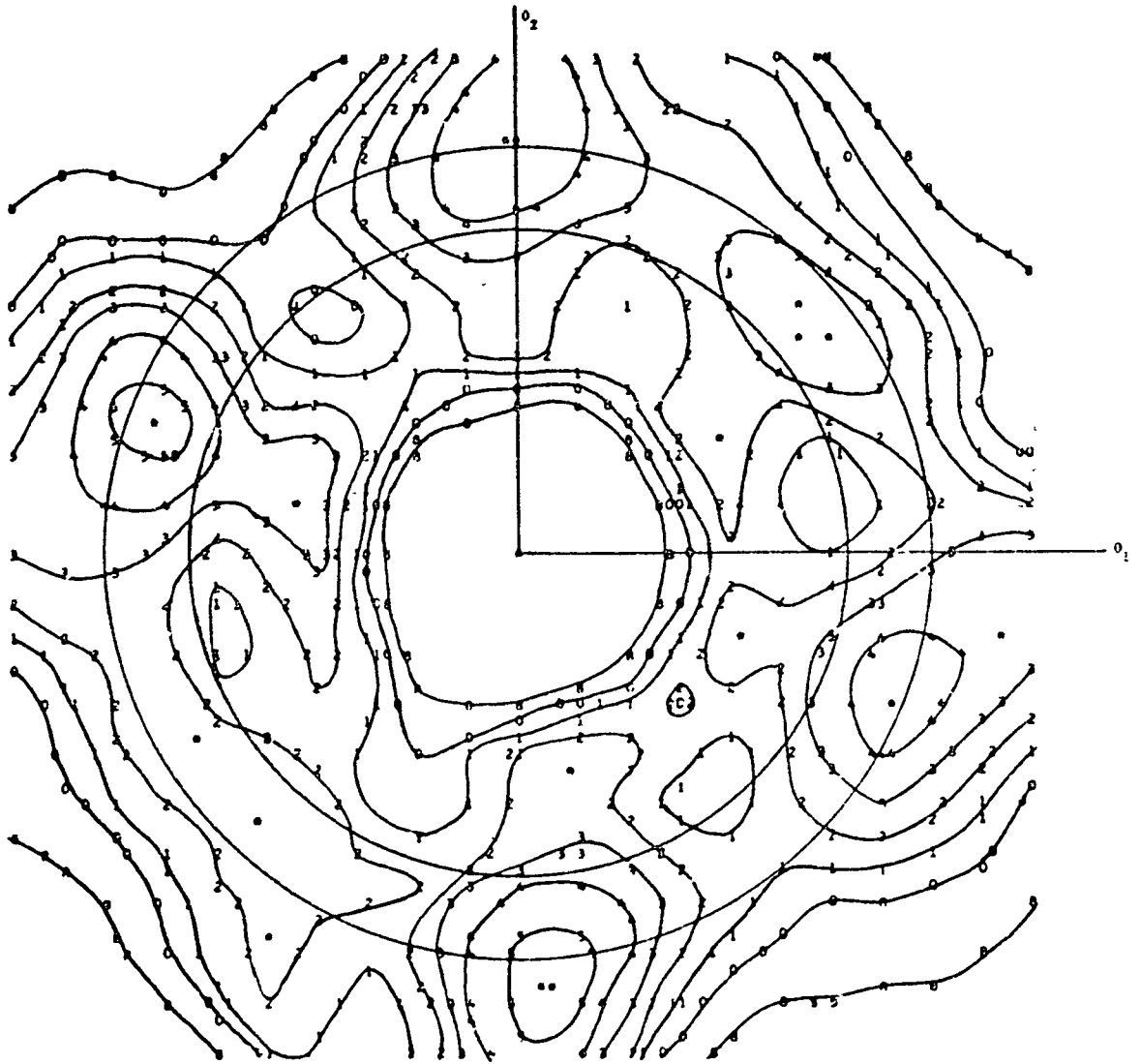


Figure 10-10 Circular polarization, $\delta = 1725$, $\lambda = 5320 \text{ \AA}$

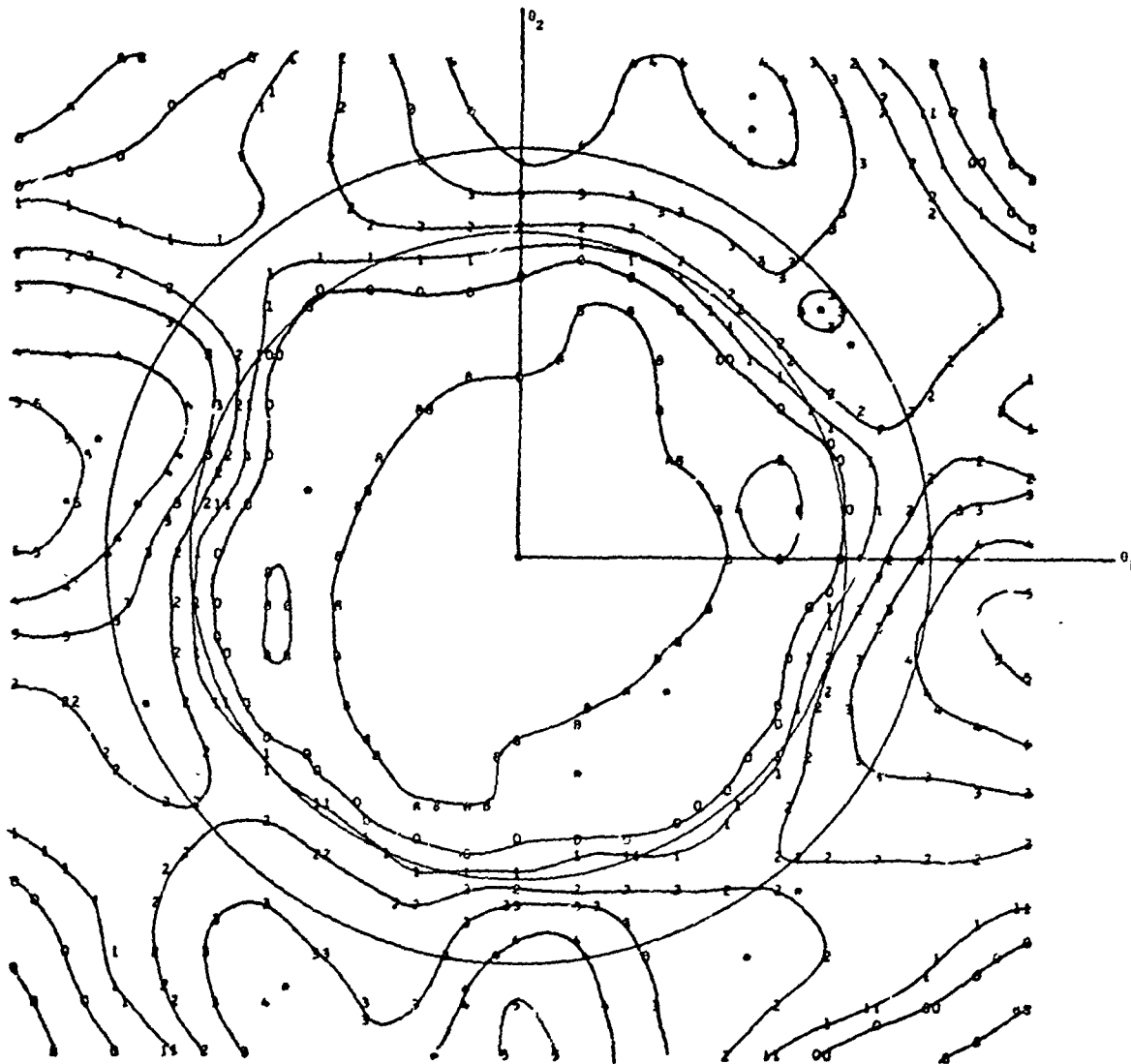


Figure 10-11. Circular polarization, $\delta = 1^{\circ}75$, $\lambda = 5320 \text{ \AA}$

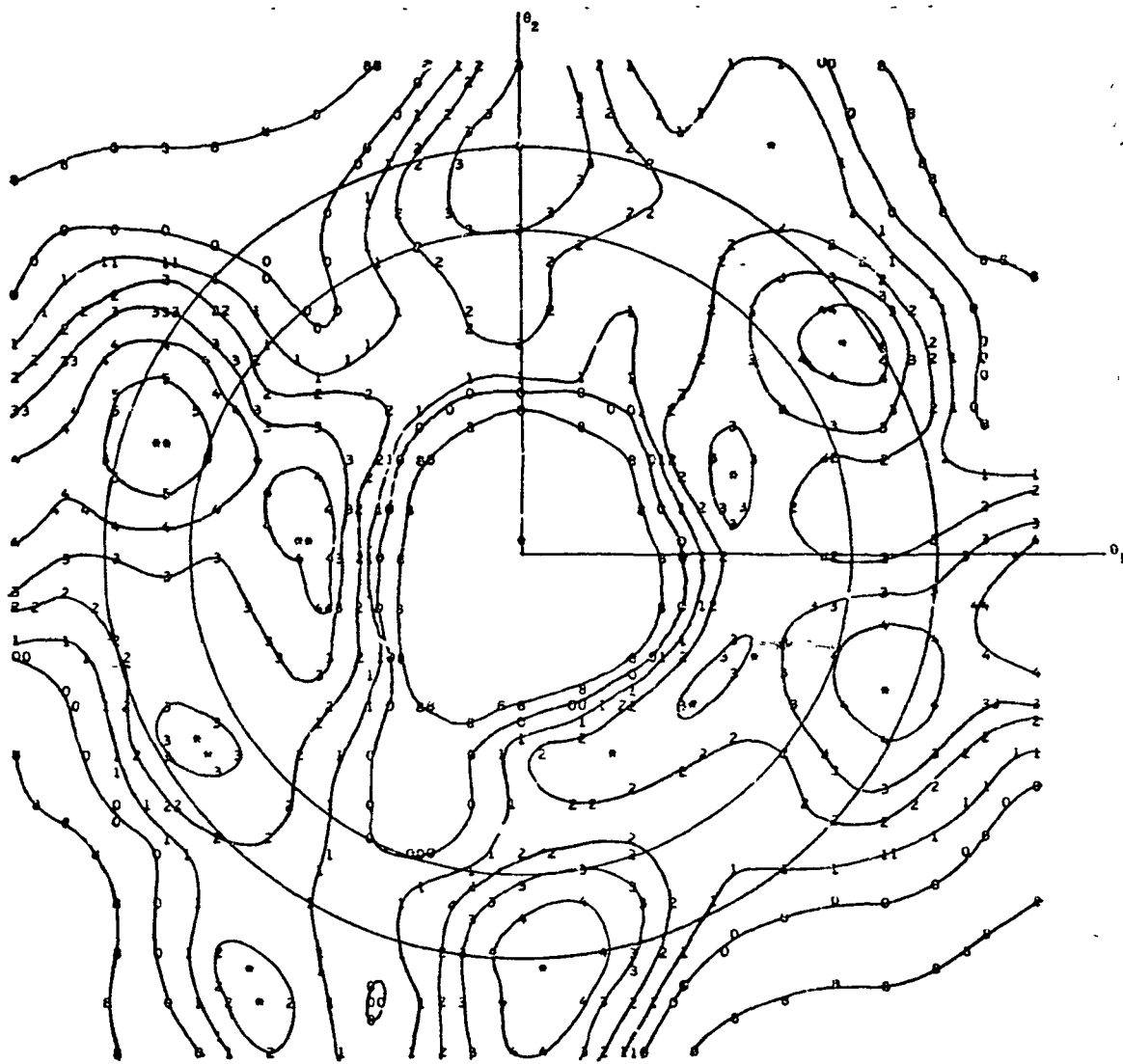


Figure 10-12. Circular polarization, $\bar{\delta} = 1'25$ (mixed dihedral angles), $\lambda = 5320 \text{ \AA}$.

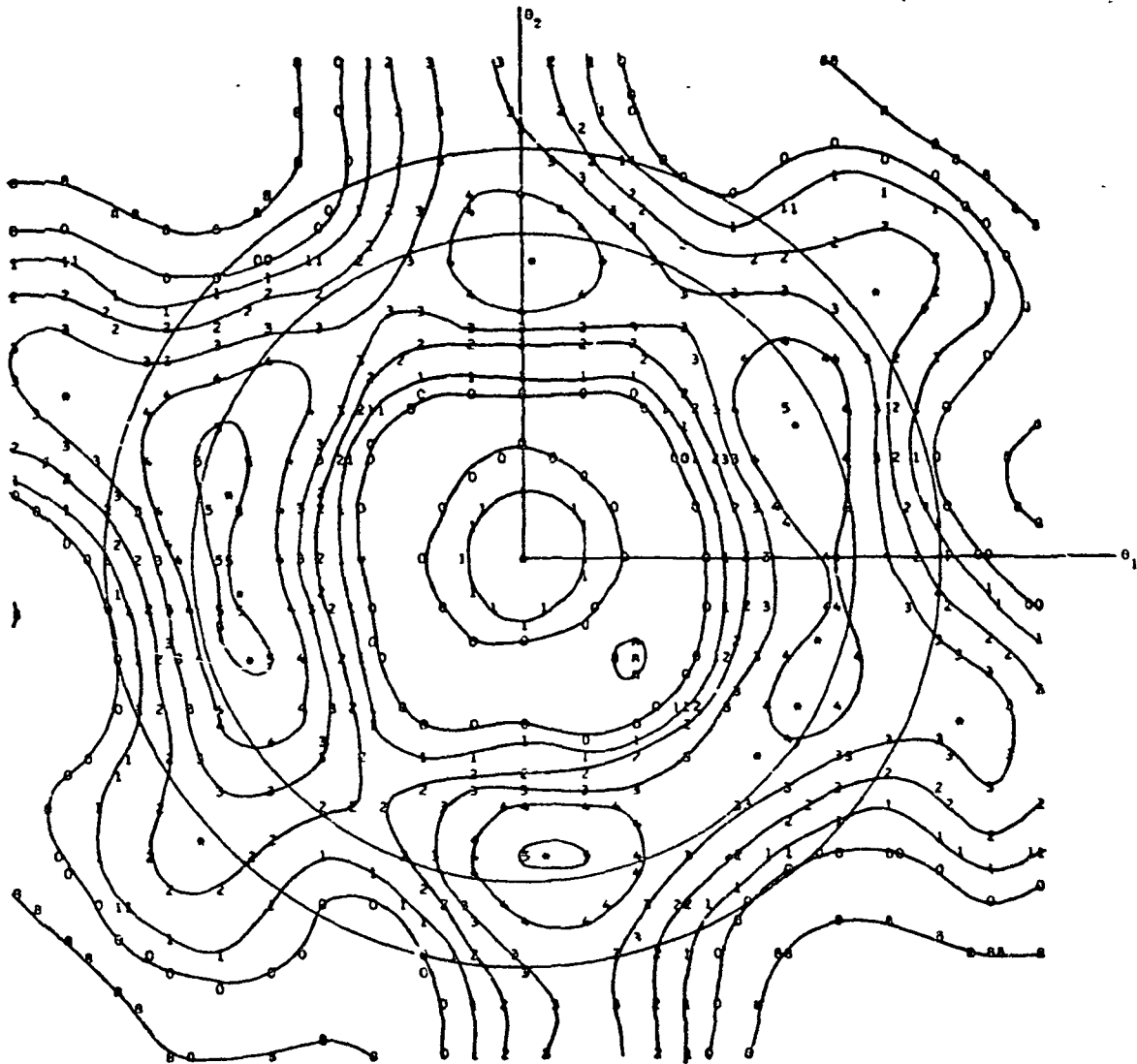


Figure 10-13. Circular polarization, $\theta = 0^\circ 75$, $\lambda = 6943 \text{ \AA}$

This figure is a reproduction of the original document. It is not a photograph of the original document. It is a reproduction of the original document.

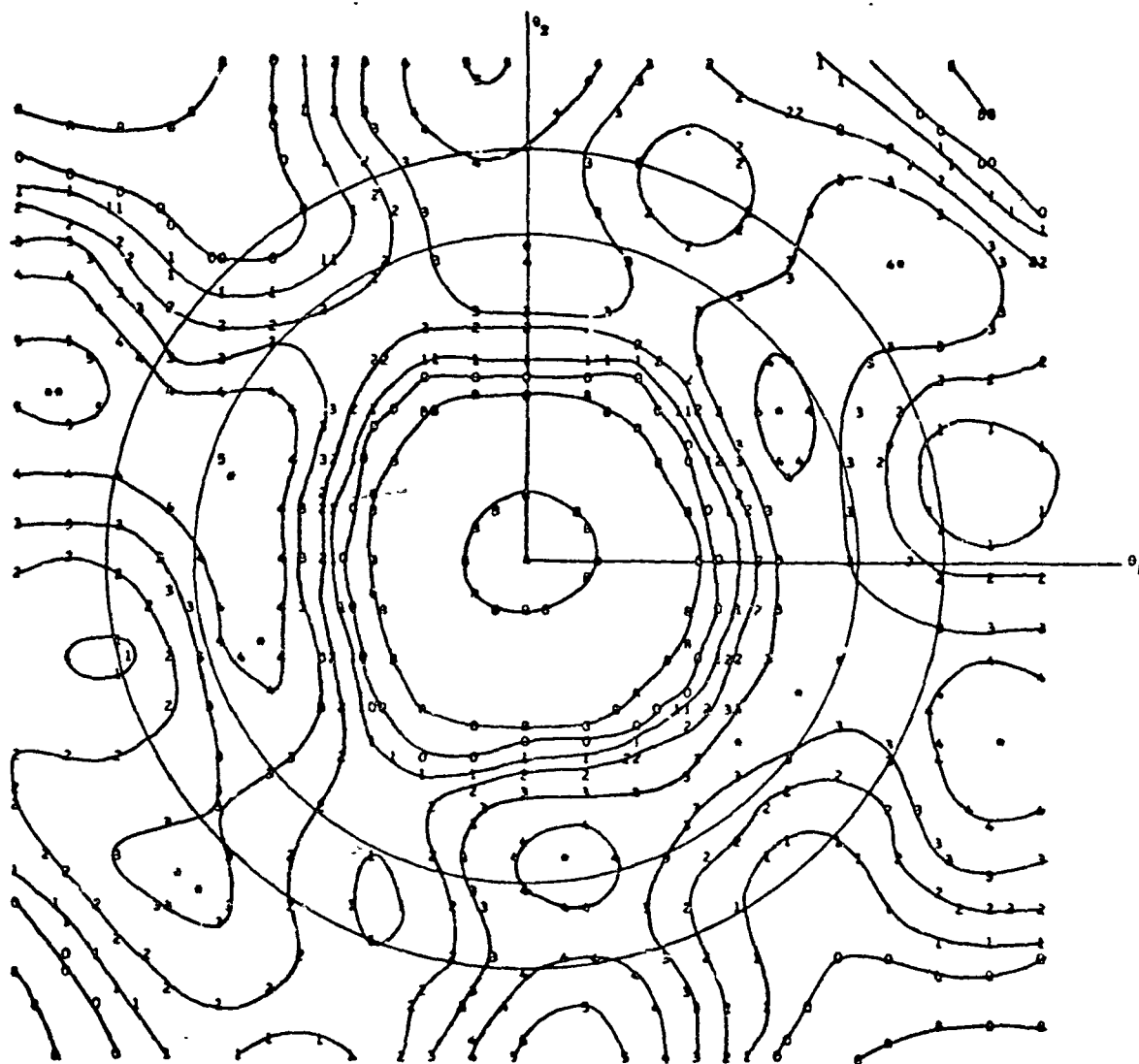


Figure 10-14 Circular polarization, $\delta = 1''25$, $\lambda = 6943 \text{ \AA}$.

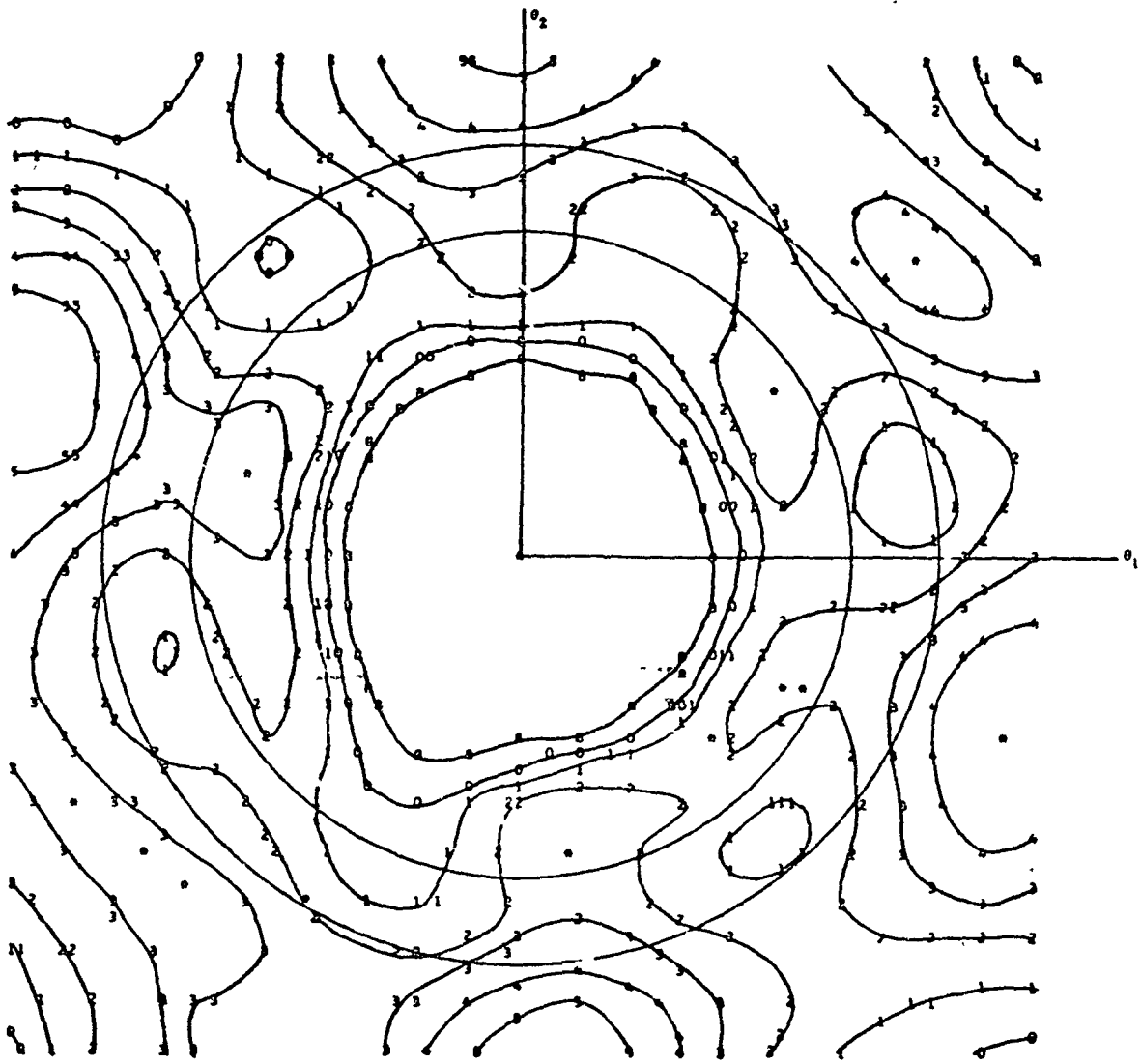


Figure 10-15. Circular polarization, $\delta = 1.775$ $\lambda = 6943 \text{ \AA}$.

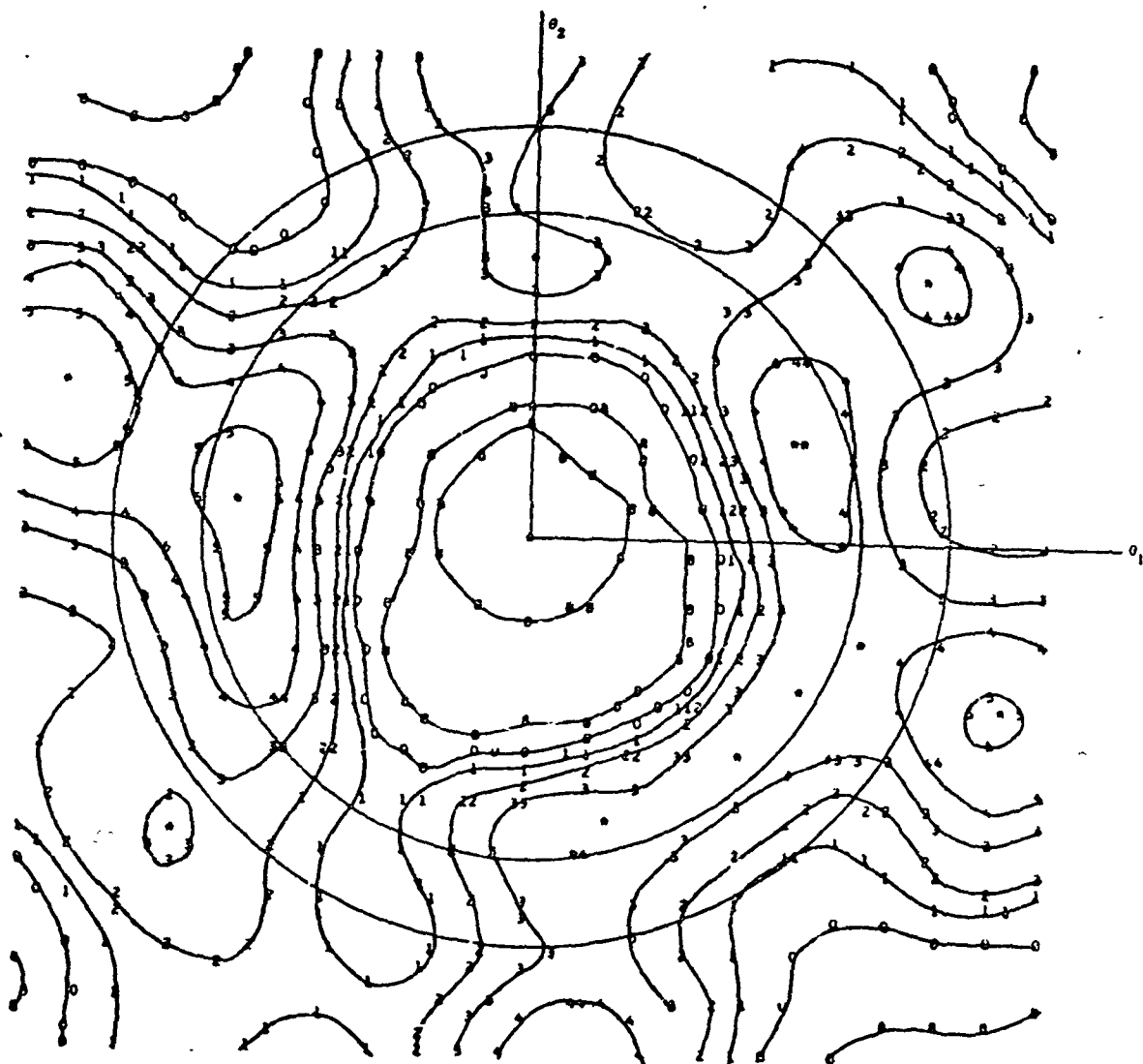


Figure 10-16. Circular polarization, $\bar{\tau} = 1.725$ (mixed dihedral angles), $\lambda = 6943 \text{ \AA}$.

“PAGE MISSING FROM AVAILABLE VERSION”

p. 158

11. EFFECT OF OPTICAL COHERENCE

The range corrections given in Section 10 were derived by adding the intensities of the reflections from each cube corner to construct the return pulse. Since slight changes in the direction of illumination of the satellite give different phase relationships among the reflections from individual cube corners, the shape and strength of the laser echo from Lageos varies from pulse to pulse when the individual reflections are added coherently. The variation of the return energy is described by the Rayleigh distribution. The effect on the range correction for various pulse lengths and pulse detection methods has been analyzed by constructing a set of coherent returns by using a pseudo random number generator to assign phases to the individual reflections. It can be shown mathematically that the incoherent centroid range correction is the average of the coherent centroid range corrections when each pulse is weighted by its intensity. This result is only approximately true for other pulse detection methods.

Table 16 gives a statistical summary of the set of coherent range corrections constructed for three different pulse lengths. The table lists the coherent average minus the incoherent value (Δ), the standard deviation of an individual pulse (σ), the number of coherent returns in the sample (N), the standard deviation of the average ($\sigma_m = \sigma/\sqrt{N}$), and the ratio of the difference Δ to the standard deviation of the mean (σ_m). The last column is a measure of the statistical significance of Δ . The variation of the range correction (σ) due to coherent interference increases as the pulse length increases, and reaches a value of about 40 mm for the 20-nsec pulse length. The greatest variations occur for the weakest pulses. When each return is weighted by its intensity, the standard deviation of a pulse of average energy is found to be on the order of 10 mm. For long pulses, the return pulse shape is nearly the same as the transmitted pulse shape. As a result, there is no difference between the range correction for different pulse detection methods and no bias in the average coherent range correction. For the shortest pulse length (0.2 nsec), there is a small but statistically significant bias in the coherent average for all pulse detection methods, which is made possible by the asymmetry of the contributions to the return along the line of sight. Weighting by signal strength removes all the bias for centroid detection, most of the bias for half-area detection, and a little of the bias for half-maximum detection.

PRECEDING PAGE BLANK NOT FILMED

Table 16. Difference between the average range correction for a set of coherent returns and the range correction for the incoherent return. The pulse length is in nsecs; Δ , σ , and σ_m are in mm.

Pulse length	Δ	σ	N	σ_m	Δ/σ_m
Centroid, Equal Weighting					
0.2	-2.16	8.67	400	0.43	-4.98
5.0	0.09	26.07	1000	0.82	0.11
20.0	-2.01	37.17	1000	1.18	-1.71
Centroid, Weighted by Signal Strength					
0.2	0.04	7.03	400	0.35	0.11
5.0	0.02	10.81	1000	0.34	0.07
20.0	-0.23	11.34	1000	0.36	-0.65
Half-Area, Equal Weighting					
0.2	-2.55	10.07	400	0.50	-5.06
5.0	0.02	28.27	1000	0.89	0.02
20.0	-2.16	40.17	1000	1.27	-1.70
Half-Area, Weighted by Signal Strength					
0.2	-0.82	7.72	400	0.39	-2.12
5.0	-0.01	10.81	1000	0.34	-0.02
20.0	-0.24	11.32	1000	0.36	-0.68
Half-Maximum, Equal Weight					
0.2	-3.47	9.84	400	0.49	-7.06
5.0	0.34	26.78	1000	0.85	0.40
20.0	-2.43	44.82	1000	1.42	-1.72
Half-Maximum, Weighted by Signal Strength					
0.2	-2.54	6.93	400	0.35	-7.33
5.0	-0.16	10.51	1000	0.33	-0.48
20.0	-0.29	11.27	1000	0.36	-0.82

Figure 11 gives some sample coherent and incoherent pulse shapes for three pulse lengths. Only one coherent return is given for the 20- and 5-nsec pulse lengths since the effect of coherent interference is primarily a displacement of the pulse rather than a distortion of the shape for long pulses. Ten sample coherent pulses are given at 0.2 nsec. The position, in meters, listed in the first column of Figure 11, is measured with respect to the center of the pulse that would be received from a point reflector at the center of gravity of the satellite. The intensity in the second column is in normalized units such that the area under the curve is equal to the signal strength in equivalent number of cube corners at normal incidence.

POSITION (METERS)	INTENSITY	20. NANOSECOND PULSE	INCOHERENT RETURN
-9.2328	.0010		
-8.6778	.0026		
-8.3220	.0030		
-8.3670	.0037		
-8.7130	.0045		
-8.0580	.0056		
-7.9030	.0068		
-7.7481	.0083		
-7.5931	.0101		
-7.4382	.0122		
-7.2832	.0147		
-7.1282	.0177		
-6.9733	.0212		
-6.8183	.0253		
-6.6633	.0300		
-6.5084	.0354		
-6.3534	.0416		
-6.1985	.0487		
-6.0435	.0577		
-5.8885	.0675		
-5.7336	.0782		
-5.5786	.0906		
-5.4237	.1049		
-5.2687	.1201		
-5.1137	.1375		
-4.9588	.1560		
-4.8038	.1763		
-4.6488	.1982		
-4.4939	.2228		
-4.3389	.2501		
-4.1840	.2800		
-4.0290	.3125		
-3.8740	.3488		
-3.7191	.3902		
-3.5641	.4368		
-3.4091	.4881		
-3.2541	.5451		
-3.0992	.6080		
-2.9443	.6771		
-2.7893	.7521		
-2.6343	.8330		
-2.4793	.9200		
-2.3243	1.0140		
-2.1693	1.1160		
-2.0143	1.2260		
-1.8593	1.3440		
-1.7043	1.4700		
-1.5493	1.6040		
-1.3943	1.7460		
-1.2393	1.8960		
-1.0843	2.0540		
-0.9293	2.2200		
-0.7743	2.3940		
-0.6193	2.5760		
-0.4643	2.7660		
-0.3093	2.9640		
-0.1543	3.1700		
0.0000	3.3840		
0.1450	3.6060		
0.2900	3.8460		
0.4350	4.1040		
0.5800	4.3700		
0.7250	4.6440		
0.8700	4.9260		
1.0150	5.2160		
1.1600	5.5140		
1.3050	5.8200		
1.4500	6.1340		
1.5950	6.4560		
1.7400	6.7860		
1.8850	7.1240		
2.0300	7.4700		
2.1750	7.8240		
2.3200	8.1860		
2.4650	8.5560		
2.6100	8.9340		
2.7550	9.3200		
2.9000	9.7140		
3.0450	10.1160		
3.1900	10.5260		
3.3350	10.9440		
3.4800	11.3700		
3.6250	11.8040		
3.7700	12.2460		
3.9150	12.6960		
4.0600	13.1540		
4.2050	13.6200		
4.3500	14.0940		
4.4950	14.5760		
4.6400	15.0660		
4.7850	15.5640		
4.9300	16.0700		
5.0750	16.5840		
5.2200	17.1060		
5.3650	17.6360		
5.5100	18.1740		
5.6550	18.7200		
5.8000	19.2740		
5.9450	19.8360		
6.0900	20.4060		
6.2350	20.9840		
6.3800	21.5700		
6.5250	22.1640		
6.6700	22.7660		
6.8150	23.3760		
6.9600	23.9940		
7.1050	24.6200		
7.2500	25.2540		
7.3950	25.8960		
7.5400	26.5460		
7.6850	27.2040		
7.8300	27.8700		
7.9750	28.5440		
8.1200	29.2260		
8.2650	29.9160		
8.4100	30.6140		
8.5550	31.3200		
8.7000	32.0340		
8.8450	32.7560		
8.9900	33.4860		
9.1350	34.2240		
9.2800	34.9700		
9.4250	35.7240		
9.5700	36.4860		
9.7150	37.2560		
9.8600	38.0340		
10.0050	38.8200		

Figure 1: Sample incoherent and coherent reflected pulse shapes. The intensity is plotted vs. the distance along the line of sight.
Figure 11-1

ORIGINAL PAGE IS
OF POOR QUALITY

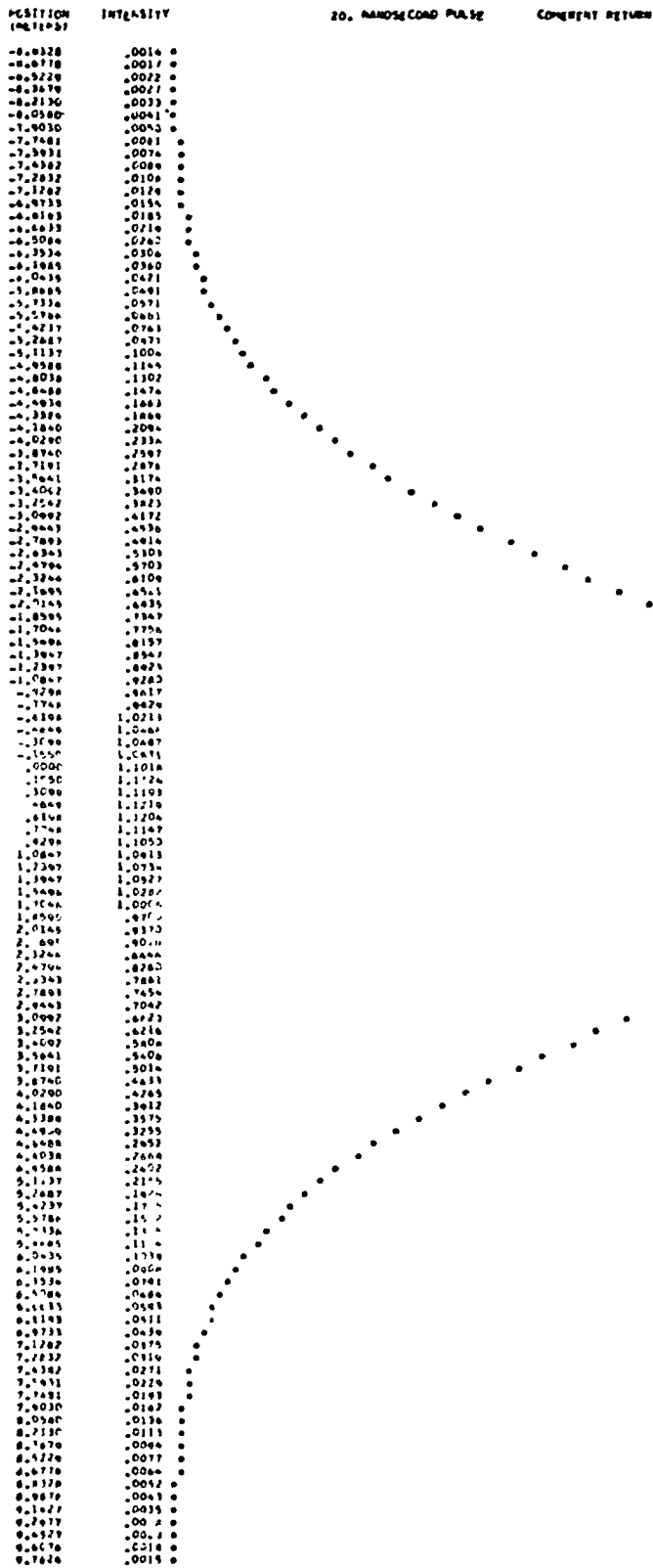


Figure 11.2

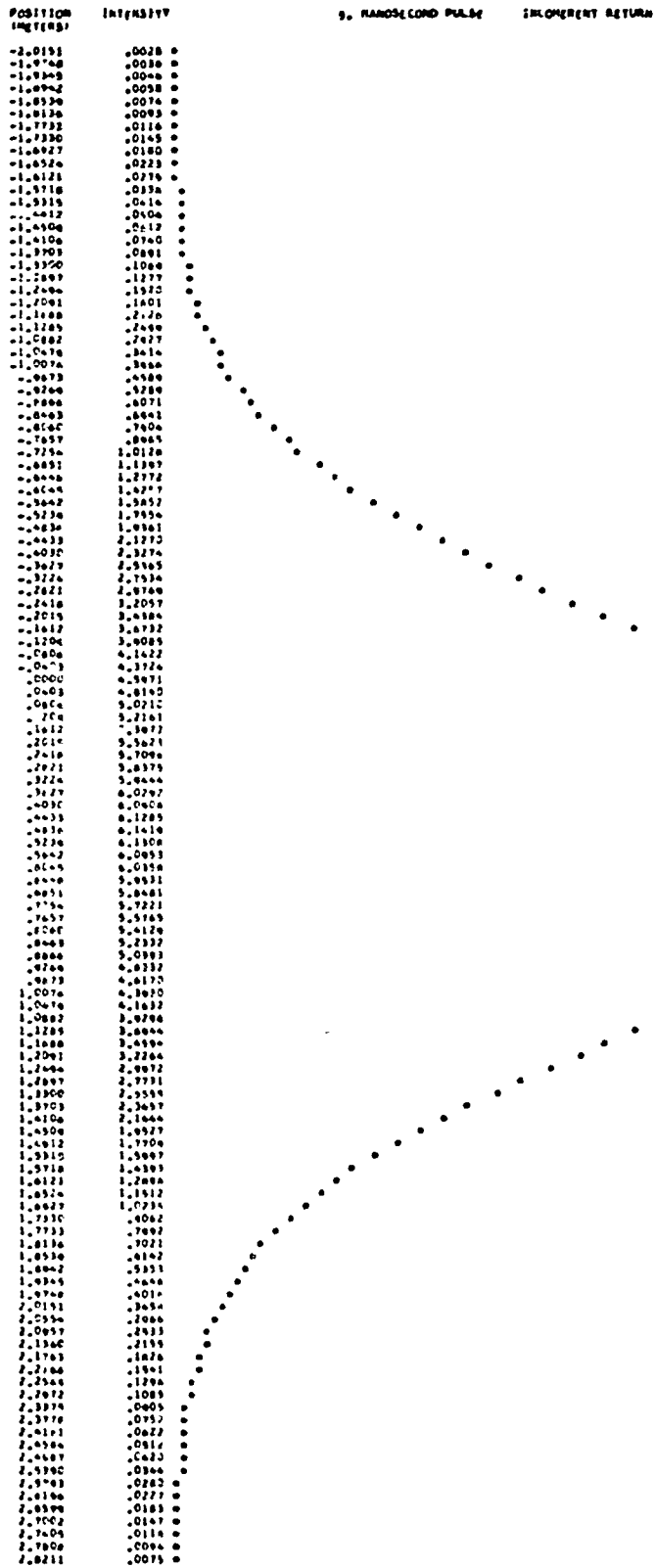


Figure 11.3

POSITION
SPE (kHz)

5. NANOSECOND PULSE

COMBENT RETURN

POSITION SPE (kHz)	INTENSITY
-2.0151	.0172
-1.9744	.0156
-1.9345	.0203
-1.8942	.0237
-1.8539	.0275
-1.8136	.0310
-1.7733	.0354
-1.7330	.0401
-1.6927	.0450
-1.6524	.0500
-1.6121	.0552
-1.5718	.0606
-1.5315	.0662
-1.4912	.0720
-1.4509	.0780
-1.4106	.0841
-1.3703	.0904
-1.3300	.0968
-1.2897	.1034
-1.2494	.1102
-1.2091	.1172
-1.1688	.1244
-1.1285	.1318
-1.0882	.1394
-1.0479	.1472
-1.0076	.1552
-.9673	.1634
-.9270	.1718
-.8867	.1804
-.8464	.1892
-.8061	.1982
-.7658	.2074
-.7255	.2168
-.6852	.2264
-.6449	.2362
-.6046	.2462
-.5643	.2564
-.5240	.2668
-.4837	.2774
-.4434	.2882
-.4031	.2992
-.3628	.3104
-.3225	.3218
-.2822	.3334
-.2419	.3452
-.2016	.3572
-.1612	.3694
-.1209	.3818
-.0806	.3944
-.0403	.4072
.0000	.4202
.0400	.4334
.0800	.4468
.1200	.4604
.1600	.4742
.2000	.4882
.2400	.5024
.2800	.5168
.3200	.5314
.3600	.5462
.4000	.5612
.4400	.5764
.4800	.5918
.5200	.6074
.5600	.6232
.6000	.6392
.6400	.6554
.6800	.6718
.7200	.6884
.7600	.7052
.8000	.7222
.8400	.7394
.8800	.7568
.9200	.7744
.9600	.7922
1.0000	.8102
1.0400	.8284
1.0800	.8468
1.1200	.8654
1.1600	.8842
1.2000	.9032
1.2400	.9224
1.2800	.9418
1.3200	.9614
1.3600	.9812
1.4000	1.0012
1.4400	1.0214
1.4800	1.0418
1.5200	1.0624
1.5600	1.0832
1.6000	1.1042
1.6400	1.1254
1.6800	1.1468
1.7200	1.1684
1.7600	1.1902
1.8000	1.2122
1.8400	1.2344
1.8800	1.2568
1.9200	1.2794
1.9600	1.3022
2.0000	1.3252
2.0400	1.3484
2.0800	1.3718
2.1200	1.3954
2.1600	1.4192
2.2000	1.4432
2.2400	1.4674
2.2800	1.4918
2.3200	1.5164
2.3600	1.5412
2.4000	1.5662
2.4400	1.5914
2.4800	1.6168
2.5200	1.6424
2.5600	1.6682
2.6000	1.6942
2.6400	1.7204
2.6800	1.7468
2.7200	1.7734
2.7600	1.8002
2.8000	1.8272
2.8400	1.8544
2.8800	1.8818
2.9200	1.9094
2.9600	1.9372
3.0000	1.9652
2.0211	.0334

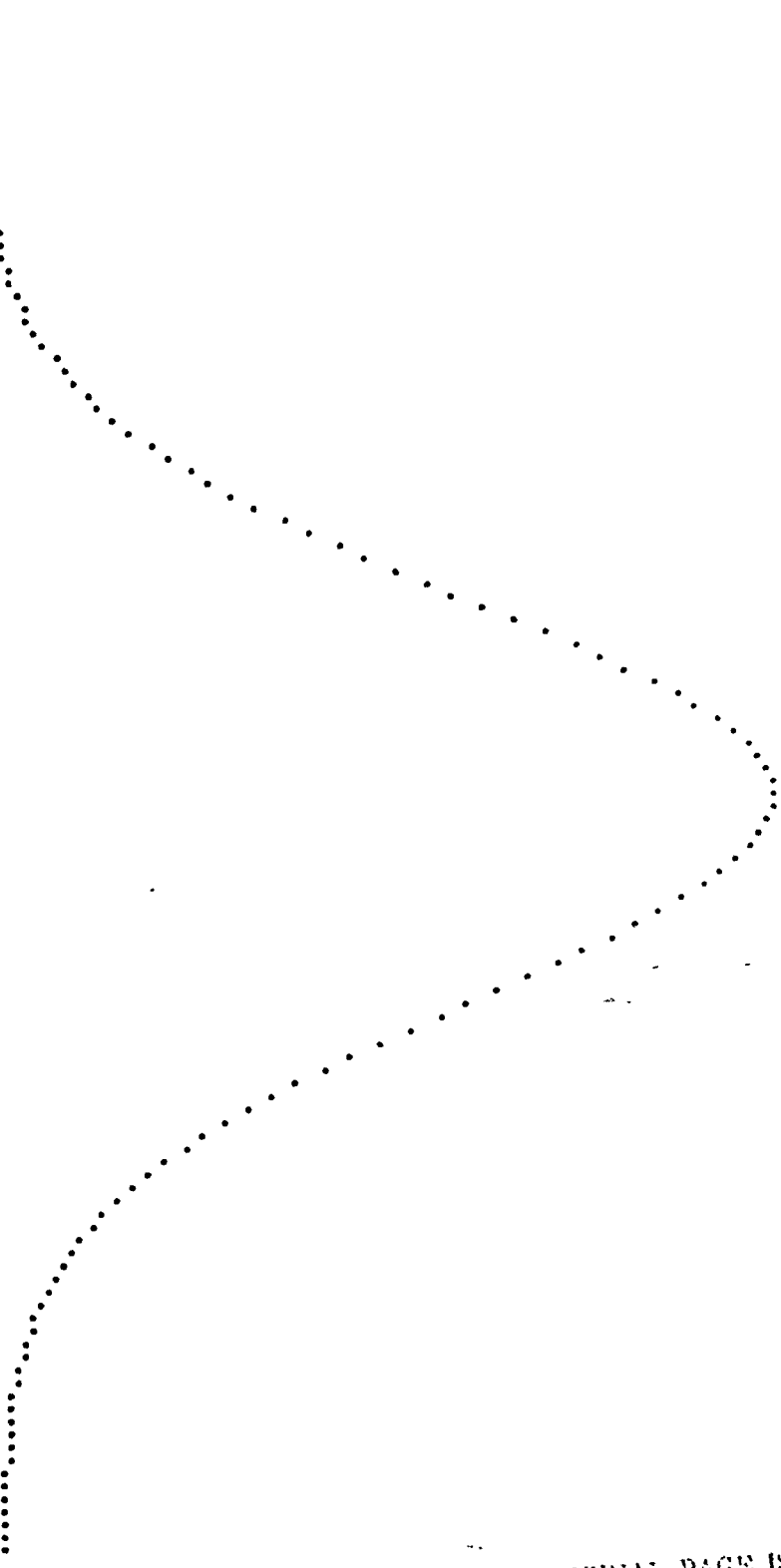


Figure 11-4

ORIGINAL PAGE IS
OF POOR QUALITY

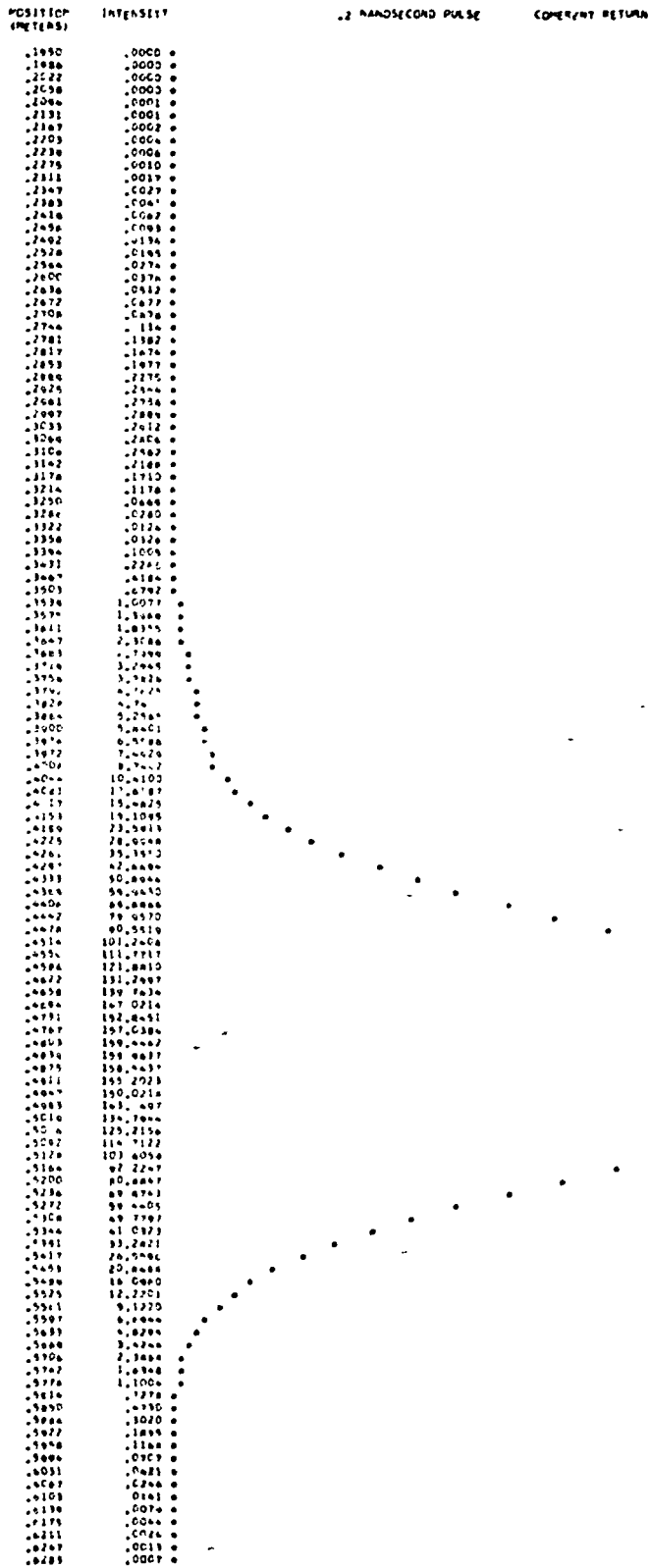


Figure 11.6

.1986	.0000
.2022	.0000
.2058	.0000
.2094	.0001
.2131	.0001
.2167	.0002
.2203	.0003
.2239	.0005
.2275	.0008
.2311	.0012
.2347	.0018
.2383	.0027
.2419	.0040
.2456	.0057
.2492	.0079
.2528	.0109
.2564	.0147
.2600	.0194
.2636	.0250
.2672	.0316
.2708	.0397
.2744	.0474
.2781	.0540
.2817	.0647
.2853	.0729
.2889	.0801
.2925	.0856
.2961	.0893
.2997	.0900
.3033	.0886
.3069	.0856
.3105	.0824
.3142	.0814
.3178	.0865
.3214	.1030
.3250	.1377
.3286	.1896
.3322	.2492
.3358	.4490
.3394	.6630
.3431	.9565
.3467	1.3457
.3503	1.6448
.3539	2.4709
.3575	3.2364
.3611	4.1528
.3647	5.2283
.3683	6.4473
.3719	7.8731
.3755	9.5429
.3792	11.3739
.3828	13.3622
.3864	15.1047
.3900	17.3011
.3936	19.6563
.3972	22.1815
.4008	24.8862
.4044	27.8784
.4081	31.0137
.4117	34.4037
.4153	38.3119
.4189	42.5084
.4225	47.1133
.4261	52.1384
.4297	57.5703
.4333	63.3602
.4369	69.5021
.4405	75.6199
.4442	81.7843
.4478	87.7030
.4514	93.1377
.4550	97.8332
.4586	101.5503
.4622	104.6610
.4658	105.1904
.4694	104.5235
.4731	102.9194
.4767	99.5179
.4803	94.7374
.4839	88.7667
.4875	81.8496
.4911	74.2454
.4947	66.1072
.4983	58.2400
.5019	50.3425
.5055	42.8423
.5092	35.9771
.5128	29.6814
.5164	24.1586
.5200	19.3761
.5236	15.3741
.5272	11.9552
.5308	9.2034
.5344	6.9932
.5381	5.2460
.5417	3.8858
.5453	2.8422
.5489	2.0529
.5525	1.4647
.5561	1.0412
.5597	.7171
.5633	.4824
.5669	.3338
.5706	.2235
.5742	.1478
.5778	.0965
.5814	.0623
.5850	.0398
.5886	.0251
.5922	.0157
.5958	.0097
.5994	.0059
.6031	.0036
.6067	.0022
.6103	.0013
.6139	.0007
.6175	.0004
.6211	.0002
.6247	.0001
.6283	.0001

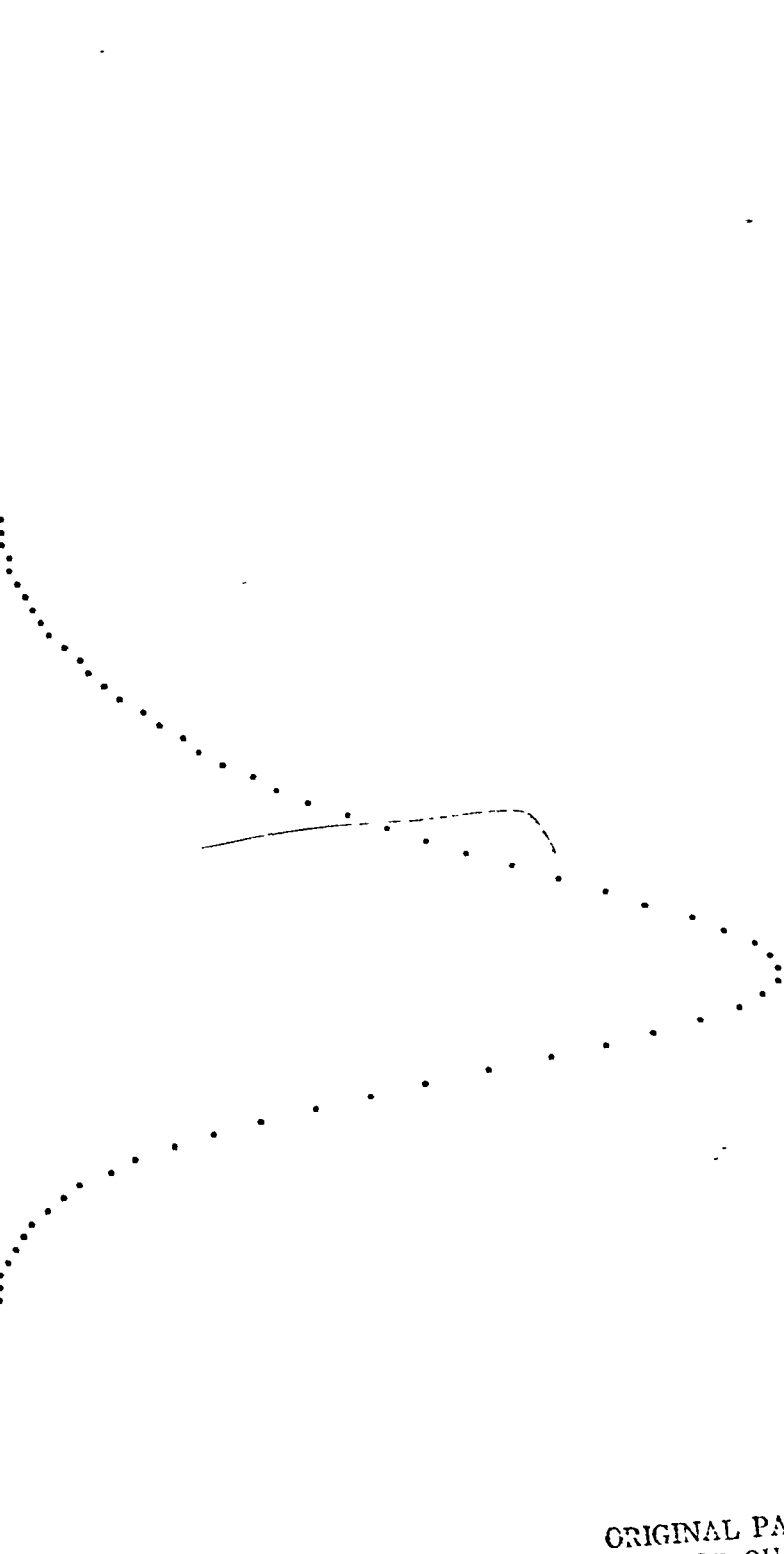


Figure 11-7

ORIGINAL PAGE IS
OF POOR QUALITY

POSITION
(METERS)

INTENSITY

.2 NANOSECOND PULSE

COHERENT RETURN

.1930	.0003
.1980	.0004
.2022	.0005
.2058	.0006
.2094	.0007
.2131	.0008
.2167	.0009
.2203	.0010
.2239	.0011
.2275	.0012
.2311	.0013
.2347	.0014
.2383	.0015
.2419	.0016
.2455	.0017
.2492	.0018
.2528	.0019
.2564	.0020
.2600	.0021
.2636	.0022
.2672	.0023
.2708	.0024
.2744	.0025
.2780	.0026
.2817	.0027
.2853	.0028
.2889	.0029
.2925	.0030
.2961	.0031
.2997	.0032
.3033	.0033
.3069	.0034
.3105	.0035
.3141	.0036
.3177	.0037
.3214	.0038
.3250	.0039
.3286	.0040
.3322	.0041
.3358	.0042
.3394	.0043
.3431	.0044
.3467	.0045
.3503	.0046
.3539	.0047
.3575	.0048
.3611	.0049
.3647	.0050
.3683	.0051
.3719	.0052
.3755	.0053
.3792	.0054
.3828	.0055
.3864	.0056
.3900	.0057
.3936	.0058
.3972	.0059
.4008	.0060
.4044	.0061
.4081	.0062
.4117	.0063
.4153	.0064
.4189	.0065
.4225	.0066
.4261	.0067
.4297	.0068
.4333	.0069
.4369	.0070
.4405	.0071
.4441	.0072
.4477	.0073
.4513	.0074
.4549	.0075
.4585	.0076
.4621	.0077
.4657	.0078
.4693	.0079
.4729	.0080
.4765	.0081
.4801	.0082
.4837	.0083
.4873	.0084
.4909	.0085
.4945	.0086
.4981	.0087
.5017	.0088
.5053	.0089
.5089	.0090
.5125	.0091
.5161	.0092
.5197	.0093
.5233	.0094
.5269	.0095
.5305	.0096
.5341	.0097
.5377	.0098
.5413	.0099
.5449	.0100
.5485	.0101
.5521	.0102
.5557	.0103
.5593	.0104
.5629	.0105
.5665	.0106
.5701	.0107
.5737	.0108
.5773	.0109
.5809	.0110
.5845	.0111
.5881	.0112
.5917	.0113
.5953	.0114
.5989	.0115
.6025	.0116
.6061	.0117
.6097	.0118
.6133	.0119
.6169	.0120
.6205	.0121
.6241	.0122
.6277	.0123

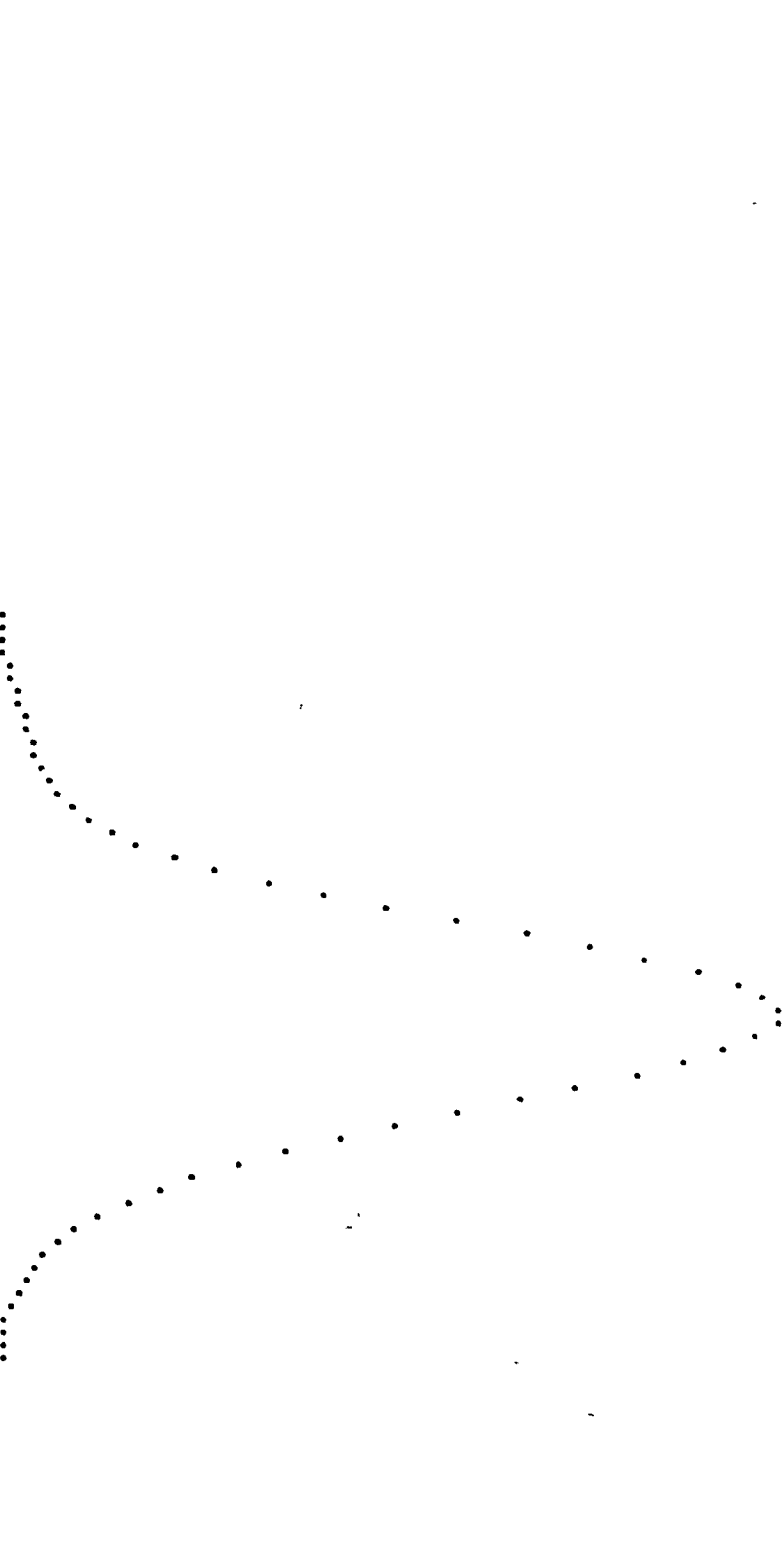


Figure 11-4

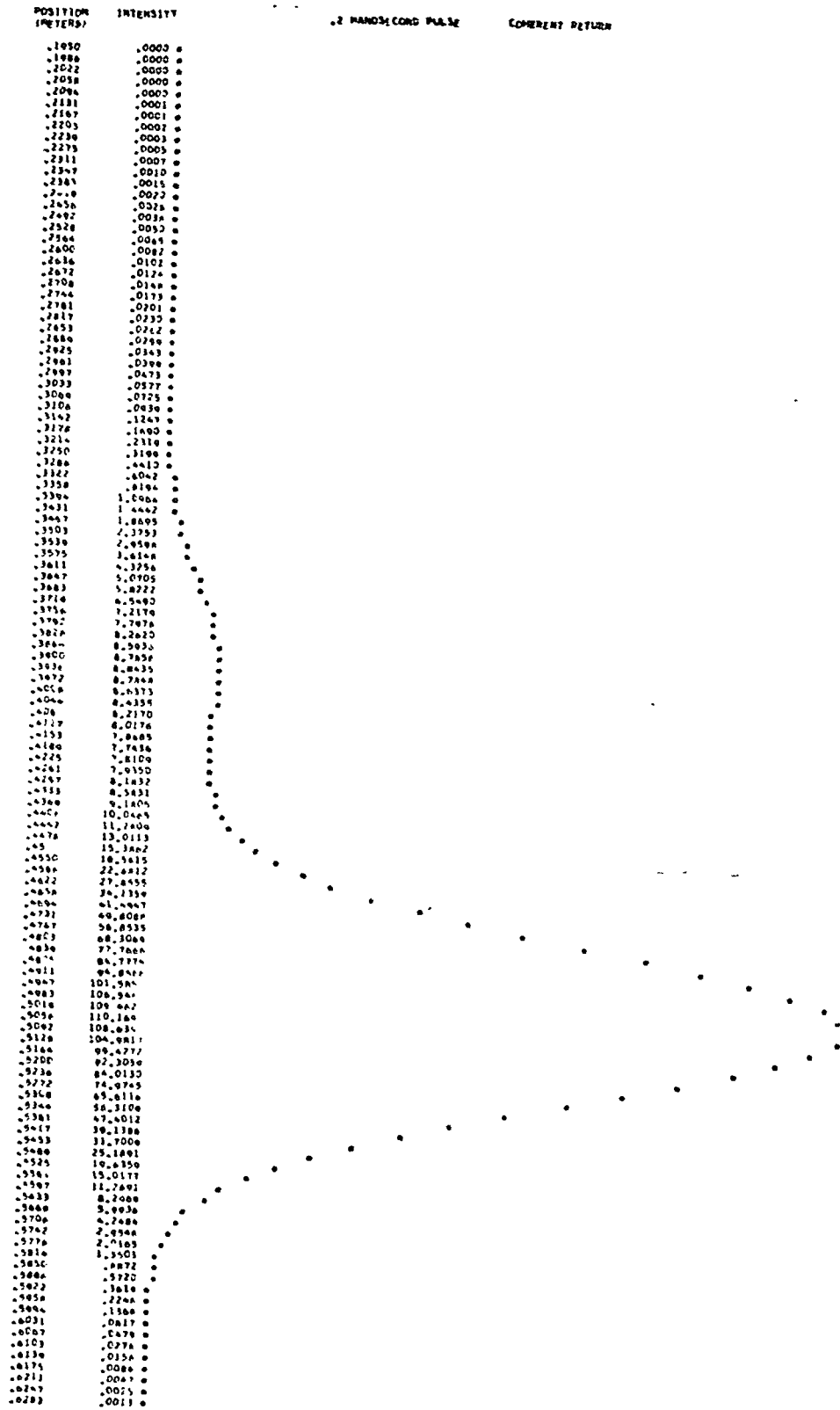


Figure 11.9
170

POSITION (METERS)	INTENSITY	.2 NANSECOND PULSE	COMMENT RETURN
.1950	.0000		
.1986	.0003		
.2022	.0000		
.2058	.0000		
.2094	.0001		
.2131	.0001		
.2167	.0002		
.2203	.0004		
.2239	.0007		
.2275	.0011		
.2311	.0018		
.2347	.0028		
.2383	.0044		
.2419	.0072		
.2456	.0104		
.2492	.0164		
.2528	.0247		
.2564	.0350		
.2600	.0480		
.2636	.0707		
.2672	.0970		
.2708	.1318		
.2744	.1767		
.2781	.2329		
.2817	.3024		
.2853	.3865		
.2889	.4855		
.2925	.6011		
.2961	.7364		
.2997	.8853		
.3033	1.0484		
.3069	1.2228		
.3105	1.4038		
.3142	1.5863		
.3178	1.7735		
.3214	1.9675		
.3250	2.1698		
.3286	2.3817		
.3322	2.5926		
.3358	2.7953		
.3394	2.9923		
.3430	3.1844		
.3467	3.3817		
.3503	3.5747		
.3539	3.7644		
.3575	3.9557		
.3611	4.1481		
.3647	4.3421		
.3683	4.5376		
.3719	4.7340		
.3755	4.9315		
.3792	5.1303		
.3828	5.3297		
.3864	5.5294		
.3900	5.7292		
.3936	5.9291		
.3972	6.1290		
.4008	6.3290		
.4044	6.5290		
.4081	6.7290		
.4117	6.9290		
.4153	7.1290		
.4189	7.3290		
.4225	7.5290		
.4261	7.7290		
.4297	7.9290		
.4333	8.1290		
.4369	8.3290		
.4405	8.5290		
.4441	8.7290		
.4477	8.9290		
.4513	9.1290		
.4549	9.3290		
.4585	9.5290		
.4621	9.7290		
.4657	9.9290		
.4693	10.1290		
.4729	10.3290		
.4765	10.5290		
.4801	10.7290		
.4837	10.9290		
.4873	11.1290		
.4909	11.3290		
.4945	11.5290		
.4981	11.7290		
.5017	11.9290		
.5053	12.1290		
.5089	12.3290		
.5125	12.5290		
.5161	12.7290		
.5197	12.9290		
.5233	13.1290		
.5269	13.3290		
.5305	13.5290		
.5341	13.7290		
.5377	13.9290		
.5413	14.1290		
.5449	14.3290		
.5485	14.5290		
.5521	14.7290		
.5557	14.9290		
.5593	15.1290		
.5629	15.3290		
.5665	15.5290		
.5701	15.7290		
.5737	15.9290		
.5773	16.1290		
.5809	16.3290		
.5845	16.5290		
.5881	16.7290		
.5917	16.9290		
.5953	17.1290		
.5989	17.3290		
.6025	17.5290		
.6061	17.7290		
.6097	17.9290		
.6133	18.1290		
.6169	18.3290		
.6205	18.5290		
.6241	18.7290		
.6277	18.9290		
.6313	19.1290		
.6349	19.3290		
.6385	19.5290		
.6421	19.7290		
.6457	19.9290		
.6493	20.1290		
.6529	20.3290		
.6565	20.5290		
.6601	20.7290		
.6637	20.9290		
.6673	21.1290		
.6709	21.3290		
.6745	21.5290		
.6781	21.7290		
.6817	21.9290		
.6853	22.1290		
.6889	22.3290		
.6925	22.5290		
.6961	22.7290		
.6997	22.9290		
.7033	23.1290		
.7069	23.3290		
.7105	23.5290		
.7141	23.7290		
.7177	23.9290		
.7213	24.1290		
.7249	24.3290		
.7285	24.5290		
.7321	24.7290		
.7357	24.9290		
.7393	25.1290		
.7429	25.3290		
.7465	25.5290		
.7501	25.7290		
.7537	25.9290		
.7573	26.1290		
.7609	26.3290		
.7645	26.5290		
.7681	26.7290		
.7717	26.9290		
.7753	27.1290		
.7789	27.3290		
.7825	27.5290		
.7861	27.7290		
.7897	27.9290		
.7933	28.1290		
.7969	28.3290		
.8005	28.5290		
.8041	28.7290		
.8077	28.9290		
.8113	29.1290		
.8149	29.3290		
.8185	29.5290		
.8221	29.7290		
.8257	29.9290		
.8293	30.1290		

FIGURE 11-10

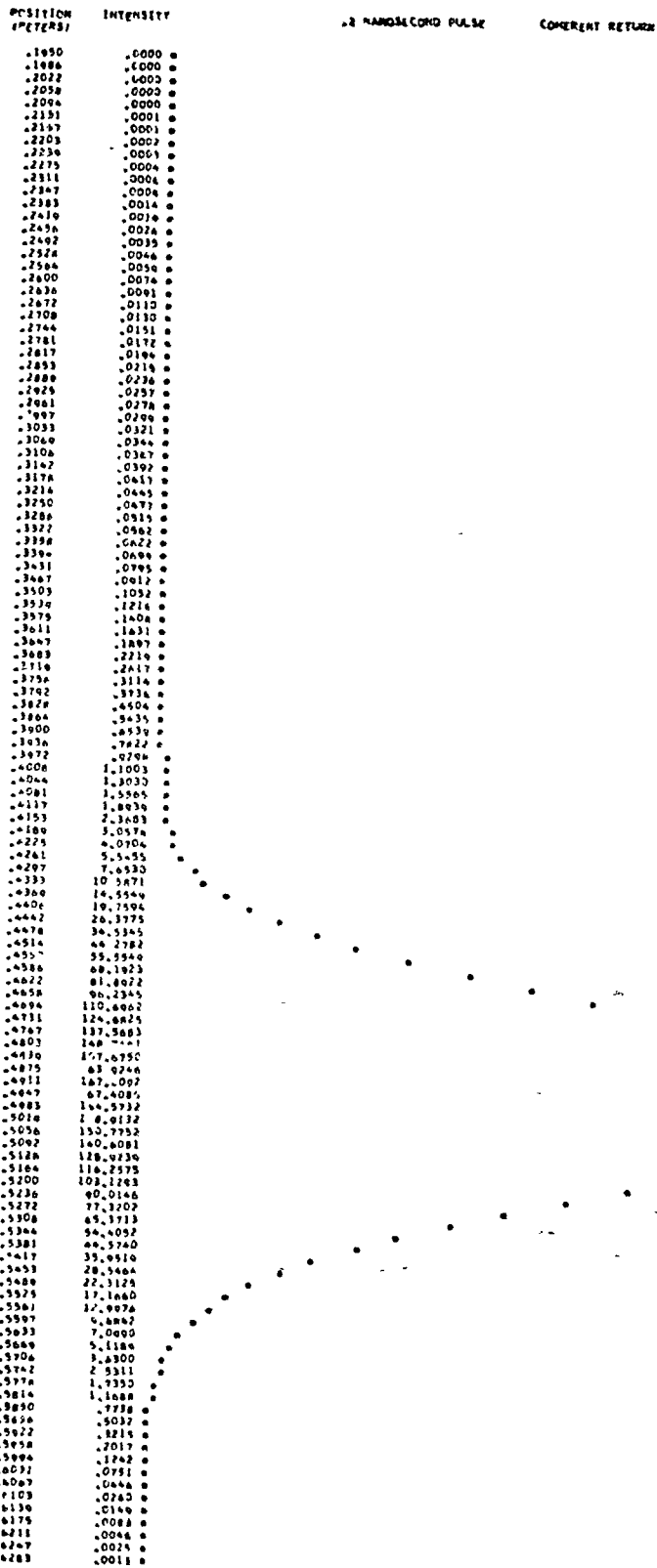


Figure 11.11

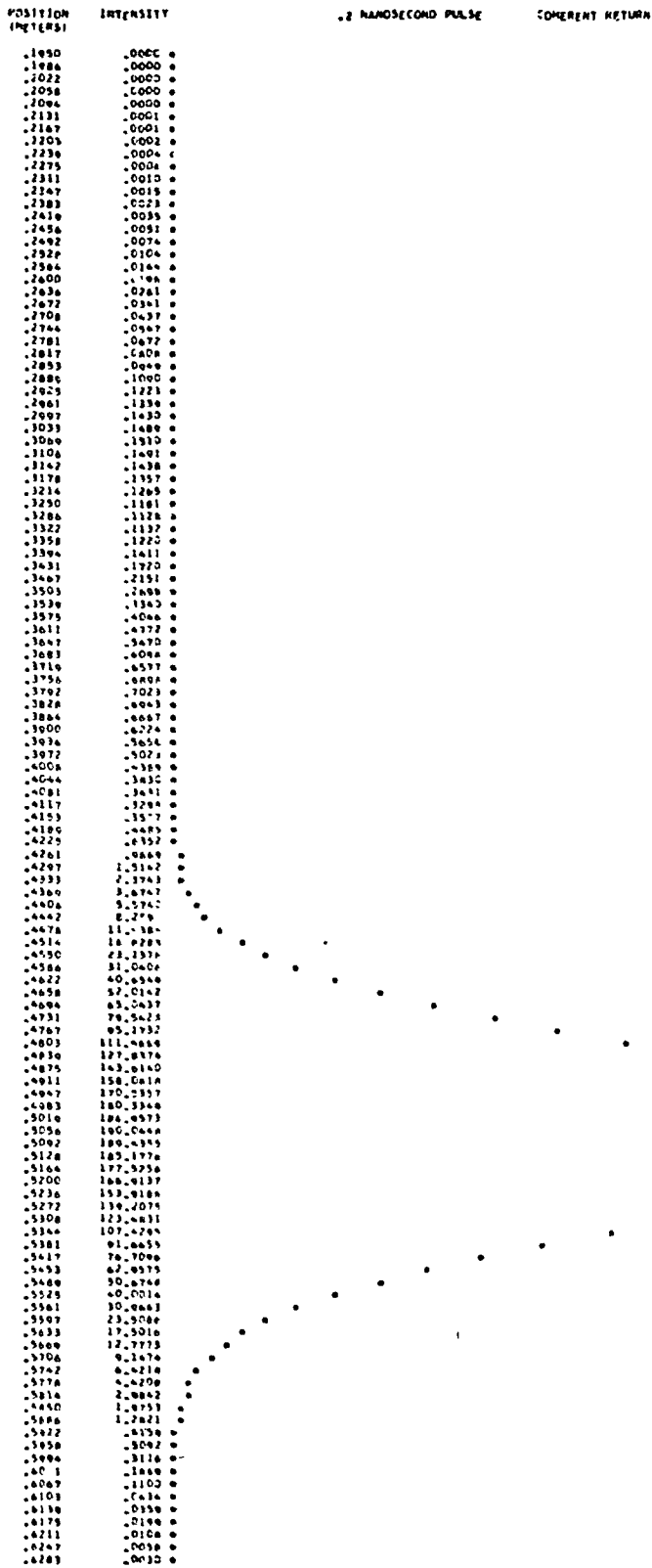


Figure 11-12

POSITION (METERS)	INTENSITY	.2 NANSECOND PULSE	COHERENT RETURN
.1890	.0300		
.1880	.0000		
.2027	.0000		
.2058	.0000		
.2064	.0001		
.2181	.0001		
.2167	.0002		
.2203	.0003		
.2239	.0004		
.2275	.0004		
.2311	.0014		
.2337	.0024		
.2383	.0041		
.2419	.0065		
.2456	.0107		
.2492	.0157		
.2528	.0237		
.2564	.0353		
.2600	.0517		
.2636	.0746		
.2672	.1050		
.2708	.1480		
.2744	.2036		
.2781	.2756		
.2817	.3668		
.2853	.4857		
.2889	.6203		
.2925	.7879		
.2961	.9857		
.2997	1.2146		
.3033	1.4787		
.3069	1.7830		
.3106	2.1287		
.3142	2.5250		
.3178	2.9827		
.3214	3.5000		
.3250	4.0842		
.3286	4.7461		
.3322	5.4876		
.3358	6.3196		
.3394	7.2415		
.3431	8.2641		
.3467	9.3878		
.3503	10.6225		
.3539	11.9681		
.3575	13.4240		
.3611	14.9904		
.3647	16.6673		
.3683	18.4547		
.3719	20.3526		
.3755	22.3610		
.3792	24.4800		
.3828	26.7105		
.3864	29.0525		
.3900	31.5060		
.3936	34.0710		
.3972	36.7475		
.4008	39.5350		
.4044	42.4335		
.4081	45.4430		
.4117	48.5635		
.4153	51.7950		
.4189	55.1375		
.4225	58.5910		
.4261	62.1555		
.4297	65.8310		
.4333	69.6175		
.4369	73.5150		
.4406	77.5235		
.4442	81.6430		
.4478	85.8735		
.4514	90.2150		
.4550	94.6675		
.4586	99.2310		
.4622	103.9055		
.4658	108.6910		
.4694	113.5875		
.4731	118.5950		
.4767	123.7135		
.4803	128.9430		
.4839	134.2835		
.4875	139.7350		
.4911	145.2975		
.4947	150.9710		
.4983	156.7555		
.5019	162.6510		
.5056	168.6575		
.5092	174.7750		
.5128	180.9035		
.5164	187.1430		
.5200	193.4935		
.5236	199.9550		
.5272	206.5275		
.5308	213.2110		
.5344	220.0055		
.5381	226.9110		
.5417	233.9275		
.5453	241.0550		
.5489	248.2935		
.5525	255.6430		
.5561	263.1035		
.5597	270.6750		
.5633	278.3575		
.5669	286.1510		
.5706	294.0555		
.5742	302.0710		
.5778	310.1975		
.5814	318.4350		
.5850	326.7835		
.5886	335.2430		
.5922	343.8135		
.5958	352.4950		
.5994	361.2875		
.6031	370.1910		
.6067	379.2055		
.6103	388.3310		
.6139	397.5675		
.6175	406.9150		
.6211	416.3735		
.6247	425.9430		
.6283	435.6235		

Figure 11-12.

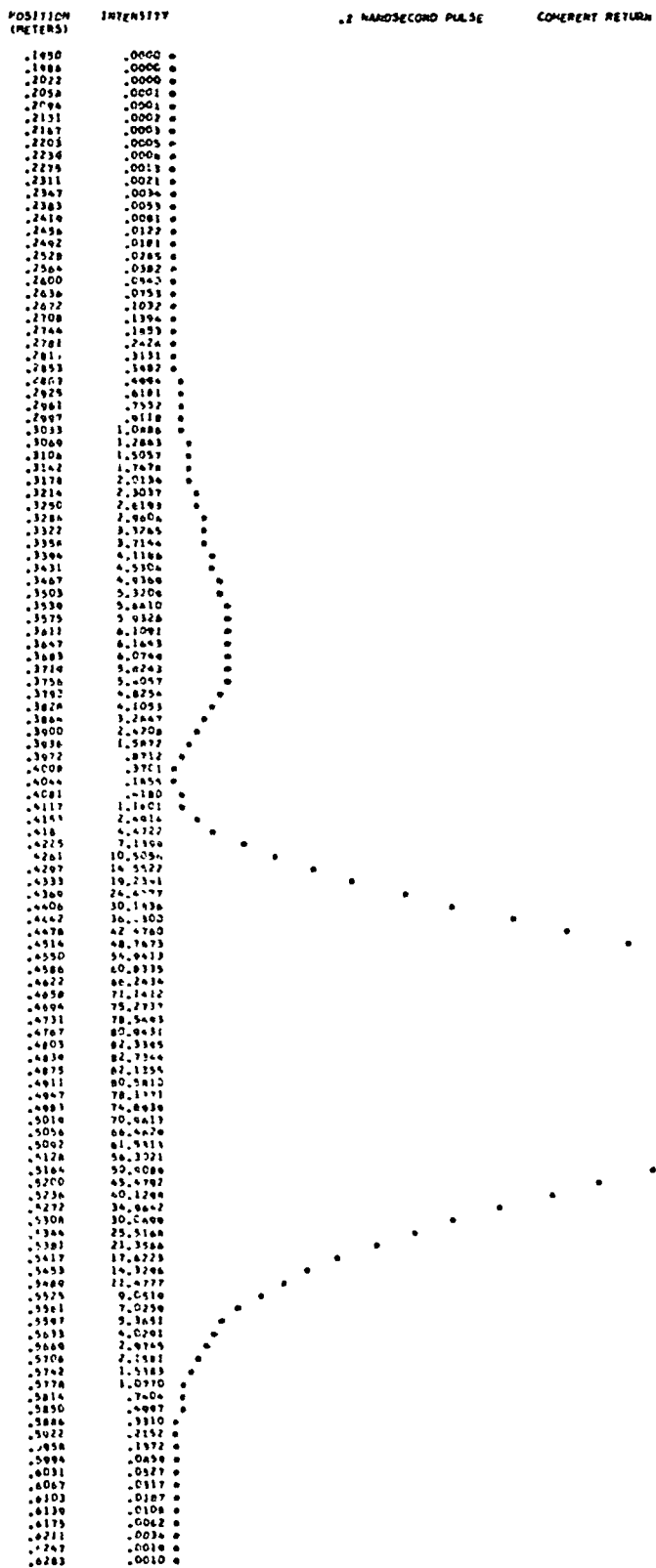


Figure 11-14

POSITION (METERS)	INTENSITY	.2 NANOSECOND PULSE	CONCURRENT RETURN
.1990	.0000		
.1998	.0000		
.2027	.0000		
.2058	.0000		
.2094	.0001		
.2131	.0002		
.2167	.0003		
.2203	.0005		
.2238	.0008		
.2275	.0013		
.2311	.0020		
.2347	.0032		
.2383	.0050		
.2419	.0076		
.2456	.0114		
.2492	.0168		
.2528	.0242		
.2564	.0343		
.2600	.0477		
.2636	.0651		
.2672	.0875		
.2708	.1140		
.2744	.1445		
.2781	.1800		
.2817	.2216		
.2853	.2705		
.2888	.326		
.2925	.389		
.2961	.4612		
.2997	.5413		
.3033	.6275		
.3069	.7208		
.3104	.8213		
.3142	.9303		
.3178	1.0478		
.3214	1.1748		
.3250	1.3113		
.3286	1.4573		
.3322	1.6128		
.3358	1.7780		
.3394	1.9530		
.3431	2.1378		
.3467	2.3324		
.3503	2.5368		
.3539	2.7509		
.3575	2.9748		
.3611	3.2085		
.3647	3.4520		
.3683	3.7053		
.3719	3.9684		
.3755	4.2413		
.3791	4.5240		
.3827	4.8165		
.3863	5.1188		
.3899	5.4309		
.3935	5.7528		
.3971	6.0845		
.4007	6.4260		
.4043	6.7773		
.4079	7.1384		
.4115	7.5093		
.4151	7.8900		
.4187	8.2805		
.4223	8.6808		
.4259	9.0909		
.4295	9.5108		
.4331	9.9405		
.4367	10.3799		
.4403	10.8290		
.4439	11.2878		
.4475	11.7563		
.4511	12.2345		
.4547	12.7224		
.4583	13.2201		
.4619	13.7275		
.4655	14.2446		
.4691	14.7713		
.4727	15.3076		
.4763	15.8535		
.4799	16.4090		
.4835	16.9741		
.4871	17.5488		
.4907	18.1331		
.4943	18.7270		
.4979	19.3305		
.5015	19.9436		
.5051	20.5663		
.5087	21.1986		
.5123	21.8405		
.5159	22.4920		
.5195	23.1531		
.5231	23.8238		
.5267	24.5041		
.5303	25.1940		
.5339	25.8935		
.5375	26.6026		
.5411	27.3213		
.5447	28.0496		
.5483	28.7875		
.5519	29.5350		
.5555	30.2921		
.5591	31.0588		
.5627	31.8351		
.5663	32.6210		
.5699	33.4165		
.5735	34.2216		
.5771	35.0363		
.5807	35.8606		
.5843	36.6945		
.5879	37.5380		
.5915	38.3911		
.5951	39.2538		
.5987	40.1261		
.6023	41.0080		
.6059	41.8995		
.6095	42.8006		
.6131	43.7113		
.6167	44.6316		
.6203	45.5615		
.6239	46.5010		
.6275	47.4501		
.6311	48.4088		
.6347	49.3771		
.6383	50.3550		
.6419	51.3425		
.6455	52.3396		
.6491	53.3463		
.6527	54.3626		
.6563	55.3885		
.6599	56.4240		
.6635	57.4691		
.6671	58.5238		
.6707	59.5881		
.6743	60.6620		
.6779	61.7455		
.6815	62.8386		
.6851	63.9413		
.6887	65.0536		
.6923	66.1755		
.6959	67.3070		
.7000	68.4481		
.7040	69.5988		
.7080	70.7591		
.7120	71.9290		
.7160	73.1085		
.7200	74.2976		
.7240	75.4963		
.7280	76.7046		
.7320	77.9225		
.7360	79.1500		
.7400	80.3871		
.7440	81.6338		
.7480	82.8901		
.7520	84.1560		
.7560	85.4315		
.7600	86.7166		
.7640	88.0113		
.7680	89.3156		
.7720	90.6295		
.7760	91.9530		
.7800	93.2861		
.7840	94.6288		
.7880	95.9811		
.7920	97.3430		
.7960	98.7145		
.8000	100.0956		
.8040	101.4863		
.8080	102.8866		
.8120	104.2965		
.8160	105.7160		
.8200	107.1451		
.8240	108.5838		
.8280	110.0321		
.8320	111.4900		
.8360	112.9575		
.8400	114.4346		
.8440	115.9213		
.8480	117.4176		
.8520	118.9235		
.8560	120.4390		
.8600	121.9641		
.8640	123.4988		
.8680	125.0431		
.8720	126.5970		
.8760	128.1605		
.8800	129.7336		
.8840	131.3163		
.8880	132.9086		
.8920	134.5105		
.8960	136.1220		
.9000	137.7431		
.9040	139.3738		
.9080	141.0141		
.9120	142.6640		
.9160	144.3235		
.9200	145.9926		
.9240	147.6713		
.9280	149.3596		
.9320	151.0575		
.9360	152.7650		
.9400	154.4821		
.9440	156.2088		
.9480	157.9451		
.9520	159.6910		
.9560	161.4465		
.9600	163.2116		
.9640	164.9863		
.9680	166.7706		
.9720	168.5645		
.9760	170.3680		
.9800	172.1811		
.9840	174.0038		
.9880	175.8361		
.9920	177.6780		
.9960	179.5295		
1.0000	181.3906		

Figure 11-16.

12. ACCURACY OF RESULTS

Individual range measurements to the Lageos retroreflector array can vary due to a number of factors. Some variations are random and some systematic. The design goal accuracy of ± 5 mm refers to systematic errors since truly random errors can be averaged out in analysis. In practice, photon quantization at the detector is the largest single source of random noise and depends on signal level and pulse length. For example, a single photoelectron return gives an rms range variation of 1.3, 0.3, and 0.013 m at pulse lengths of 20, 5, and 0.2 nsec, respectively. The largest single source of noise due to the satellite itself is coherent interference among the reflections from individual cube corners, which produces a noise of about 1 cm at the pulse lengths considered if weighting by signal strength is used (Section 11). In principle, if the pulse length were shorter than the distance between cube corners along the line of sight, there would be no coherent interference. Calculating the return signal so that the range correction can be determined requires knowing the position and reflectivity of each cube corner contributing to the return. The range correction at a point in the far field pattern is a function of the intensity of the diffraction pattern of each cube corner at that point and the position of the cube corner along the line of sight. The positions of the cube corners on the satellite and the variation of the configuration of the cube corners from different viewing directions contribute an uncertainty of about 1 mm (Section 7). The primary source of systematic errors in computing the range correction is the variation of the range correction with position in the far field. The magnitude of the effect for Lageos can be seen from the range contour plots in Figure 10 of Section 10. In an attempt to estimate the effect of manufacturing tolerances on the range correction, calculations have been done for dihedral angle offsets of 0.75, 1.25, and 1.75 arcsec. The uncertainty in the offset is one of the primary manufacturing tolerances to be considered. Other factors affecting the far field pattern are surface curvature, material inhomogeneities, and thermal gradients that produce refractive index gradients. Optical testing of the cube corners under the expected thermal conditions showed that the variation in performance of an individual cube corner under different thermal conditions is in general less than the variation from one cube corner to another due to manufacturing differences. Looking at the range contour plots for

different dihedral angle offsets, wavelengths, and polarizations of the incident illumination shows that the extreme variations in the range correction within the annulus are from a high of about 0.2450 m to a low of about 0.2380, which gives peak-to-peak error limits of about plus 2 or 3 mm to minus 4 or 5 mm. Looking only at the plots for a mixture of angles whose mean is 1.25 arcsec, the extremes are from plus 2 or 3 mm to minus 2 or 3 mm. This is probably the best estimate of the range uncertainty since it should be a reasonable approximation for modeling the actual array.

The calculation of range corrections for other pulse detection methods at selected points in the far field shows that half-maximum and peak detection are more stable over the far field pattern than centroid or half-area detection for short pulses. The histogram in Figure 7 (Section 8) shows that the return energy is strongly peaked toward the front of the array. Half-maximum detection with a short pulse effectively detects the earliest part of the return whose location is well defined. In practice, strong signals would be required to take advantage of this fact, since the probability distribution for a single photoelectron is the energy distribution shown in the histogram, and the mean position of a photoelectron is the centroid.

In summary, the range corrections presented in this report are estimated to be accurate to 3 mm or better.

13. INFRARED TRANSFER FUNCTION

The infrared array carried by the Lageos satellite was designed to provide coverage from any direction of illumination with a minimum of interference between the reflections from different cube corners. Germanium was chosen for the material because its high index of refraction gives each cube corner a very large viewing angle so that only a small number of reflectors are required. The material has the disadvantage that it becomes opaque at around 100°C, which occurs if the cube corner faces the sun. An accurate range correction to the center of the satellite requires knowing the orientation of the satellite. In principle, the orientation can be determined from the infrared data.

The four infrared cube corners are positioned to form an approximate tetrahedron. One cube is at the north pole and the other three are in the third row below the equator in holes 1, 11, and 21. The coordinates of each cube are given in Section 3. For a perfect tetrahedron, the central angle between any pair of vertices is 109.47122°. The central angle between all pairs of infrared cube corners is listed in Table 17. The cubes are numbered starting with the pole cube as 1 and the cubes in holes 1, 11, and 21 of the third row below the equator as cubes 2, 3, and 4, respectively.

Table 17. Central angles between pairs of infrared cube corners.

Pair	Angle (°)
1-2	112.982
1-3	112.982
1-4	112.982
2-3	102.756
3-4	102.756
4-2	111.490

Since the back faces are uncoated, the infrared reflectors depend on total internal reflection. The minimum incidence angle ϕ_c at which total internal reflection can be lost is given by the formula

$$\phi_c = \sin^{-1} (n \sin \phi'_c) ,$$

where

$$\phi'_c = \tan^{-1} \sqrt{2} - \sin^{-1} (1/n) .$$

The index of refraction is $n \approx 4.00$ for germanium, so that the cutoff angle after entering the front surface is $\phi'_c = 46^\circ 258$. The angle outside the cube corner is

$$\phi_c = \sin^{-1} (2.5849) .$$

Since the sine of the cutoff angle ϕ_c is greater than unity, no loss of total internal reflection occurs.

The reflectivity of the infrared cube corners is listed in Table 18 and plotted in Figure 12 as a function of the incidence angle ϕ for $\theta = 0$, where the angles θ and ϕ are defined in Figure 4 (Section 6). Since the front face is circular and no loss of total internal reflection occurs, the reflectivity is nearly independent of θ . There is a slight dependence on θ due to polarization effects. The reflected energy is largely in the same polarization state as the input illumination, although some depolarization does occur as shown in Table 19. Except at normal incidence, the reflection losses at the front face are a strong function of the input polarization. The return is strongest when the electric vector is parallel to the plane of incidence and weakest when it is perpendicular. The signal for circular polarization is at least half as strong as the return for parallel polarization. The reflectivity listed is the average in the annulus between 32 and 41 μ rad from the center of the pattern. This is close to the top of the central lobe of the diffraction pattern, which is fairly wide at this long wavelength. The intensity has been normalized to the peak of the Airy diffraction pattern, which is the pattern for a perfect circular reflector. Reflection losses at the front face, and phase changes due to total internal reflection, which spread the pattern, together account for the fact that the intensity is down by about a factor of five from the center of the Airy

pattern. To convert the reflectivities in the table to gain the values are multiplied by G_{106000} where

$$G_{106000} = \frac{A}{\lambda^2} = \frac{11.4009 \text{ cm}^2}{(10.6 \times 10^{-4} \text{ cm})^2}$$

$$= 1.01468 \times 10^7$$

The cross section is $AR G_{106000}$ where R is the reflectivity from Table 18. At normal incidence the cross section is $2.55 \times 10^3 \text{ m}^2$ (in standard units of gain and cross section we have $4\pi \times 2.55 \times 10^3 \text{ m}^2 = 3.2 \times 10^4 \text{ m}^2$).

Table 18. The reflectivity in units of A/λ^2 for the Lageos infrared cube corners for input illumination, which is polarized parallel or perpendicular to plane of incidence or circularly polarized.

PHI	PARALLEL	PERPENDICULAR	CIRCULAR
0	.220740	.220740	.220740
5	.203725	.201985	.202860
10	.186730	.180403	.183602
15	.169991	.157213	.163702
20	.153655	.133528	.143784
25	.137848	.110358	.124401
30	.122625	.088528	.105975
35	.108039	.068704	.088851
40	.094131	.051364	.073278
45	.080858	.036751	.059349
50	.068216	.024957	.047109
55	.056140	.015884	.036482
60	.044598	.009303	.027342
65	.033539	.004866	.019503
70	.023071	.002164	.012821
75	.013469	.000743	.007221
80	.005585	.000160	.002917
83	.002277	.000040	.001176
85	.000885	.000011	.000454
86	.000450	.000005	.000231
87	.000179	.000001	.000092
88	.000045	0.000000	.000023

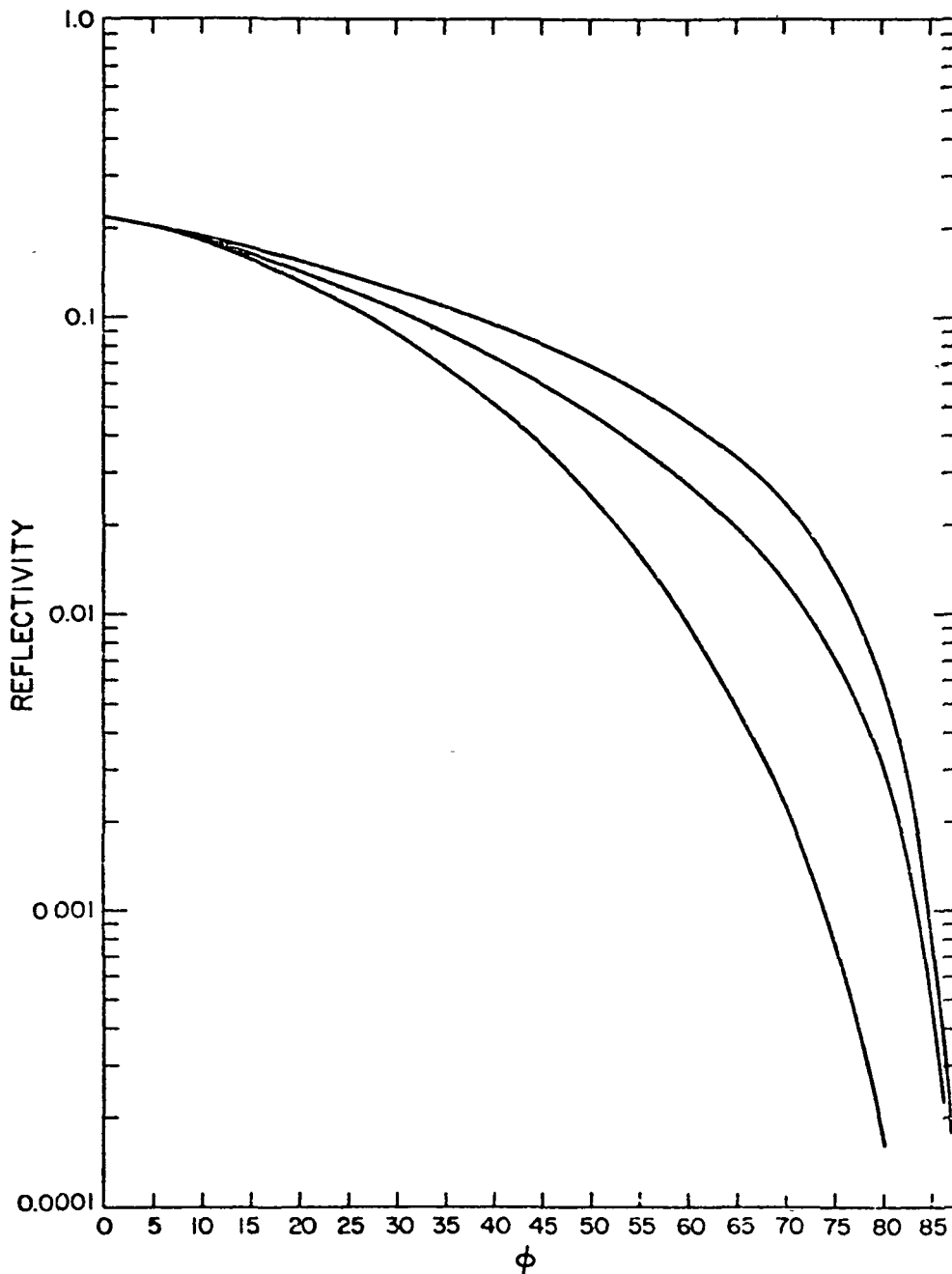


Figure 12. The reflectivity of the Lageos infrared cube corners in units of A/λ^2 . The top curve is for input illumination parallel to the plane of incidence, the bottom curve for perpendicular to the plane of incidence, and the middle curve for circularly polarized illumination.

the same polarization state as the incident illumination and the orthogonal polarization state for some sample cases.

Incidence angle (°)	Transmitted polarization	Reflected intensity	
		Original polarization	Orthogonal polarization
0	Circular	0.2207	0.000012
60	Circular	0.0234	0.003925
0	Linear	0.2207	0.000006
60	Linear (E_{\parallel})	0.0446	0.000012
60	Linear (E_{\perp})	0.0093	0.000012

The transmission factor of the germanium cube corners decreases rapidly as the temperature of the material increases. The distance traveled by the ray inside the material varies from 5.57 to 5.75 cm. In Table 20, the absorption coefficient per centimeter, and the transmission factor for the cube corner are listed for various temperatures using a path length of 5.7 cm.

Table 20. Absorptance/cm and transmission factor for the Lages infrared reflectors.

Temperature (°C)	Absorptance/cm	Transmission factor
27	0.027	0.857
40	0.028	0.852
45	0.033	0.829
50	0.045	0.774
60	0.085	0.616
70	0.143	0.443
80	0.241	0.253
90	0.386	0.111

The transmission factor should be included in the constant η when computing signal strengths using the formula in Section 5. Thermal vacuum tests run on two of the infrared cube corners gave temperatures of 104.4 and 106.7 °C with full solar illumination. The cube corners would be opaque at this temperature. With the solar illumination reduced by the factor $1/\pi$, the temperatures fell to 55.5 and 52.8 °C for the two cubes. This illumination corresponds to an incidence angle of 71.4°. With no solar illumination, the temperatures were 12.2 and 26.6°. In conclusion, the cube corners should operate well except when they are facing close to the direction of the sun.

By use of the reflectivity curve for the cube corners, calculations have been done to determine the probability over all possible viewing angles of obtaining single, double, and triple reflections. A return is considered double or triple if more than 0.1% of the reflected energy comes from a second or third cube corner. The results are tabulated for various cutoff intensities of the total signal (Table 21). The cutoff intensity is relative to the strongest return that can be obtained, which occurs when one cube corner is normal to the incident illumination. The results are shown for circular and linear polarization. A range of values is obtained for linear polarization since the reflectivity depends on the polarization angle. Strong returns are more likely to be single, and weak returns are more likely to be multiple.

Table 21. Probability over all viewing directions of getting single or multiple reflections for various cutoff levels of total intensity.

Cutoff intensity	Total probability	Single	Double	Triple
Circular Polarization				
0.01	1.000	0.223	0.632	0.135
0.1	0.980	0.233	0.632	0.115
0.2	0.781	0.233	0.516	0.031
0.5	0.256	0.206	0.050	0.000
Linear Polarization				
0.01	1.00-1.00	0.24-0.25	0.62-0.63	0.12-0.13
0.1	0.92-0.96	0.24-0.25	0.57-0.63	0.08-0.10
0.2	0.73-0.76	0.24-0.25	0.46-0.49	0.01-0.04

If the angle between the incident illumination and the normal to the front face of the infrared cube corner is known, the range correction from the apparent reflection point to the center of the satellite can be computed from the formula

$$C = R \cos \phi - L \sqrt{n^2 - \sin^2 \phi} ,$$

where

- C = the infrared range correction,
- R = the distance from the center of the satellite to the front face of the cube corner (29.807 cm),
- ϕ = the incidence angle of the illumination on the cube corner,
- L = the length of the cube corner from vertex to face (2.78384 cm),
- n = the index of refraction (4.0).

The first term is the position of the center of the front face of the cube corner along the line of sight, and the second term is the correction for optical path length in the cube corner. The range correction as a function of incidence angle is listed in Table 22. The negative values for large incidence angles indicate that the apparent reflection point is behind the center of the satellite. This effect is due to the optical path length in the cube corner.

Coherent interference can occur in the infrared reflection from Lageos in two different ways: The reflections from two or more cube corners can interfere with each other or multiply retroreflected beams from the same cube corner can interfere with each other. The beat frequency due to the first effect is $2 \Delta \dot{C} / \lambda$, where λ is the wavelength and $\Delta \dot{C}$ is the rate of change of the difference in the range corrections for the two cube corners. The second effect is due to the fact that some of the radiation is reflected back into the cube corner each time a beam exits from the front face. A pulse of radiation therefore produces a train of reflected pulses each of lower intensity than the previous one. Alternate reflections are in the same direction as the incident beam. The reflections are of significant intensity because of the high index of refraction of germanium. The optical path length difference between the primary retroreflected beam and the next beam, which is parallel to the incident beam, is

Table 22. Infrared range correction vs the angle between the incident illumination and the normal to the front face of the reflector.

PHI (DEG)	RANGE CORRECTION (METERS)
0.0	.1867
1.0	.1867
2.0	.1865
3.0	.1863
4.0	.1860
5.0	.1856
6.0	.1851
7.0	.1845
8.0	.1839
9.0	.1831
10.0	.1823
11.0	.1814
12.0	.1804
13.0	.1793
14.0	.1781
15.0	.1768
16.0	.1754
17.0	.1740
18.0	.1725
19.0	.1709
20.0	.1691
21.0	.1674
22.0	.1655
23.0	.1636
24.0	.1615
25.0	.1594
26.0	.1572
27.0	.1549
28.0	.1526
29.0	.1502
30.0	.1477
31.0	.1451
32.0	.1424
33.0	.1397
34.0	.1369
35.0	.1340
36.0	.1310
37.0	.1280
38.0	.1249
39.0	.1217
40.0	.1184
41.0	.1151
42.0	.1117
43.0	.1083
44.0	.1048
45.0	.1012
46.0	.0975
47.0	.0938
48.0	.0900
49.0	.0862
50.0	.0823
51.0	.0783
52.0	.0743
53.0	.0703
54.0	.0661
55.0	.0620
56.0	.0577
57.0	.0535
58.0	.0491
59.0	.0448
60.0	.0403
61.0	.0358
62.0	.0313
63.0	.0268
64.0	.0222
65.0	.0175
66.0	.0128
67.0	.0081
68.0	.0033
69.0	-.0015
70.0	-.0063
71.0	-.0112
72.0	-.0161
73.0	-.0210
74.0	-.0259
75.0	-.0309
76.0	-.0359
77.0	-.0409
78.0	-.0460
79.0	-.0511
80.0	-.0562
81.0	-.0613
82.0	-.0664
83.0	-.0715
84.0	-.0767
85.0	-.0819
86.0	-.0870
87.0	-.0922
88.0	-.0974
89.0	-.1026
90.0	-.1078

$$\frac{4n L}{\cos \phi'} = \frac{4n^2 L}{\sqrt{n^2 - \sin^2 \phi}},$$

where

n = the index of refraction (4.0),

L = the length of the cube corner (2.78384 cm),

ϕ = the incidence angle on the cube corner,

ϕ' = the angle of the beam after refraction at the front face.

As the angle of incidence on the cube corner changes, the optical path length between the two retroreflected beams changes. The beat frequency due to this change is

$$\frac{\dot{\phi}}{\lambda} \frac{d}{d\phi} \left(\frac{4n^2 L}{\sqrt{n^2 - \sin^2 \phi}} \right) = \frac{\dot{\phi}}{\lambda} \frac{4Ln^2 \sin \phi \cos \phi}{(n^2 - \sin^2 \phi)^{3/2}}.$$

The cutoff angle for this interference is $66^\circ 59'$ because the active reflecting area for secondary retroreflection goes to zero at this angle.

In order to use infrared data for deriving satellite positions to an accuracy better than 10 cm, it is necessary to know the orientation of the satellite. The orientation and angular velocity of the satellite affect the return signal in various ways that can, in principle, be used to infer the orientation as a function of time. If the satellite is spinning rapidly compared to the orbital frequency, the reflected intensity and measured range to each cube corner vary periodically. However, if the spin rate is low, or the change in orientation of the satellite relative to the observer is due only to the orbital motion, the variations in range and intensity would be difficult to separate from the variations due to orbital motion or other factors. The coherent interference between pairs of cube corners provides a precise measure of the change in distance to the two cube corners along the line of sight. The coherent interference between the primary and secondary retroreflected signals from one cube corner is a function of the incidence angle of the illumination on the cube corner. The rate of change of phase with incidence angle is zero at normal incidence and reaches a maximum value of 24 cycles/deg at 46° for a wavelength of 106000 Å. Except at normal incidence, the

reflected intensity for linearly polarized illumination is a function of the angle of the polarization vector with respect to the plane of incidence on the cube corner. If the plane of polarization is rotated, the maximum intensity will occur when the polarization vector is in the plane of incidence, and the minimum will occur when it is perpendicular. The ratio of the maximum to the minimum is a function of the angle of incidence. Aside from an ambiguity of 180° in azimuth, such a measurement indicates the angle between the line of sight and the normal to the cube corner, and the azimuth of the cube corner about the line of sight.

14. ACKNOWLEDGMENTS

The author wishes to express his appreciation to all those people who provided information used in this report. In particular, Mr. William Johnson of Marshall Space Flight Center provided technical data on the design of the satellite and retro-reflectors, and Mr. John Brueger of Bendix Aerospace Systems Division provided data on the thermal vacuum testing of the infrared cube corners.

15. REFERENCES

ARNOLD, D.A.

- 1972. Calculation of retroreflector array transfer functions. Final Technical Report, NASA Grant NGR 09-015-196, December. [This report gives results computed for satellites BE-B (6406401), BE-C (6503201), Geos 1 (6508901), D1C (6701101), D1D (6701401), Geos 2 (6800201), Peole (7010001), and Geos 3].
- 1974. Optical transfer function of NTS-1 retroreflector array. Technical Report RTOP 161-05-02, NASA Grant 09-015-002, Supplement No. 57, October.
- 1975a. Optical transfer function of Starlette retroreflector array. Technical Report RTOP 161-05-02, NASA Grant NGR 09-015-002, Supplement No. 57, February.
- 1975b. Optical and infrared transfer function of the Geos 3 retroreflector array. Technical Report RTOP 161-05-02, NASA Grant NGR 09-015-002 Supplement No. 57, October.

FITZMAURICE, M.W., MINOTT, P.O., ABSHIRE, J.B., and ROWE, H.E.

- 1977. Prelaunch testing of the laser geodynamic satellite (Lageos), March.

WEIFFENBACH, G.C.

- 1973. Use of a passive stable satellite for earth physics applications. Final Report, NASA Grant NGR 09-015-164, April.

PRECEDING PAGE MISSING NOT FILMED